

**COMPOSITE FOUNDATIONS ON MALAYSIAN SOFT CLAY SOIL:
APPLICATIONS OF INNOVATIVE TECHNIQUES**

KHAIRUL NIZAR B MOHD YUSOF

Submitted in accordance with the requirements for the degree of
Doctor of Philosophy

The University of Leeds
School of Civil Engineering

February 2012

The candidate confirms that the work submitted is his own and that
appropriate credit has been given where reference has been made to the
work of others

This copy has been supplied on the understanding that it is copyright material
and that no quotation from the thesis may be published without proper
acknowledgement

ACKNOWLEDGEMENTS

I would like to express my sincere thanks and appreciation to my supervisor, Prof. B.G. Clarke, for suggesting this thesis topic, and for encouragement, and insightful suggestions. I sincerely feel that without his help and guidance this work would not have been possible. It has been both a pleasure and an honour to have worked with him.

Much thankful also for Ministry of Higher Education of Malaysia and University Tun Hussein Onn Malaysia for fees funding and scholarship.

Sincere appreciation is extended to the school of civil engineering, staff and fellow graduate students at the University of Leeds for their encouragement, support and friendship. In particular, I am thankful to Mr M Marsden for his expertise, cooperation and patience in this laboratory investigation. Thanks are also extended to Mrs M Martell and Prof. D.C. Wijeyesekera for their assistance and devotion.

I also wish to thank the mechanical workshop, the concrete wet lab, and the engineering store for their technical assistance.

I would like to personally thank Dr Rafidah Hamdan, Dr Norwati Jamaluddin, Dr Norshuhaila Mohamed Sunar, Dr Saiful Azhar Ahmad Tajuddin, Dr Aziman Madun, Dr Adnan Zainorabidin, Mr Godwin Eton, Mr Chris Robson, Mr Apo Peter Zaproš, Mr Umberto Armani, Mr Marco-Felipe King Costello, Mr Vu Thanh Son, Ms Floriane, Mr Steve, and also Mr Richard Vine for their assistance and encouragement, and most of all for wonderful friendship they have rewarded me. Extra thanks are extended to Assoc. Prof. Ir Azizan Abd Aziz, Prof. Dato' Dr Ismail Bakar, and JKIG's staff members for their encouragement.

Finally, without these guys, Mr Faslie Subari, Mr Knott Abdul Hamid, Mr Uzair Abdul Nasir, and Mr Hirman Sudairi Sugiman, their moral support, their understanding whilst am in Leeds, abit of their support this thesis would never have been completed. And not to forget, Mr Safian Ahmad and Mr Nazrey Omar.

ABSTRACT

An innovative technique of electro osmosis coupled with vertical surcharge loading to accelerate the consolidation and stiffen Kaolin (China Clay Grade E) was investigated in this study. The geotechnical properties of this China Clay Kaolin Grade E and the design of electro osmotic consolidation chamber are discussed together with an explanation of the procedural concept of the electro osmotic consolidation chamber (i.e., the preparation of the apparatus and the clay sample, assembling of the electro osmotic consolidation chamber; and the experimental work).

The plastic limit, liquid limit and plasticity index were 35%, 53% and 18% respectively. Therefore, China Clay Kaolin Grade E is classified as MH soil, and it is predominantly a silt with high plasticity. The specific gravity of the soil is 2.65. To ensure the kaolin is saturated, all samples were prepared in a similar manner with deaired water to produce a slurry at 150% of the liquid limit (initial moisture content of 79.5%).

The electro osmotic consolidation chamber was cylindrical and consisted of the body, the base and the top cap. The body and the base of the chamber were constructed of polyvinyl chloride (PVC) tube with a wall thickness of 10.9 mm, 345 mm high and 251 mm inner diameter. The electro osmotic consolidation chamber was assembled together with a 45 mm thick flange and collar. The top cap of this chamber was based on that of a Rowe cell of similar diameter.

Twenty one tests were performed in this study with an applied voltage and one test was a control test. The test samples in the twenty one tests were all consolidated to three different phases. In Phases 1 and 2, the samples were consolidated at 15 kPa while in the Phase 3, 50 kPa was used. The electro osmotic process was only performed during Phase 2. The time of treatment, numbers of electrodes, the arrangement of electrodes, and the applied voltages were investigated in these tests.

Results from these tests indicated that the China Clay Kaolin Grade E in a 79.5% slurry form responded well to electro osmotic treatment and that electro osmotic process increased the overall stiffness of the soil as indicated by the reduced relative settlement in Phase 3 with a pressure of 50kPa.

The water content around the anodes was less than that at the cathode creating zones of higher average constrained stiffness. The tests demonstrated that the longer the time of treatment, the greater the numbers of anodes, the shorter distance between the electrodes and the higher the applied voltages associated with electro osmosis increased the average stiffness of the soil mass confirming the concept of an electro osmotic pile.

Keywords: electro osmotic merged vertical loading and electro osmotic, consolidation, electro osmotic consolidation chamber, stiffening.

CONTENTS

Acknowledgements	ii
Abstract	iii
List of Tables	viii
List of Figures	x
Abbreviations and Symbols	xvi
CHAPTER 1 INTRODUCTION	
1.1 Introduction	1
1.2 Background to the problem	3
1.3 Objectives of study	6
1.4 The composite foundation	6
1.5 Scope of thesis	7
CHAPTER 2 LITERATURE REVIEW	
2.1 General	8
2.2 Peninsular Malaysian Soft Clay	8
2.2.1 Soft clay definition	10
2.2.2 Soft clay soil profiles in Peninsular Malaysia	10
2.2.3 Problems with soft clay soils	10
2.2.4 Soil improvement in Southeast Asia areas	12
2.3 Electro kinetic occurrence in clays	17
2.4 Electro osmosis	22
2.4.1 The theory of electro osmosis	22
2.4.2 Consolidation via electro osmosis	28
2.4.2.1 Excess pore water pressure production and consolidation by electro osmosis	28
2.4.2.2 Combined electro osmosis and external load induced consolidation	31
2.5 Historical review of electro osmosis consolidation	39
2.6 Costs of electro osmosis consolidation	41

2.7	Suitable applications for electro osmotic piles	47
2.7.1	Improvng friction pile capacity	47
2.7.2	Trenching and excavation sites	49
2.7.3	Prevent swelling and shrinkage in foundations	50
2.7.4	Stabilise the unstable slope	52
2.7.5	Review of case histories of electro osmotic strengthening of piles	54
2.8	Effectiveness and efficiency of electro osmotic treatment	56
2.8.1	Energy consumption, E	56
2.8.2	Electro osmotic flow efficiency	56
2.8.3	Electro osmotic transport efficiency, k_t	57
2.9	Conclusions	58

CHAPTER 3 THE LABORATORY PROCESS USED TO ACCESS ELECTRO OSMOTIC PILES

3.1	Introduction	60
3.2	The principles	60
3.3	The design	61
3.3.1	The electro osmotic consolidation chamber of its general Assembly	61
3.3.2	Test chamber	63
3.3.3	The base of the cell	64
3.3.3.1	Plugs	68
3.3.4	The top of the cell	70
3.3.4.1	Top plate and o-ring	70
3.3.4.2	Clamping bolts	71
3.3.5	The electrodes	71
3.3.6	The control systems	75
3.4	The procedure	76
3.4.1	Preparation of the apparatus	76
3.4.2	Electro osmotic consolidation chamber assembly	77
3.5	Experimental work	82
3.5.1	Kaolin sample	82
3.5.1.1	Soil classification test	83
3.5.1.2	Preparation of kaolin slurry	83
3.5.2	Loading stages	83

3.5.3	Electro osmotic piles series	84
3.5.4	Control test	89
3.5.5	Parameters determination	89
3.6	An examples of the osmotic test	89
3.7	Conclusions	97

CHAPTER 4 RESULTS AND DISCUSSIONS

4.1	General	98
4.2	Control tests	103
4.2.1	Test conditions	103
4.2.2	Test results	103
4.3	Electro osmotic piles tests	105
4.3.1	Vertical displacement and water expelled versus time curves	106
4.3.1.1	Time of treatment tests series	108
4.3.1.2	Numbers of electrodes and arrangement of electrodes tests series	111
4.3.1.3	Different applied voltage tests series	115
4.3.2	Vertical displacement multiplied by area versus water expelled lines	119
4.3.3	Water expelled and current versus time curves	120
4.3.3.1	Time of treatment tests series	121
4.3.3.2	Numbers and arrangement of electrodes tests series	122
4.3.3.3	Different applied voltage tests series	123
4.3.4	Effect on water content, w_c	130
4.3.5	Effect on coefficient of volume compressibility, m_v	135
4.3.6	Effect on constrained stiffness, $E_{stiffness}$	138

CHAPTER 5 SUMMARY, CONCLUSIONS AND RECOMMENDATIONS FOR FUTURE RESEARCH

5.1	Summary and conclusions	146
5.2	Recommendations for future research	148

References	149
Appendices	159

LIST OF TABLES

Table 1.1	The hierarchy for construction on soft clays	4
Table 2.1	Soft clay soils thickness in Peninsular Malaysia (Abdullah and Chandra, 1987)	10
Table 2.2	Upper and lower depth ranges for a west costs deposits of Peninsular Malaysia (Aziz, 1993)	11
Table 2.3	Upper and lower depth ranges for a west costs deposits of Peninsular Malaysia (Aziz, 1993)	12
Table 2.4	Survey of existing methods for improving cohesive soils (after Eggestad, 1983)	15
Table 2.5	Range of particle sizes for various soil Improvement approaches (reproduced From Hausmann, 1990, Lee et al., 1985)	16
Table 2.6	Streaming potential, electro phoresis and sedimentation definitions (reproduced from Mitchell and Soga, 2005; Mitchell, 1993)	22
Table 2.7	Coefficients of electro osmotic permeability, k_e	25
Table 2.8	Direct costs of the field tests as Performed (reproduced from Burnotte et al., 2004)	42
Table 2.9	Weight constituent of total costs (reproduced from Alshawabkeh, 2001; Alshawabkeh et al., 1999a)	43
Table 2.10	Cost of the treatment for stabilizing the Norwegian Quick Clay (reproduced from Bjerrum et al., 1967: 226)	44
Table 2.11	Impact of electrode configuration on electrode requirements and size of in ineffective areas (reproduced from Alshawabkeh et al., 1999a:620)	47
Table 3.1	Atterberg's limits and specific gravity of Kaolin grade E used in the tests	82
Table 3.2	Chemical features of grade E white kaolin	82
Table 3.3	Electrode layout	85
Table 3.4	Series of experimental works	88
Table 3.5	Summary of experiments after electro osmosis for Q3 sample treated with 5 Volts for 24 hours	96
Table 4.1	Summary of the electro osmotic piles test	99
Table 4.2	Computed results	103

Table 4.3	Summary of settlement for test series of number of anodes and the distance between the electrodes	114
Table 4.4	Summary of settlement for test series of different applied Voltage	118
Table 4.5	Volume changed at the end of primary Consolidation on Phase 2	121
Table 4.6	End of time for primary consolidation and osmotic treatment under numbers and arrangement of electrodes tests series	123
Table 4.7	End of time for primary consolidation and osmotic treatment under different applied voltage	124
Table 4.8	Summary of A1V5 test series: e_o , m_v , $E_{stiffness}$, $E_{pre-treatment}$ and $E_{build\ phase}$ results	129
Table 4.9	Summary of water content test, w_c (%)	132
Table 4.10	Summary of numbers and arrangement of electrodes test series: numbers of anodes and cathodes applied voltage, distance between electrode, ΔH and W	135

LIST OF FIGURES

Figure 1.1	Flow chart to select appropriate deep ground improvement technique (reproduced from Bergado et al., 1994)	2
Figure 2.1	Soft deposits distribution in Peninsular Malaysia map (Malaysian Highway Authority, 1989)	8
Figure 2.2	Soft clay soils profile in Peninsular Malaysia (Abdullah and Chandra, 1987)	11
Figure 2.3	Variation of electrical potential with distance from a charged surface (reproduced from Mitchell and Soga, 2005; Mitchell, 1993)	17
Figure 2.4	Double layer structure near the surface of the positively charged particles (reproduced from Mitchell and Soga, 2005; Mitchell, 1993)	19
Figure 2.5(a)	Helmholtz-Smoluchowski model for electro kinetic phenomena (reproduced from (reproduced from Mitchell and Soga, 2005; Mitchell, 1993)	20
Figure 2.5(b)	Electro osmotic flow in rigid-straight capillaries (reproduced From Casagrande, 1952b)	20
Figure 2.6	Electro osmosis (reproduced from Mitchell and Soga, 2005; Mitchell, 1993)	21
Figure 2.7	Hydraulic flow in a capillary (reproduced from Casagrande, 1952b)	22
Figure 2.8	k_e vs k_h for impervious type of drainage	27
Figure 2.9	Pore water pressure induced at balance for the case of open cathode and closed anode (reproduced from Mitchell and Soga, 2005; Mitchell, 1993)	30
Figure 2.10	Pore pressure distributions – electro osmotic consolidation superimposed on direct loading consolidation: $u_a/u_o = -1.0$ (after Wan and Mitchell, 1976)	33
Figure 2.11	Pore pressure distributions – electro osmotic consolidation superimposed on direct loading consolidation: $u_a/u_o = -2.0$ (after Wan and Mitchell, 1976)	33
Figure 2.12	Pore pressure distributions – electro osmotic consolidation superimposed on direct loading consolidation: $u_a/u_o = -4.0$ (after Wan and Mitchell, 1976)	34

Figure 2.13	Average pore pressure versus time factor during electro osmotic superimposed on direct loading consolidation (after Wan and Mitchell, 1976)	34
Figure 2.14	Degree of consolidation versus time factor for merged electro osmosis and direct loading (after Wan and Mitchell, 1976)	36
Figure 2.15	Result of experimental investigation: excess pore water pressure at anode versus time for recompression from 49 kPa to 98.1 kPa (after Wan and Mitchell, 1976)	37
Figure 2.16	Result of experimental investigation: measured at anode and current density versus time during electro osmotic consolidation of remoulded kaolinite (after Wan and Mitchell, 1976)	45
Figure 2.17	Approximate evaluation of ineffective areas for (a): 1-D and (b): 2-D electrode configurations (after Alshawabkeh et al., 1999a: 621)	46
Figure 2.18	Pile converted to anodes (Pugh, 2002)	48
Figure 2.19	Pile converted to cathodes (Pugh, 2002)	48
Figure 2.20	Single phase treatments (Pugh, 2002)	49
Figure 2.21	Double phase treatments (Pugh, 2002)	50
Figure 2.22	Shrinkage treatments (Pugh, 2002)	50
Figure 2.23	Swelling treatments (Pugh, 2002)	51
Figure 2.24	Collapsing treatments (Pugh, 2002)	51
Figure 2.25	Vertical installations (Pugh, 2002)	53
Figure 2.26	Incline installations (Pugh, 2002)	53
Figure 3.1(a)	General arrangement of the electro osmotic consolidation chamber	61
Figure 3.1(b)	Dial gauge and other parts	62
Figure 3.2	Schematic diagram of electro osmotic consolidation chamber	62
Figure 3.3(a)	Elevation of the osmotic chamber	64
Figure 3.3(b)	Plan view of the osmotic chamber A: clamping bolt type 1; B: clamping bolt type 2	64
Figure 3.4	The whole view from upper part of bottom base (A) and (B): locating bolts holder; (C): flange slot; (D): drainage port; (E): gland	65

Figure 3.5	Upper plan view base of the cell (A) and (B): locating bolts holder; (C): flange slot; (D): drainage port; (E): gland slots	66
Figure 3.6	Bottom plate on top of the base of the cell and (B): locating bolts holder; (F): flange slots	66
Figure 3.7	Vertically copper coiled spring electrodes together with the folded cylindrical filter paper	67
Figure 3.8	Schematic diagram of the anode plug Installation	67
Figure 3.9	Photograph of anode plug	68
Figure 3.10	Photograph of cathode plug	68
Figure 3.11	Schematic diagram of the cathode plug installation	69
Figure 3.12	Blanking plug	69
Figure 3.13	Schematic diagram of the blank plug Installation	70
Figure 3.14	Clamping down bolt type 1(A) and 2(B)	71
Figure 3.15	Copper coiled spring electrodes showing the brass mandrel, and (b) the spring	72
Figure 3.16	Copper coiled spring electrodes together with the filter paper core	73
Figure 3.17	Top section fitted with the hangar and solids steel	74
Figure 3.18	The side view of hangar and the holder	74
Figure 3.19	Elevation view of the gland	75
Figure 3.20	Connected drainage connector from the base of the cell view	76
Figure 3.21	Location of small o-ring seals	77
Figure 3.22	Location of filter paper	78
Figure 3.23	Pouring and shaking process	79
Figure 3.24	Filter paper on the top of the top slurry surface	80
Figure 3.25	Drainage valve	81
Figure 3.26	Particle size distribution graph for grade E kaolin	83
Figure 3.27	Approximate evaluation of ineffective areas for (a) 1-D and (b) 2-D electrode configurations	87
Figure 3.28	Hexagonal layout for primary experimental work	87
Figure 3.29	Results for Q3 on phase 1: vertical displacement versus time	90
Figure 3.30	Results for Q3 on phase 2: vertical displacement versus time	91

Figure 3.31	Results for Q3 on phase 3: vertical displacement versus time	91
Figure 3.32	Results for Q3 on phase 1: water expelled versus time	92
Figure 3.33	Results for Q3 on phase 2: water expelled versus time	92
Figure 3.34	Results for Q3 on phase 3: water expelled versus time	93
Figure 3.35	Results for Q3: vertical displacement*area versus water expelled	94
Figure 3.36	Results of Q3V516d test: water expelled and current versus time	95
Figure 3.37	Results of Q3V516d test: moisture content versus distance	96
Figure 3.38	Voids ratio for Q3V5 and control sample	97
Figure 4.1	Result of control test: relative vertical displacement versus Time	104
Figure 4.2	Result of control test: relative water expelled versus time	104
Figure 4.3	Result of control test: vertical displacement*area versus water expelled	105
Figure 4.4	Phase 1 results of A1V5 tests series: settlement versus time curves	106
Figure 4.5	Phase 1 results of A1V5 tests series: water expelled versus time curves	107
Figure 4.6	Phase 3 results of A1V5 tests series: settlement versus time curves	107
Figure 4.7	Phase 2 results of A1V5 tests series: settlement versus time curves	108
Figure 4.8	Phase 1 results of Q3V5 tests series: settlement versus time curves	109
Figure 4.9	Phase 1 results of Q3V5 tests series: water expelled versus time curves	109
Figure 4.10	Phase 3 results of Q3V5 tests series: settlement versus time curves	110
Figure 4.11	Phase 2 results of Q3V5 tests series: settlement versus time curves	110
Figure 4.12	Phase 1 results for numbers and arrangement of electrodes test series: settlement versus time curves	112
Figure 4.13	Phase 2 results for numbers and arrangement of electrodes test series: settlement versus time curves	112

Figure 4.14	Phase 3 results for numbers and arrangement of electrodes test series: settlement versus time curves	113
Figure 4.15	Phase 1 results for different applied voltage test series: settlement versus time curves	116
Figure 4.16	Phase 2 results for different applied voltage test series: settlement versus time curves	116
Figure 4.17	Phase 3 results for different applied voltage test series: settlement versus time curves	117
Figure 4.18	Result of A1V5 for 1 day test: settlement*area versus water expelled	119
Figure 4.19	Result of A1V53d days test: water expelled and current versus time	120
Figure 4.20	Q3V5 test series: voids ratio versus time	125
Figure 4.21	Q3V5 test series: voids ratio versus current in Phase 2	125
Figure 4.22	A1V5 test series: voids ratio versus time	126
Figure 4.23	A1V5 test series: voids ratio versus current in Phase 2	126
Figure 4.24	Numbers and arrangement of electrodes test series: voids ratio versus time	127
Figure 4.25	Numbers and arrangement of electrodes test series: voids ratio versus current in Phase 2	127
Figure 4.26	Different applied voltage test series: voids ratio versus time	128
Figure 4.27	Different applied voltage test series: voids ratio versus current in Phase 2	128
Figure 4.28	Result of treatment of time tests series: w_c average versus Time	133
Figure 4.29	Result of numbers and arrangement of electrode tests series: w_c average versus number of anodes	133
Figure 4.30	Different applied voltage tests series: w_c average versus applied voltage	134
Figure 4.31	Correlation graph of all results: m_v average e_o	134
Figure 4.32	Result of A1V5 test series: m_v versus t	136
Figure 4.33	Result of Q3V5 test series: m_v versus t	136
Figure 4.35	Result numbers and arrangement of electrode test series: m_v versus number of anodes	137
Figure 4.35	Result of different applied voltage test series: m_v versus V	137
Figure 4.36	Result of A1V5 test series: $E_{stiffness}$ versus t	140

Figure 4.37	Result of Q3V5 test series: $E_{\text{stiffness}}$ versus t	140
Figure 4.38	Result of numbers and arrangement of electrode test series: $E_{\text{stiffness}}$ versus t	141
Figure 4.39	Result of different applied voltage test series: $E_{\text{stiffness}}$ versus t	141
Figure 4.40	Relationship between $E_{\text{stiffness}}$ and number of anodes test series: at the end of Phase 3	142
Figure 4.41	Relationship between $E_{\text{stiffness}}$ and different applied voltage test series: at the end of Phase 3	142
Figure 4.42	Relationship between $E_{\text{build phase}}$ and $E_{\text{pretreatment}}$ and A1V5 test series: at the end of Phase 3	143
Figure 4.43	Relationship between $E_{\text{build phase}}$ and $E_{\text{pretreatment}}$ and Q3V5 test series: at the end of Phase 3	143
Figure 4.44	Relationship between $E_{\text{build phase}}$ and $E_{\text{pretreatment}}$ and arrangement of electrode test series: at the end of Phase 3	144
Figure 4.45	Relationship between $E_{\text{build phase}}$ and $E_{\text{pretreatment}}$ and different applied voltage test series: at the end of Phase 3	144

ABBREVIATIONS AND SYMBOLS

K_2O, Na_2O	alkalis (%)
Al_2O_3	aluminium (III) oxide (%)
V	applied voltage (V)
ϕ_{max}	applied voltage (V)
ΔE	applied voltage (V)
a	area (m^2)
A_{cell}	area of cell
$E_{stiffness}$	average constrained stiffness (kPa)
CAN	Canadian dollar
q_a	capillary of flow rate (V/m per m^2)
k_e	coefficient of electro osmotic permeability (m^2/Vs)
k_h	coefficient of hydraulic conductivity (cm/s or m/s)
m_v	coefficient of volume compressibility (m^2/MN)
H_s	comparable height of surcharge (m)
C_1	cost of electrodes per unit length ($\$L^{-1}$)
C_3	cost of electrodes of the chemical agent ($\$M^{-1}$)
C_4	cost of treatment per unit volume of the electrolyte (effluent) collected ($\$L^{-3}$)
nA	cross-sectional area of a void
I	current (A)
U	degree of consolidation (%)
R_d	delaying factor (dimensionless)
DC	direct current
δ	distance between the wall and the centre of the plabe of mobile charge
x	distance to the cathode (m)
Q	drainage rate (cm^3/s)
σ^*	effective electric conductivity of the soil medium
u^*	effective ionic mobility of the ion (m^2 per sec-V)
C_2	electric energy cost ($\$$ per kWhour)
ϵ	electrical energy requirements per gallon discharged (kWh)
$\frac{dV}{dL}$	electric field, or known as voltage gradient (V/m)

$V(x)$	electric potential at position x relative to the potential at the cathode at $x = 0$ (V)
k_i	electro osmotic transport efficiency ($\text{cm}^3/\text{Ampere-hours}$)
L	electrode spacing (m)
R_e	electrode radial spacing (m)
E	energy consumption (kWh per m^3)
u_a	excess pore pressure (kN/m^2)
F	Faraday's constant ($96485 \text{ C/mol-electron}$)
α	factor depending upon the stoichiometry of the neutralizing reaction, dimensionless;
Fe_2O_3	ferum (III) oxide (%)
v	flow velocity
Q_h	flow rate induced by hydraulic gradient
Q_e	flow rate induced by voltage gradient
η	fluid viscosity (Ns/m^2)
i_e, i_r	gradients
A	gross total cross-sectional area normal to the direction of flow (m^2)
A_{ineff}	ineffective area
u_o	initial excess pore pressure due to fill loading (kN/m^2)
L	length of the sample (m)
ΔL	layer thickness difference
w_L	liquid limit (%)
MHA	Malaysian Highway Authority
M_w	molecular weight of the neutralizing chemical (M/W)
H_e	negative pore water head generated by electro osmosis at $x = L/2$ (m)
Ψ	negative potential
N	number of capillaries (non dimensional)
F_1	number of electrodes per cell
N	number of electrodes per unit surface area ($\text{\$/L}^{-2}$)
ϵ	permittivity of fluid (F/m)
w_p	plastic limit (%)
I_p	plasticity index (%)
PVC	polyvinyl chloride
u	pore water pressure (kN/m^2)
ζ	potential across the capillary, or known as zeta potential (V)
Ψ_o	potential at the surface

B	reactive transport rate of a species relative to the electric conductivity of a medium
v	sample volume (L)
SiO ₂	silicon oxide (%)
G _s	specific gravity
c _v	Terzhagi's coefficient of consolidation (m ² /year)
T _v	time factor (non dimensional)
C _{total}	total costs per unit volume of soil to be treated (\$L ⁻³)
h	total hydraulic head (m)
t	total time (h)
Q	total water expelled (cm ³)
Q	total volume flow rate (m ³ /s)
γ _w	unit weight of water (kN/m ³)
C ₅	variable daily cost (monitoring, insurance, rentals, etc) (\$L ⁻³ T ¹)
v _h	velocity of water induced by hydraulic gradient
v _e	velocity of water induced by voltage gradient
e _o	voids ratio (nondimensional)
ΔE	voltage difference
H ₂ O	water
w _c	water content (%)

LIST OF APPENDICES

APPENDIX A	Soil improvement approaches (reproduced from Hausmann, 1990; Lee et al., 1985)	159
APPENDIX B	Outline of several of the earlier electro osmosis experiments	166
APPENDIX C	Figure C1 Plan slot for clamping bolt type 1 (A)	177
	Figure C2 Elevation view for clamping bolt type 1 (A) from section AA	177
	Figure C3 Elevation view of slot clamping bolt type 1 (A) from section BB	178
	Figure C4 Plan of slot for clamping down bolt type 2 (B)	178
	Figure C5 Elevation view for clamping bolt type 2 (B) from section AA	178
	Figure C6 Elevation view of slot clamping bolt type 2 (B) from section BB	179
	Figure C7 Elevation view for bottom base	180
	Figure C8 Plan view of slot for clamping bolts and holding down	181
	Figure C9 Elevation view	181
	Figure C10 Plan view	181
	Figure C11 Plan view of bottom plate	182
	Figure C12 Details for white flat slotted screw	183
	Figure C13 Details for locating plastic screw holder	183
	Figure C14 Section for holding down plastic screw	183
	Figure C15 Section of anode plug	184
	Figure C16 Plan view of anode plug	184
	Figure C17 Section of cathode plug	184
	Figure C18 Plan view of cathode plug	184
	Figure C19 Section of solid plug	185
	Figure C20 Plan view of solid plug	185
	Figure C21 Top plate	185
	Figure C22 Details for gland locations	186
	Figure C23 Schematic diagram for wire access glands	186
	Figure C24 Elevation view for wire access glands	186
	Figure C25 Section of sealing plug	187

Figure C26 Details for drainage port	187
APPENDIX D Table D1 Summary of control test results	188
Table D2 Summary of A1V51d test results	189
Table D3 Summary of A1V53d test results	190
Table D4 Summary of A1V55d test results	191
Table D5 Summary of A1V57d test results	192
Table D6 Summary of A1V515d test results	193
Table D7 Summary of A1V519d test results	194
Table D8 Summary of Q3V51d test results	195
Table D9 Summary of Q3V53d test results	196
Table D10 Summary of Q3V55d test results	197
Table D11 Summary of Q3V57d test results	198
Table D12 Summary of Q3V515d test results	199
Table D13 Summary of Q3V517d test results	200
Table D14 Summary of Q1V515d test results	201
Table D15 Summary of Q2V516d test results	202
Table D16 Summary of Q4V516d test results	203
Table D17 Summary of A2V517d test results	204
Table D18 Summary of A2V1016d test results	205
Table D19 Summary of Q2V1015d test results	206
Table D20 Summary of Q4V1014d test results	207
Table D21 Summary of Q4V2012d test results	208
Figure D1 Phase 2 results of A1V5 test series: water expelled versus time curves	209
Figure D2 Phase 3 results of A1V5 test series: water expelled versus time curves	209
Figure D3 Phase 2 results of Q3V5 test series: water expelled versus time curves	210
Figure D4 Phase 3 results of Q3V5 test series: water expelled versus time curves	210
Figure D5 Phase 1 results for numbers and arrangement of electrodes test series: water expelled versus time curves	211
Figure D6 Phase 2 results for numbers and arrangement of electrodes test series: water expelled versus time curves	211
Figure D7 Phase 3 results for numbers and arrangement of electrodes test series: water expelled versus time curves	212

Figure D8 Phase 1 results for different applied voltage test series: water expelled versus time curves	212
Figure D9 Phase 2 results for different applied voltage test series: water expelled versus time curves	213
Figure D10 Phase 3 results for different applied voltage test series: water expelled versus time curves	213
Figure D11 Result of A1V5 test series: settlement*area versus water expelled	214
Figure D12 Result of Q3V5 test series: settlement*area versus water expelled	214
Figure D13 Result of numbers and arrangement of electrodes test series: settlement*area versus water expelled	215
Figure D14 Result of different applied voltage on A2 test series: settlement*area versus water expelled	215
Figure D15 Result of different applied voltage on Q2 test series: settlement*area versus water expelled	216
Figure D16 Result of different applied voltage on Q4 test series: settlement*area versus water expelled	216
Figure D17 Results of A1V51d test: water expelled and current versus time	217
Figure D18 Results of A1V55d test: water expelled and current versus time	217
Figure D19 Results of A1V57d test: water expelled and current versus time	218
Figure D20 Results of A1V515d test: water expelled and current versus time	218
Figure D21 Results of A1V519d test: water expelled and current versus time	219
Figure D22 Results of Q3V51d test: water expelled and current versus time	219
Figure D23 Results of Q3V53d test: water expelled and current versus time	220
Figure D24 Results of Q3V55d test: water expelled and current versus time	220

Figure D25 Results of Q3V57d test: water expelled and current versus time	221
Figure D26 Results of Q3V515d test: water expelled and current versus time	221
Figure D27 Results of Q3V517d test: water expelled and current versus time	222
Figure D28 Results of Q1V517d test: water expelled and current versus time	222
Figure D29 Results of Q2V516d test: water expelled and current versus time	223
Figure D30 Results of Q4V516d test: water expelled and current versus time	223
Figure D31 Results of A2V517d test: water expelled and current versus time	224
Figure D32 Results of A2V1016d test: water expelled and current versus time	224
Figure D33 Results of Q2V1015d test: water expelled and current versus time	225
Figure D34 Results of Q4V1014d test: water expelled and current versus time	225
Figure D35 Results of Q4V2012d test: water expelled and current versus time	226
Figure D36 Results of A1V51d test: water content versus distance	226
Figure D37 Results of A1V53d test: water content versus distance	227
Figure B38 Results of A1V55d test: water content versus distance	227
Figure D39 Results of A1V57d test: water content versus distance	228
Figure D40 Results of A1V515d test: water content versus distance	228
Figure D41 Results of A1V519d test: water content versus distance	229

Figure D42 Results of Q3V51d test: water content versus distance	229
Figure D43 Results of Q3V53d test: water content versus distance	230
Figure D44 Results of Q3V55d test: water content versus distance	230
Figure D45 Results of Q3V57d test: water content versus distance	231
Figure D46 Results of Q3V515d test: water content versus distance	231
Figure D47 Results of Q3V517d test: water content versus distance	232
Figure D48 Results of Q1V515d test: water content versus distance	232
Figure D49 Results of Q2V516d test: water content versus distance	233
Figure D50 Results of Q4V516d test: water content versus distance	233
Figure D51 Results of A2V517d test: water content versus distance	234
Figure D52 Results of A2V1016d test: water content versus distance	234
Figure D53 Results of Q2V1015d test: water content versus distance	235
Figure D54 Results of Q4V1014d test: water content versus distance	235
Figure D55 Results of Q4V2012d test: water content versus distance	236

CHAPTER 1

INTRODUCTION

1.1 INTRODUCTION

Soft clays and peat soils are two kinds of soils which are known to have low strengths and low stiffnesses. The first is often a product of weathered material deposited in a marine environment; the second is derived from the decaying process of animals and plants. The mechanical characteristics of these soils are a function of their composition, history and current state. Engineering solutions have to be considered to alter these characteristics when building on or in these materials. These solutions range from permanent, hard solutions such as piled foundations, to time dependent improvement of the soil through consolidation. Piled solutions are often preferred as it reduces the risk of failure and excessive settlement but they are expensive and not sustainable given the use of primary resources. The alternative is to improve the ground using techniques such as preloading, often combined with prefabricated vertical drains and vertical sand drains; stone columns; mixing the soils with lime/cement (dry mixed method); stiffened columns; vacuum consolidation; and electro kinetics dewatering. A flow chart (Figure 1.1) developed by Bergado, et al. (1994) is a guide to the selection of the most appropriate ground improvement technique.

One method not shown on that chart yet has been in use for many years is that of electro osmotic consolidation in which water is forced out of the soil by passing an electric current through the soil between two electrodes. The technique is known to be successful at improving the mechanical characteristics but there are a number of challenges to overcome which means that the techniques has not been widely used. One of the key challenges is the breakdown of the electrodes with time stopping the process and contaminating the groundwater. Recent developments in electrodes have overcome these problems offering an alternative ground improvement technique.

An alternative approach is to use electro osmotic consolidation to create stiff soil columns within soft clay and combine that with a stiff granular layer to create a composite foundation. There is potential to use this composite foundation in soft clays in many parts of the world including Malaysia where much of the infrastructure of mainland Malaysia is built on the coastal plain.

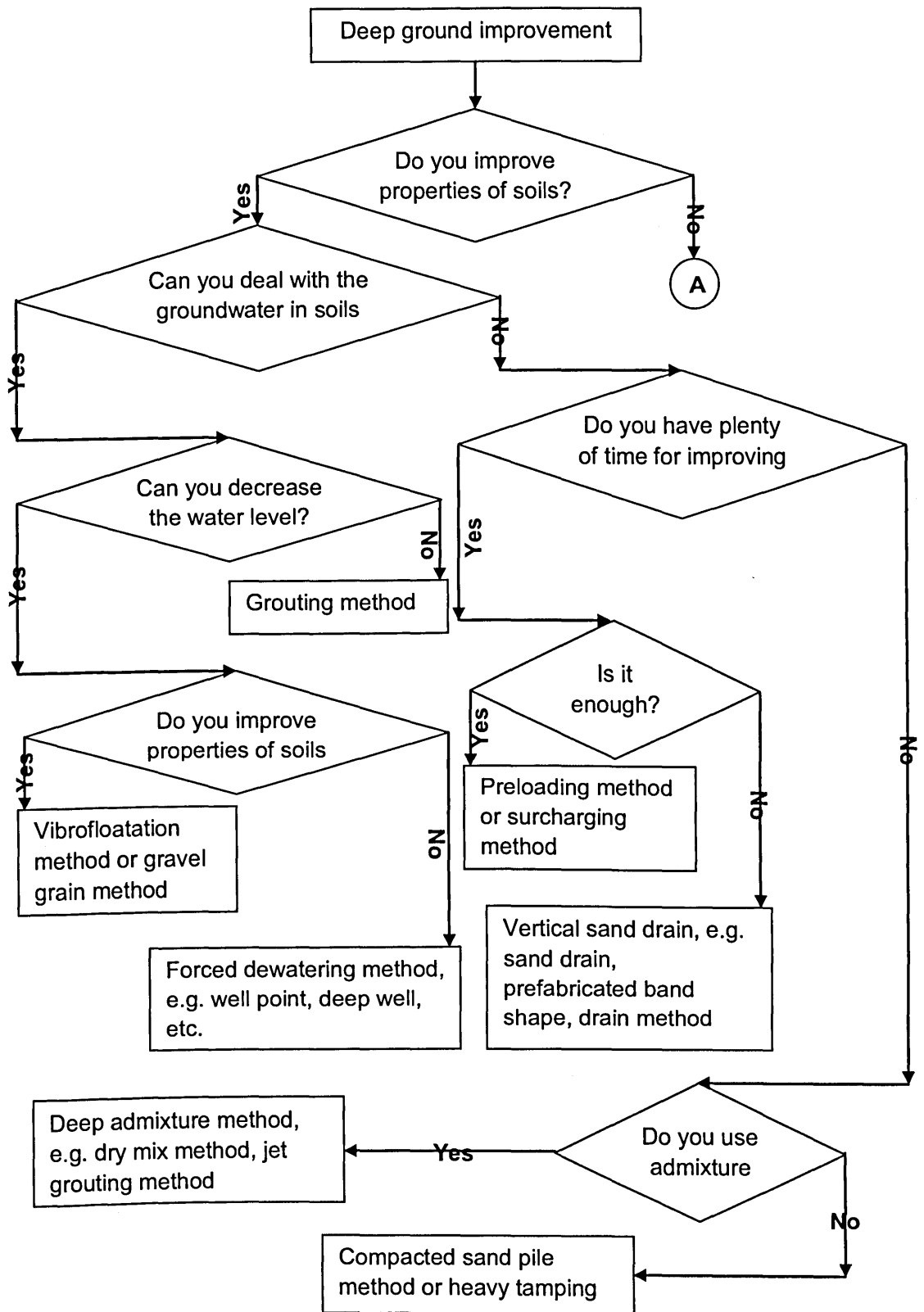


Figure 1.1 Flow chart to select appropriate deep ground improvement technique (reproduced from Bergado et al., 1994)

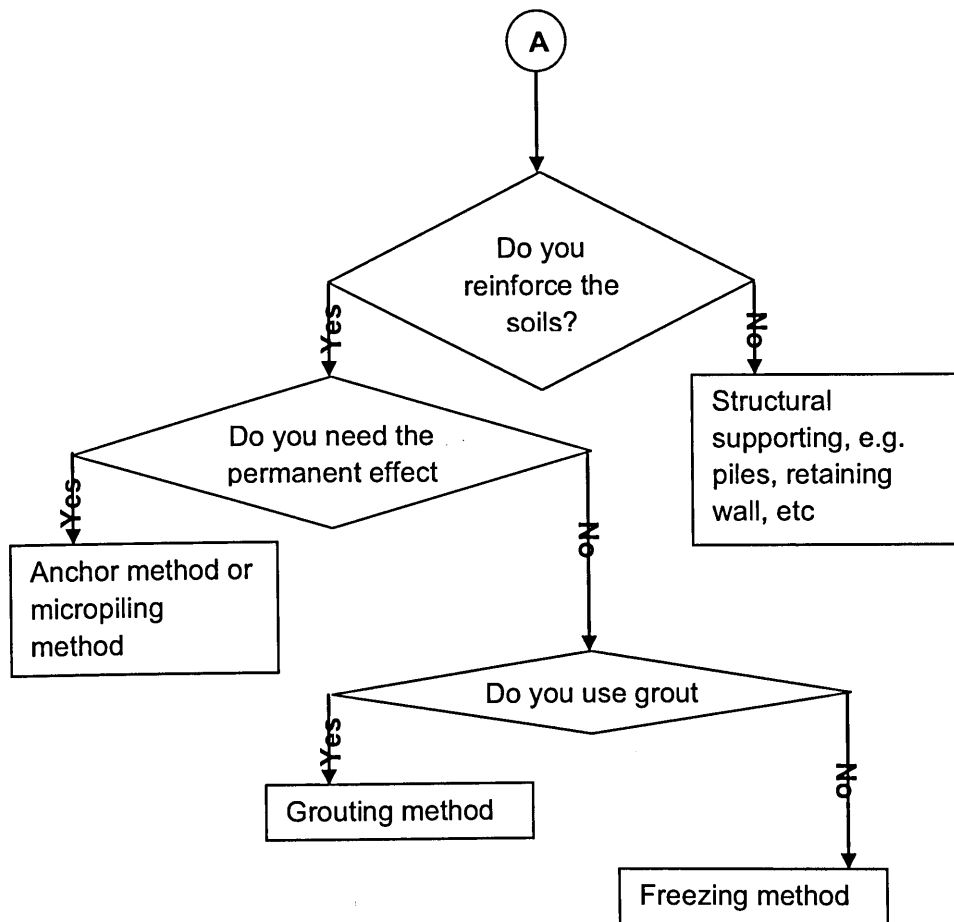


Figure 1.1 Flow chart to select appropriate deep ground improvement technique (reproduced from Bergado et al., 1994)

1.2 BACKGROUND TO THE PROBLEM

It is difficult to build on or in soft fine grained soils because of the pore pressures generated during loading or unloading and subsequent volume changes as the pore pressures dissipate. This can lead to catastrophic failure and excessive deformation. Yet these soils are common especially in floodplains where there is significant development of the built environment. A hierarchy is followed in order to develop on these soils as indicated in Table 1.1. The first solution, to excavate and replace, is the most costly and damaging to the environment; consolidation either by preloading or electro osmosis is the least damaging to the environment but there is a time element to consider.

The main advantage of electro osmotic consolidation over preloading is that there is no need to import fill and failure will not occur during ground improvement. Degradation of the electrodes and potential contamination of the ground water are no longer issues as a result of recent developments in electrically conductive polymers used as electrodes.

Table 1.1 The hierarchy for construction on soft clays

Technique	Description	Disadvantage	Advantage
Excavate and replace	The soft clays are excavated by mechanical means and either used as landscaping material or disposed to landfill. Granular material is used as a replacement	Cost of excavation and disposal of soft clay; stability of excavation; cost of fill and placement of fill; use of primary resources	Removes problem completely
Concrete, steel or timber piles	Piles are driven or bored through the soft clays into the underlying bearing strata.	Working platform for pile construction; potential negative friction on piles; material, transportation and installation costs.	Bypasses problem; provides permanent hard solution
Stone columns	Stone columns created by vibro compaction transferring the load into the underlying bearing strata.	Working platform for stone column construction; use of primary resources which may not be available locally; potential negative friction on stone columns; potential failure of stone columns due to insufficient lateral support	Bypasses problem;
Lime/cement columns	Lime/cement soil columns created by in situ nixing techniques transferring the load into the underlying bearing strata	Working platform for construction plant; use of manufactured material; potential contamination; potential negative friction on columns.	Bypasses problem; reduced quantity of imported material

Chemical stabilization	Chemicals mixed in place or injected into the soil to react with the water thus reducing the water content or cementing the soil particles	Working platform for construction plant; use of manufactured material; potential contamination	Uniform modified/stabilised soil with known properties
Preloading	together. Imported fill used to increase the pore pressures which dissipate with time as the clay consolidates	Cost of importing fill and disposing of that fill; instability of preload; time for consolidation to occur; disposal of water.	Creates a permanent solution which relies on the improved properties of the soil
Electro osmotic loading	Create stiffened soil columns through electro osmotic consolidation	Working platform for construction plant; disposal of water; cost of electrodes and electricity; degradation of electrodes limits life of process	Creates a composite foundation using modified soil

1.3 OBJECTIVES OF STUDY

The aim of this work is to establish whether electro osmotic consolidation can be used to create a composite foundation in soft fine grained soils. The objectives of the programmes are:-

1. to undertake a critical assessment of the literature on the use of electro osmosis in geotechnical engineering;
2. To introduce the concept of osmotic piles which are created by vertically installed anodes and their part in a composite foundation in which a working platform spreads the load onto the soil reinforced by the osmotic piles;
3. To establish from the literature review the criteria that governs the behaviour of the composite foundation;
4. To design an experiment to determine the relationship between the performance of the composite foundation and applied load using the criteria established from the critical assessment of the literature;
5. To undertake experiments to determine the relationships between the treatment needed to create the osmotic piles and the improvements in the mechanical characteristics of the soft clays.

1.4 THE COMPOSITE FOUNDATION

The composite foundation is a combination of electrically stiffened soil columns with a granular capping layer. This is comparable to a foundation created with stone columns but it avoids the use of primary resources and relies on the intrinsic strength and stiffness of the soil. For those reasons it is considered a sustainable solution.

Electro kinetic vertical drains installed on a grid pattern create a number of stiffened soil columns. The drains acted as electrodes and by passing current between the electrodes it is possible to dewater the soil through a process of osmosis thus increasing the strength and stiffness of the soil. The grid can be varied to determine the optimum array which, with a granular raft to spread the load of the structure onto the soil columns, should produce an economical composite foundation.

1.5 SCOPE OF THESIS

The thesis contains six chapters and seven appendices.

Chapter 2 presents the literature review of Peninsular Malaysia soft clay soils showing the relationship between the distribution of these soils and the built environment; and the principle of electro osmosis and its application to geotechnical engineering.

Chapter 3 describes principles of the experiment used to validate the concept of osmotic piles. A description of the equipment and how it was used are presented.

The experimental results are presented in Chapter 4. It covers the effects of electrode spacing, time of treatment and voltage.

Chapter 5 draws together the results of the tests to make observations of how this technique can be used in ground improvement

Chapter 6 includes a summary of the studies, conclusions and recommendations for future study.

Appendix A summarises in tabulated forms. It briefly describes the soil improvement approaches about its principle, most suitable soils and types, suitable depth that can be installed by certain types, and also discusses its advantages and limitations.

Appendix B and Appendix C describe the range of particle sizes for various soil improvement approaches, and outlines of several of the earlier electro osmotic experiments.

Appendix D compiles of the drawing details for the electro osmotic chamber and certain important parts.

Appendix E describes the summary data for the tested samples under series of time of treatment, numbers and arrangement of electrodes, and different applied voltage. Analyses graphs are presented, i.e., water expelled versus time curves, settlement*area versus water expelled, water expelled and current versus time, and also water content versus distance.

CHAPTER 2

LITERATURE REVIEW

2.1 GENERAL

This thesis describes the potential of using electro osmotic piles in Peninsular Malaysia. The review centres around three major topics; Peninsular Malaysia soft clay soils, electro osmosis piles, and effective and efficient of electro osmosis treatment.

2.2 PENINSULAR MALAYSIAN SOFT CLAY SOIL

In Peninsular Malaysia, soft soil can usually be found along the west coast, i.e., in Johor, Melaka, Port Kelang, Alor Setar and some parts of the east coast, such as Port Kuantan and Terengganu. Soft soil thickness in these areas can reach 40 m in thickness. Figure 2.1 shows the soft deposits distribution in Peninsular Malaysia.

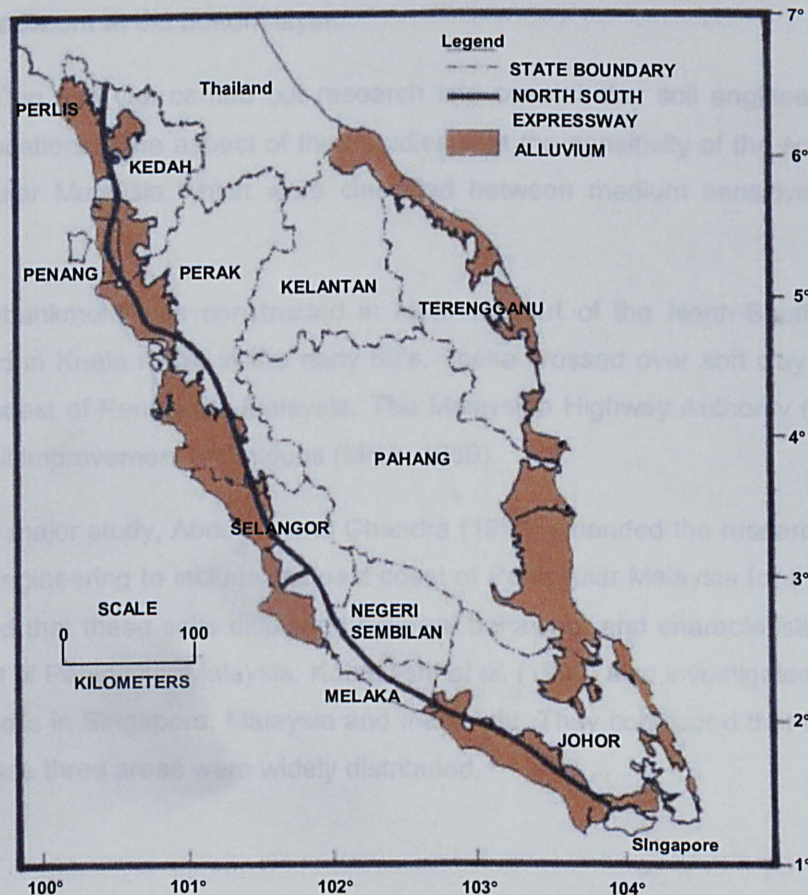


Figure 2.1 Soft deposits distribution in Peninsular Malaysia map (Malaysian Highway Authority, 1989)

Due to industrialisation and drastic urbanisation growth, the majority of future planned construction projects are located on these soft soil deposits. These coastal areas consist of soft soils alluvial sediments which originated during the Cainozoic era. The time scale would probably 1.5 million years ago. This area covers 20% of the Peninsular Malaysia (Aziz, 1993).

Coz (1968, 1970) studied the formation and engineering characteristics of clay soils in East Asia. Most of the primary research works that were carried out on the clay soils in Malaysia were focussed on construction projects. Among these was primary research into the Muda Irrigation Planning in northern part of Peninsular Malaysia. Ledgerwood (1961) investigated geology in the area, whilst Taylor and James (1967) discussed the geotechnical characteristics. Howell (1970) explained the methods used to construct a canal and a dam in these soils.

More detailed studies of soft clay behaviour were carried out by investigating wooden pile installation in soft clay soils in the Prai area (Ting and Chan, 1971). Ting *et al.* (1975) who analysed pile behaviour in a similar area reported at least 6.0 m thick of fine and coarse sand layers separating the soft sediment layers at the upper layer and the hard sediment at the bottom layer.

In 1977, Ting and Ooi carried out research into coastal clay soil engineering at four different locations. One aspect of their studies was the sensitivity of the soft clay soils in Peninsular Malaysia which were classified between medium sensitive and quick types.

A trial embankment was constructed in Muar as part of the North-South Highways project and in Kuala Perlis in the early 80's. These crossed over soft clay soils along the west coast of Peninsular Malaysia. The Malaysian Highway Authority (MHA) used several soil improvement techniques (MHA, 1989).

In another major study, Abdullah and Chandra (1987) extended the research works on soft clay engineering to include the east coast of Peninsular Malaysia for the first time. They found that these soils displayed different behaviour and characteristics from the west coast of Peninsular Malaysia. Kobayashi *et al.* (1990) also investigated the marine soft clay soils in Singapore, Malaysia and Indonesia. They concluded that the soft clay soils in these three areas were widely distributed.

2.2.2 Soft clay definition

In geotechnical engineering, clay soil is a type of soil that contains particles which are less than 2 μm . Clay is formed from the weathering process, hydrothermal activity or through settled sediment. According to the Unified Soil Classification System, clay is a fine material of soil of which 50% weight can pass through a No. 200 or US standard of 0.074 mm sieve. Clay contains clay particles usually in the shape of platelet, when examined under the scanning electron microscope. Normally consolidated clay are usually soft.

Soft clay soil is classified as a soil that has unconfined shear strength between 25 kPa and 50 kPa. It is a fine natural material which produces plasticity characteristics when it is mixed with water, i.e., non-reversible changes of shape when forces are applied. Soft clay soils also have very high water content of over 85%. It has also been found to be sensitive to compression and can easily be disturbed (Brand and Brenner, 1981).

2.2.3 Soft clay soil profiles in Peninsular Malaysia

Abdullah and Chandra (1987) claimed that the soft clay soil thickness varied as shown in Table 2.1. This table shows that the soft clay soil stratum on the west coast has a thickness from 5 m to 35 m whilst on east coast it varies 3 m to 20 m.

**Table 2.1 Soft clay soils thickness in Peninsular Malaysia
(Abdullah and Chandra, 1987)**

Locations		Thickness (m)
Perlis – Kedah	West	5 – 12
Sungai Kedah dam area		8 – 12
Alor Setar airport area		12
Prai area and Pulau Pinang bridge		12 – 25
along the Butterworth – Changkat Jering highways		5 – 15
Sungai Kerian area		10
Bagan Datoh road – Teluk Intan		5 – 11
Port Klang area		8 – 30
Kg. Acheh area – Port Merin	East	3 – 7
West Johor agricultural development projects area		10 – 35
Kuantan area		3 – 20
Sungai Kuantan bridge area		5 – 12
Port Kuantan area		3 – 15
Chukai area		4 – 8
Semerak – Kemasin area		3 – 10

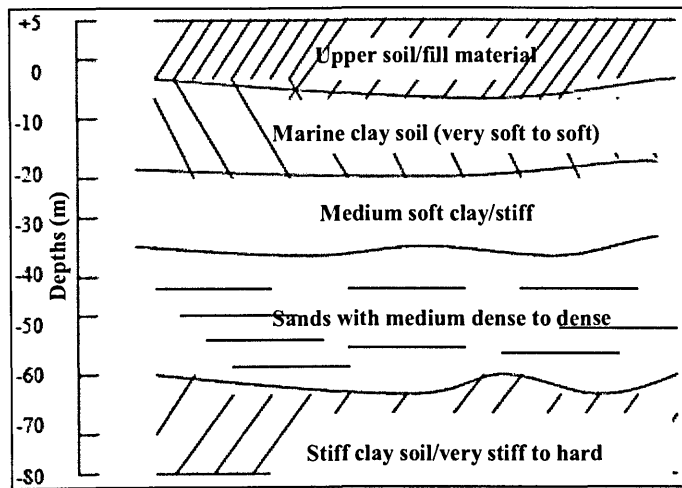


Figure 2.2 Soft clay soils profile in Peninsular Malaysia (Abdullah and Chandra, 1987)

Figure 2.2 shows a typical profile of soft clay in Peninsular Malaysia. The upper layer with thickness of 5 m to 7 m is the upper soil or fill material, and below it there is typically 18 m of soft to very soft marine clay soil. The next layer is medium soft clay or stiff clay which is approximately 15 m thickness. Below that there are 25 m and 20 m of medium dense to dense sands, and stiff clay and very stiff to hard clays.

Soft clay soils are split into upper clay soil and lower clay soil shown in Table 2.2. According to Aziz (1993), the upper and lower soft clay soil layers occurred because of sea level changes in the Pleistocene era. This could be due to weathering. These changes produced thin sand layers which divided those upper and lower soft clay soils. Balasubramaniam *et al.* (1985) concluded that soft clay soils were generally light gray in colour and contained sea shells fragments. Their classification can be seen in Table 2.3.

Table 2.2 Upper and lower depth ranges for west coasts deposits of Peninsular Malaysia (Aziz, 1993)

Locations	Depth Ranges (m)	
	Upper	Lower
Kuala Perlis, Perlis	0 – 6	6 – 9
Alor Setar, Kedah	0 – 9	9 – 16
Prai, Juru, Pulau Pinang	0 – 12	12 – 22
Bagan Datok, Perak	0 – 11	11 – 22
Sabak Bernam, Selangor	0 – 10	10 – 23
Port Klang, Selangor	0 – 11	11 – 20
Muar, Johor	0 – 9	9 – 18
Pontian, Johor	0 – 10	10 – 17

Table 2.3 Upper and lower depth ranges for west coasts deposits of Peninsular Malaysia (Aziz, 1993)

Soil layer	Thickness (m)	Colour	Remarks
Upper ↓	2 – 6	Light grey or light brown	Reclamation sand with shell fragments or upper soil
	10 – 32	Grey greenish or grey	With loose sand layers 2 m to 3 m thick, varying amount of shell and organic matter
	3 – 11	Light brown or brown greyish	With fine sand bands
	4 – 25	Light grey or grey yellowish	Not homogeneous, with medium or stiff clay layer, stiff or very stiff clay stiff layer
Lower	-	Light brown or grey	Varying from peat bands to sandy gravel bands

2.2.4 Problems with soft clay soils

Soft clay is a fine-grained soil which can undergo significant volume changes even with lightly loaded structures. The water content can be greater than the liquid limit. The amount of water that can be held by a soil increases with the clay content in the soil. These clays are strongly influenced by the presence of water due to their high surface activity (Miura and Ngaraj, 2001).

These soils can exhibit extreme variations such as heaving and loss of shear strength and settlement and shrinkage as the water content alters. The presence of organic matter also may increase the water content considerably. However, when a soil contains an appreciable quantity, say 20% or more by weight of material finer than 63 μm size, a description based on water content alone is insufficient. Atterberg's limits are empirical and somewhat arbitrary divisions, in term of water content between states of clay. The water content between the liquid and plastic states is known as the liquid limit. The water content between the plastic limit and semisolid state is the plastic limit. If the water content of natural firm clay is allowed to increase, the clay will soften and become more compressible. The plasticity of such a fine soil has an important effect on engineering properties such as shear strength and compressibility.

Generally, high plasticity clays are more compressible and tend to consolidate more over a period of time under load than clays of low plasticity. Additionally, according to Head (1992), high plasticity clays are more difficult to compact when used as a fill material.

2.2.5 Soil improvement in general

Malaysia has seen rapid economic expansion which requires additional land for housing, building and other related infrastructure in the coastal strip which is underlain by soft clay soil. It has been a normal practice to implement a structural solution using piles, or substitute inappropriate materials, i.e. soft clay soil, with properly compacted fill.

For construction in areas that are distributed with layers of non-engineered soil or natural deposits of inappropriate soils, the common method is to implement a solution with structural support or to eliminate and substitute the inappropriate materials with properly compacted fill. For a case of construction on an embankment, the solution would be partially structural where the positioning of piles are maintained with caps or rafts. The solution with substructural construction is too costly.

Coarse or fine granular materials can be used as a backfill material if the ground water level is below the excavation. Full replacement is appropriate in construction areas where they is a shallow deposit of inappropriate materials. Typically it can be used up to 3 m thick. For exceptional cases, it can be used up to 6 m thick provided the soil shear strength of the side slopes is adequate. In the main, the excavation could be able to retain side slopes of 1:4 in the problematic soils. For thicker layers of problematic soils it is more difficult to retain the stability of side slopes, to handle the soils and prevent the excavation from flooding. There is also the difficulty of disposing of the excavated materials especially in the municipal areas and the cost of imported materials. The viability and cost of this approach is questionable.

Several trials of ground improvement have been successfully implemented in Southeast Asia. They are: vertical drains and dynamic compaction in international airport at Changi, Singapore in 1975; sandwich drains in Bangkok Clay, in Bangkok, Thailand; vacuum consolidation in Bangkok, Thailand; vibro compaction in Pasir Panjang, Singapore; dynamic replacement columns in Kuala Lumpur, Malaysia; stone column in Hong Kong; grouting for a dam in Malaysia, transit system in Singapore, sewerage in Taipei city, and trial tunnel in Kowloon Peninsula; lime stabilisation for an embankment in Thailand and Singapore; electro osmosis in Singapore; reinforced earth for an embankment wall in Hong Kong, retaining wall to a slope in Johor, road embankment wall in Kuala Lumpur and Penang, Malaysia; soil nailing for a transit station in Singapore; and geotextiles for a highways in Singapore, Malaysia and Thailand.

Yee and Ong (2006), Lee *et al.* (1985), and Eggestad (1983) highlighted several characteristics that influence the factors; (1) types of soil and soil states; (2) impact of the construction progression on adjacent structures; (3) environmental aspects; (4) construction period; (5) acceptance after the construction displacement; (6) rate of construction; (7) accessibility of backfill matters; (8) expenditure and maintenance; (9) available equipment; and (10) local practice.

The alternative to excavate and replace the ground or provide a full structural solution is to improve the ground. Soil improvement includes densification, cementation, reinforcement, soil modification or substitution, drainage and other water content controls. An outline of existing methods for improving cohesive soils, can be seen in Table 2.4, and other types of soil improvement approaches can be seen in APPENDIXES A. Table 2.4 is a review of the processes and impact of the methods of improving cohesive soils and the range of soil particle sizes applicable for these soil improvement approaches is displayed in Table 2.5.

Table 2.4 Survey of existing methods for improving cohesive soils (after Eggestad, 1983)

Method	Basic effect				Primary improvement			Curing time days			Equipment size		
	Chemical	Physical	Mechanical	Structural	Bearing capacity	Rate of consolidation	Permeability	0 ~ 10	10 ~ 100	100 ~ 1000	Small	Medium	Large
Columns of stab. soil	●		○	●	●	○		○	●	○		●	○
Columns of pure chemical	○		●		●				●	○	●	○	
Hydraulic injection	●		○		●				●	○	●		
El. chemical injection	●	●			●				●	○	●		
Electro osmosis	○	●			●				●		●		
Freezing		●			○		●		●		○	●	
Heating		●			●			●	○		○	●	
Grouting			●				●	●			●		
Dynamic consolidation			●		●	○	○		●	○		○	●
Preloading			●		●					●	○	●	
Vertical drains			●			●			●	○		●	○
Stone columns			○	●	●	○		●	○			●	○
Embankment piles				●	●			●	○			●	○
Micropiles				●	●			●			●	○	
Nailing				●	●			●			●		
Reinforced earth				●	●	○		●			●		

●: primary; ○: secondary. (1) Chemical effects: chemicals introduced into the soil by mixing, flowing or diffusion, (2) Physical effects: freezing, heating or electric treatment, (3) Mechanical effects: loading, pore pressure release, etc, (4)Structural effects: all kinds of reinforcing elements, (5) Bearing capacity: includes also reduced compressibility, (6) Rate of consolidation: where increasing the rate itself is the objective, (6) Permeability: where an increase or decrease of permeability is the objective, (7) Curing time: the time necessary for a major part of the effect to develop, (7) Small equipment: equipment that can be lifted by a normal building crane, (8) Medium equipment: ordinary self moving construction equipment accessible at most sites, (9)Large equipment: very large or highly specialized equipment.

**Table 2.5 Range of particle sizes for various soil improvement approaches
(reproduced from Hausmann, 1990, Lee *et al.*, 1985)**

Gravel	Sand	Silt	Clay
Particulate grouting			
Vibratory rollers			
Vibrofloatation			
Compaction piles			
Chemical grouting			
Dynamic compaction			
Sand compaction piles, Jet grouting			
Terraprobe			
Blasting			
Compaction grout			
Stone columns			
Preloading, Surcharge fills			
Lime stabilisation			
Electro kinetic injection			
Electro osmosis			

Table 2.4 shows that almost all of the methods of improvement increase the bearing capacity as a primary improvement. Table 2.5 shows that the electro osmosis method can be apply within silt and clay particle sizes. There are other types of improvement for these soils including preloading, surcharge fills, lime stabilisation, electro kinetic injection, stone columns, compaction grout, and sand compaction piles and jet grouting.

Although there are various types of soil improvement methods available the research is particularly interested in electro osmosis because there a lack of expertise regarding this type of improvement and it has not been implemented in any construction in Malaysia.

Hence, the scope of this study is to implement electro osmosis to stiffen soft clay soils which alters them from normally consolidated clays to overconsolidated clays leading to an increase in stiffness. Electro osmosis primarily affects its physical characteristics; chemical effects are secondary (Table 2.4). It only requires 10 days to 100 days to function and limited equipment size for installation purposes.

2.3 ELECTRO KINETIC OCCURRENCE IN CLAYS

Mitchell (1993) states that clay particles are crystalline particles. Das (1999) states those clays minerals are principally hydrous alumina silicates. Mitchell (1993) notes that, for clay minerals, there is link between the clay mineralogical composition and the engineering properties. The clay particle surfaces are negatively charged due to replacement of isomorphous and the existence of fragmented bonds. Lambe (1958), through his studies on Guoy-Chapman theory, showed that when clay particles were in water, the adsorbed cations and the diffuse double layer on a surface will produce neutrality electrical. The established distribution for adjoining ions to a negatively charged clay particles is illustrated in Figure 2.3. In 1993, Mitchell maintained that the electro kinetic property for a mineral in the main is governed by a diffuse double layers structure on a wet clay surface.

Electro kinetics describes the behaviour of fluid and particles in an electric field. An external force acts on the double layer to generate movement. Electro kinetics includes electro osmosis, the movement of water; which is the most interesting for ground improvement as it can lead to a reduction in water content and hence an increase in stiffness.

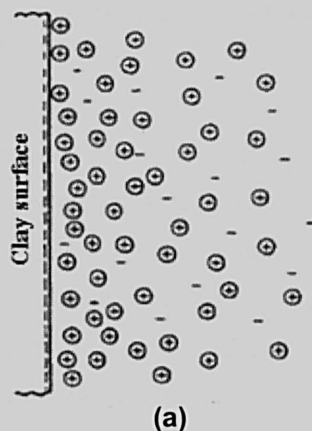


Figure 2.3 Variation of electrical potential with distance from a charged surface (reproduced from Mitchell, 1993)

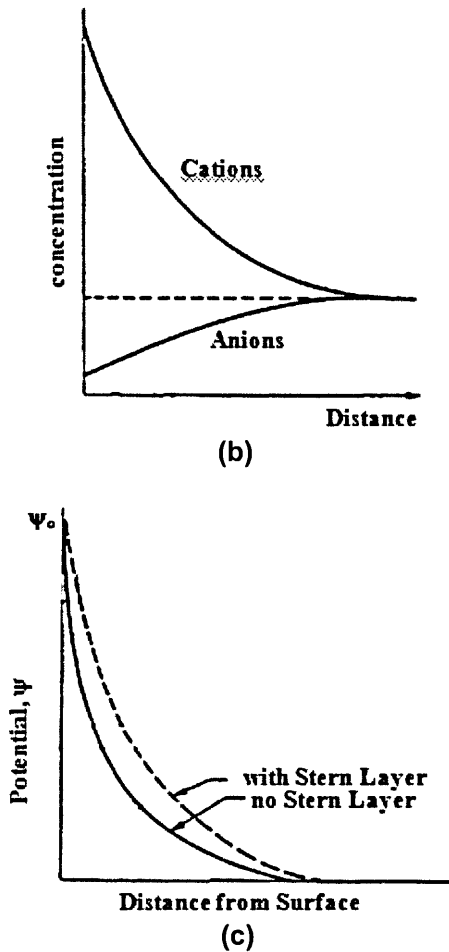


Figure 2.3 Variation of electrical potential with distance from a charged surface (reproduced from Mitchell, 1993)

Figure 2.3(a) shows the distribution of cations and anions near to the surface of a clay particle. The concentration decreases with distance from the surface (Figure 2.3(b)). The Stern Layer is the term for those positively charged ions immediately adjacent to the clay surface (Figure 2.4). There is a gradual increase in the number of negatively charged ions with distance from the surface of the clay particle through the diffuse layer. Thus there is a drop in potential with distance from the surface of the clay particle (Figure 2.3c). The Stern Layer, predicted from the Guoy-Chapman theory, contributes to the inter particle repulsion (Mitchell, 1993). The Stern Layer remains attached to the clay particle; the diffuse layer is mobile thus forming a slip plane at the boundary with the Stern Layer. The potential at the slip plane governs the movement of the ions in the diffuse layer.

Figure 2.4 is a combination of the figures in Figure 2.3. It shows that the double layer structure on the surface of the clay particles is separated from the diffuse layer by the

Stern layer. The diffuse layer is a layer of free ions which move in the fluid under the influence of electric attraction.

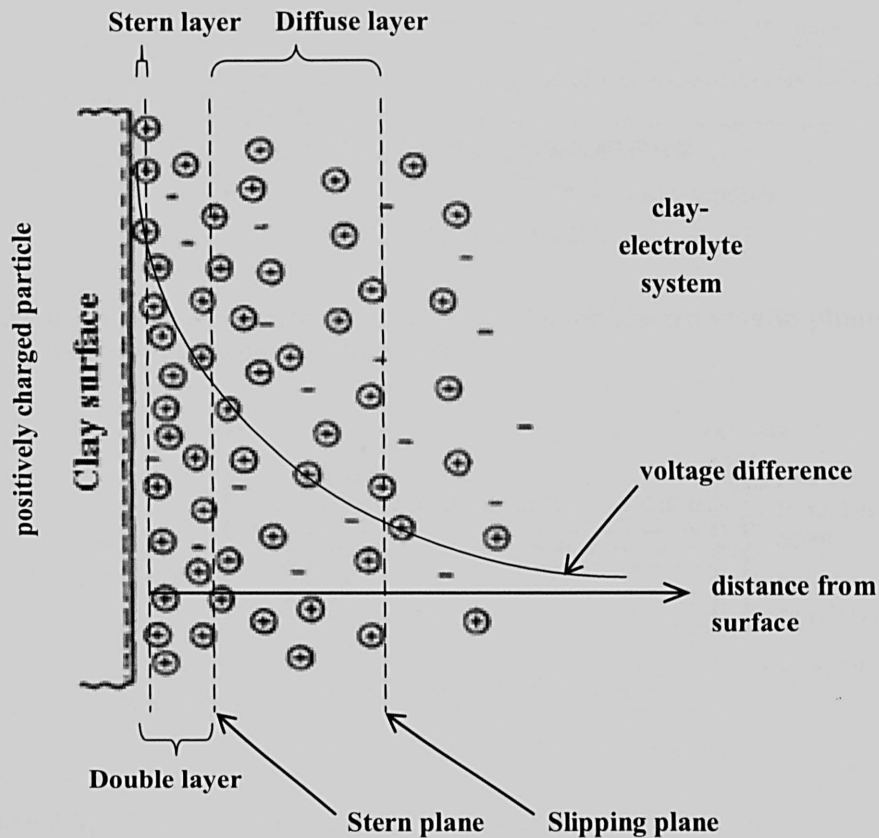


Figure 2.4 Double layer structures near the surface of the positively charged particles

The double layer leads to an electrically charged surface. This electrically charged surface then creates an electrostatic field, which affects the ions in the clay-electrolyte-system. By combining the thermal motion of the ion, the electrostatic field and thermal motion will develop a counter charge. This counter charge produces a net electric charge similar in magnitude to the net surface charge. However, the net electric charge has the opposite polarity to the net surface charge. As a result, the whole system is electrically neutral, where the cations and anions curves overlapped at some point far from the clay surface. This can be seen in Figure 2.3(b)..

If a voltage difference is applied across two adjacent clay particles, then the negative ions move towards the positive terminal (+) and positive ions towards the negative terminal (-). This can be seen in Figure 2.5. These two figures explain the movement of

water, noted as velocity distribution, from the positive terminal to the negative terminal through the wall capillary.

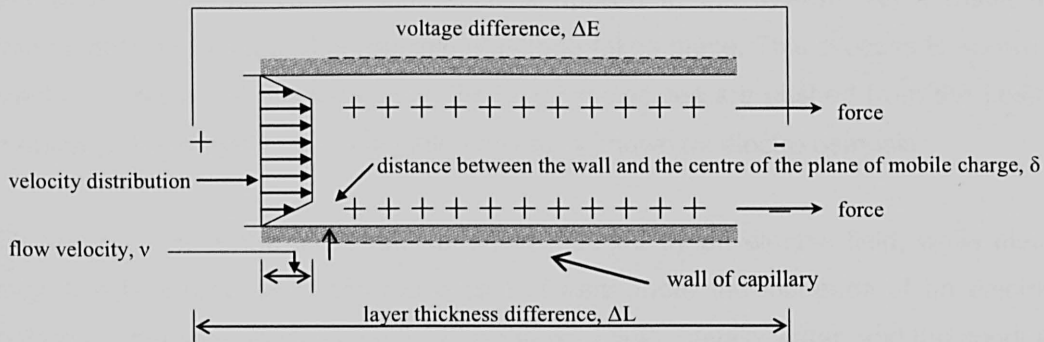


Figure 2.5(a) Helmholtz-Smoluchowski model for electro kinetic phenomena (reproduced from Mitchell, 1993)

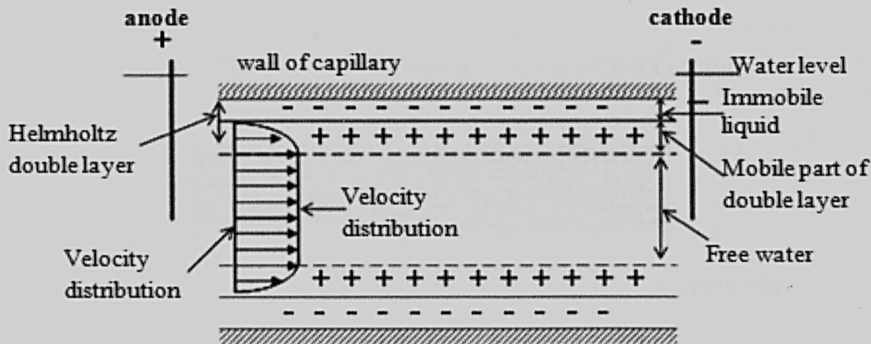


Figure 2.5(b) Electro osmotic flow in rigid-straight capillaries (reproduced from Casagrande, 1952b)

The discovery regarding the movement of water molecules with the presence of voltage difference was made by Reuss in 1807 and Helmholtz in 1879 (Mitchell, 1993, and Casagrande, 1952(b)). Reuss discovered that the water molecules moved through the capillaries towards the negative terminal with the application of voltage differences. Voltage difference marked ΔE in Figure 2.5(a) and the transportation of water molecules is via the mobile part of double layer in Figure 2.5(b). In Figure 2.5(b), Casagrande (1952(b)) labelled the mobile part of the double layer as the Helmholtz double layer. The idea of this double layer named after Helmholtz was from Helmholtz's theory which was an improvement on Reuss's theory of 1879. The detail of this mathematical model is described in Mitchell (1993).

The double layer lies between the wall of the capillary and free water. There are two parts to this layer. Adjacent to the wall of the capillary, there is a very thin layer which is the Stern layer. This very thin layer labelled as water immobile liquid on Figure 2.5b

negatively charged. The other layer within the double layer, or the thicker layer is known as the mobile part of the double layer. This thicker zone of double layer is developed when the voltage difference is applied to the system. As a result, the transportation of ions to the opposite electrode takes place. This process is known as electro migration. At the same time the water molecules are pushed from the positive terminal to the negative terminal, this process is known as electro osmosis.

Electro osmosis is the movement of liquid induced by an electric field, while electro migration is a process of the movement of ions under the influence of an electrical potential difference. In clays the liquid is the pore fluid, usually water, and the conduit is the connected pore space between the particles. This Stern layer, as can be seen in Figure 2.4, only exists with the presence of a voltage difference (Mitchell, 1993, and Casagrande, 1952(b)).

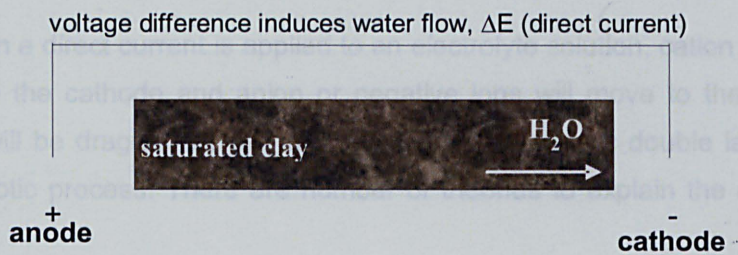


Figure 2.6 Electro osmosis (reproduced from Mitchell, 1993)

The voltage difference, as can be seen in Figure 2.6, creates electro osmosis flow as water moves from the positive terminal to the negative terminal. The velocity distribution of the free water, as in Figure 2.5, is constant. Two factors contribute to this constant rate. The first one is due to the cylinder of free water within the system. The second factor is due to the electro migration process; that is the transportation of ions to the opposite terminal (Figure 2.5). Electro migration means the movement of charged particles like clay is relative to its concentration, as an example during gravitational settlement. The effect it produces is a potential difference. This is due to viscous drag from water which retards the movement.

There are three other processes taking place in addition to electro osmosis and electro migration. There are the streaming potential, electrophoresis and sedimentation potential and Table 2.6 summarises the definitions of these three terms.

Table 2.6 Streaming potential, electrophoresis and sedimentation

definitions (reproduced from Mitchell, 1993)

Terms	Definitions
Streaming potential	The difference in electric potential between a diaphragm, capillary, or porous solid and a liquid that is forced to flow through it
Electrophoresis	The migration of charged colloidal particles or molecules through a solution under the influence of an applied electric field usually provided by immersed electrodes
Sedimentation	The process of depositing sediment

2.4 ELECTRO OSMOSIS

2.4.1 The theory of electro osmosis

When a direct current is applied to an electrolyte solution, cation or positive ions will move to the cathode and anion or negative ions will move to the anode. Water molecules will be dragged by the ions moving in the electric double layer due to the electro osmotic process. There are number of theories to explain the electro osmotic phenomena.

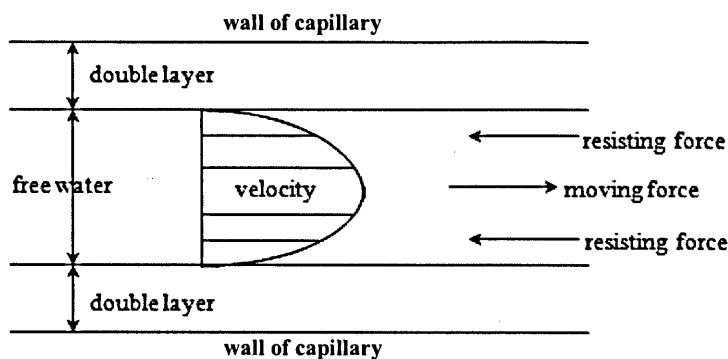


Figure 2.7 Hydraulic flows in a capillary (reproduced from Casagrande, 1952(b))

Figure 2.7, based on Figure 2.5, shows a simple interpretation of the electro osmotic flow of water. The Helmholtz-Smoluchowski's theory states that the rate of water flow caused by electro osmosis is governed by the electrical forces which results in the motion of water and the friction due to the double layer. Therefore, the velocity is given by:

$$v = \frac{\varepsilon \zeta}{\eta} \frac{dV}{dL} \quad (2.1)$$

where:

$\frac{dV}{dL}$ = electric field, or known as voltage gradient, unit in V/m;

ζ = potential across the capillary, or known as zeta potential, unit in V;

ε = permittivity of fluid, unit in F/m; and

η = fluid viscosity, unit in Ns/m².

Note that typical units are given. As Mitchell (1993) states: "for most cases in clay, the values of ζ are in the range of 0 mV to 50 mV and the charge of the mobile ions is positive, plus the lowest values are associated with excessive pore water salt concentrations". For a single capillary for area of $a = \pi r^2$, where r is the radius of the capillary. The flow rate, q_a , is:

$$q_a = va = \frac{\varepsilon \zeta}{\eta} \frac{dV}{dL} a \quad (2.2)$$

where:

q_a = capillary of flow rate, unit in V/m per m²; and

a = area, unit in m².

For a bunch of N capillaries of radius, r^2 within the total of cross-section area, A (m²), grossly normal to the flow direction, the total volume flow rate, Q would be:

$$Q = Nq_a = vN\pi r^2 = \frac{\varepsilon \zeta}{\eta} \frac{dV}{dL} N\pi r^2 \quad (2.3)$$

where:

Q = total volume flow rate, unit in m³/s; and

N = number of capillaries, non dimensional.

In a porous medium, the cross-sectional area of a void is nA , which must be equivalent to $N\pi r^2$, consequently equation (2.3) be converts into equation (2.4):

$$Q = \frac{\varepsilon \zeta}{\eta} \frac{dV}{dL} \eta A \quad (2.4)$$

Casagrande suggests: "by analogy with Darcy's law, the relationship between the volume flow rate, Q , and the imposed gradient $\frac{dV}{dL}$, for a porous medium defined in equation (2.4) may be re-defined as (Casagrande, 1952b: 289; 1949: 161):

$$Q = k_e \frac{dV}{dL} A \quad (2.5)$$

where:

k_e = coefficient of electro osmotic permeability, unit in m^2/Vs ; and

A = gross total cross-sectional area normal to the direction of flow, unit in m^2 .

The coefficient of electro osmotic conductivity, k_e , is a characteristic of a porous medium, and is the average linear hydraulic flow velocity under a unit voltage gradient (Mitchell, 1993). It resembles the hydraulic conductivity which is an average linear hydraulic flow velocity under a unit of hydraulic gradient. The coefficient of electro osmotic conductivity, k_e , for Helmholtz-Smoluchowski's model is:

$$k_e = \frac{\epsilon \zeta \eta}{\eta} \quad (2.6)$$

The coefficient of electro osmotic conductivity, k_e , is not dependent on the pore size. This is unlike the coefficient of hydraulic conductivity, k . k_e depends on the zeta potential, ζ . The zeta potential has a very low value, and effects k_e , the k_e frequently reacts actively in the pore fluid if the pore fluid contains a very high salt concentration (Mitchell, 1993). Numerous researchers have studied electrokinetic reactions with various types of soils to resolve the k_e value. Table 2.7 summarises the published data. It shows that for most soils k_e varies between $1 \times 10^{-5} \text{ cm}^2/sV$ and $1 \times 10^{-4} \text{ cm}^2/sV$. The value of $5 \times 10^{-5} \text{ cm}^2/sV$ was put forward by Casagrande (1952b) as a typical value for all soils. According to Mitchell: "measurement of k_e is made by determination of the flow rate of water through a soil sample of known length and cross section under a known electrical gradient" (Mitchell, 1993).

Table 2.7 Coefficients of electro osmotic permeability, k_e

No	Researcher and Materials	w_c (%)	k_e in 10^{-4} (cm^2/sV)	k_h (cm/s)*
Mohamedelhassan (1998)				
	Marine Sediment, Korea	65.5 ~ 127	0.3373 ~ 0.6289	5.28×10^{-8} ~ 3.44×10^{-7}
		81.3 ~ 142.7	0.6118 ~ 0.8082	6.118×10^{-7} ~ 8.082×10^{-7}
		80.9 ~ 143	0.4822 ~ 0.6591	1.63×10^{-7} ~ 4.11×10^{-7}

Shang (1997b,c)			
Brown Clay, Timmons, ON	61.0	0.286	-
Shang (1997b); and Shang and Lo (1997)			
Phosphatic Clay, Florida	244.8	0.07	-
Segall and Bruell (1992)			
Kaolinite	-	1.20	3×10^{-8}
Silt	-	0.448	6×10^{-5}
Sandy Clay	-	0.18	5×10^{-8}
Clayey Silt	-	0.43 ~ 0.47	$1.8 \times 10^{-6} \sim 1.3 \times 10^{-5}$
Hamir (1997)			
Kaolin Grade E	82.0	0.12 ~ 0.37	$2.3 \times 10^{-7} \sim 4.4 \times 10^{-7}$
Bjerrum <i>et al.</i> (1967)			
Ås Quick Clay	31.0	2.0 ~ 0.25	2×10^{-8}
Fetzer (1967)			
Silty Clay, West Branch Dam	32.0	0.3 ~ 0.6	$1.2 \times 10^{-8} \sim 6.5 \times 10^{-8}$
Gray and Mitchell (1967)			
Kaolinite	73.7	0.94	9.4×10^{-7}
	61.7	0.81	8.1×10^{-7}
	52.2	0.67	6.7×10^{-7}
	42.7	0.54	8.3×10^{-3}
Silty Clay	50.1	0.35	6.55×10^{-7}
	41.9	0.28	3.71×10^{-7}
	32.0	0.20	1.81×10^{-7}

*: approximate; - : no experimental work has been carried out.

Table 2.7 Coefficients of electro osmotic permeability, k_e

No	Researcher and Materials	w_c (%)	k_e in 10^{-4} (cm ² /sV)	k_h (cm/s)*
Gray and Mitchell (1967)				
	Illitic Clay	102.0	0.85	6.12×10^{-7}
		84.0	0.56	1.27×10^{-7}
		59.1	0.29	2.7×10^{-8}
		98.0	0.73	-
		78.6	0.50	1.49×10^{-7}
		56.6	0.38	3.40×10^{-8}
Casagrande <i>et al.</i> (1961)				

Clayey Silt, Little Pic, River, ON	26.0	0.15	2×10^{-5}
Ballou (1955)			
Na-Kaolinite	92	1.14	1.41×10^{-6}
	57	0.94	3.5×10^{-7}
	41	0.82	1.21×10^{-7}
Casagrande (1952b)			
London Clay	52.3	0.58	1×10^{-8}
Boston Blue Clay	50.8	0.51	1×10^{-8}
Commercial Kaolin	67.7	0.57	1×10^{-7}
Clayey Silt (England)	31.7	0.50	1×10^{-6}
Rock Flour (Hartwick, N.Y.)	27.2	0.45	1×10^{-7}
Na-Bentonite	170.0	0.20	1×10^{-9}
Na-Bentonite	2000.0	1.20	1×10^{-8}
Mica Powder	49.7	0.69	1×10^{-5}
Fine Sand	26.0	0.41	1×10^{-4}
Quartz Powder	23.5	0.43	1×10^{-4}

*: approximate; - : no experimental has been carried out.

Figure 2.8 shows a correlation between electro osmotic conductivity, k_e , and coefficient of hydraulic conductivity, k_h , using data from Table 2.6. The graph shows that there is no significant correlation indicating that the two coefficients are dependent on different factors.

Mitchell (1993) states that the relationship between osmotic conductivity and hydraulic conductivity is that the hydraulic head difference in 1 cm per unit water needed in a system is the same as 1 unit of flow of rate in an osmotic flow. Osmotic flow is affected by salt concentration, in the ratio of 1:10, thus whenever the salt concentration increase, the flow rate will decrease 10 times. The same effect also occurs with hydraulic conductivity, where increase in salt concentration, will increase in hydraulic conductivity in the ratio of 10.

Where else in the relationship between electro osmotic conductivity and hydraulic conductivity, the head difference is needed for balance. In determining the head difference for the hydraulic conductivity, the head difference can be compared to salt concentration. This balance is effected by the difference in value of 1 Volts in the electrical potential positioned at the opposing layered part. During the consolidation process, the hydraulic conductivity is reduced gradually. However, the ratio between osmotic conductivity and hydraulic conductivity increases significantly. This shows that osmotic flow and electro osmosis is relative to the increase in total flow.

According to Mitchell (1993), the relationship between osmotic conductivity and hydraulic conductivity was based on a study using a kaolinite sample. Kaolin is capable of providing an accurate average estimate of the electro osmotic and osmotic flow. This is due to the coupling effect in kaolinite is usually smaller in comparison to active clay.

In a system which contains confined layered clay that reacts to electric chemical gradient, Darcy's rule may not be effective in estimating rate of hydraulic flow, especially if the clay contains high plasticity clays. This situation is common with clay which are placed in a very deep layer, clay shales and densely compacted clays.

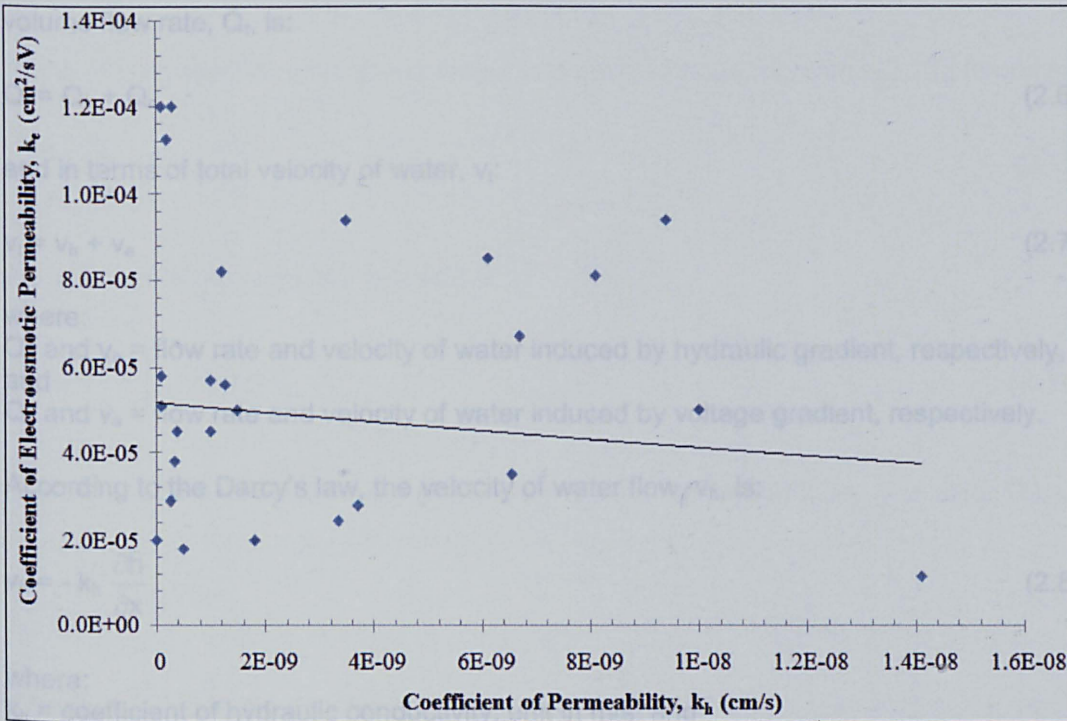


Figure 2.8 k_e vs k_h for impervious type of drainage

2.4.2 Consolidation via electro osmosis

2.4.2.1 Excess pore water pressure production and consolidation by electro osmosis

Applying a direct electric current between two electrodes inserted into a clay soil creates a difference in potential between the electrodes. The electro osmotic process drags water to the negative terminal from the positive terminal. Water is expelled via the negative terminal, and if the positive terminal is closed, the water is not replaced. As a result, consolidation between these two terminals takes place. As water is dragged from the positive terminal, most consolidation occurs at the positive terminal and none at the negative terminal. The total stress, σ , in the system remains constant but the effective stress increases at the positive terminal because of the reduction in pore pressure caused by electro osmosis. The effective stress remains the same at the negative terminal if it is open.

The voltage difference in the system causes a difference in hydraulic potential. This state continues until the system reaches a balance where the electro osmotic force driving water to the cathode is equal to reverse flow due to the hydraulic gradient.

For one dimensional flow induced with electrical and hydraulic gradients, the total volume flow rate, Q_t , is:

$$Q_t = Q_h + Q_e \quad (2.6)$$

and in terms of total velocity of water, v_t :

$$v_t = v_h + v_e \quad (2.7)$$

where:

Q_h and v_h = flow rate and velocity of water induced by hydraulic gradient, respectively, and

Q_e and v_e = flow rate and velocity of water induced by voltage gradient, respectively.

According to the Darcy's law, the velocity of water flow, v_h , is:

$$v_h = -k_h \frac{\partial h}{\partial x} \quad (2.8)$$

where:

k_h = coefficient of hydraulic conductivity, unit in m/s; and

h = total hydraulic head, unit in m.

The velocity of the water due to the electrical potential depends on the voltage gradient, $\frac{\partial V}{\partial x}$. Hence,

$$v_e = -k_e \frac{\partial V}{\partial x} \quad (2.9)$$

Thus, from the equation (2.7):

$$v_t = -k_h \frac{\partial V}{\partial x} - k_e \frac{\partial h}{\partial x} \quad (2.10)$$

Darcy's equation, equation (2.8), in a term of excess pressure is (Terzhagi *et al.*, 1996):

$$v_h = \frac{k_h}{\gamma_w} \frac{\partial u}{\partial x} \quad (2.11)$$

where:

γ_w = unit weight of water, unit in kN/m³; and

u = pore water pressure, unit in kN/m^2 .

Placing equation (2.11) into equation (2.10), will generate:

$$v_t = - \frac{k_h}{\gamma_w} \frac{\partial u}{\partial x} - k_e \frac{\partial V}{\partial x} \quad (2.12)$$

At the of consolidation with closed anode and open cathode, equation (2.12), becomes:

$$- \frac{k_h}{\gamma_w} \frac{\partial u}{\partial x} = - k_e \frac{\partial V}{\partial x} \quad (2.13)$$

Thus, the pore pressure at the anode is:

$$u = - \left(\frac{k_e}{k_h} \right) \gamma_w V(x) + C \quad (2.14)$$

At $x = 0$ m at the cathode; $V(x) = 0$ V and $u = 0$ kN/m^3 at the cathode, C is zero. Thus,

$$u = - \left(\frac{k_e}{k_h} \right) \gamma_w V(x) \quad (2.15)$$

Equation (2.15) is the negative pore pressure created by electro osmosis at the end of the consolidation process. The magnitude of negative pore pressure depends on the proportion of $\left(\frac{k_e}{k_h} \right)$ and applied voltage. The negative pore pressure induced will be higher in a soil with a low hydraulic conductivity.

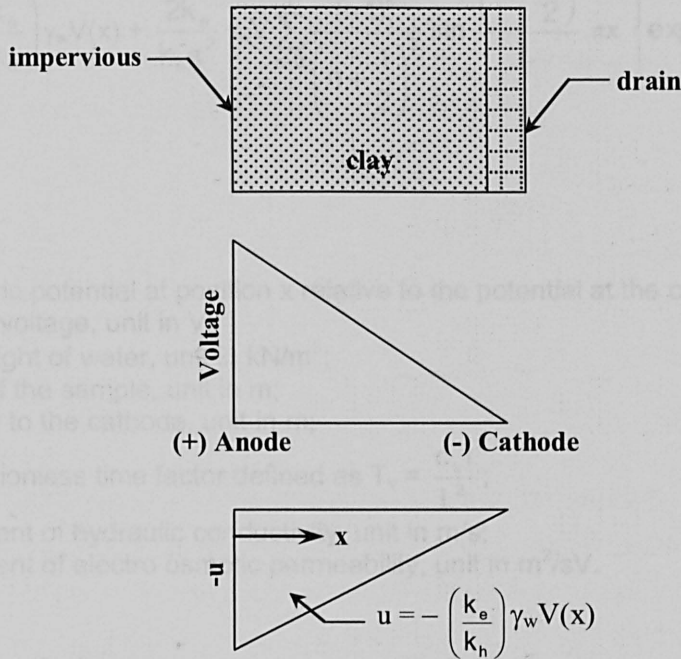


Figure 2.9 Pore water pressure induced at balance for the case of open cathode and closed anode (reproduced from Mitchell, 1993)

Terzaghi's equation for consolidation also applies to electro osmotic consolidation for a constant voltage gradient setting in motion the dummy variable, ξ .

$$\frac{\partial^2 \xi}{\partial x^2} = \frac{1}{c_v} \frac{\partial \xi}{\partial t} \quad (2.16)$$

where Esrig (1968) found out that:

$$\xi = u + \left(\frac{k_e}{k_h} \right) \gamma_w V(x); \text{ and } c_v = \frac{k_h}{\gamma_w m_v} \text{ known as Terzaghi's coefficient of consolidation.}$$

Therefore, the one dimensional consolidation equation induced by an imposed electric field (Esrig, 1968):

$$\frac{\partial^2 u}{\partial x^2} + \left(\frac{k_e}{k_h} \right) \gamma_w \frac{\partial^2 V}{\partial x^2} = \frac{1}{c_v} \frac{\partial \xi}{\partial t} \quad (2.17)$$

u and V are shown in Figure 2.9.

For a closed system at the anode and open at the cathode, the pore pressure, $u(x,t)$ in a unit of kN/m^2 , at the point x within the soil sample at time, t , is:

$$u(x,t) = - \left(\frac{k_e}{k_h} \right) \gamma_w V(x) + \frac{2k_e}{k_h \pi^2} \gamma_w V \sum_{n=0}^{\infty} \frac{(-1)^n}{\left(n + \frac{1}{2} \right)^2} \sin \frac{\left(n + \frac{1}{2} \right) \pi x}{L} \left\{ \exp \left[- \left(n + \frac{1}{2} \right)^2 \pi^2 T_v \right] \right\} \quad (2.18)$$

where:

$V(x)$ = electric potential at position x relative to the potential at the cathode at $x = 0$ (V);

V = applied voltage, unit in V;

γ_w = unit weight of water, unit in kN/m³;

L = length of the sample, unit in m;

x = distance to the cathode, unit in m;

T_v = dimensionless time factor defined as $T_v = \frac{c_v t}{L^2}$;

k_h = coefficient of hydraulic conductivity, unit in m/s;

k_e = coefficient of electro osmotic permeability, unit in m²/sV.

This equation (2.18), at time, t , moves towards the limit,

$$u(x,\infty) = - \left(\frac{k_e}{k_h} \right) \gamma_w V(x) \quad (2.19)$$

This equation (2.19), shows the distribution of induced pore water pressure in the soil during the treatment.

2.3.2.2 Combined electro osmosis and external load induced consolidation

Wan and Mitchell (1976) investigated combining consolidation due to voltage and hydraulic gradients. They assumed that k_e , k_h and m_v were constant. Wan and Mitchell (1976) contemplated the case when the excess pore water pressure was induced in a soil mass by direct loading, and the soil consolidation started before the electrical field was generated. Electro osmosis accelerates the dissipation of excess pore water pressure.

Boundary states ($0 < t < \infty$) where at the open cathode ($x = 0$)($u = 0$); and

at the closed anode ($x = L$), $v_t = |_{x=L} = 0$ or $\frac{\partial u}{\partial x} = |_{x=L} = \frac{V_e \gamma_w}{k_h}$ from equation (2.7) and

equation (2.13).

Initial value of pore pressure at the start of electro osmosis, where $t = 0$;

$$u_i(x) = u_0 \quad (2.20)$$

where:

u_i = initial positive excess pore water pressure induced by direct loading.

Wan and Mitchell in 1976 have stated where the clarification from equation (2.16) for the boundary and preliminary conditions given earlier is:

$$u = \frac{v_e \gamma_w X}{k_h} + \sum_{n=0}^{\infty} \frac{2}{\left(n + \frac{1}{2}\right)\pi} \left[u_o - \frac{(-1)^n}{\left(n + \frac{1}{2}\right)\pi} \left(\frac{v_e \gamma_w X}{k_h} \right) \right] \left\{ \frac{\sin\left(n + \frac{1}{2}\right)\pi}{L} \exp\left[-\left(n + \frac{1}{2}\right)^2 \pi^2 T_v\right] \right\}$$

(2.21)

Applying equation (2.21), between the anode and the cathode and at various time intervals, the distribution of excess pore water pressure can be seen in Figures 2.10 until 2.12. All of these figures are used to determine the excess pore water pressure for

different ratios, $r = \frac{u_a}{u_o}$. Plus, $u_a = -\left(\frac{k_e}{k_h}\right) \gamma_w V(x)$ as an equilibrium negative excess pore

water pressure at the anode is generated. The final pore pressure distribution is zero at the cathode and varies linearly to a maximum excess negative pore water pressure (Wan and Mitchell, 1976) at the anode. The solution for the average pore water pressure is displayed in Figure 2.13.

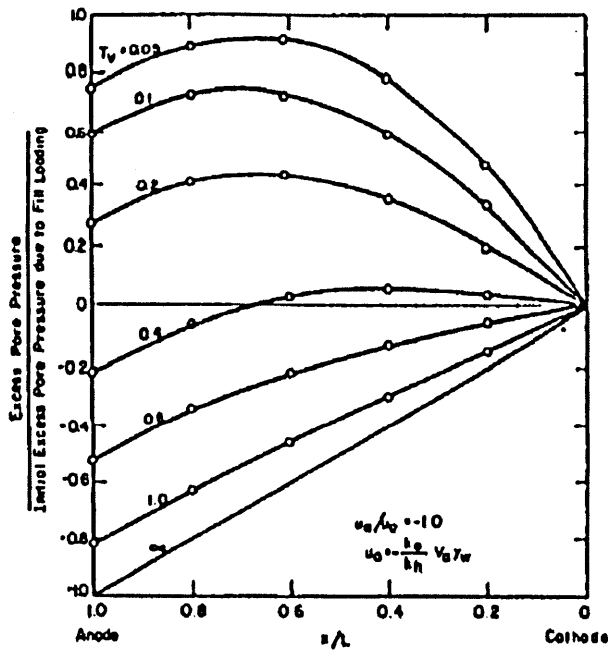


Figure 2.10 Pore pressure distributions – electro osmotic consolidation superimposed on direct loading consolidation: $u_a/u_o = -1.0$ (after Wan and Mitchell, 1976)

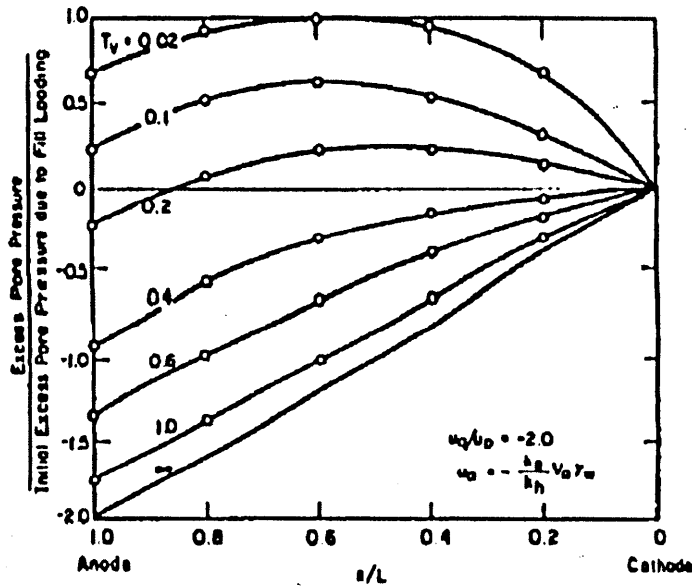


Figure 2.11 Pore pressure distributions – electro osmotic consolidation superimposed on direct loading consolidation: $u_a/u_o = -2.0$ (after Wan and Mitchell, 1976)

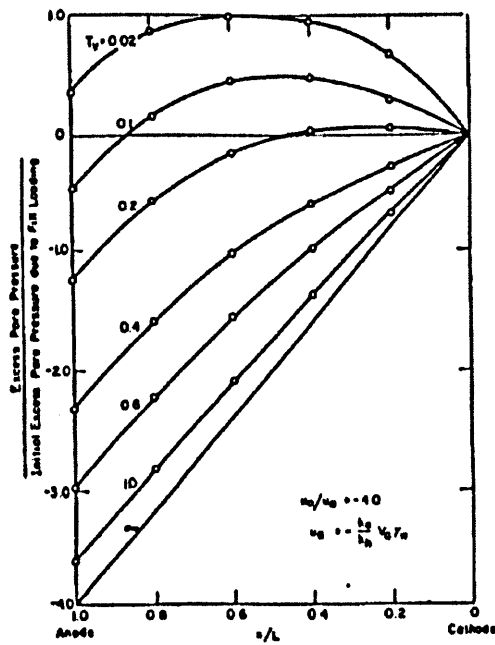


Figure 2.12 Pore pressure distributions – electro osmotic consolidation superimposed on direct loading consolidation: $u_a/u_o = -4.0$ (after Wan and Mitchell, 1976)

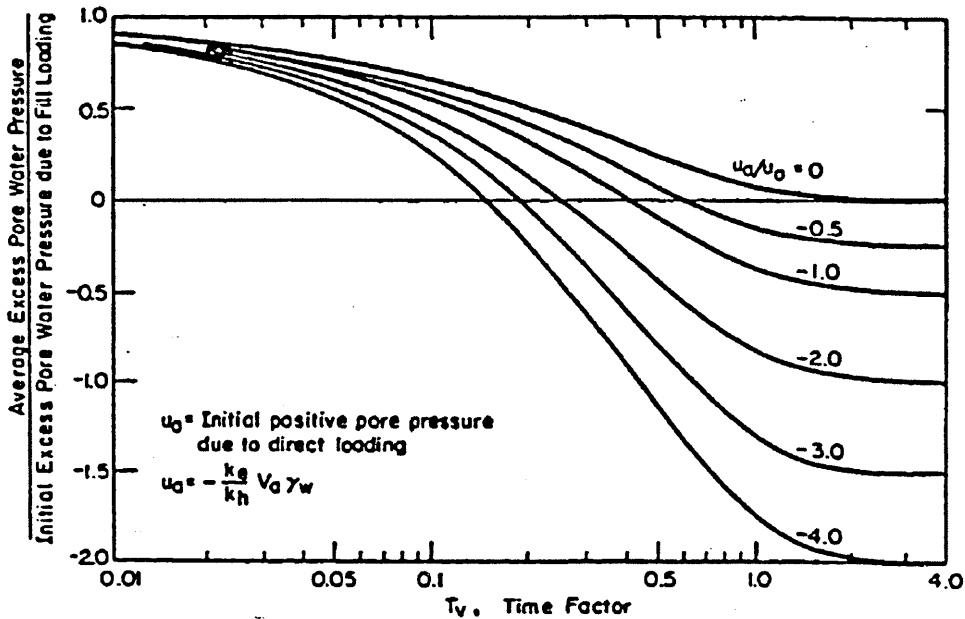


Figure 2.13 Average pore water pressure versus time factor during electro osmotic superimposed on direct loading consolidation (after Wan and Mitchell, 1976)

This electro osmotic process stops when $T_v = T_{v_0}$. The comparable height of surcharge, H_s to create the same effect as electro osmosis is (Wan and Mitchell, 1976):

$$H_s = \frac{\gamma_w}{\gamma_s} H_e \quad (2.22)$$

where:

γ_s = unit weight of the surcharge, unit in N/m^3 ; and

H_e = negative pore water head generated by electro osmosis at $x = L/2$ and expressed

$$\text{as } H_e = - \frac{\bar{v}k_e}{k_h}, \text{ unit in m.}$$

By applying equation (2.21), the degree of consolidation, U , at the beginning when $u_i(x) = u_0$, is (Wan and Mitchell, 1976):

$$U = \frac{1}{1 - \frac{r}{2}} \left(1 - \left[\frac{r}{2} + \sum_{n=0}^{\infty} \frac{2}{\left(n + \frac{1}{2}\right)^2 \pi^2} \left[1 - \frac{(-1)^n}{\left(n + \frac{1}{2}\right)^2 \pi} \exp \left[- \left(n + \frac{1}{2}\right)^2 \pi^2 T_v \right] \right] \right) \right) \quad (2.23)$$

where:

$$r = \frac{u_a}{u_0}$$

Figure 2.14 shows equation (2.23) for different values of $r = u_a/u_0$. In addition, this value highlights that in this case the correlation among the degree of consolidation and time factor depends on both initial excess pore water pressure and the voltage.

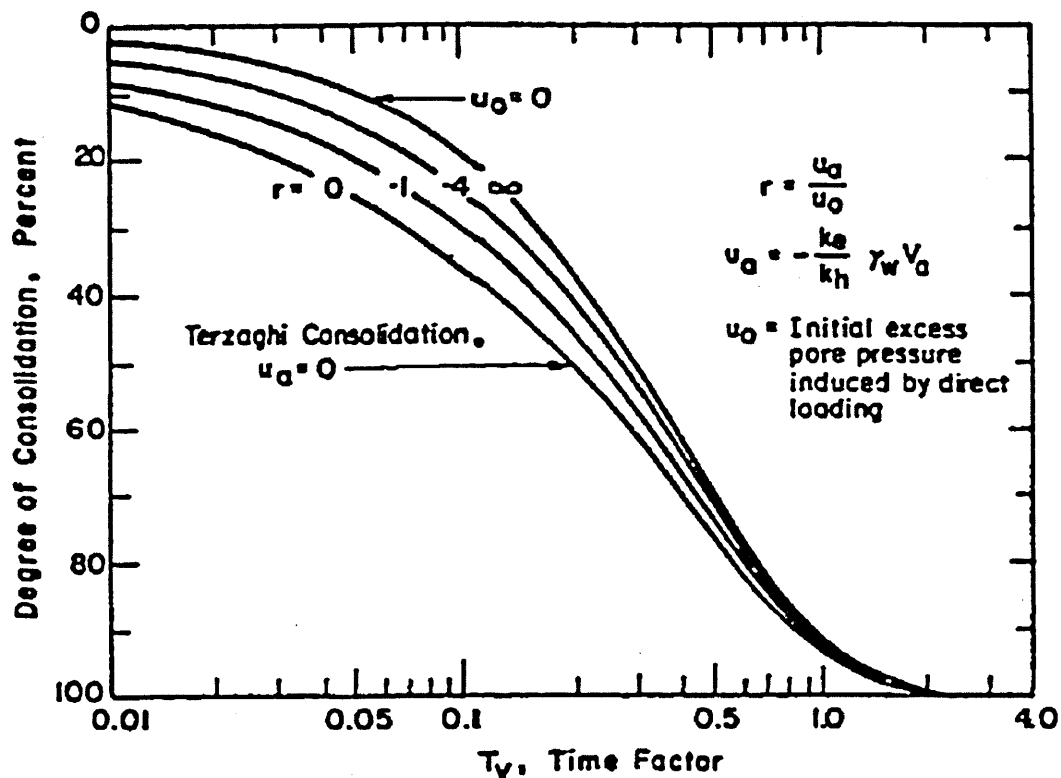


Figure 2.14 Degree of consolidation versus time factor for merged electro osmosis and direct loading (after Wan and Mitchell, 1976)

Wan and Mitchell (1976) carried out a series of laboratory tests to show that this assumption was correct. Fully saturated samples of remoulded kaolin with dimensions of 60 mm x 200 mm x 200 mm were used. The sample was initially consolidated to an effective vertical pressure of 686.7 kPa and then allowed to swell under a pressure at 49 kPa. This produced an overconsolidated specimen which meant that the assumption that k_h , k_e and m_v were constant would be valid. Figure 2.15 shows the dissipation of excess pore pressures with a vertical stress of 98 kPa.

A voltage gradient of 75 V/m was then applied across the sample.

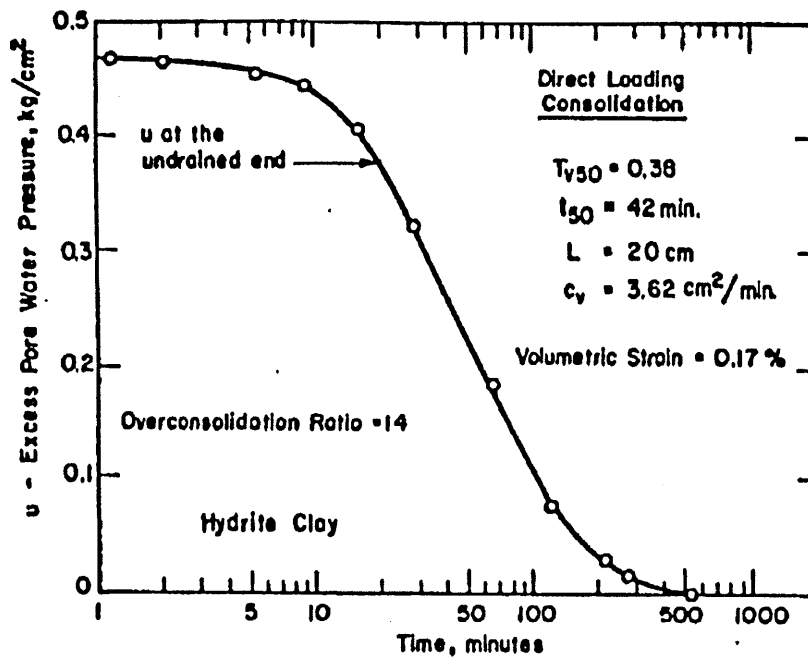


Figure 2.15 Result of experimental investigation: excess pore water pressure anode versus time for recompression from 49 kPa to 98.1 kPa (after Wan and Mitchell, 1976)

The excess pore water pressure was computed at the closed anode and current density with time, and shown in Figure 2.16. From this figure, it shows that the ultimate negative excess pore water pressure was 1.17 kg/cm^2 (or equivalent to 114.3 kN/m^2) at the anode and it's equally to the value of 0.92 kg/cm^2 (or equivalent to 89.84 kN/m^2). These two values were calculated using equation (2.19). The volumetric strain for the same experiment was measured as 0.16%.

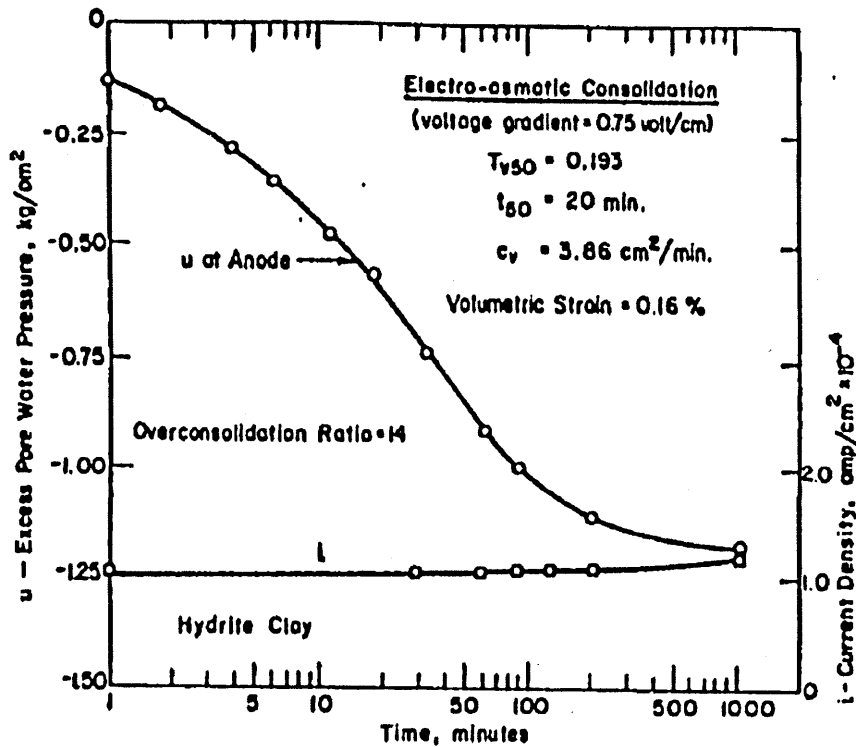


Figure 2.16 Result of experimental investigation: negative pore water pressure measured at anode and current density versus time during electro osmotic consolidation of remoulded kaolinite (after Wan and Mitchell, 1976)

These tests was exposing from the theory of Esrig (1968) who subjected a sample to consolidation under the integrated effect of direct loading and electro osmosis. However, Esrig's theory may differ from what happens in the field. In situ, the electrode is normally installed in a vertical direction. This creates a radial field. Therefore, the results from the in situ conditions may not be same as predicted from Esrig's theory which applies to a one dimensional condition.

2.5 HISTORICAL REVIEW OF ELECTRO OSMOSIS CONSOLIDATION

APPENDIX C summarises several of the earlier electro osmotic experiments. This is a summary of the objectives of the research, voltage, voltage gradient, current density, types and shapes of electrodes, and whether the tests were either consolidated by electro osmosis only, or by a combination of electro osmosis with direct loading.

These past experiments were performed predominantly on soil samples ranging from silt to clay, submerged or not submerged in water or seawater. Ten types of electrodes have been used:- (1) aluminium, (2) carbon, (3) copper, (4) ferum, (5) graphite, (6) platinum, (7) polypropylene, (8) reinforcing bars, (9) silver, and (10) titanium. Sixteen shapes of electrodes were used in the experiments, namely (1) bars, (2) cylinders, (3) disks, (4) fibres, (5) H-piles, (6) mesh, (7) non woven sheet, (8) perforated pipes, (9) pipes, (10) plates, (11) ribbons, (12) rods, (13) sheet, (14) sheet piles, (15) tubes, and (16) wire stringer.

The tests were conducted in a range of tanks including cylindrical, rectangular and square. The applied voltage, voltage gradient and current density were also varied from 1 V to 240 V for direct current, and for alternate current by Shang and Dunlap (1998, 1996) in the range 7000 V to 30 000 V, and Lo and Shang (1994) up to 18 000 V.

The conclusions that can be derived from the range of tests include:-

- (i). Settlement.
 - (a). The discharge of water was observed at the cathode where the water discharge was greenish due to corrosion of copper (Bergado *et al.*, 2003).
 - (b). The electro kinetic treatment results in an increase in the apparent preconsolidation pressure for treated soil samples where the greatest increase occurred in the soil closest to the anode. The results of the consolidation tests also showed that the electro kinetic treatment transformed a normally consolidated clay into an overconsolidated clay (Micic *et al.*, 2003b). Lo and Ho (1992), and Lo *et al.* (1991a) also agreed regarding the preconsolidation pressure, where they concluded the increase in preconsolidation pressure after treatment provides additional direct evidence that the soft clay is actually consolidated by the electrical potential which is analogous to mechanical loading. When the electro osmotic consolidation occurs, the increase in preconsolidation pressure is a result of the negative pore pressure generated, which is equivalent to an

internal effective stress under which the soil consolidates. The samples were therefore virtually overconsolidated by the electro osmotic process and this is a reason why the effects of treatment are permanent.

- (c). In Lo *et al.* (1992) studies, they reached the conclusion the higher the applied electric potential and the deeper the electrode depth, the larger the settlement. On the effect of the electrode depth, the higher settlement corresponding to the deeper electrode depth is due to the larger volume of the soil mass treated. And if the soil mass used in the experiment is limited in size, more water can be extracted from the soil mass in the same period of treatment time, and this will lead to higher settlement.
- (d). Morris *et al.* (1985) studies suggested that the void ratio reduced, the reduction increasing with time of treatment. They concluded that the consolidation reduces the water content of the soil especially near to the anode. This is due to the flow of water from the anode to the cathode. With time the rate of settlement decreased gradually where the current had increased (Bjerrum *et al.*, 1967).
- (e). In 1977 and 1976, Mitchell and Wan, and Wan and Mitchell, respectively, conducted studies in relation to excess pore pressure and the installation of vertical drainage through the soils. The studies showed an increment of effective stress because consolidation settlement occurred from this result where in a saturated soil, both a reduction of excess positive pore water pressure as in direct loading consolidation, and an increase of excess negative pore water pressure as in electro osmotic consolidation can result in an increase to the effective stress. Finally, a more rapid dissipation of the excess pore pressure will take place by combining the vertical loading or preloading with the electro osmotic process compared to the electro osmotic process itself.

(ii). Water content

- (a). Soo *et al.* (2006) found that the final water content was less than the initial water content at the anode and increased in the vicinity of the cathode. Similar results were found in Alshawabkeh *et al.* (2004), Shang *et al.* (2004), Bergado *et al.* (2003), Micic *et al.* (2003b, 2003a, 2002b), Hamir (1997), Shang and Dunlap (1996), Lo and Shang (1994), Lo *et al.* (1994), Mitchell (1991), Gray (1990, 1968), Bjerrum *et al.* (1967, 1952).

- (b). The decrease in water content at the anode is assumed to be due to the evaporation of pore water as the temperature increases and pore water flow to the cathode due to electro osmosis under direct current electric fields. Electro kinetic treatment also develops apparent soil cohesion, attributed to the electro-cementation bonding and the effect of electric decomposition of the anode. The electro chemical effects also changed the plastic and liquid limits (Soo *et al.*, 2006, Alshawabkeh *et al.*, 2004, Shang *et al.*, 2004, Micic *et al.*, 2003b, 2003a, 2002b, Hamir, 1997, Bjerrum *et al.*, 1967).
- (c). According to Bergado *et al.* (2003) the reduction in water content which reduced the void ratio was generally in agreement with the corresponding values obtained from settlements. The reduction of water content at the anode implies an increase in shear strength due to a reduction in the void ratio and physico-chemical forces of interaction or electro kinetic forces (Shang and Dunlap, 1996). The electric field drives the clay particles close to one another and that results in an increase of electro static attractions thus leading to higher shear strengths.

2.6 COSTS OF ELECTRO OSMOSIS CONSOLIDATION

Pugh (2002), Burnotte *et al.* (2004), Alshawabkeh *et al.* (1999), and Bjerrum *et al.* (1967) briefly discussed the costs for the selective items of electro osmotic consolidation tests. Despite everything, all the studies reviewed so far suffer from the fact that the life span of electrodes materials is short especially the anodes which are likely to corrode during electro osmosis treatment. Hamir (1997) employed the electro kinetic geosynthetics in which a sheet metal of electrodes is sandwiched between geosynthetics fabrics. This study showed an increase in the life span during treatment of the anode. A new material, termed MMO, has the ability to prevent corrosion, so creating reusable electrodes.

The costs are shown in Table 2.7 From this table, it's clearly shown that the most contribution to the cost of electro osmotic improvement are electrode installation and connecting the power line; 30% and 27%, respectively, of the total cost. The rest of the items are each less than 10% from the total cost.

To improve a 7m high embankment on soft clay, anodes were installed at the site to a length of 5.0 m. They were at depths of 25.5 m to 33 m, and 26.5 m to 31.5 m or 9.0 m to 14.0 m below the berm surface. The steel anodes were tied to PVC tubes of equal

diameter to the ground surface. The cathodes were made from steel tubes and installed from the ground surface to a depth of 14.0 m.

To ensure that water was flowing completely at the cathode end, an ejector was attached at the bottom of each cathode end and then connected with plastic tubes to collect the water that flowed out.

The anode and cathode were assembled with two rows of cathodes and anodes placed at 3 m interval. Each row had six electrodes at 2 m interval between them. A total of 24 electrodes were assembled within an area of 9 m x 10 m. However, the researchers did not disclose the detail costing but only provided a brief cost as in Table 2.7.

**Table 2.7 Direct costs of the field tests as performed
(reproduced from burnotte *et al.*, 2004)**

Remarks	Cost	%
Electrodes (L = 14.5 m)	12731	16
Electrode Installation	23956	30
Power line to the site and connection to Hydro-Québec network	20976	27
Electrode connection	3980	5
Pumping system	7012	9
Access road, fence and miscellaneous	4969	6
Electricity	5508	7
Total	79132	100

Cost as in Canadian Dollar in 2004, % as in total percentage for the whole costs of the construction project.

Burnotte *et al.*(2004) claims (1): the cost of connection for the network and establishing the power were similar; (2): 15% of the power consumed was for the pumping system with CAN\$5500 estimated at CAN\$0.07 kW per hour; (3): the highest cost was for the installation of the electrodes, and it would have been more if the electrodes had to be installed through the present embankment. Consequently, they recommended placing the electrodes from the natural ground surface.

Alshawabkeh *et al.* (1999) and Alshawabkeh (2001) presented a paper that highlighted the cost of carrying out electro kinetic remediation in-situ. Table 2.8 underlines the five components of the cost, which is fabrication and installation of electrodes, electric energy, enhancement agents (if necessary), any post treatment (if necessary), fixed costs.

Table 2.8 Costs of electro osmotic treatment (reproduced from Alshawabkeh, 2001; and Alshawabkeh *et al.*, 1999)

Constituent	Remarks
Fabrication and installation of electrodes	Electrode costs
Electric energy	Soil properties, contaminant properties, electrode configuration, and processing time
Enhancement agents, if necessary	To improve the efficiency of electrokinetic remediation
Any post-treatment, if necessary	Be considered if effluent treatment is required
Fixed costs	(1): mobilisation and demobilisation costs of various equipment, site preparation, security, progress monitoring, insurance, labour, contingency, and miscellaneous expenses; (2): capital costs; (3): depreciation costs; (4) rental costs

Alshawabkeh (2001) and Alshawabkeh *et al.* (1999) identified seven examples of total costs that contributed to in-situ construction. These are (1): mobilisation costs of a drilling rig and labour costs of two man operating crew \$1000 per day; (2) costs of drilling is \$15 per m; (3): fabrication and installation of electrodes is \$5 per m where the electrodes are reusable; (4): electricity costs is \$0.04 per kWh; (5): variable costs for two man crew plus 14 hour per week which is \$50 per two man per hour; (6): variable rate which is \$0.001 per m³-hour plus 30% increase for insurance; and (7): post treatment and fixed costs which is \$25 per m³. The total cost is:-

$$C_{\text{total}} = C_{\text{electrode}} + C_{\text{energy}} + C_{\text{chemical}} + C_{\text{post-treat}} + C_{\text{fixed}} + C_{\text{variable}} \quad (2.24)$$

$$C_{\text{electrode}} = C_1 N \quad (2.25)$$

$$C_{\text{energy}} = \frac{C_2 \phi_{\text{max}}}{3600000\beta} \quad (2.26)$$

$$C_{\text{chemical}} = \frac{C_3 M_w}{\beta \alpha F} \quad (2.27)$$

$$C_{\text{post-treat}} = C_4 \frac{n R_d k_e}{u^* + k_e} \quad (2.28)$$

$$C_{\text{variable}} = \frac{C_5}{\beta} \frac{L}{\sigma^* i_e} \quad (\text{for one dimensional}) \quad (2.29)$$

$$C_{\text{variable}} = \frac{C_5}{\beta} \frac{R_e^2}{i_r'} \quad (\text{for radial}) \quad (2.30)$$

where:

C_{total} : total costs per unit volume of soil to be treated, unit in $\text{\$L}^{-3}$;

N : number of electrodes per unit surface area, unit in $\text{\$L}^{-2}$;

C_1 : cost of electrodes per unit length; unit in $\text{\$L}^{-1}$;

C_2 : electric energy cost, unit in $\text{\$}$ per kWhour;

ϕ_{max} : applied voltage, unit in V ;

β : the reactive transport rate of a species relative to the electric conductivity of a medium, i.e.,

$$\beta = \frac{u^* + k_e}{R_d \sigma^*} \quad \text{where } u^*: \text{effective ionic mobility of the ion, unit in } \text{m}^2 \text{ per sec-V; } k_e:$$

coefficient

of electro osmotic conductivity, unit in $\text{m}^2 \text{ per sec-V}$; R_d : delaying factor, dimensionless;

σ^* : effective electric conductivity of the soil medium.

C_3 : cost of electrodes of the chemical agent, unit in $\text{\$M}^{-1}$;

M_w : molecular weight of the neutralizing chemical, unit in M/W ;

α : factor depending upon the stoichiometry of the neutralizing reaction, dimensionless;

F : Faraday's constant (96485 C/mol-electron);

C_4 : cost of treatment per unit volume of the electrolyte (effluent) collected, unit in $\text{\$L}^{-3}$;

C_5 : variable daily cost (monitoring, insurance, rentals, etc), unit in $\text{\$L}^{-3}\text{T}^{-1}$;

L : electrode spacing, unit in m ;

i_e : gradients;

R_e : electrode spacing, unit in m ;

i_r' : gradients;

Bjerrum *et al* (1967) presented the cost of stabilising Norwegian Quick Clay. The details of the costs are summarised in Table 2.9 where roughly 8 N.Cr. per cubic metre of direct costs to stabilise the problematic soft clay.. From their projects, they claimed 30000 kWh of electricity was consumed throughout this project. Approximately 100 m^3 of water was drained out and 2000 m^3 of clay was stiffened. To stiffen one cubic metre of clay, they had calculated only 17 kWh was needed.

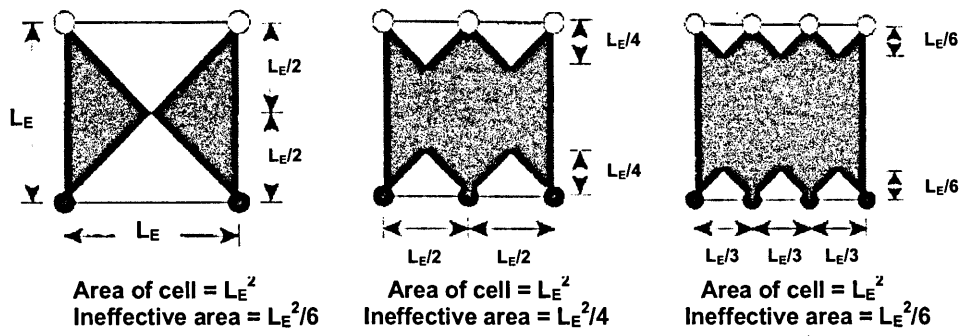
Table 2.9 Cost of the treatment for stabilising the Norwegian Quick Clay (reproduced from Bjerrum *et al.*, 1967: 226)

Items	Costs (N.Cr.)
Electrode steel and attachments	6000
Electricity	4000
Hire of transformers	2000
Labour costs	4000
Total	16000

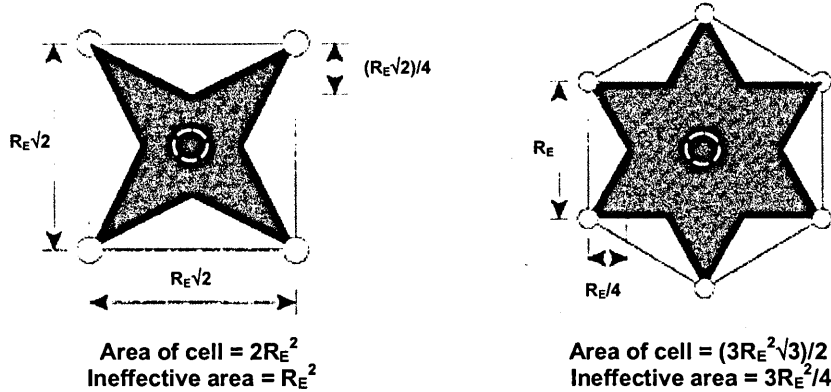
All of these studies indicate that the costs of installation and power together account for about 50% of the cost of the electro osmotic treatment.

The installation costs can be reduced by reducing the number of electrodes. Reducing the number of electrodes increases the spacing between the electrodes which means that more power is needed to generate the same voltage gradient. Hence there is an optimum spacing for a given electrode distribution. Alshawabkeh et al. (1999) studied the spacing (Figure 2.17) and came to the conclusion that the most effective layout was the hexagonal layout with six anodes for every cathode.

Based on Figure 2.17(b) and Table 2.10, the study by Alshawabkeh et al. (1999) found that the percentage of zone of ineffective areas for square shape and hexagonal were 50% and 29% accordingly. They concluded that hexagonal shapes with six anodes to one cathode are better and more effective. Alshawabkeh et al. (1999) also mentioned that in using electro osmosis for soil consolidation, the number of anodes should be very much more than the number of cathodes. The soil surrounding the anode will consolidate more reducing the water content and increasing the shear strength. If the same hexagonal shape is used but with one anode and six cathodes then the soil for that area will experience less consolidation because of the ability of the single anode to disperse the water from the anode to the cathode area is low.



(a)



(b)

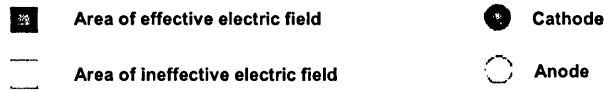


Figure 2.17 Approximate Evaluation of Ineffective Areas for (a): 1-D and (b): 2-D Electrode Configurations (after Alshwabkeh *et al.*, 1999: 621)

Table 2.10 Impact of electrode configuration on electrode requirements and size of ineffective areas (reproduced from Alshawabkeh *et al.*, 1999: 620)

Config.	Spacing		F ₁	A _{cell}	Σelectrodes/area		Ineffective Area	
	Opp.	Same			N	%	A _{ineff}	% of A _{cell}
1-D	L _E	L _E	1	L _E ²	1/L _E ²	0	L _E ² /2	50
1-D	L _E	L _E /2	2	L _E ²	2/L _E ²	100	L _E ² /4	25
1-D	L _E	L _E /3	3	L _E ²	3/L _E ²	200	L _E ² /6	17
Square	R _E	√2 R _E	2	2R _E ²	1/R _E ²	0	R _E ²	50
Hex.	R _E	R _E	3	$\frac{3\sqrt{3}}{2} R_E^2$	$\frac{\sqrt{4}}{\sqrt{3} R_E^2}$	15.5	3R _E ² /4	29

Config.: configuration; Hex.: hexagonal; Spacing: electrode spacing; Opp.: opposite charge; Same: same charge; F₁: number of electrodes per cell; A_{cell}: area of cell; Σelectrodes/area: number of electrodes per unit area; %: increase percentages; A_{ineff}: ineffective area; % of A_{cell}: percentages of area of cell.

2.7 SUITABLE APPLICATIONS FOR ELECTRO OSMOTIC PILES

Following the pioneering work of Casagrande in 1961 and 1952(b) and others such as Burnotte *et al.* (2004), Lo and Ho (1991c, 1991b), Eggestad and Føyn (1983), Butterfield and Johnston (1980), Chappell and Burton (1975), Bjerrum *et al.* (1967), and Soderman and Milligan (1961), the consolidation of soft clays using electro osmosis has generated much interest in geotechnical engineering. Electro osmosis has been applied to improve friction pile capacity, to stabilise trenches and excavations, to prevent swelling and shrinkage in foundation soils, and to stabilise slopes.

2.7.1 Improving friction pile capacity

Electro osmosis can help with piling in two ways. Steel piles are used as anodes, after they have been installed to increase the capacity of the pile. This has the disadvantage that there has to be some sacrificial steel included in the design. The alternative is to use the steel piles as cathodes to facilitate driving. In this case water is driven to the piles thus reducing the installation friction. The electrodes are shown in Figures 2.18 and 2.19. The cathodes are perforated to allow water to be removed.

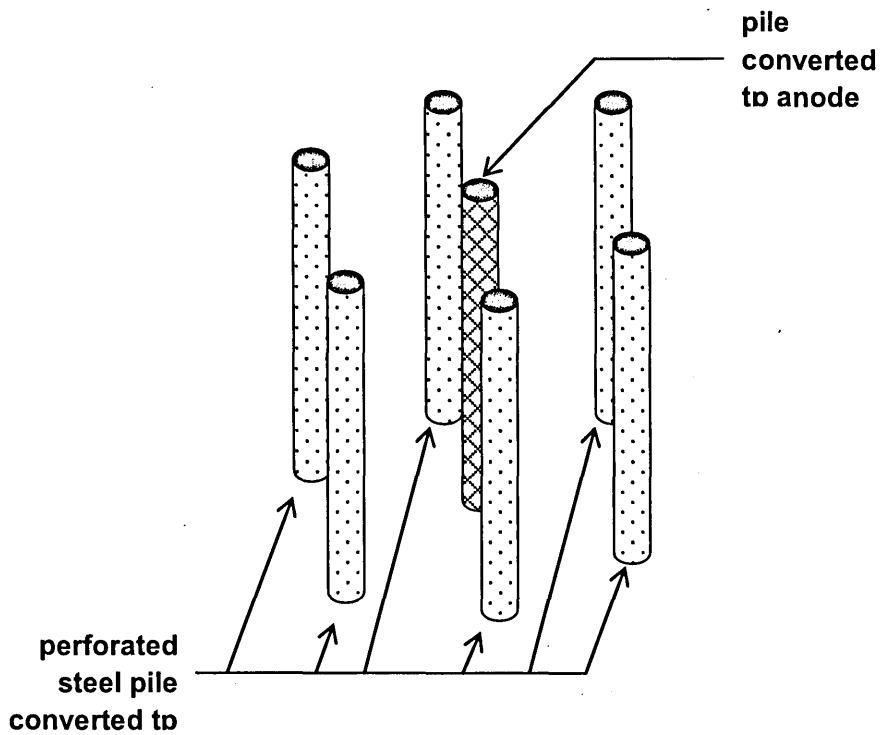


Figure 2.18 Pile converted to anodes (Pugh, 2002)

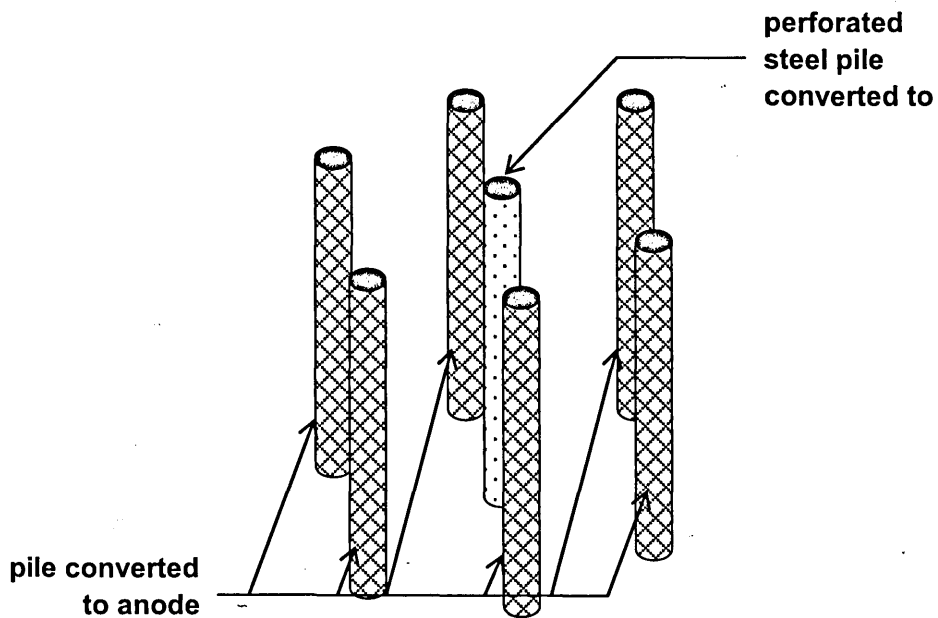


Figure 2.19 Pile converted to cathodes (Pugh, 2002)

Anodes are installed close to the piles. At the end of installation the electric current is switched off and equilibrium re-established with time. This would be enhanced by reversing the electric current.

2.7.2 Trenching and Excavation Sites

Electro osmosis can be used to enhance the lowering of the ground water level. Cathodes are used as wells. Anodes are installed in the area to be excavated (Figure 2.20 and 2.21) Electro osmotic improvement can be carried out either in single phase or double phase. Single phase is performing with the installation of anodes in the excavated area and cathodes are installed near to the anodes (Figure 2.20). Single phase is conduct without pumping water from the cathodes. This reduces the time to lower the ground water level. Double phase is when water is pumped from the cathodes used as well points. Fig 2.21 displays schematically the double phase. Pumping out the water via cathode as a well point can reduce the ground water level in a shorter time.

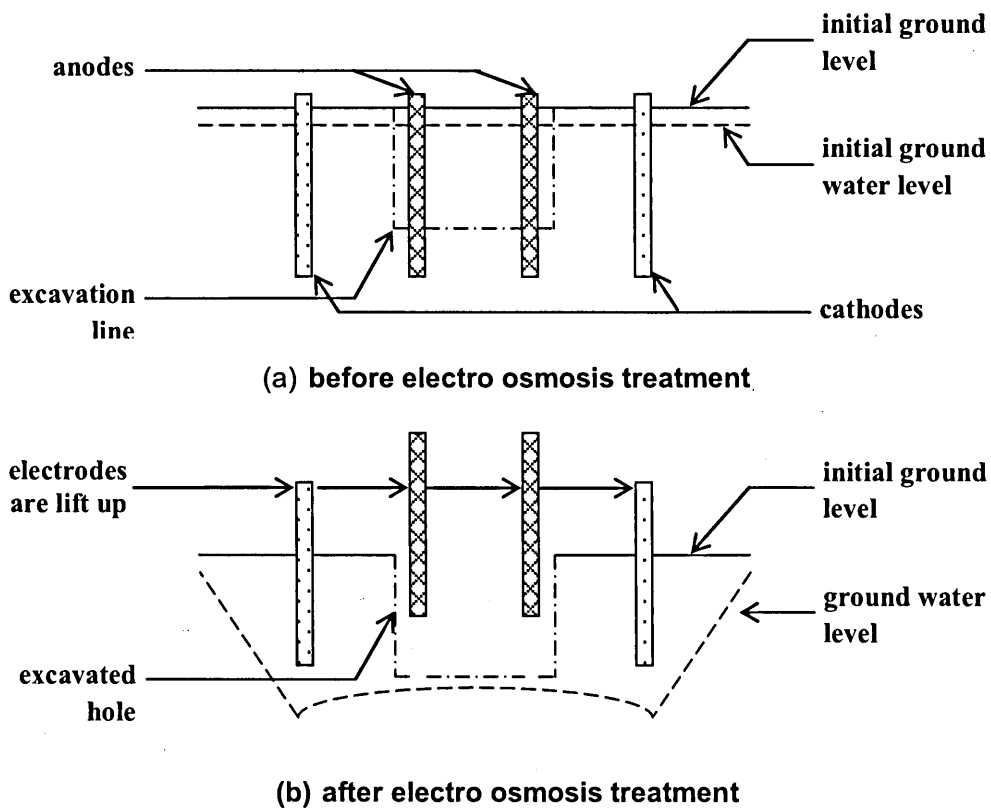


Figure 2.20 Single phase treatment (Pugh, 2002)

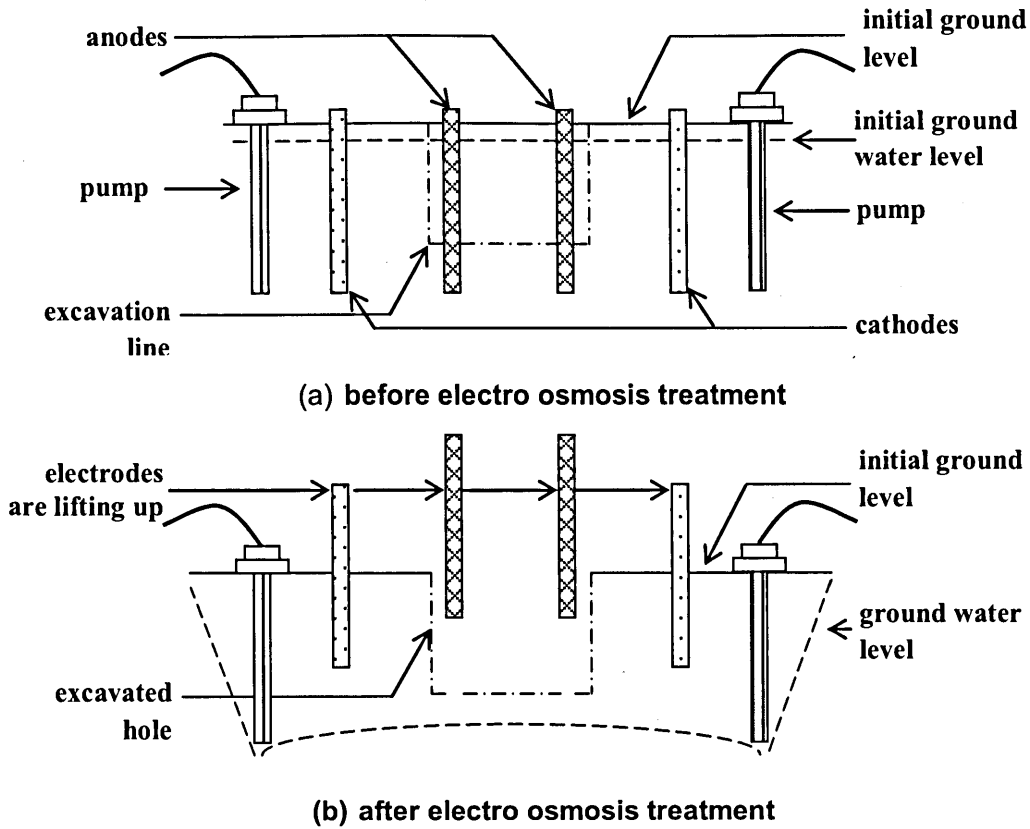


Figure 2.21 Double phase treatment (Pugh, 2002)

2.7.3 Prevent swelling and shrinkage in foundations

Electro osmosis can be used to control swelling and shrinking of soils by maintaining the water content through the appropriate use of anodes and cathodes. The electrodes are installed near the foundations as shown in Figures 2.22 and 2.23. The electro osmotic piles will transport the water either out or into the problematic layers, and control the volume of soils.

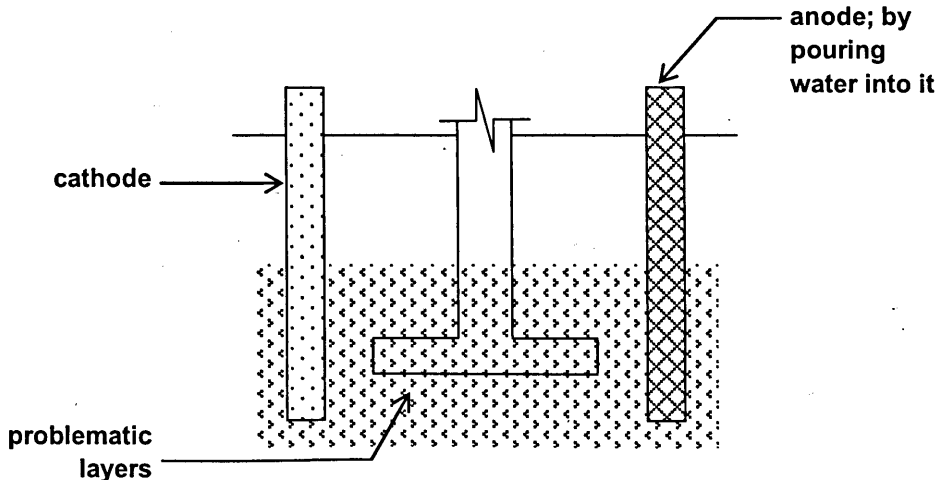


Figure 2.22 Shrinkage treatment (Pugh, 2002)

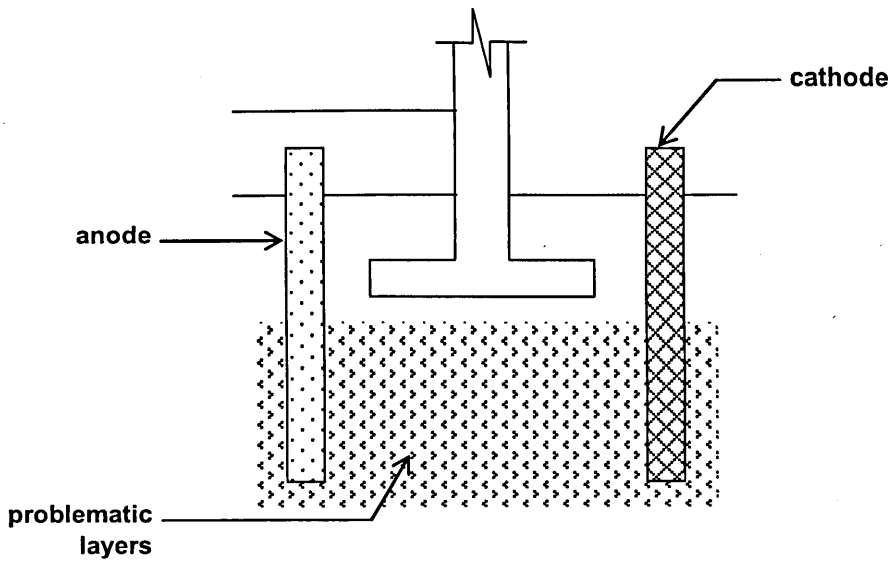
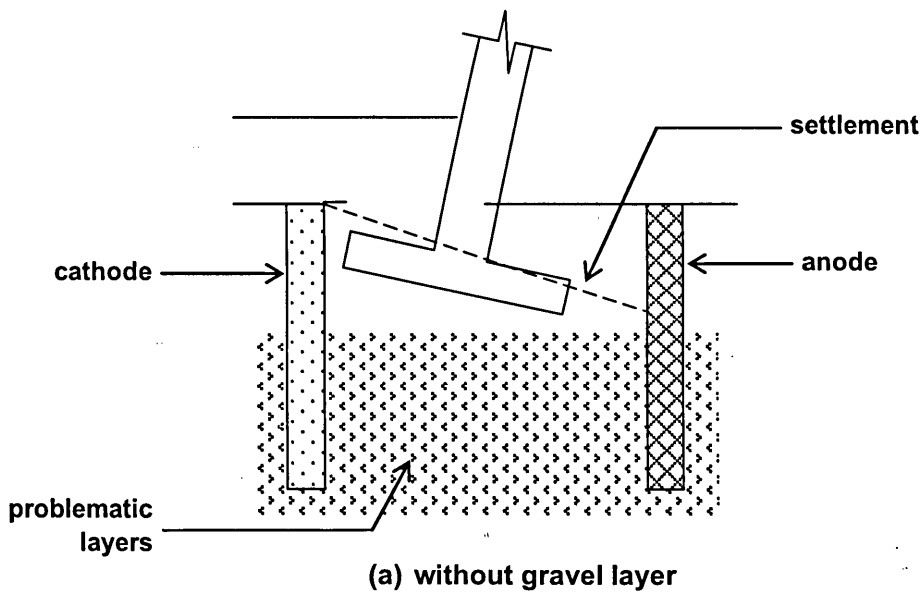


Figure 2.23 Swelling treatment (Pugh, 2002)

During the initial phase of the construction, cracking can occur in a building due to differential settlement due to the effects of electro osmosis (Figure 2.24a). This can be solved by spreading a layer of gravel underneath the foundation. This gravel layer is placed before the construction of the building foundation. Therefore, to ensure the uniformity of settlement especially at the anode after electro osmotic treatment, the gravel is compacted in layers (Figure 2.24b).



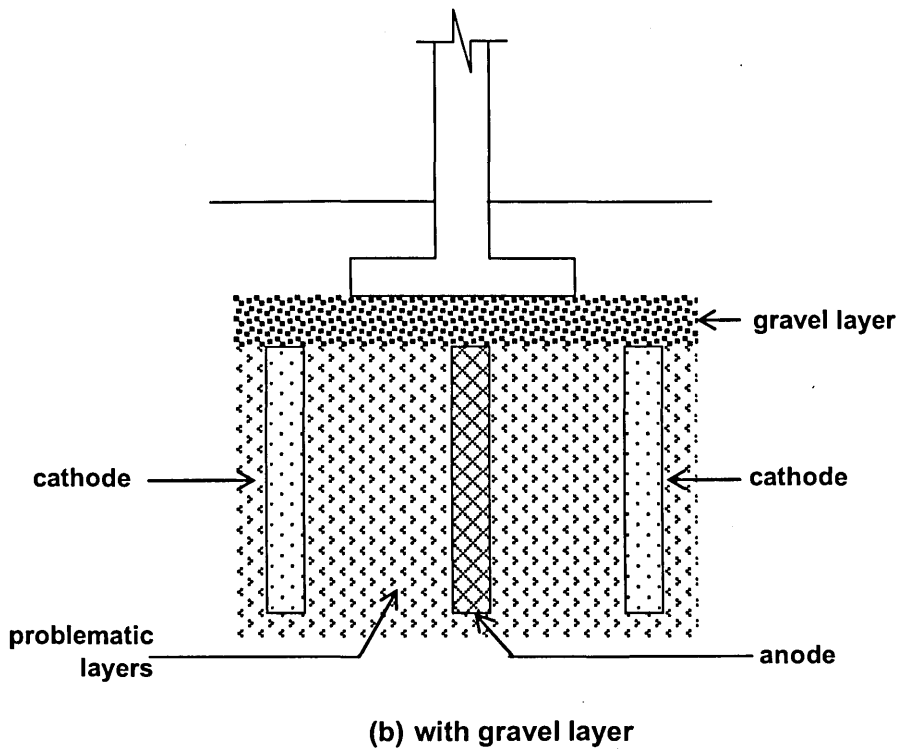


Figure 2.24 Collapsing treatment (Pugh, 2002)

2.7.4 Stabilise the unstable slope

Unstable slopes are common in Peninsular Malaysia such as at Taman Hillview, Hulu Kelang in 2002, and Gua Tempurung, Gopeng in 2004 (Berita Harian, 22 November 2002, and 1 November 2004). The expansion of the built environment means that there is an increase in the number of excavations and slopes. Installing electro osmotic electrodes on slopes it are possible to stiffen the unstable slope by decreasing the pore water pressure. Figures 2.25 and 2.26 illustrate schematically the installation of electrodes on a slope.

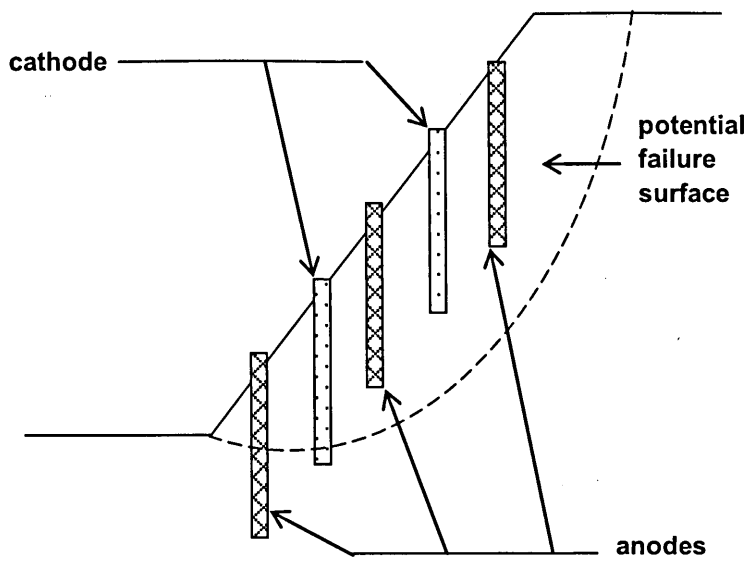


Figure 2.25 Vertical installation (Pugh, 2002)

A negative pore water pressure is generated at the anodes on the unstable slope. The water is forced to the cathode which also acts as a drain. Thus, the strength of the soil is increased in places and the ground water level is lowered.

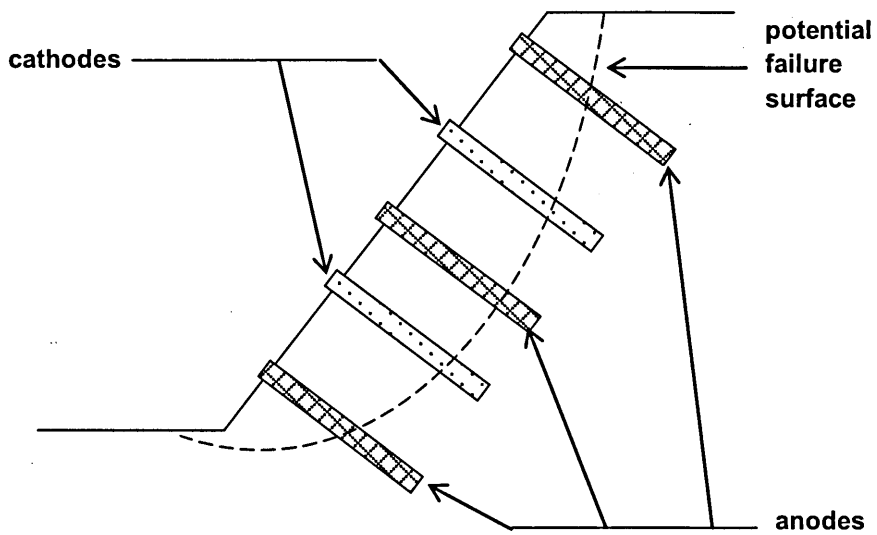


Figure 2.26 Inclined installation (Pugh, 2002)

2.7.5 Review of case histories of electro osmotic strengthening of piles

Electro osmosis treatment techniques have already been applied to problematic sites since the process of soil treatment was created by Casagrande et al. in 1947. A direct current was been applied at the ground surface to treat the problematic sites by these researchers. They were conducting research to obtain a fundamental knowledge about the electro osmosis treatment. Several cases using electro osmosis treatment to increase the bearing capacity of piles are reported.

(a) Big Pic River, Ontario, Canada

Electro osmosis was used to increase the pile bearing capacity of piles by Soderman and Miligan in 1961 on a highway bridge project in Big Pic River, Canada. The subsurface contained 3.0 m to 6.1 m of alluvial soils overlying 12.2 m to 18.3 m of varved clay from soft to firm. The clay concerned was found to be layered with more than 76.2 m of silt and silty fine sand. The layer of silty fine sand was under artesian pressure. the artesian pressure exceeded the hydrostatic head, therefore the capacity of a long friction pile was small compared with a short pile. A test on the pile driven into the soil showed that it had a lower load capacity compared with piles which are extended just below the clay layer. In view of the shorter pile length, it was not possible to support the designed load, 36 300 kg. A suggestion was carried out to increase the pile's bearing capacity by electro osmosis by using piles as electrodes. Tests in the laboratory and field confirmed the validity of the suggestion.

After driving the H pile to a depth of 17 m for each pier, the cathodes of a length of 213 m were attached surrounding the overall depth of pile and were installed starting from the ground surface. The average distance between the piles and the cathode is 7.0 m. Power supply was delivered a 70 Volts to 120 Volts using a generator. Average current for each pile was 15 Ampere. After four weeks of carrying out the treatment, the pile bearing capacity increased between 63 500 kg to 90 700 kg. This translates to an increase in capacity of 2.5 times to 3 times that before treatment. Some of the piles were outside the pier foundation to allow load testing. This was to ensure that the capacity could be checked to ensure that it was permanent. It is believed that this study is the first example using electro osmosis process to increase the capacity of skin friction pile.

A further study was done by Miligan (1995) for 36 years to evaluate an change in pile capacity. No reduction in bearing capacity of pile was recorded and the settlement reading for the bridge foundation was small.

(b) Highway at Berthierville, Quebec, Canada

A study on the location mentioned above was done by Bozozuk and Labrecque in the year 1969. The location is above a compressible marine clay fill. At 80 km east of Montreal in Berthierville, the road meets and crosses a railway network and Highway 41. At the junction crossing, a bridge was constructed at the highway and is supported by six 1 m diameter piles of 82.3 m in length and placed and driven into bedrock by 2.4 m to 3.0 m. The piles are 13 mm thick steel and filled with concrete. The weight of each pile was 20 400 kg and it was numbered with 18-S and the material was made by reinforced ferum. This composite pile was designed to a total capacity of 1.814×10^6 kg with 1.09×10^6 kg allowed to take the negative skin friction. The subsoil at the site is marine clays from the Champlain Sea. The upper 18 m encompasses sandy soil, silty clay, sand and layered silt and layered clayey silt. Between 18 m to 73 m, the soil layer changes to a firmer grey silty clay. The grey silty clay lies over 9 m thickness of fine sand. The fine sand was found to be above the bedrock layer. The consolidation test shows that the soil is normally consolidated until a depth of 12 m and overconsolidated below 21 m depth. Reliable settlement is expected to occur because of the consolidation which happens in the top 12 m.

Two piles marked B-2 and B-3 experienced elongation after placement of concrete due to the cement hydration process. This was startling because the piles were expected to experience compression under negative skin friction loading. This observation shows that the relative movement may reduce the bonding between the concrete and the steel tube thus effecting the lateral loading resistance. Thus the movement should have been avoided. An attempt was made to expel skin friction loading using the electro osmotic process with the composite steel tube as the cathode. 50 kW of electric power was generated from the gas which was produced by the generator. The power was supplied until there was a reduction in the length of the pile. For pile marked B-3 with an average flow supply of 475 Ampere and 20.5 Volts for duration of 1.5 hours the pile finally shortened for 0.25 hour. New valves or a new redesigned valve was installed within the pile. The purpose of this new redesigned valve was to reduce the electro osmosis process to occur, especially to occur at half the effectiveness at the corner end of the pile. However, in their findings about the electro osmosis process, they found that there is no direct method in identifying the electro osmosis process effectiveness occurring in eliminating the negative skin friction loading which has begun to increase as soon as experiment is completed.

2.8 EFFECTIVENESS AND EFFICIENCY OF ELECTROOSMOTIC TREATMENT

There are several parameters that can be determined experimentally to determine the effectiveness and efficiency of electro osmosis consolidation treatment. Those parameters are (1) water content, w_c ; (2) constrained stiffness, $E_{\text{stiffness}}$; (3) void ratio, e_o ; (4) coefficient of volume compressibility, m_v ; (5) the energy consumption, E ; (6) the electro osmotic flow efficiency; and (7) the electro osmotic transport efficiency, k_i . Parameters such as water content, constrained stiffness, void ratio, and coefficient of volume compressibility are essential to determine the effectiveness of electro osmotic treatment. Parameters such as the energy consumption, the electro osmotic flow efficiency, and the electro osmotic transport efficiency are important and related to the low cost of soil improvement which applies to the field works. These three parameters are defined as the economic efficiency of electro osmotic treatment.

2.8.1 Energy Consumption, E

Energy consumption is the amount of energy that is applied in the electro osmotic consolidation phase. According to Lefebvre and Burnotte (2002), the energy consumption, E , is scale dependent and stated in kWh per m^3 . The energy consumption is configured using the following equation:

$$E = \frac{VIt}{v} * \text{scaling factor} \quad (2.31)$$

where:

V = mean applied voltage (V);

I = mean current (A);

t = total time (h);

v = sample volume (L);

scaling factor = electrode spacing of 0.15 cm in the laboratory to a spacing of 3 m in the field.

2.8.2 Electro osmotic Flow Efficiency

Efficiency is defined as the ratio of total flow quantity to total energy consumed. Details of total flow per power consumed was discussed by Eykholt and Daniel (1994), and Gray and Mitchell (1967). The efficiency of total flow per power consumed can be defined as:

$$\frac{Q}{E} = \frac{\text{Total water expelled}}{\text{Energy consumption}} \quad (2.32)$$

where:

Q = total water expelled (cm^3); and

E = energy consumption as calculated from equation (2.41).

2.8.3 Electro osmotic Transport Efficiency, k_i

The efficiency and economics of electro osmosis depends on the total amount of water transferred per unit electrical charged passed. For clay with negative charge, the greater the variation between the concentrations of cations and anions, the greater the net drag on the water in the direction toward the cathode during electro osmosis. The electro osmotic transport efficiency may be described by:

$$k_i = \frac{Q}{It} = \frac{\text{Total water expelled}}{\text{Current} * \text{time}} \quad (2.33)$$

or

$$k_i = \frac{Q}{It} = \frac{\text{Total water expelled}}{\text{Current}} \quad (2.34)$$

where:

Q = total water expelled (cm^3); and

I = mean current passed through soil sample (Ampere); and

t = total time (h).

The electro osmotic transport efficiency, k_i , is a function of the electrical conductivity of the soil and it may vary. According to Mitchell (1991), the variations are due to electrolyte concentration, water content, and soil type. Dielectric constants and viscosity of the pore fluids, changes in pH, existence of current carried during the electro osmosis process also contribute to the variations of k_i . Hamir *et al.* (2001), Hamir (1997), Pamukcu (1997), Acar *et al.* (1990), and Gray and Mitchell (1967) presented and discussed the k_i 's parameter in their research paper.

Electro osmotic flow efficiency and transport efficiency varies in clayey soils. Both of these parameters define the electro osmotic energy requirements. The voltage drop and current consumption in a system control the electro osmotic dewatering process. Gray and Mitchell (1967) suggested the applied voltage, ΔE , and the electrical energy requirements per gallon discharged, ϵ , are the other two efficiency indicators that can be obtained besides equations (2.32) and (2.34). By computing the voltage drop, it shows the dewatering rate in a soil together with electrode spacing and electro osmotic permeability, k_e . For one dimensional flow, the voltage drop relationship is (Gray and Mitchell, 1967):

$$\Delta E = \frac{Q}{k_e} \Delta L \quad (2.35)$$

where:

ΔE = the applied voltage (V);

Q = drainage rate (cm^3/s);

A = cross sectional area (cm^2);

ΔL = electrode spacing (cm); and

k_e = electro osmotic permeability, which is 5×10^{-5} (cm^2/sV).

The electrical energy requirements per gallon discharged, ϵ , in kWh, defines the critical voltage which would cause extreme heating in the system. ϵ can also be an indicator of the maximum applied voltage in the system (Gray and Mitchell, 1967). ϵ can be estimated from (Gray and Mitchell, 1967):

$$\epsilon = \frac{\Delta E}{k_i} \times 10^{-3} \quad (2.36)$$

where:

ΔE = the applied voltage (V);

k_i = electro osmotic transport efficiency (gallon/Amp-h) as calculated from equation (2.33) or (2.34).

2.9 CONCLUSIONS

The literature review chapter began by introducing the soft clay soils distribution in Peninsular Malaysia. This section defined soft clay, distribution profiles in Peninsular Malaysia, the problems that exist, the available soil improvement techniques and the types to improve the problematic soils. The available approaches for fine and coarse grained soils were then discussed in detail.

The electro kinetic occurrence in clays was then introduced beginning with a description of the Helmholtz theory, the double layer and Stern layer. Diagrams of double layer are used to explain these important theories. When the applied voltage is applied electro osmosis, streaming potential, electrophoresis and sedimentation potential also occur within soil.

The next section then explained the theory of electro osmosis. This part discusses the introduction of the fundamental principles of electro osmosis as to why the electro osmotic process occurs within soft clay soils and how consolidation via electro osmosis with direct loading takes place. A historical review was also mentioned in this chapter. It summarises the past research studies highlighting several important parameters

which have been applied in their studies. Those important parameters are the applied voltage, voltage gradient, current density and types of electrodes. Tests were carried out in the field and laboratory. A series of suitable applications for electro osmotic piles were suggested in this chapter.

Finally, the effective and efficiency of electro osmosis treatment were discussed and several indicators were introduced. This section concludes the energy requirements for electro osmotic dewatering. Effective parameters are water content, constraint stiffness, voids ratio, and the coefficient of volume compressibility. The efficiency parameters are energy requirement, electro osmotic flow efficiency, electro osmotic transport efficiency, maximum applied voltage, and electrical energy requirements.

CHAPTER 3

THE LABORATORY PROCESS USED TO ACCESS ELECTRO OSMOTIC PILES

3.1 INTRODUCTION

This chapter describes the laboratory equipment and the procedure followed to validate the concept of electro osmotic piles and determine characteristics of that system.

The aims of the laboratory work were to show that electro osmotic consolidation could increase the average stiffness of a clay soil by creating zones of stiffened soil within the soil mass; and to investigate the relationship between electrical input and the resulting mass stiffness.

3.2 THE PRINCIPLES

Various approaches have been developed to investigate electro osmotic consolidation. The principal effect of applying a voltage to a wet soil mass is to push water from the positive terminal to the negative terminal. The water content at the negative terminal will decrease. Hence, the soil at the positive terminal will gain in stiffness and strength. In fact, the effect is similar to consolidation in which water is expelled due to external loading; therefore, consolidation theory can be customised to calculate the effect of electro osmosis consolidation. Therefore, to study electro osmotic consolidation, several principles were followed. The key principles of these experiments were: (1) the test chamber had to be non conductive, to ensure the cell did not affect the current flow; (2) the ability to apply a vertical pressure to ensure a positive pressure at all time to prevent fracturing due to electro osmosis; (3) the sample has to be constrained to move vertically to provide a one dimensional study; (4) to measure the volume changes by measuring changes in water content and settlement; (5) to apply voltage difference across sample and measure the current; and (6) to use copper as the electrodes to increase the lifespan of the electrode.

3.3 THE DESIGN

This section briefly describes each component of the osmotic cell and its purpose. These are: (1) the general assembly of the osmotic cell; (2) the test chamber; (3) the base of the cell; (4) the top of the cell; and (5) supplementary equipment. The supplementary equipment included; copper coiled spring electrodes, volume measuring system; direct current power supply, and the hangar and holder. All of these components are numbered and shown in Figures 3.1 and 3.2.

3.3.1 The electro osmotic consolidation chamber

Figure 3.1(a) shows the general assembly of the electro osmotic consolidation chamber and the ancillary equipment. Figure 3.1(b) shows details of the control and measuring systems on top of the cell. Figure 3.2 shows a section through the consolidation chamber. The measuring cylinder (5 in Figure 3.1) and the settlement gauge (7) were used to monitor the volume change of the sample. The control systems were the direct current power supply (8) and air pressure supply (9). Pressure was applied to the top of the sample using a modified Rowe's cell pressure system (4). The pressure system consisted of semi-flexible rubber diaphragm, labelled (21 in Figure 3.2). The test chamber and the base of the cell are discussed in brief in Section 3.3.2 and 3.3.3. The schematic diagrams of the electro osmotic consolidation chamber are displayed in Figures C1 until C26 in the APPENDIX C.

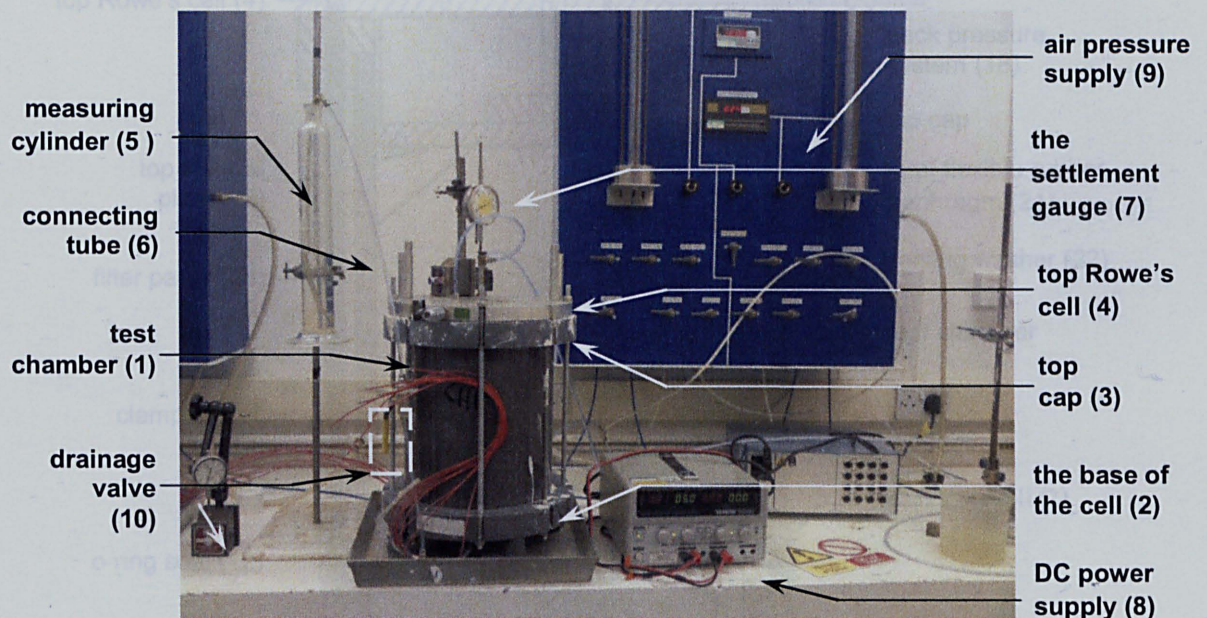


Figure 3.1(a) General arrangement of the electro osmotic consolidation chamber

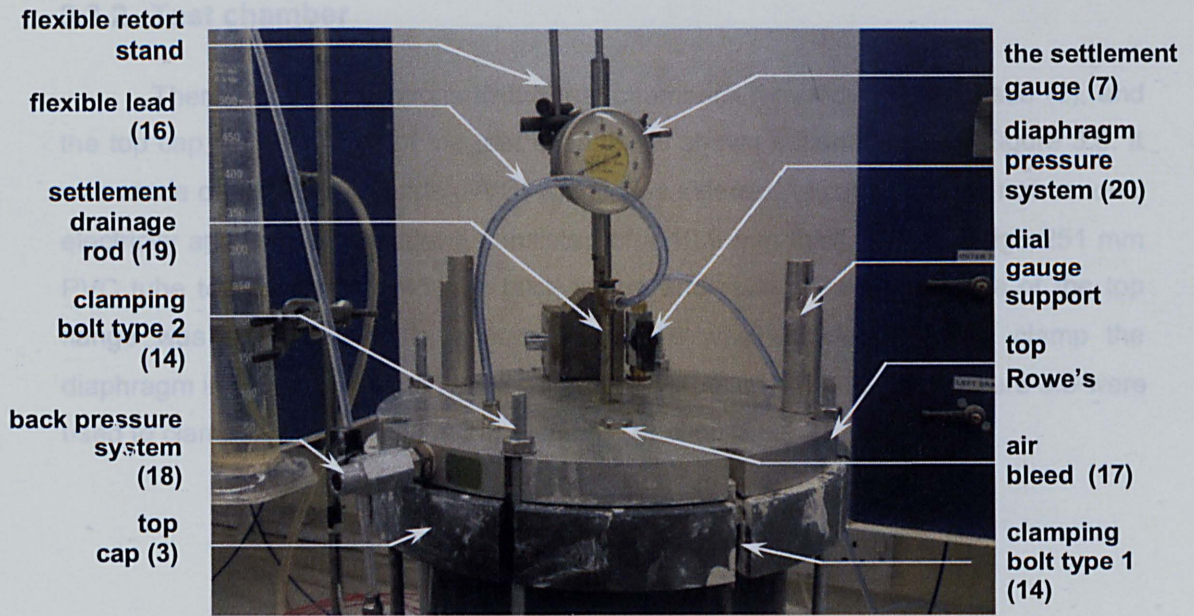


Figure 3.1(b) Dial gauge and other parts

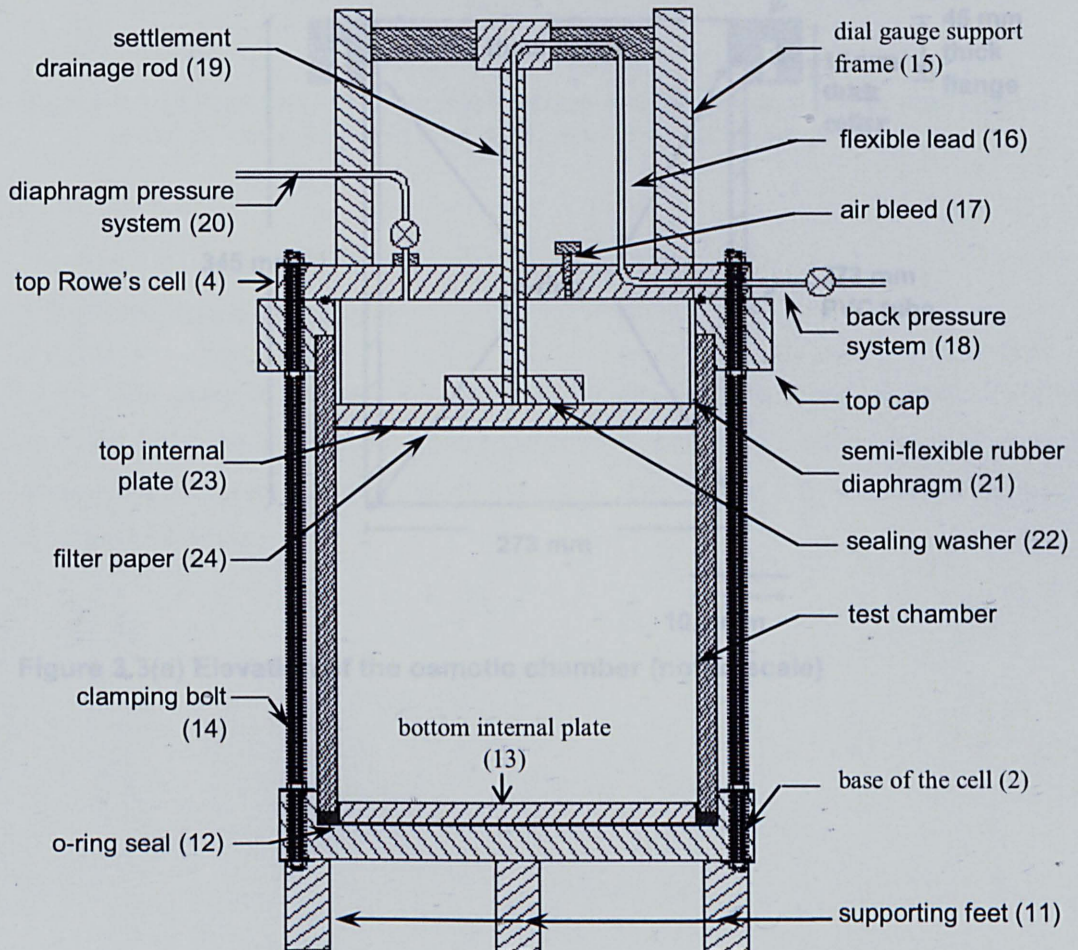


Figure 3.2: Schematic diagram of the electro osmotic consolidation chamber

3.3.2 Test chamber

There are three sections to the test chamber:- the body (1), the base (2), and the top cap (3). The body of the test chamber is shown schematically in Figure 3.5. It was made of polyvinyl chloride (PVC) which was selected because it does not conduct electricity and will not corrode. It consisted of a 10.9 mm thick, 345 mm high 251 mm PVC tube together with a 45 mm thick flange and collar. The flat surface of the top flange was 56 mm wide to ensure that there was sufficient area to clamp the diaphragm in place. The slots type 1 and type 2, labelled (A) and (B) in Figure 3.3 were used to clamp down the bolts as discussed in Section 3.3.4.2.

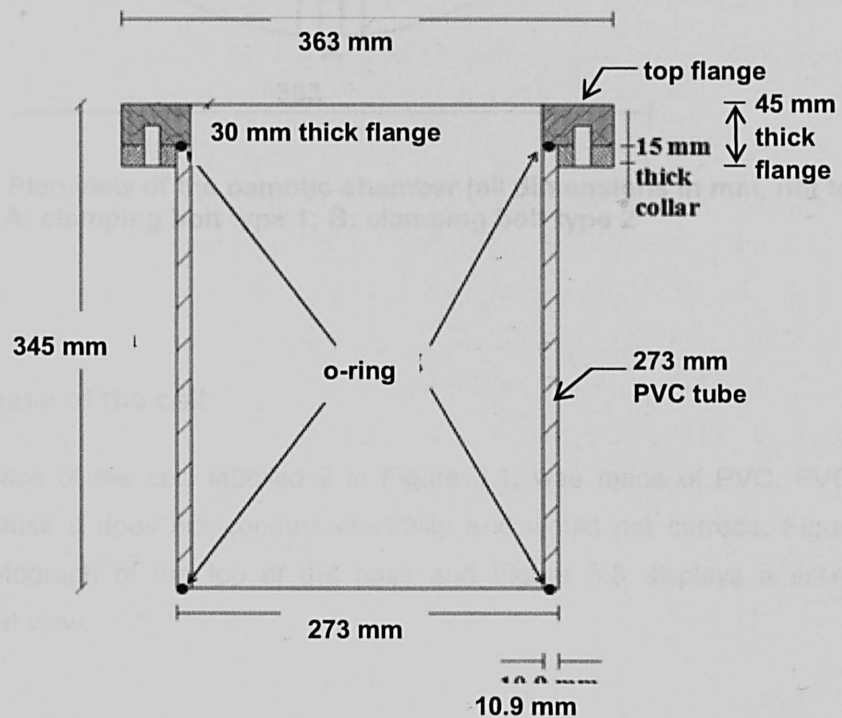


Figure 3.3(a) Elevation of the osmotic chamber (not to scale)

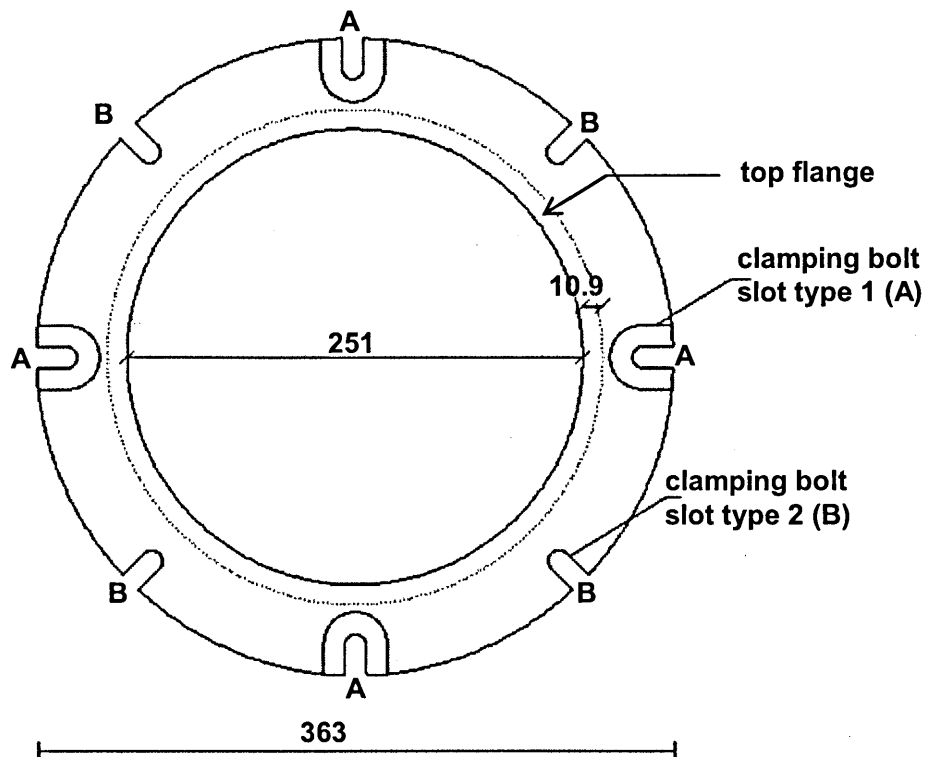


Figure 3.3(b) Plan view of the osmotic chamber (all dimensions in mm, not to scale) A: clamping bolt type 1; B: clamping bolt type 2

3.3.3 The base of the cell

The base of the cell, labelled 2 in Figure 3.1, was made of PVC. PVC was selected because it does not conduct electricity and would not corrode. Figure 3.4 shows a photograph of the top of the base and Figure 3.5 displays a schematic diagram of that view.

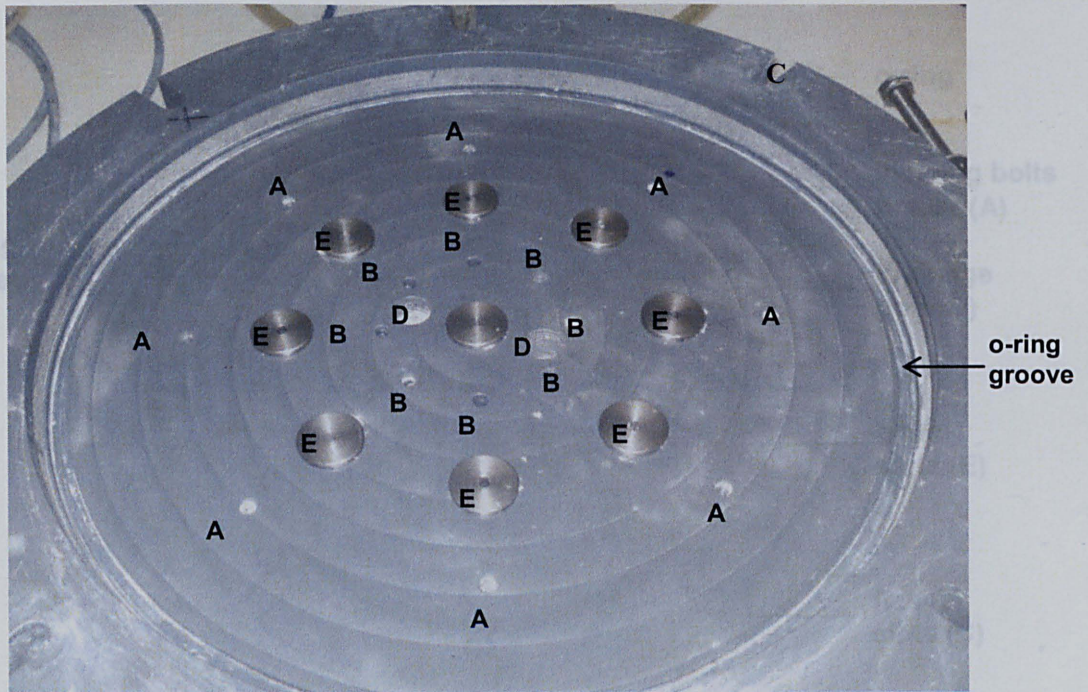


Figure 3.4 The whole view of the upper part of bottom base (A) and (B): locating bolts holder; (C): flange slot; (D): drainage port; (E): gland

The base of the cell was designed to provide the drainage outlets, marked (D); to house the stainless steel access glands; marked E; and to support the bottom internal plate which held the electrodes formed of vertical copper springs. Figure 3.6 displays the bottom internal plate located on the base of the cell. A and B in the base plate and internal plate were the positions of the locating bolts. Figure 3.7 shows the vertical electrodes installed in the bottom plate. O-rings were placed around the locating bolts to ensure a leak proof seal when the internal plate was clamped into the base. The O-rings also provided support to the internal plate.

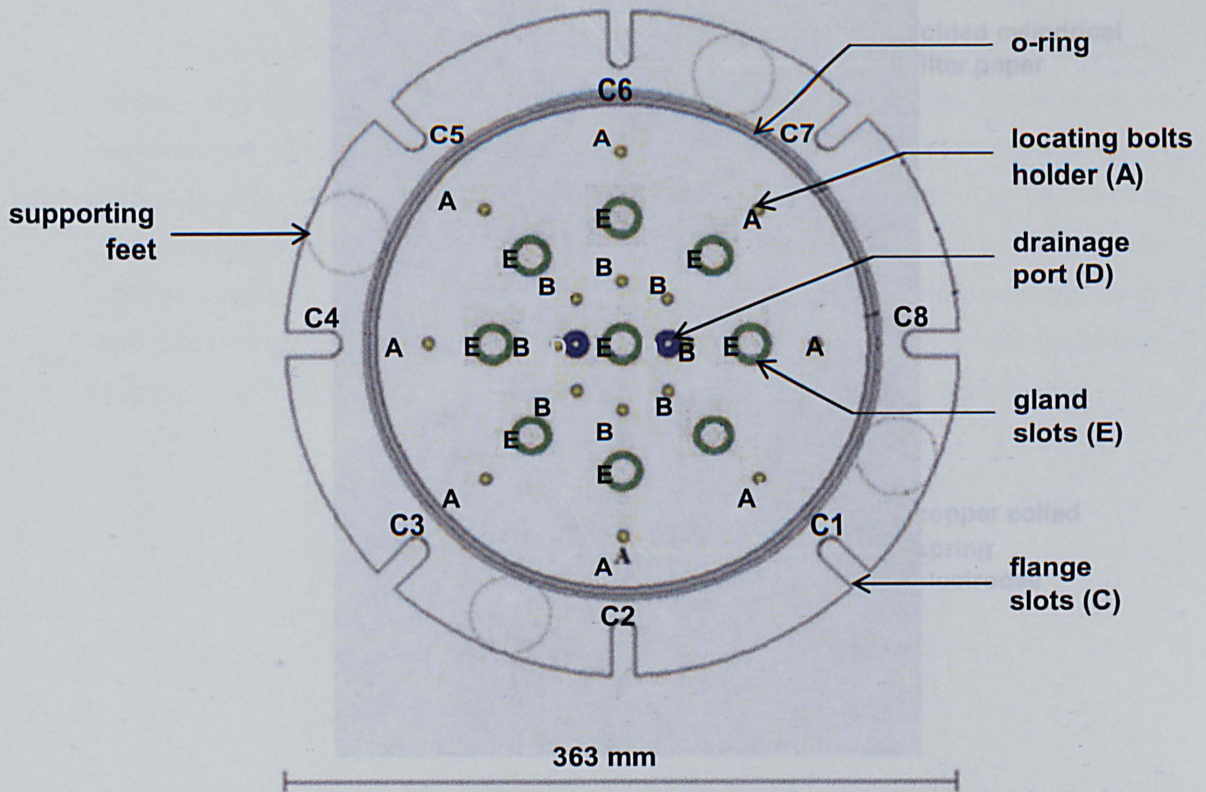


Figure 3.5 Upper plan view base of the cell (A) and (B): locating bolts holder; (C): flange slot; (D): drainage port; (E): gland slots

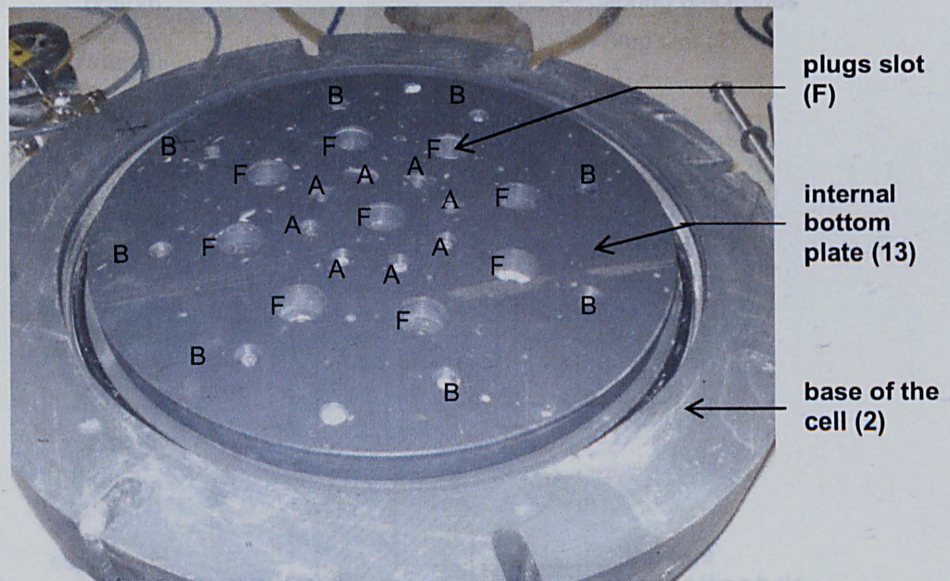


Figure 3.6 Bottom plate on top of the base of the cell (A) and (B): locating bolts holder; (F): plugs slot

3.3.3.1 Plugs

There were cathode and blank electrodes at that electrodes in place. pass through to the water flowing in the Note that O-rings were Figures 3.9 to 3.13

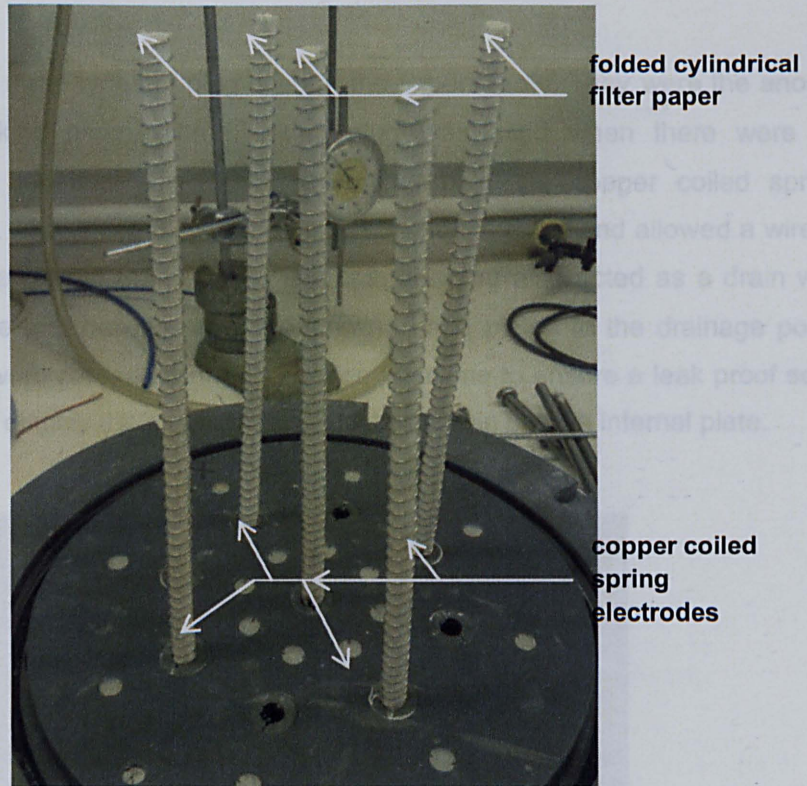


Figure 3.7 Vertically copper coiled spring electrodes together with the folded cylindrical filter paper

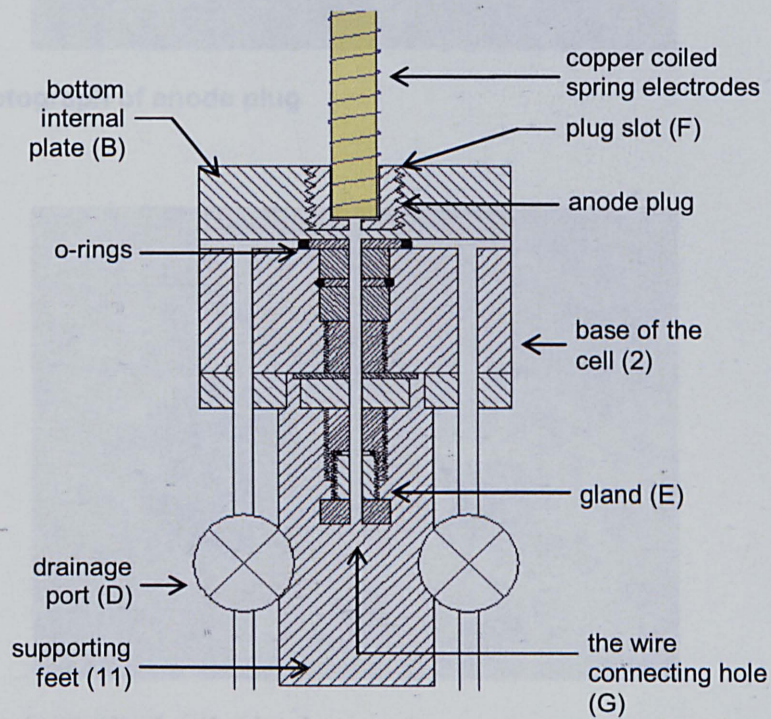


Figure 3.8 Schematic diagram of the anode plug installation

3.3.3.1 Plugs

There were three types of plug used in the experiments. They were the anode, cathode and blanking plugs. The blanking plug was used when there were no electrodes at that location. The other two plugs held the copper coiled spring electrodes in place. These two plugs held the electrodes in place and allowed a wire to pass through to the glands in the base. The cathode plug also acted as a drain with water flowing in the gap between the internal and base plates to the drainage ports. Note that O-rings were placed around the anode locations to ensure a leak proof seal. Figures 3.9 to 3.13 display the plugs and their installation in bottom internal plate.



Figure 3.9 Photograph of anode plug



Figure 3.10 Photograph of cathode plug

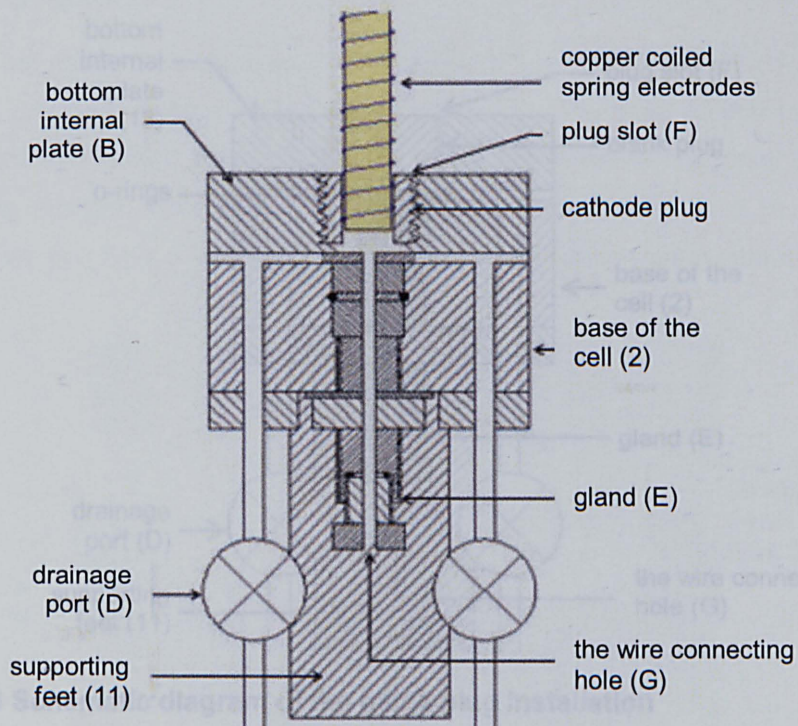


Figure 3.11 Schematic diagram of the cathode plug installation



Figure 3.12 Blanking plug

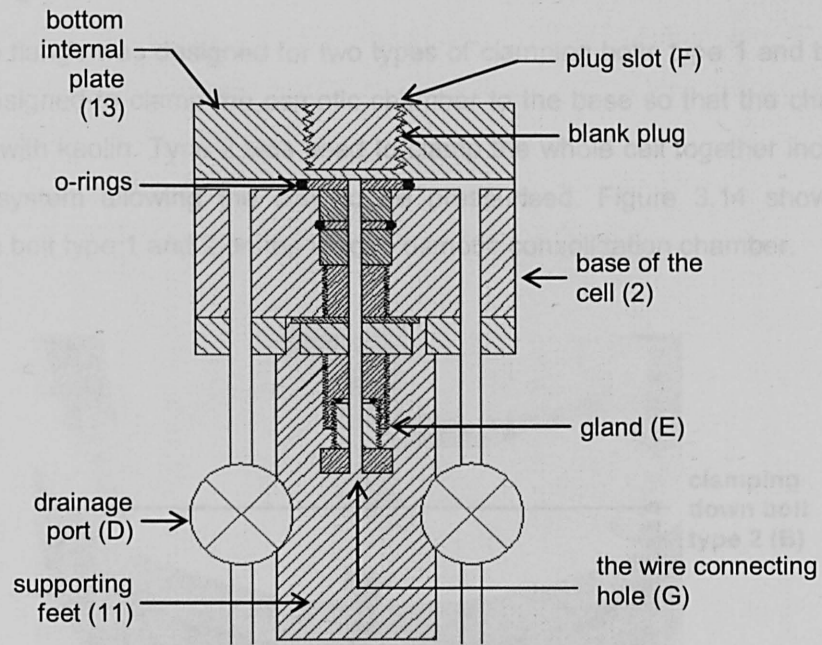


Figure 3.13 Schematic diagram of the blank plug installation

3.3.4 The top of the cell

The osmotic cell consisted of three parts: the top Rowe cell; the test chamber, labelled (1), and the base of the cell, labelled (2). The top of the cell is divided into two parts:- a pressure chamber based on a Rowe cell and a top cap. The Rowe cell is a standard piece of equipment adapted for this experiment. The Rowe cell and top cap are labelled (3) and (4) in Figures 3.1 and 3.2.

Various ports in the Rowe cell cap that is the rim drain (17), the air bleed (18) and the back pressure system were not needed in these experiments. Therefore, they were closed off. The semi-flexible rubber diaphragm in the Rowe cell cap provided an efficient pressure system to allow substantial settlement as a result of osmotic consolidation to take place. Water was used to pressurise the system.

3.3.4.1 Top plate and o-ring

The other essential parts of the top of the cell are the top internal plate (23) and O-ring. The PVC internal top plate was 251 mm diameter and 15 mm thick allowing the plate to move freely within the chamber but maintaining a rigid loading system. When the pressure was applied, it was assumed that an evenly distributed load was transferred to the kaolin sample.

3.3.4.2 Clamping bolts

The top flange was designed for two types of clamping bolts type 1 and type 2. Type 1 was designed to clamp the osmotic chamber to the base so that the chamber could be filled with kaolin. Type 2 was used to clamp the whole cell together including the pressure system allowing the clay to be pressurised. Figure 3.14 shows the clamping down bolt type 1 and 2 on the electro osmotic consolidation chamber.

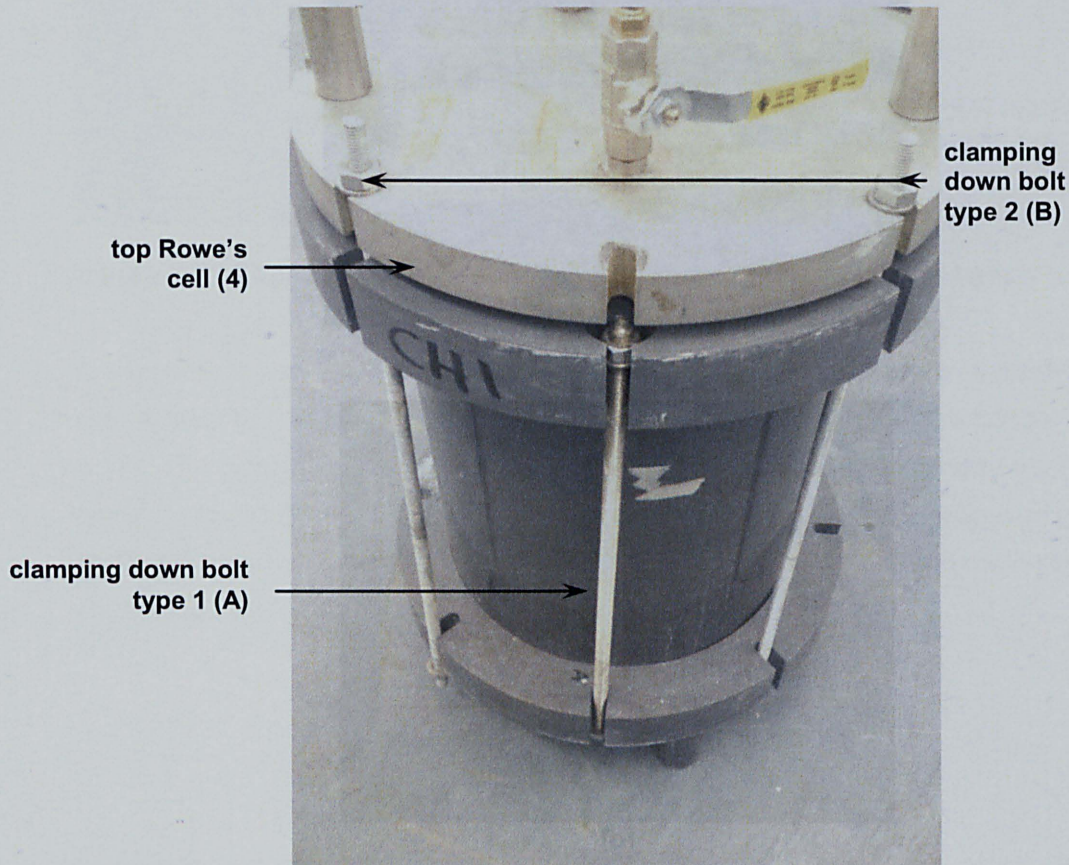


Figure 3.14 Clamping down bolt type 1 (A) and 2 (B)

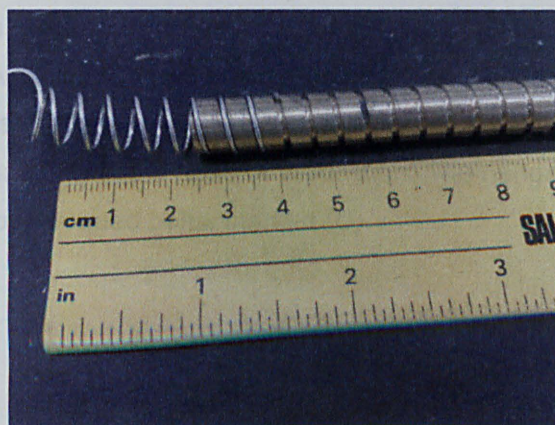
3.3.5 The electrodes

The electrodes used were purpose made springs. A spring was made by winding copper wire around a 8 mm diameter brass cylindrical mandrel as shown in Figure 3.15. Copper was chosen because it is ductile metal and its electrical properties are known and more importantly, the degradation of copper due to osmosis is less than that of steel. A spring was used to allow the electrode to compress as the soil consolidated either due to the external applied pressure or the induced osmotic pore pressure. The electrode was in direct contact with the kaolin. A cylinder of filter paper, as can be seen in Figure 3.7, was used to prevent kaolin entering the core of the

electrode. Figure 3.16 displays the welded copper coiled spring electrode together with the cylindrical folded filter paper. The electrode was supported by the plug (F) in the base plate. The wire connecting the electrode to the power supply was passed through a gland (E) (Figures 3.8 and 3.11).



(a)



(b)

Figure 3.15 Copper coiled spring electrodes showing (a) the brass mandrel, and (b) the spring

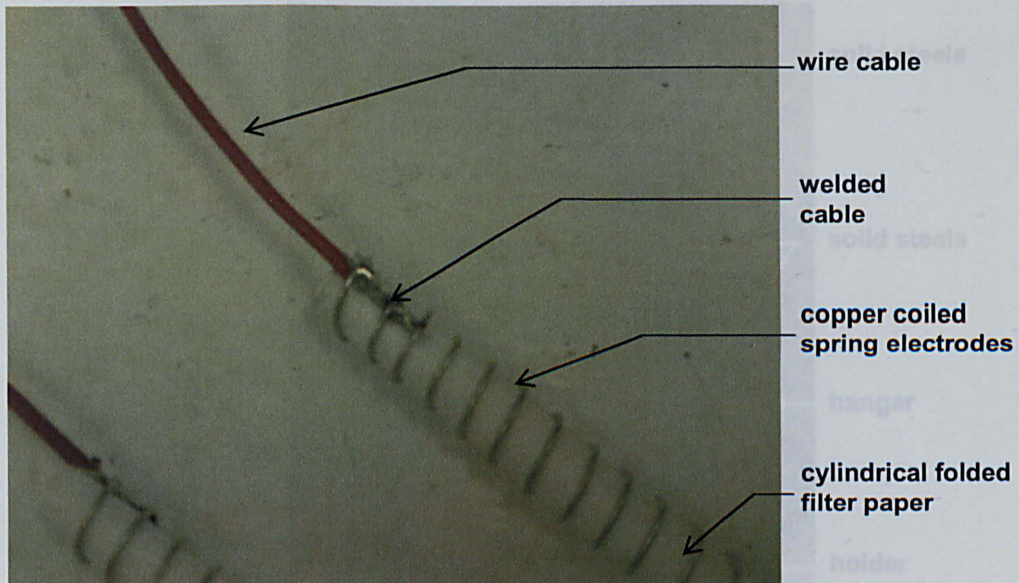


Figure 3.16 Copper coiled spring electrodes together with the filter paper core

A hangar was used to hold the electrodes in position when the soil was placed in the cell. A steel rod was inserted in an electrode and held in place by the hangar (Figure 3.17). The hangar was made of two parts, namely the hangar (labelled A) and the holder (labelled B) as shown in Figures 3.18. The hangar and the holder were made of PVC. PVC was chosen due to the ease of production. The hangar and the holder were connected together by threaded bolts, marked (C).



Figure 3.18 The side view of hangar and the holder

Figures 3.4, 3.5 and 3.10 display the gland (labelled (E)). It was made of stainless steel to limit corrosion. The gland was clamped into the bottom internal plate (13) of the base of the cell. The wire was clamped in place within the gland by an O-ring to ensure that the gland was leak tight (Figures 3.6, 3.11 and 3.13).

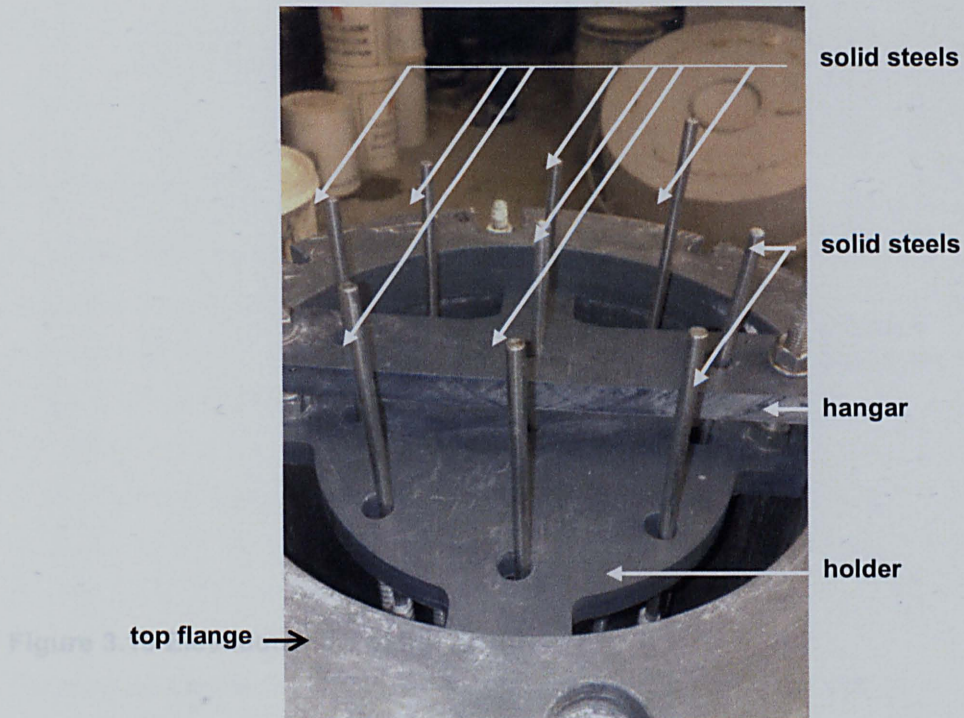


Figure 3.17 Top section fitted with the hangar and solids steel

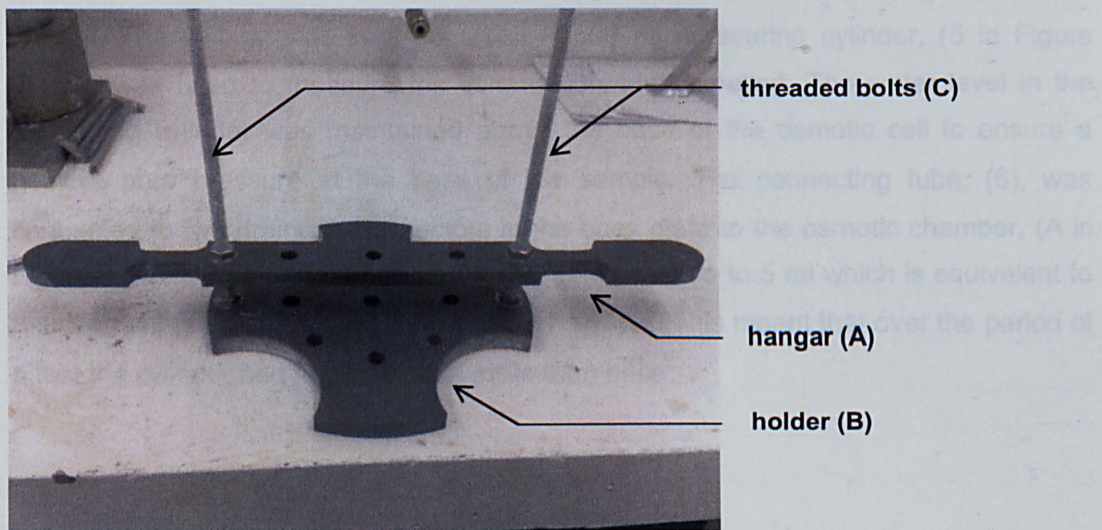
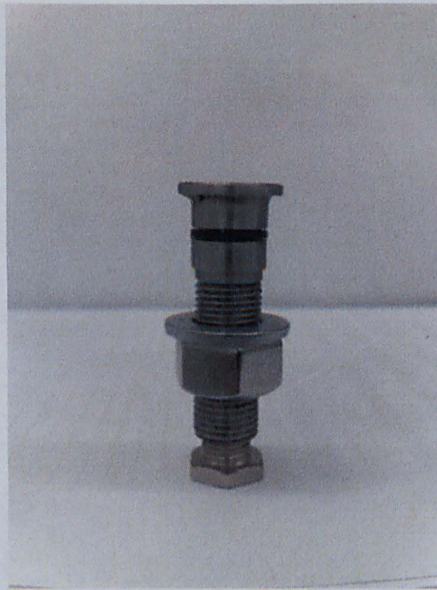


Figure 3.18 The side view of hangar and the holder

Figures 3.4, 3.5 and 3.19 display the gland labelled (E). It was made of stainless steel to limit corrosion. The gland was clamped into the bottom internal plate (13) of the base of the cell. The wire was clamped in place within the gland by an O-ring to ensure that the gland was leak tight (Figures 3.8, 3.11 and 3.13).



drainage
connector

Figure 3.19 Elevation view of the gland

Figure 3.20 Connected drainage connector at the base of the cell

3.3.6 The control systems

Three measurements were taken during a test:- water expelled, settlement and current. The voltage was kept constant. A 500 ml measuring cylinder, (5 in Figure 3.1(a)), was used to measure the volume of water expelled. The water level in the measuring cylinder was maintained above the base of the osmotic cell to ensure a positive pore pressure at the base of the sample. The connecting tube, (6), was connected to two drainage connectors in the base plate to the osmotic chamber, (A in Figure 3.20). It was possible to read a change in volume to 5 ml which is equivalent to a settlement of 0.106 mm occurs in the clay sample. This meant that over the period of a test the cylinder had to be emptied more than once.

3.4.1 Preparation of the apparatus

All equipment was thoroughly cleaned and dried before assembly. It was particularly important to ensure that the o-rings and o-ring grooves were cleaned to ensure a seal. Silicone grease was applied to the rubber diaphragm and settlement rod to ensure that they would move freely without affecting the experimental process. The silicone grease also acted as a seating compound.

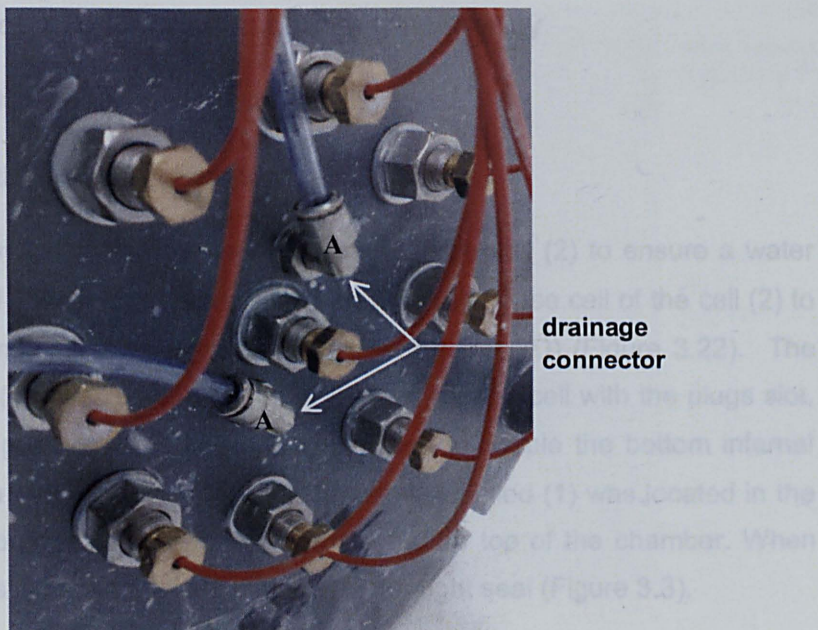


Figure 3.20 Connected drainage connector at the base of the cell

A direct current (dc) power supply was used to control the voltage gradient. Two types of power supply were used, Thurlby Electronics PL 320 that had a maximum capacity of 1 Ampere and 240 Volts, reading to 0.1 Volts and 0.1 Ampere and an SJ Electronics GPS-3303 which a maximum capacity of 15 Ampere and 250 Volts, and reading 0.1 Volts and 0.01 Ampere.

3.4 THE PROCEDURE

This section summarises the procedure of assembling the electro osmotic chamber and conducting the experimental programmes. There were several steps to be followed starting with the assembly of the apparatus until the end stage, which was to clean the apparatus. The steps were (1) assembling the osmotic chamber; (2) installing the electrodes; (3) filling the chamber with clay; (4) assembling the top Rowe cell and other parts; (5) loading the sample; and (6) disassembling the cell.

3.4.1 Preparation of the apparatus

All equipment was thoroughly cleaned and dried before assembly. It was particularly important to ensure that the o-rings and o-ring grooves were cleaned to ensure a seal. Silicone grease was applied to the rubber diaphragm and settlement rod to ensure that they would move freely without affecting the experimental process. The silicone grease also acted as a sealing compound.

3.4.2 Electro osmotic consolidation chamber assembly

The electro osmotic chamber assembly was as follows:-

Step 1: assembling the osmotic chamber

An o-ring was fitted in the o-ring groove in the base of the cell (2) to ensure a water tight seal (Figure 3.21). Filter paper was placed on top of the base cell of the cell (2) to prevent flow of soil material through the drainage port outlet, (D) (Figure 3.22). The bottom internal plate (13) was placed on top of the base of the cell with the plugs slot, (F), aligned with the glands, (E). 16 screws were used to couple the bottom internal plate (13) to the base of the cell (2). The test chamber, labelled (1) was located in the base resting on the o-rings. An o-ring was located on the top of the chamber. When bolt type A flange was clamped in place, it was a water tight seal (Figure 3.3).

Figure 3.22 Location of filter paper

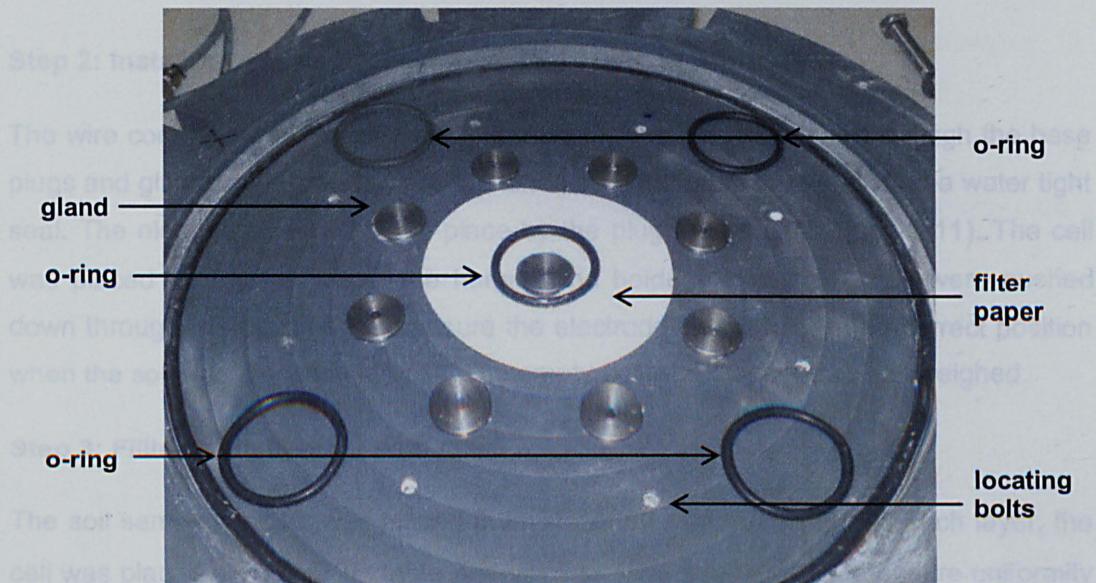


Figure 3.21 Location of small o-ring seals

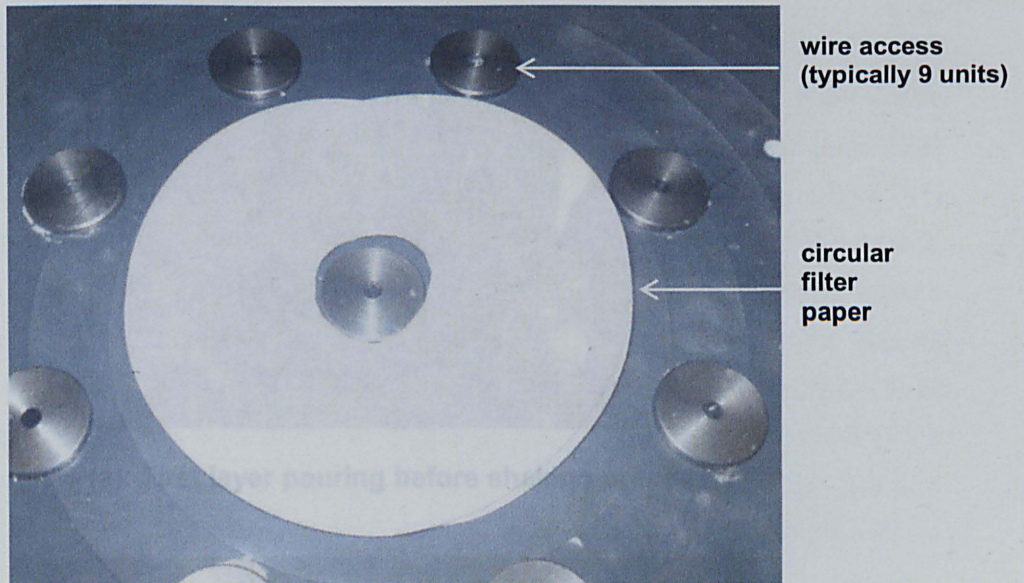


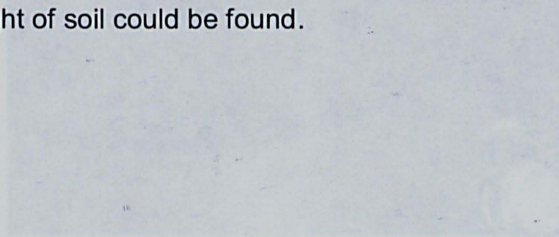
Figure 3.22 Location of filter paper

Step 2: installing the electrodes

The wire connecting the electrodes to the power supply was passed through the base plugs and glands. The glands were tightened onto the base thus providing a water tight seal. The electrodes were held in place by the plugs (Figures 3.8 and 3.11). The cell was placed up right to install the hangar and holder. Solid steel rods were pushed down through the electrodes to ensure the electrodes remained in the correct position when the soil was placed in the cell. The empty cell with electrodes were weighed.

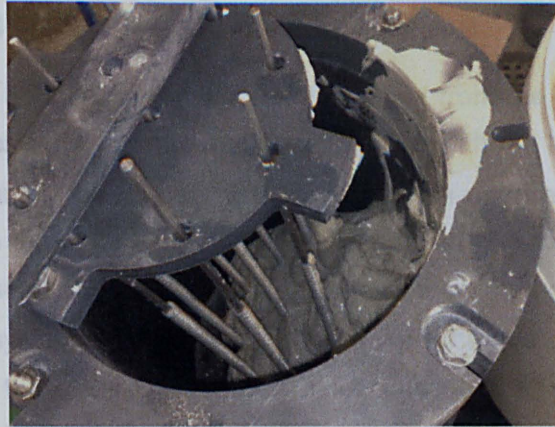
Step 3: Filling the chamber with clay

The soil sample, kaolin, was placed in layers of 50 mm. After pouring each layer, the cell was placed on a shaking table and vibrated for a few minutes to ensure uniformity of the sample and remove entrapped air. This can be seen in Figure 3.23. This was repeated until the total depth of soil was about 300 mm. The cell and soil were weighed so that the initial weight of soil could be found.



(c). First layer after the shaking process

Figure 3.23 Pouring and shaking process



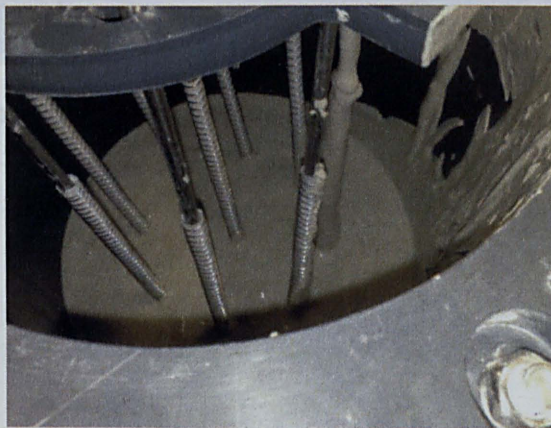
(a): First layer pouring before shaking process



chamber

shaking table

(b): Shaking process



(c): First layer after the shaking process

Figure 3.23 Pouring and shaking process

Step 4: Assembling the control sample

The steel bars, and hangar and holder were removed from the chamber. Filter paper was placed on top of the soil to prevent direct contact with the top plate (Figure 3.24) ensuring that the sample would not stick to the smooth surface. The diaphragm (21) was placed over the top plate and flange of the chamber. Four clamping bolts type 2, labelled (B), were used to clamp the top of the Rowe cell onto the diaphragm to ensure a sealed pressure system. The following checks were carried out before the start of each test to ensure the electro osmotic chamber functioned effectively, namely (1) all valves were closed at the start of a test; (2) the drainage valve was connected to the volume change cylinder; (3) the pressure system was connected to the air pressure valve; and (4) the dial gauge was put in contact with the central rod through the Rowe cell cap.

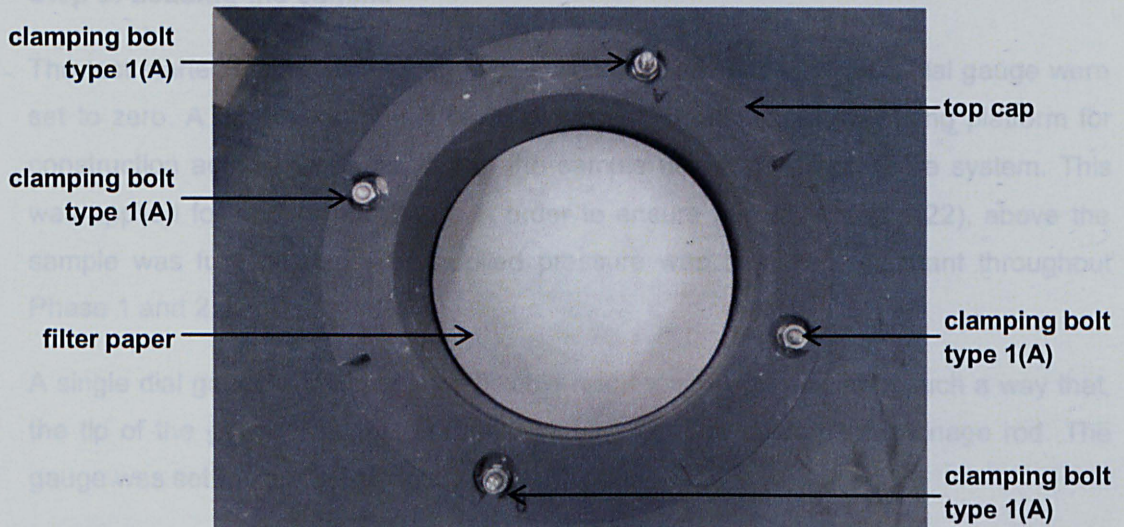


Figure 3.24 Filter paper on the top of the top slurry surface

(1) Phase 1: application of 15 kPa to simulate a working platform and to limit potential cracking at the surface
(2) Phase 2: application of electro osmotic pressure
(3) Phase 3: application of 50 kPa to simulate a surcharge such as that due to a shallow foundation or raising the ground level by about 3m.

In each phase the settlement of the top plate and the volume of water expelled were recorded. Since this was a consolidation test, readings were taken at a frequency used in standard consolidation tests, i.e., 0.07 min, 0.25 min, 0.5 min, 1 min, 2 mins, 4 mins, 8 mins, 15 mins, 30 mins, 60 mins, 120 mins, 240 mins, 480 mins, 1440 mins, 1680 mins, 1920 mins, 2880 mins, 4320 mins, 5760 mins, ... 10080 mins.

drainage valve →

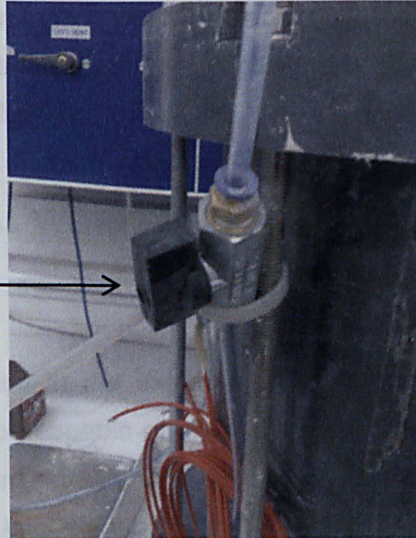


Figure 3.25 Drainage valve

Step 5: Loading the sample

The test started when the drainage valve was opened. The timer and dial gauge were set to zero. A predefined pressure of 15 kPa which simulates a working platform for construction activities was applied to the sample using the air pressure system. This was applied for about three hours in order to ensure the diaphragm, (22), above the sample was fully inflated. The applied pressure was then kept constant throughout Phase 1 and 2.

A single dial gauge supported by a flexible retort stand was placed in such a way that, the tip of the gauge was just in direct contact with the settlement drainage rod. The gauge was set to zero before the start of the tests.

There were three phases in each test:-

- (1) Phase 1: application of 15 kPa to simulate a working platform and to limit potential cracking at the surface.
- (2) Phase 2: application of electro osmotic pressure.
- (3) Phase 3: application of 50 kPa to stimulate a surcharge such as that due to a shallow foundation or raising the ground level by about 3m.

In each phase the settlement of the top plate and the volume of water expelled were recorded. Since this was a consolidation test, readings were taken at a frequency used in standard consolidation tests, i.e, 0.167 min, 0.25 min, 0.5 min, 1 min, 2 mins, 4 mins, 8 mins, 15 mins, 30 mins, 60 mins, 120 mins, 240 mins, 480 mins, 1440 mins, 1680 mins, 1920 mins, 2880 mins, 4320 mins, 5760 mins, ..., 10080 mins.

Phases 1 and 3 were terminated when primary consolidation had ceased. This was when no further water was expelled. The length of time for osmotic consolidation was one of the variables investigated.

3.5 EXPERIMENTAL WORKS

3.5.1 Kaolin sample

The soil to be used in the experiment had to have sufficiently low enough hydraulic permeability to be capable of electro osmotic consolidation treatment; and it had to be uniform to ensure repeatability. China Clay Grade E kaolin was chosen. The classification data for that kaolin are given in Table 3.1. The chemical characteristics of the kaolin are given in Table 3.2.

Table 3.1 Atterberg's limits and specific gravity of kaolin grade E used in the tests

Soil Indexes	Hamir (1997)	Researcher (2010)
Plastic Limit, w_p (%)	34%	35%
Liquid Limit, w_L (%)	55%	53%
Plasticity Index, I_p (%)	20%	18%
Specific Gravity, G_s	2.60*	2.65*
Soil Classification	MH	MH

*obtained from manufacturer's documentation.

Kaolin has been used in many studies, for instance Andreou *et al.* (2008), Suter (2008), Kalumba (2006), Hamir (1997), and Al-Tabbaa and Wood (1987). This meant that there is a significant body of knowledge of the properties of kaolin. Kaolin has been chosen because it is supplied in powder form which means that the spatial variability of samples can be controlled. This means that samples can be prepared with the same properties. Kaolin is supplied as a white powder made up of, in the main, by a hydrous aluminium silicate clay mineral kaolinite.

Table 3.2 Chemical features of grade E white kaolin

Features	(%)
Silicon Oxide (quartz), SiO_2	50%
Aluminium (III) Oxide (diaspore), Al_2O_3	35%
Loss on Ignition	11%
Alkalis, K_2O , Na_2O	2.7%
Ferum (III) Oxide, Fe_2O_3	1.1%
Water-soluble salt content	0.15%
Ph at 10% solids	5.0 ± 0.5
w_c maximum	1.5%

3.5.1.1 Soil classification test

The liquid limits, w_L , and plastic limits, w_P , were determined using the procedure described in BS 1377: Part 2: 1990, Clause 4.3 for liquid limits with cone penetrometer, and Clause 5.3 for plastic limits. The particle size distribution, obtained from the manufacturer's technical specification, is displayed in Figure 3.26. The kaolin is defined as well graded very fine clay (British Standard 1377-2:1990).

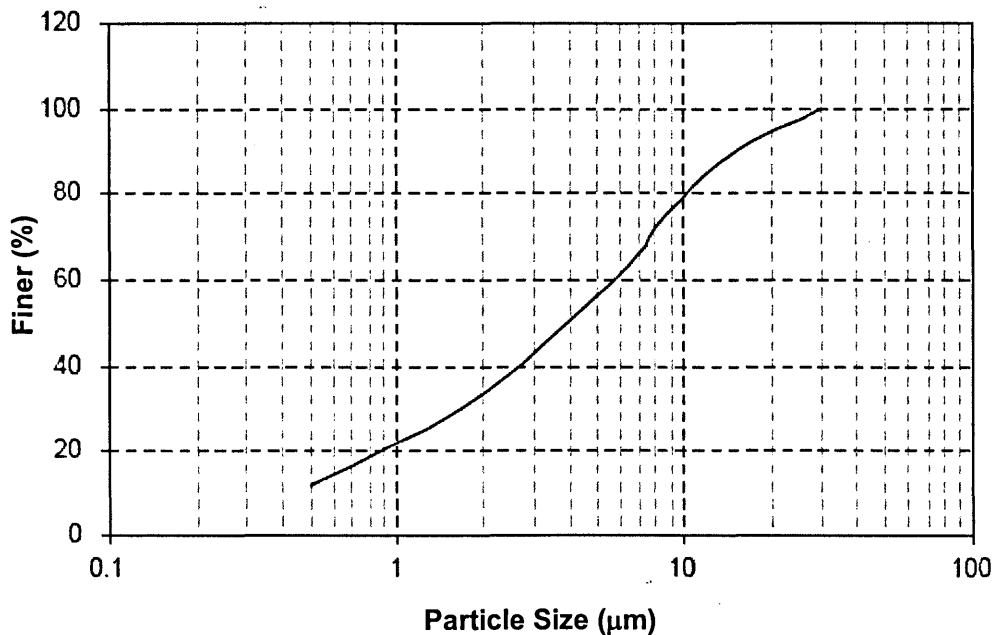


Figure 3.26 Particle size distribution graph for grade E kaolin

3.5.1.2 Preparation of kaolin slurry

All samples were prepared in the same way. Kaolin powder was mixed with deaired water to produce a slurry at 150% of the liquid limit. This helped ensure a saturated sample. The mixture was put aside for a few days to ensure homogeneity. Typically 22 kg of kaolin was placed in the electro osmotic consolidation cell in several layers to a predetermined depth of approximating 300 mm and care was taken to minimize entrapped air.

3.5.3 Loading stages

There were three loading phases. The first was to create uniform conditions in the sample and apply a positive stress thus preventing cracking during the osmotic process. A 15 kPa pressure was applied to the top plate. Typically, it took 14 days to 16 days to reach steady state. A constant 5 Volts was applied during the second phase while still maintaining the 15 kPa external applied pressure. This was applied for 12

days to 19 days, depending on the electrode life. The current was switched off when no further water was expelled as described in Section 3.4.2 step 5, and the applied pressure increased to 50 kPa. This third phase was used to determine the impact of the osmotic process on the overall stiffness of the sample.

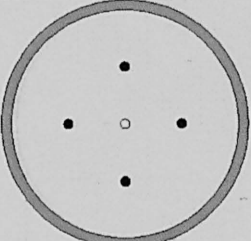
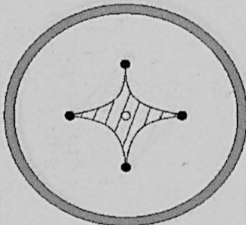
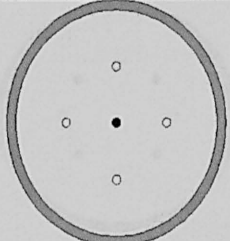
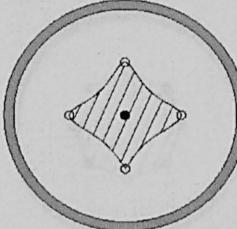
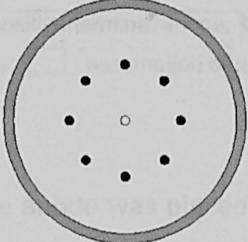
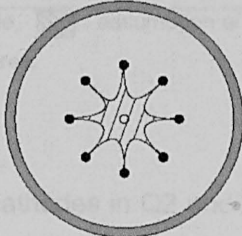
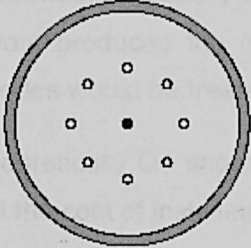
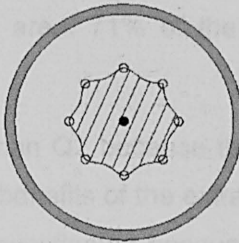
3.5.4 Electro osmotic piles series

A total of twenty three electro osmotic consolidation tests and one control test were performed in this research programme. The main objectives were to determine the most effective electro osmotic consolidation configuration with respect to stiffening of soft clay soil, and to determine the effect osmotic consolidation had upon the overall stiffness of the sample.

All the cathode locations were open while the anode was closed. This meant a negative pressure would be developed at the anode. This pore pressure can be predicted using theorems developed by Esrig (1968) and Mitchell (1993).

Table 3.3 shows the six arrangements of electrodes use in the programme. The other tests variables were the time of treatment and applied voltage.

Table 3.3 Electrode layout

Electrodes Layout	Coded	Approximate of effective treated area	Polygon Type
	Q1		Concave
	Q2		Kite octagon
	Q3		Concave octagon
	Q4		Octagon


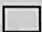
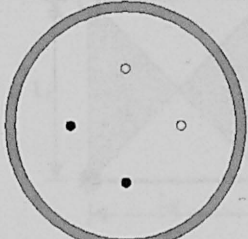
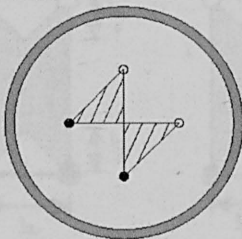
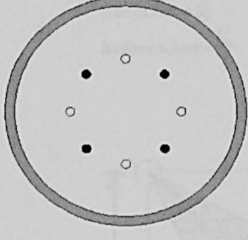
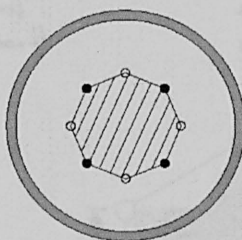


o: positive terminal/anode; ●: negative terminal/cathode,  : assumption of approximate of effective area;  : assumption of approximate of ineffective area.

Table 3.3 Electrode layout

Electrodes Layout	Coded	Approximate of effective treated area	Polygon Type
	A1		Quadrilateral
	A2		Octagon

o: positive terminal/anode; ●: negative terminal/cathode,  : assumption of approximate of effective area;  : assumption of approximate of ineffective area.

The anode was placed at the centre of the cathodes in Q2 and Q4. Previous studies by Alshawabkeh (2001) and Alshawabkeh *et al.* (1999) suggested that the hexagonal layout produced the most effective treated area. 71% of the area enclosed by the anodes would be treated.

Theoretically Q4 should be more effective than Q2 because there are more cathodes but the cost of installation might out way the benefits of the extra improvement. Q1 and Q3, the mirror image of Q2 and Q4, were investigated because of the degradation of the anodes in Q2 and Q4 may be too great leading to a reduction in the effectiveness of the improvement. The pilot study was according to the model of Alshawabkeh, 2001, and Alshawabkeh *et al.*, 1999. The octagonal layout was been selected as the first initial stage and coded as Q3.

Sample A1 was the arrangement suggested by Alshawabkeh, 2001, and Alshawabkeh *et al.*, 1999.

Sample A2 represents a modified arrangement of Q4 layout where electrode polarity is interchanged at every other position and the central node is removed. The distance between nodes is reduced from 63 mm (Q4 layout) to 49 mm (A2 layout).

Figure 3.27 shows the effective electric field for the 1D (A1 and A2) and 2D (Q2 and Q4) electrode layout. Table 3.4 summarises the aim of the tests, the layout code, the treatment time and the voltages.

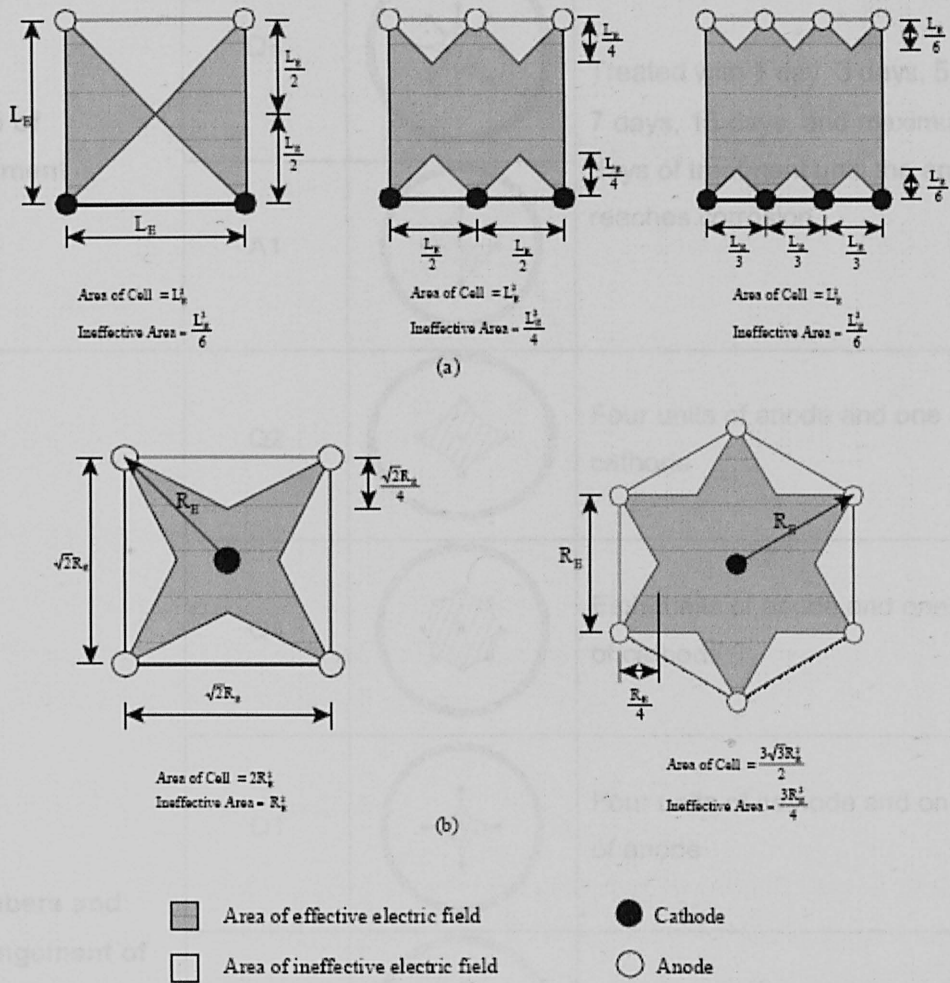


Figure 3.27 Approximate evaluation of ineffective areas for (a) 1-D and (b) 2-D electrode configurations (Alshawabkeh *et al.*, 1999; Alshawabkeh, 2001)

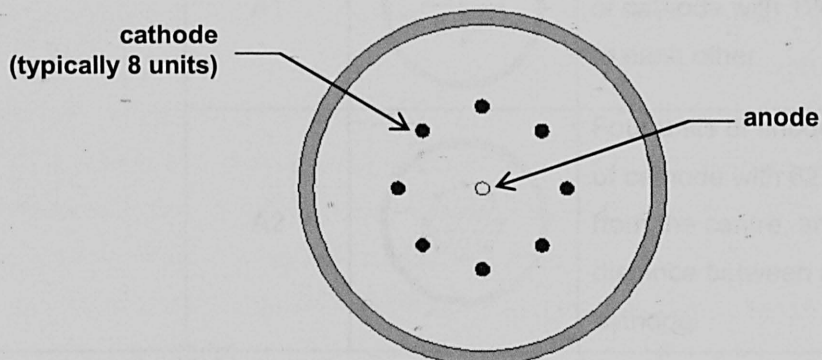
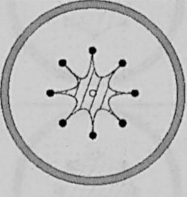
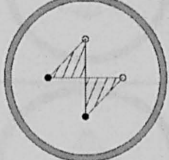
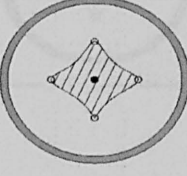
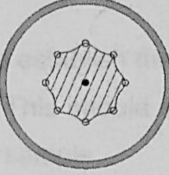
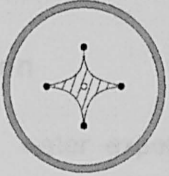
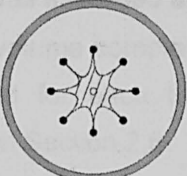
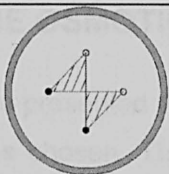
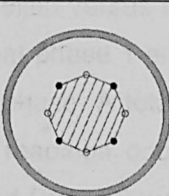
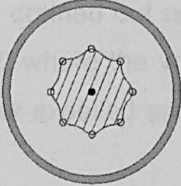
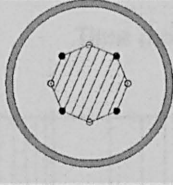
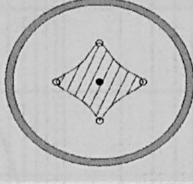


Figure 3.28 Hexagonal layout for primary experimental work
Table 3.4 Series of experimental works

Series	Layout Codes	Treated area	Remarks
Time of treatment	Q3		Treated with 1 day, 3 days, 5 days, 7 days, 15 days, and maximum days of treatment until the anode reaches corrosion
	A1		
Numbers and arrangement of electrodes	Q2		Four units of anode and one unit of cathode
	Q4		Eight units of anode and one unit of cathode
	Q1		Four units of cathode and one unit of anode
	Q3		Eight units of cathode and one unit of anode
	A1		Two units of anode and two units of cathode with 124 mm distance to each other
	A2		Four units of anode and four units of cathode with 62 mm radians from the centre, and 49 mm distance between anode to cathode

Different Applied Voltages	Q4		Treated with 5 Volts, 10 Volts, and 20 Volts
	A2		Treated with 5 Volts, and 10 Volts
	Q2		Treated with 5 Volts, and 10 Volts

3.5.4.5 Control test

The control test was used to establish the performance of the clay sample when only Phase 1 and 3 were applied. This should demonstrate the impact of Phase 2 on the overall performance of the clay sample.

3.5.5 Parameters determination

The vertical displacement, water expelled and current during a test were recorded. The water content, w_c was assessed at various positions at the end of a test. The voids ratio, e_o , coefficient of volume compressibility, m_v , and average constrained stiffness, $E_{stiffness}$, were calculated for each test. The full equations for all these parameters have been discussed in Section 2.6.

3.6 AN EXAMPLES OF THE OSMOTIC TEST

An example of the results is presented here. Configuration Q3 with 5 Volts for 24 hours of osmotic treatment was chosen. The results of the vertical displacement versus time curves, and water expelled versus time curves are shown in Figures 3.29 to 3.34. These two figures show that phase 1 and phase 3 required almost 14 days to reach the secondary compression phase. A total of 31.94 mm and 1613 ml of vertical displacement and water expelled readings occurred during Phase 1. As mentioned earlier in Section 3.5.3, Phase 1 and Phase 3 were carried out to avoid cracking and to measure average constrained stiffness, respectively.

A total of 847 ml water has been drained out and 17.47 mm of vertical displacement took place in Phase 3. In Phase 2, where the voltage was applied to treat the sample for 24 hours, it shows 24 ml water expelled and 0.49 mm of vertical readings, due to electro osmosis.

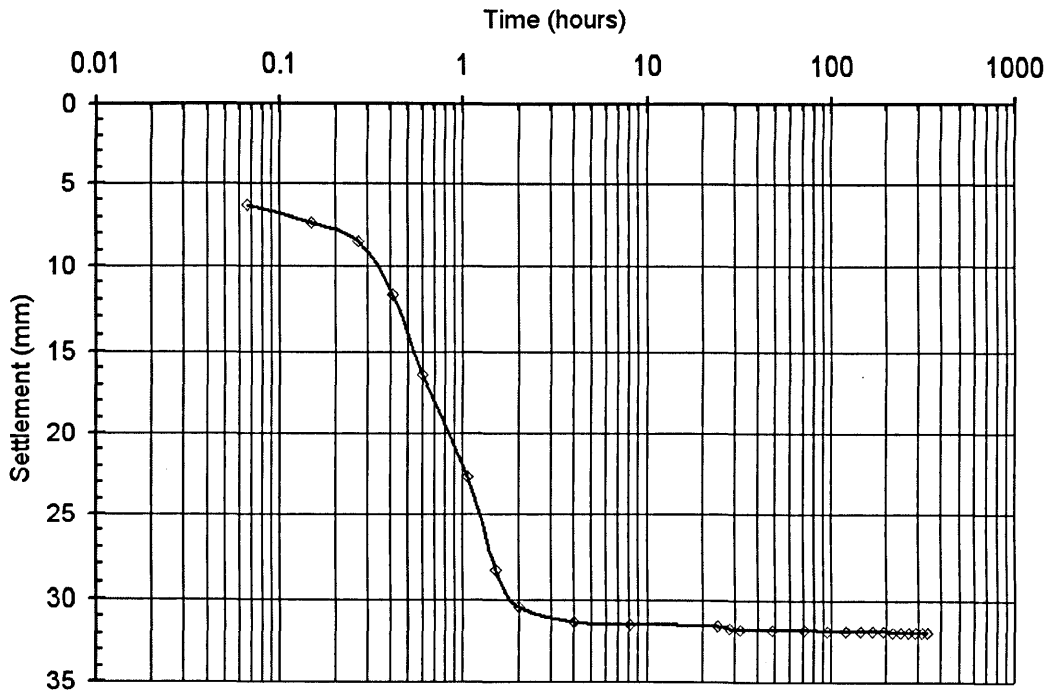


Figure 3.29 Results for Q3 on phase 1: vertical displacement versus time

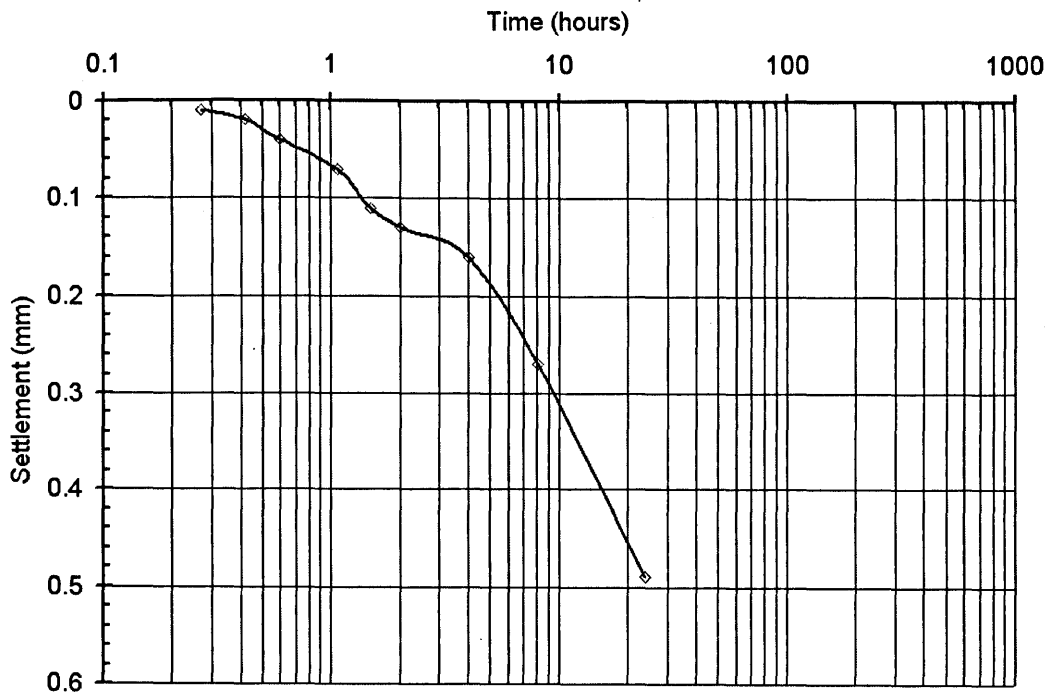


Figure 3.30 Results for Q3 on phase 2: vertical displacement versus time

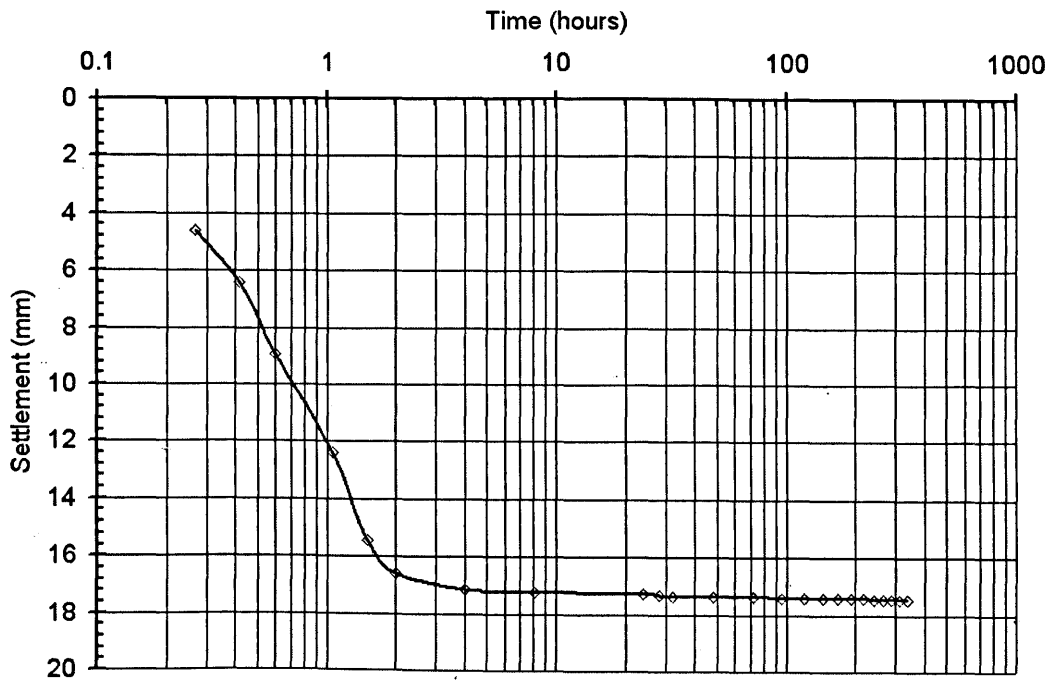


Figure 3.31 Results for Q3 on phase 3: vertical displacement versus time

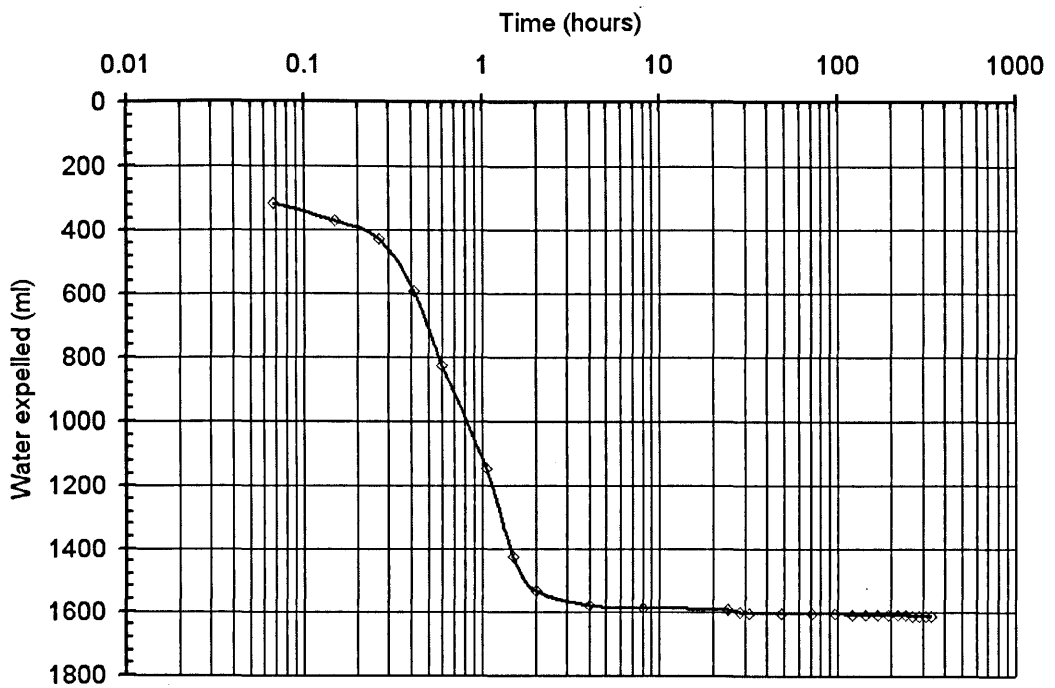


Figure 3.32 Results for Q3 on phase 1: water expelled versus time

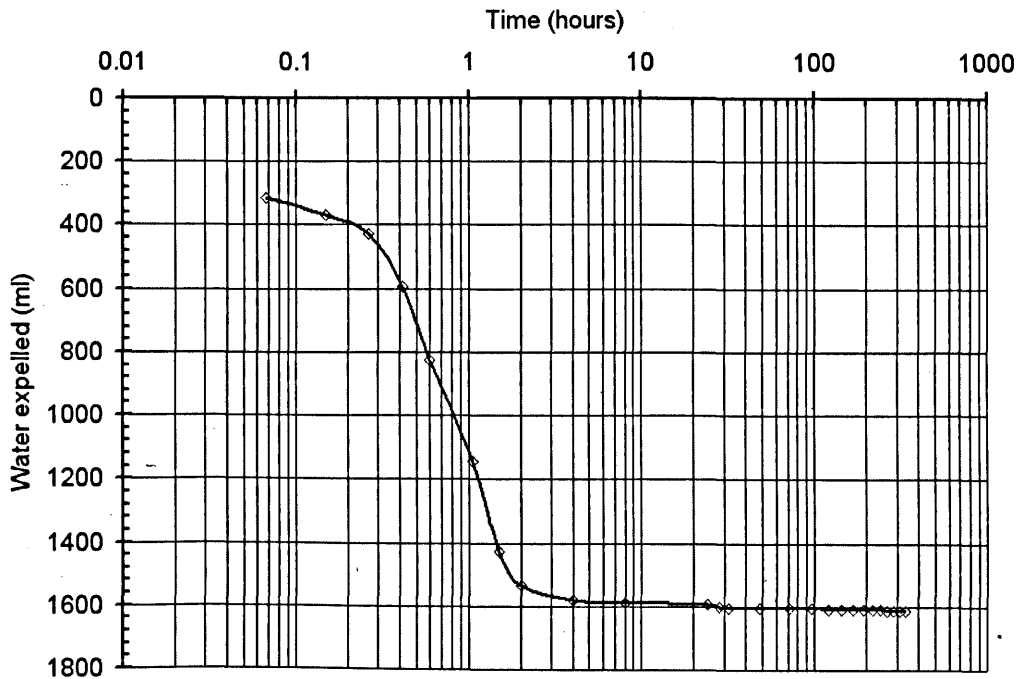


Figure 3.33 Results for Q3 on phase 2: water expelled versus time

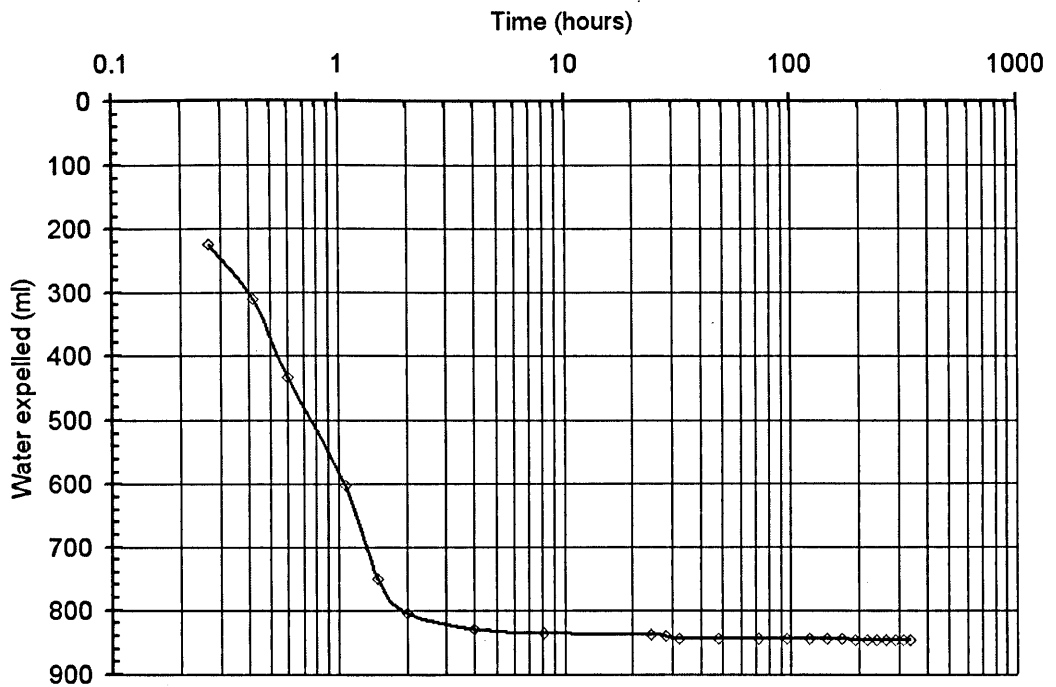


Figure 3.34 Results for Q3 on phase 3: water expelled versus time

Figure 3.35 shows the volume calculated from the volume readings plotted against the volume of water expelled. The experimental line is very nearly at 45° which suggests the accuracy of the measurements was acceptable.

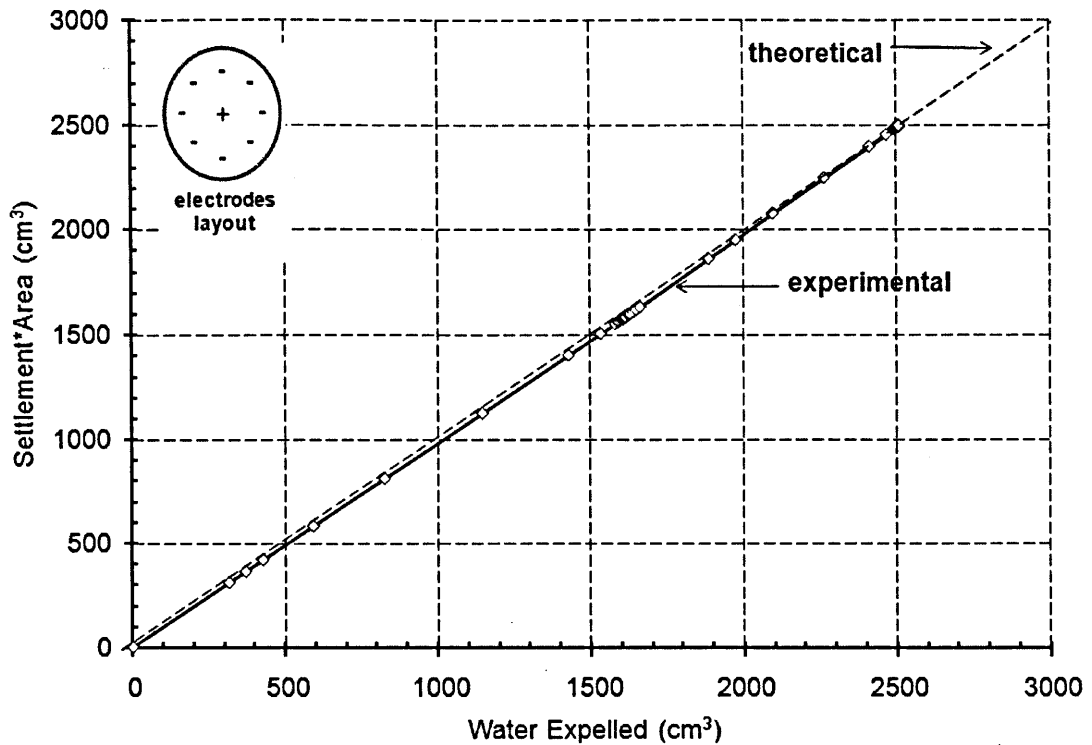


Figure 3.35 Results for Q3: vertical displacement*area versus water expelled

Figure 3.36 displays the water expelled and current readings versus time for Phase 2. The water expelled lines shows that there was a gradual rise from the start of the experiment. During treatment the applied voltage and current were monitored continuously. The applied voltage was 5 Volts, and it remained constant over the test. The electric field within the electro osmotic consolidation chamber was generated by nine copper coiled spring electrodes. The output current was observed with time and the result is presented in Figure 3.36, showing that the current dropped gradually throughout treatment from 68 mA to 26 mA. The most noticeable difference between 2 hours and 8 hours is the increase in current with time where this is attributed to the increase in electrical conductivity of the soil pore fluid. The current decreases sharply in the last 16 hours from 63 mA to 37 mA as the corrosion process of the anode starts. The decrease of current with time under a constant voltage is attributed to the conduction and polarisation behaviour in such systems is dominated by ions.

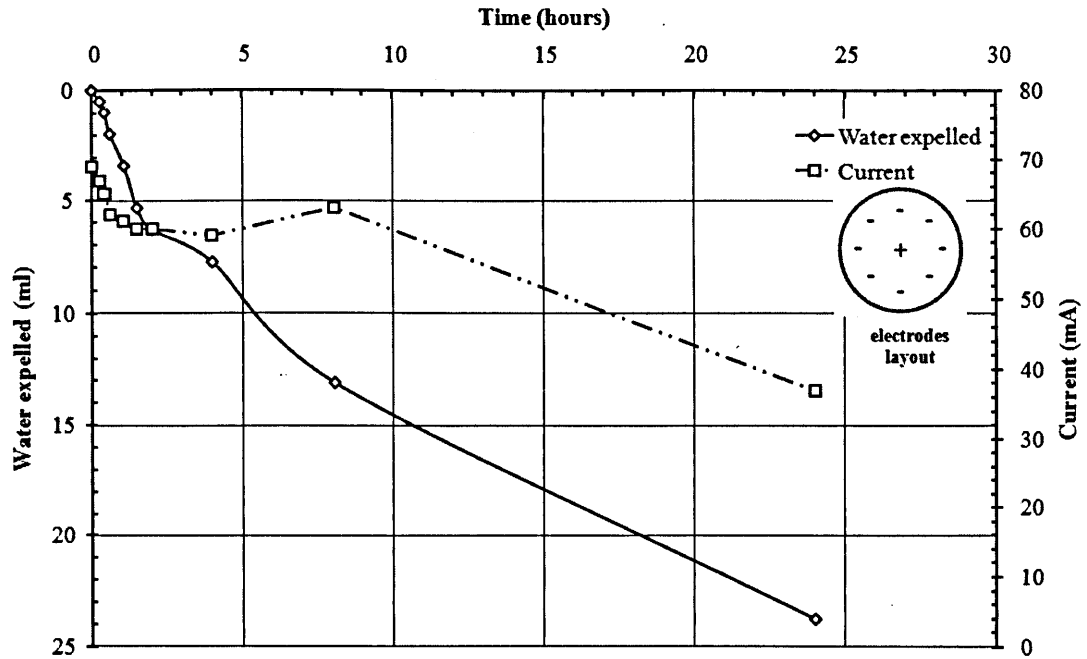


Figure 3.36 Results of Q3V51d test: water expelled and current versus time

The effect of electro osmotic consolidation treatment can be further evaluated from the water content after treatment. Figure 3.37 presents the results, where the determination of water content was only carried out at the surface near to the top internal plate. Micic *et al.* (2003b) concluded that the water content at different depth was fairly uniform. Hence measurements of water content were only made at the surface. The initial water content was 79.5%. The water content at the end of the experiment was, on average 51.0%.

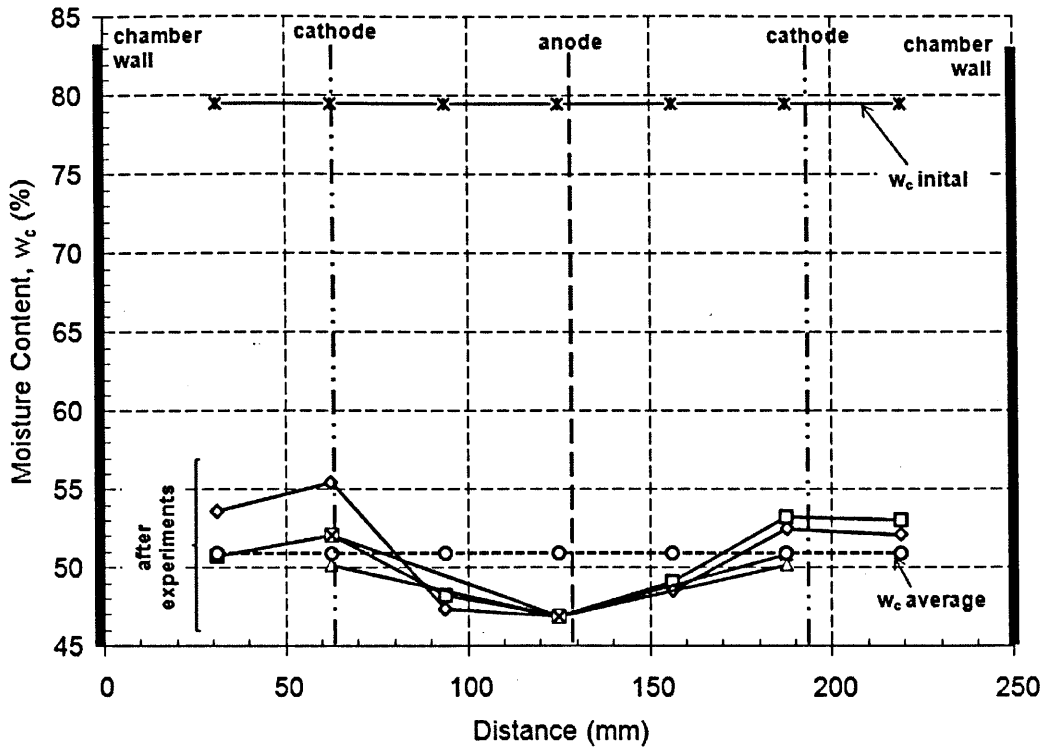


Figure 3.37 Results of Q3V51d test: water content versus distance

The voids ratio decreased from 2.123 at 0 kPa to 1.598 at 50 kPa. And at the end of Phase 3, the voids ratio shows that the value from the treated soil is slightly higher than that from the control test. Voids ratio changes for the control test are 0.200 at the end of 50 kPa compared 0.182 for treated sample (Table 3.5 and Figure 3.38).

Table 3.5 Summary of experiments after electro osmosis for Q3 sample treated with 5 Volts for 24 hours

σ' (kPa)	ΔH (mm)	e_o	Δe_o	$1 + e_{average}$	$\Delta e/\Delta\sigma'$	m_v (m^2/MN)
0	0	2.123	not applicable	2.956	0.022	0.0075
15	31.94	1.790	0.332			
15 + 5 Volts	1.02	1.780	0.011	2.689	0.005	0.0019
50	17.46	1.598	0.182			

σ' : pressure; ΔH : vertical displacement; e_o : voids ratio; Δe_o : voids ratio change; $e_{average}$: average of voids ratio; m_v : the coefficient of volume compressibility.

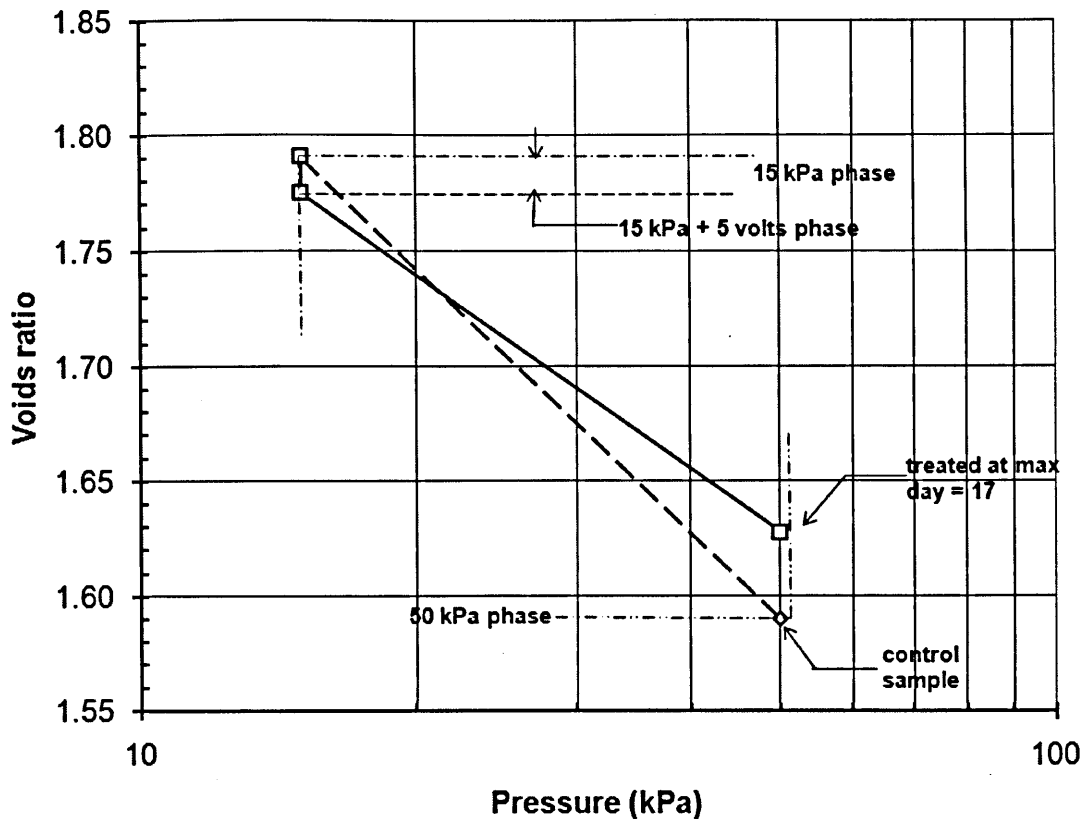


Figure 3.38 Voids ratio for Q3V5 and control sample

3.7 CONCLUSIONS

This chapter has established the principles, design, procedure, experimental works, and an example of a test. An electro osmotic consolidation chamber was designed and fabricated to measure the vertical displacement and water expelled. The design used vertical copper coiled spring setup that enabled applications of the vertical load. Those design considerations and experimental setup on the electro osmotic piles series, i.e., time of treatment, numbers of electrodes, the arrangement of electrodes, and different applied voltage, were chosen for their practicality in situ applications. During the experiment, the volume change, the voltage and current readings were monitored. Hence, the example results showed in Section 3.6, led to the conclusion that electro osmotic consolidation treatment of kaolin slurry with 79.5% with one unit of anode and eight units of cathodes for 24 hours of applied voltage is an effective method. Due to the significant stiffening effect at end of 50 kPa, this method has potential applications in stiffening soft soils at in situ. The full results on the electro osmotic piles series, i.e., time of treatment, numbers of electrodes, the arrangement of electrodes, and different applied voltage are discussed in Chapter 4.

CHAPTER 4

RESULTS AND DISCUSSION

4.1 GENERAL

In this chapter, the results of electro osmotic pile tests are presented. Factors affecting the treatment, including the time of treatment, numbers of electrodes, the arrangement of electrodes and applied voltage are examined. This was discussed in brief in Section 3.5.4.

Twenty one tests were performed on China Clay Grade E kaolin, as summarised in Table 4.1. The electrode layout and series of experimental works are listed in Tables 3.3 and 3.4, respectively. Twenty osmotic tests were carried out with applied voltage and one test without applied voltage as a control test.

Electro osmotic consolidation treatment was started after phase 1, in which the slurry was consolidated under 15 kPa vertical pressure. During the tests, the settlement (vertical displacement) and volume of water expelled were recorded, and at the end of tests the water content was determined.

The results are reported in terms of changes of sample volume (settlement and water expelled), water content and current readings. They are compared and discussed with the results obtained from the control test. The results were interpreted to produce several important parameters which are summarised in Table 4.2. These are voids ratio, e_o ; coefficient of volume compressibility, m_v ; average constrained stiffness, $E_{stiffness}$; average constrained stiffness at build phase, $E_{build\ phase}$; average constrained stiffness at pre-treatment phase, $E_{pre-treatment}$. A summary of test results are included in each section; full sets of data in the APPENDIX D. The tests are discussed in Section 4.4.

Table 4.1 Summary of the electro osmotic piles test

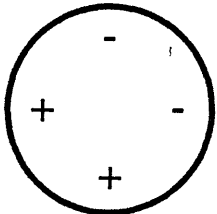
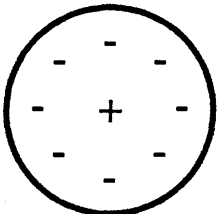
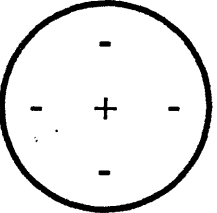
Series	Electrode layout	Code	Time of treatment (days)			Applied voltage (volts)	Distance anodes to cathodes (mm)	
			Phase 1	Phase 2	Phase 3			
Time of treatment		A1V51d	16	1	16	5	124	
		A1V53d		3				
		A1V55d		5				
		A1V57d		7				
		A1V515d		15				
		A1V519d		19				
				Q3V51d				14
	Q3V53d		3					
	Q3V55d		5					
	Q3V57d		7					
	Q3V515d		15					
	Q3V517d		17					
	Numbers and arrangement of electrodes			Q1V515d	15	15	15	

Table 4.1 Summary of the electro osmotic piles test

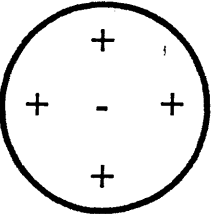
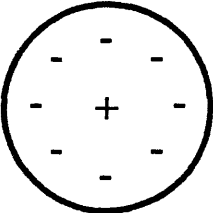
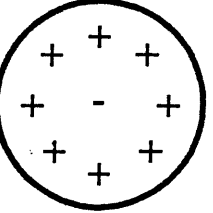
Series	Electrode layout	Code	Time of treatment (days)			Applied voltage (volts)	Distance anodes to cathodes (mm)
			Phase 1	Phase 2	Phase 3		
Numbers and arrangement of electrodes		Q2V516d	17	16	17	5	63
		Q3V517d	14	17	14	5	63
		Q4V516d	17	16	17	5	63

Table 4.1 Summary of the electro osmotic piles test

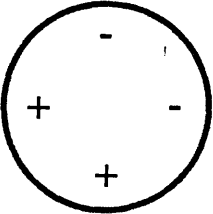
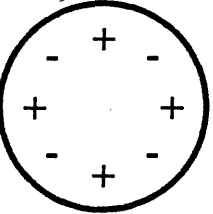
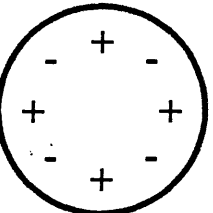
Series	Electrode layout	Code	Time of treatment (days)			Applied voltage (volts)	Distance anodes to cathodes (mm)
			Phase 1	Phase 2	Phase 3		
Numbers and arrangement of electrodes		A1V519d	16	19	16	5	124
		A2V517d	15	17	15	5	49
Different applied voltage		A2V517d	15	17	15	5	49
		A2V1016d	15	16	15	10	49

Table 4.1 Summary of the electro osmotic piles test

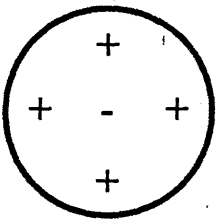
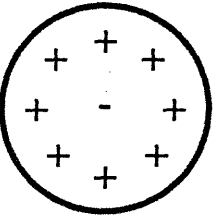
Series	Electrode layout	Code	Time of treatment (days)			Applied voltage (volts)	Distance anodes to cathodes (mm)
			Phase 1	Phase 2	Phase 3		
Different applied voltage		Q2V516d	17	16	17	5	63
		Q2V1015d	17	15	17	10	63
		Q4V516d	17	16	17	5	63
		Q4V1014d	17	14	17	10	63
		Q4V2012d	17	12	17	20	63
			17	12	17	20	63

Table 4.2 Computed results

Symbol	Notations	Unit
e_o	voids ratio	no unit
m_v	coefficient of volume compressibility	m^2/MN
$E_{stiffness}$	Average constraint stiffness	kPa
$E_{build\ phase}$	Average constraint stiffness at build phase	kPa
$E_{pre-treatment}$	Average constraint stiffness at pre-treatment phase	kPa

4.2 CONTROL TEST

4.2.1 Test conditions

The control test was loaded with 15 kPa in the first phase and 50 kPa in the second phase to provide information on the behaviour of the slurry only subject to an increase in pressure. Both drainage valves underneath the base of the cell were open during the test. The test lasted 432 hours and 336 hours for phases 1 and 2, respectively.

4.2.2 Test results

The results for the control test are presented in Figures 4.1 until 4.3. The full results of the control test are summarised in Table D1 in the APPENDIX D.

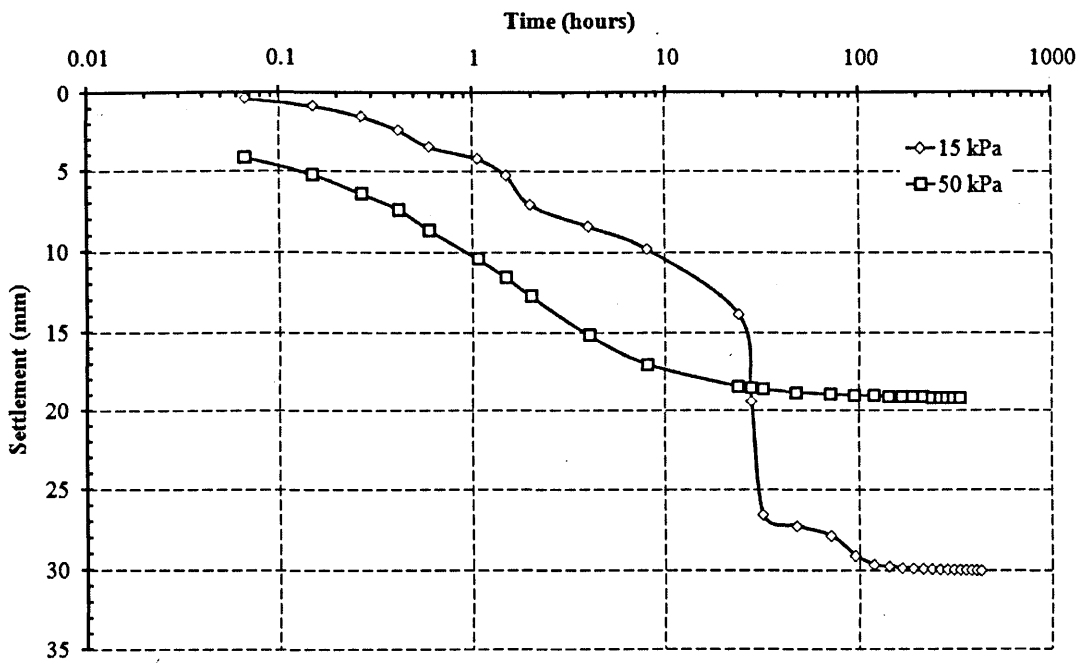


Figure 4.1 Result of Control Test: relative vertical displacement versus time

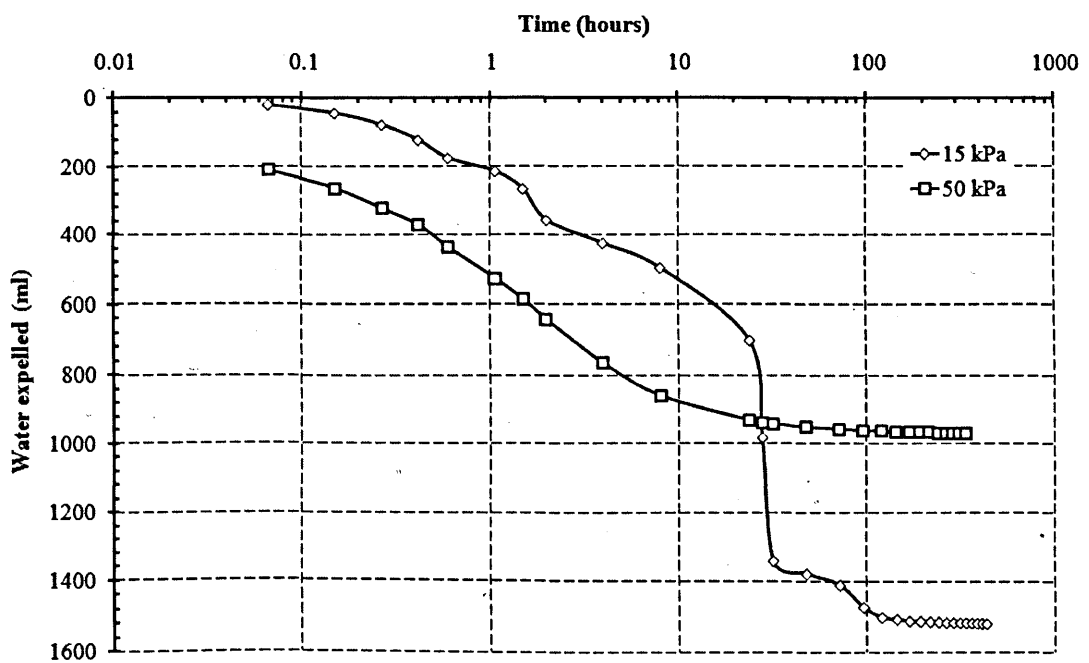


Figure 4.2 Result of Control Test: relative volume change versus time

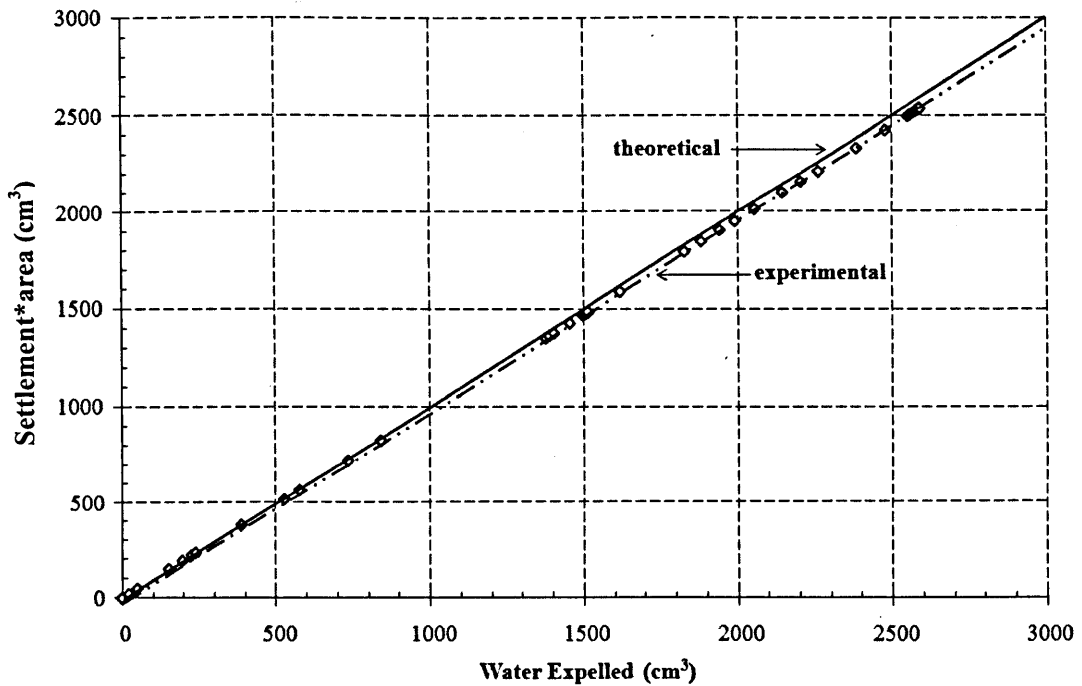


Figure 4.3 Result of Control Test: vertical displacement*area versus water expelled

Figure 4.3 shows the volume of water expelled compared to the change in volume determined from the settlement. From the figure, it can be seen that the results indicate that slightly more water was expelled than expected from the settlement readings. This could be due to leakage that occurred at top internal plate (23) and internal wall of electro osmotic consolidation chamber as some water was seen to flow between these components (Figure 3.2)

4.3 ELECTRO OSMOTIC PILES TESTS

The electro osmotic pile tests were conducted to study the effects of electro osmosis on the stiffness of the system. A pressure of 15 kPa was applied to create a normally consolidated specimen from the slurry. This pressure was maintained when the voltage was applied. The 50 kPa pressure was used to assess the stiffness of the system. The series of electro osmotic piles tests are summarised in Table 4.1. The results of all the tests in this study are presented according to the test series, namely; (1) time of treatment; (2) numbers and arrangement of electrodes; and (3) applied voltage. The computed parameters including e_o , m_v , $E_{stiffness}$, $E_{build\ phase}$, and $E_{pre-treatment}$ are discussed and correlated with the (1) treatment time, t ; (2) number of anode (nos. anode); (3) applied voltage, V ; and (4) distance between electrodes, D .

There were twelve tests conducted to investigate time (1), six tests to investigate arrangement of electrodes (2) and three tests to investigate applied voltage (3)

4.3.1 Vertical displacement and water expelled versus time curves

Figures 4.4 to 4.9 show the settlement versus time curves, and volume change versus time, respectively. The slurries were all prepared to the same water content. Figures 4.4 and 4.5, and Figure 4.6 show the settlement of all samples during Phase 1 and Phase 3, respectively. From these figures, it is clearly shown that the six tests for 1 day, 3 days, 5 days, 7 days, 15 days and 19 days are similar. This suggests that the water content and preparation of the samples were similar. All the results show that the soil was consolidated during the electro osmosis consolidation (phase 2). This can be seen in Figure 4.7. The rest of volume change measurement versus time plotted graphs, Phases 2 and 3, are shown in Figures D1 and D2 in the APPENDIX D.

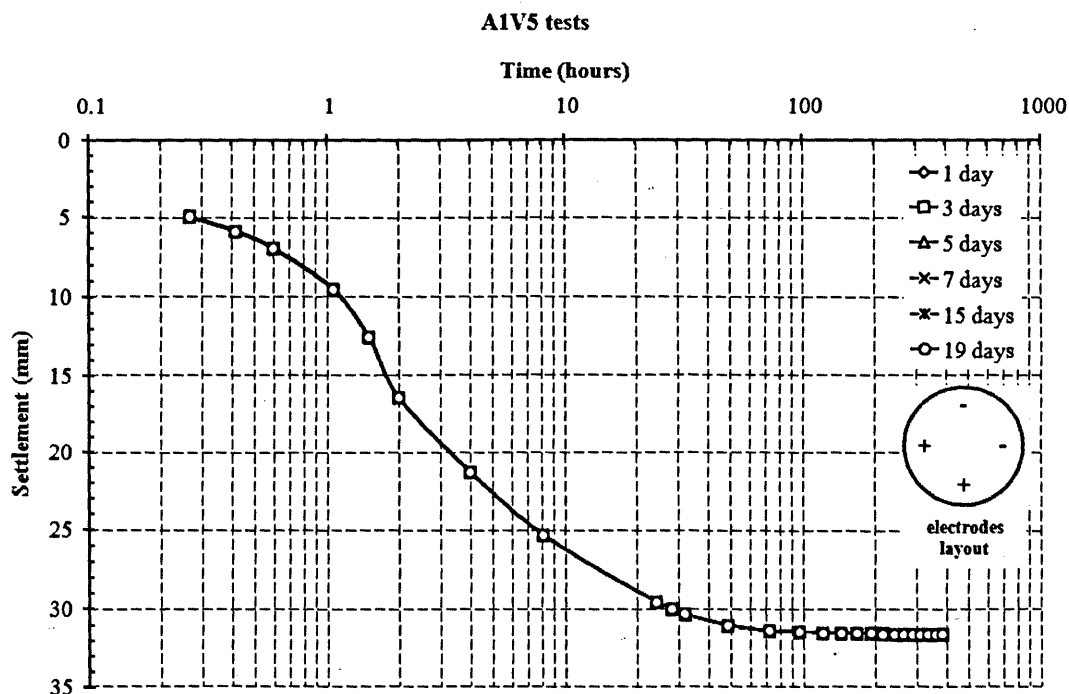


Figure 4.4 Phase 1 results of A1V5 tests series: settlement versus time curves

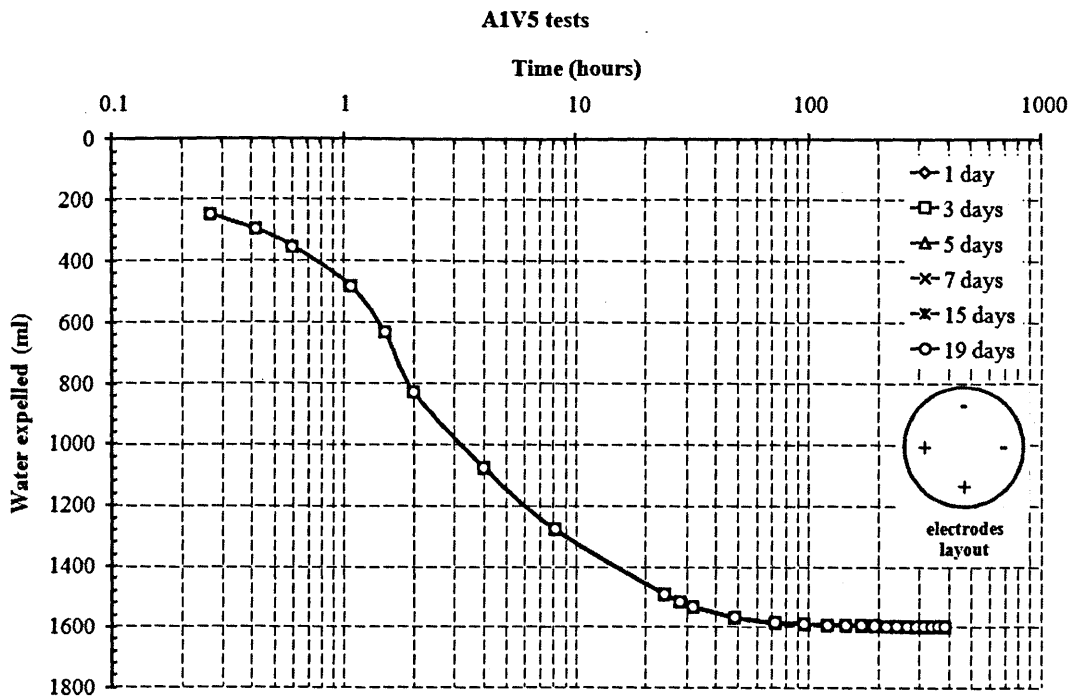


Figure 4.5 Phase 1 results of A1V5 tests series: water expelled versus time curves

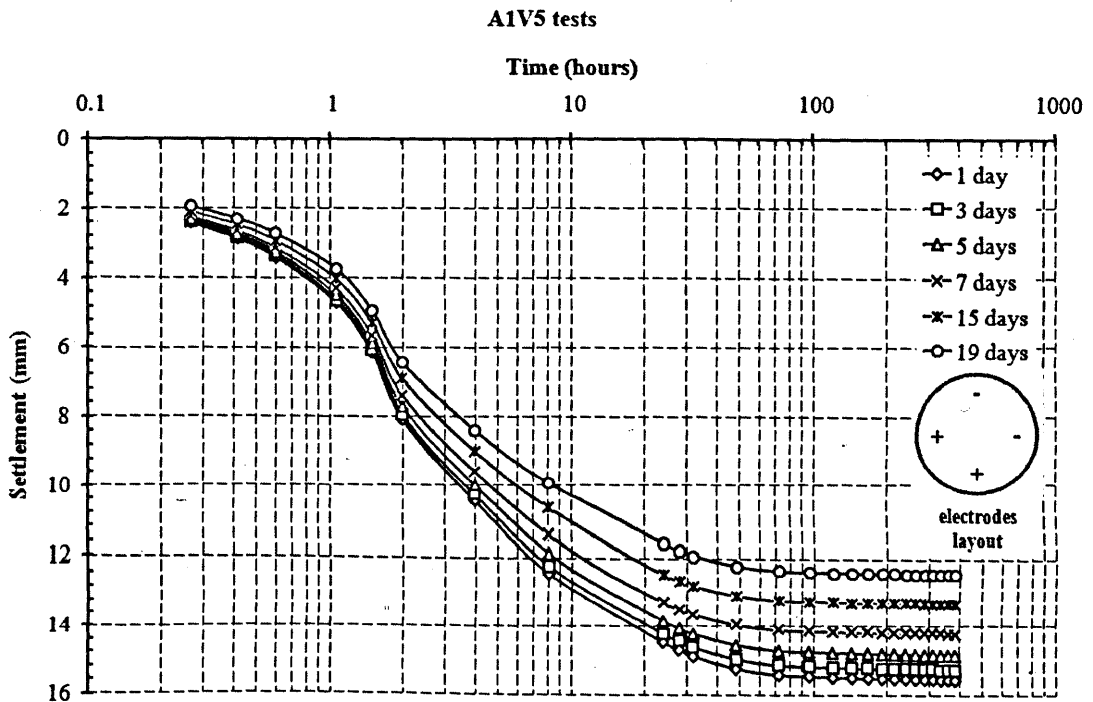


Figure 4.6 Phase 3 results of A1V5 tests series: settlement versus time curves

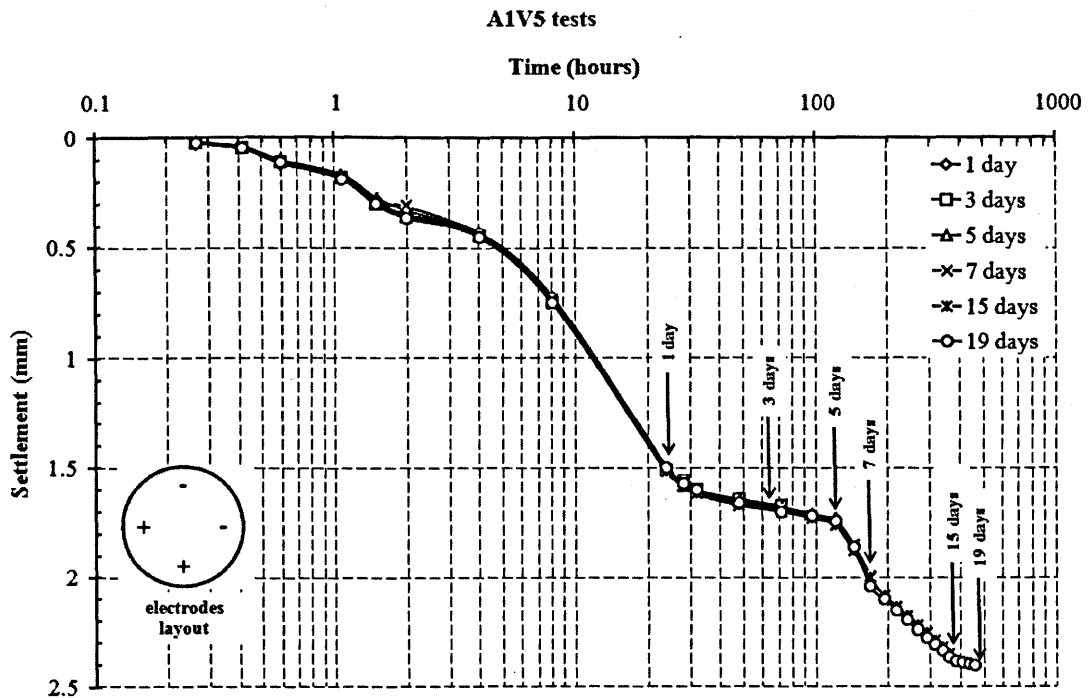


Figure 4.7 Phase 2 results of A1V5 tests series: settlement versus time curves

4.3.1.1 Time of treatment tests series

They were twelve tests series A1V5 and Q3V5 to evaluate the effect of time of electro osmotic treatment. In these tests series, a constant 5 Volts was applied. Figures 4.4 to 4.6, and Figures 4.8 to 4.10 show that initial consolidation during Phases 1 and 3 for tests series A1V5 and Q3V5, respectively, were similar for all tests. Figures 4.7 and 4.10 show that a unique curve was created for the two configurations of electrodes of all the tests are plotted on the same graph, For A1V5 the majority of the settlement occurred within the first five days. From the figure, it clearly shown that the rate of settlement for A1V5 samples is similar.

The rate of settlement increased developing a stage consolidation process. This was not shown with the single anode (Q3V5). In this test there was a change in behaviour after one day when the rate of settlement increased. Test A1V5 stopped after 19 days; test Q3V5 at 17 days. At that point the current had reduced to zero. The rest of volume change measurement versus time graphs for Phases 2 and 3, are shown in Figures D3 and D4 in the APPENDIX D.

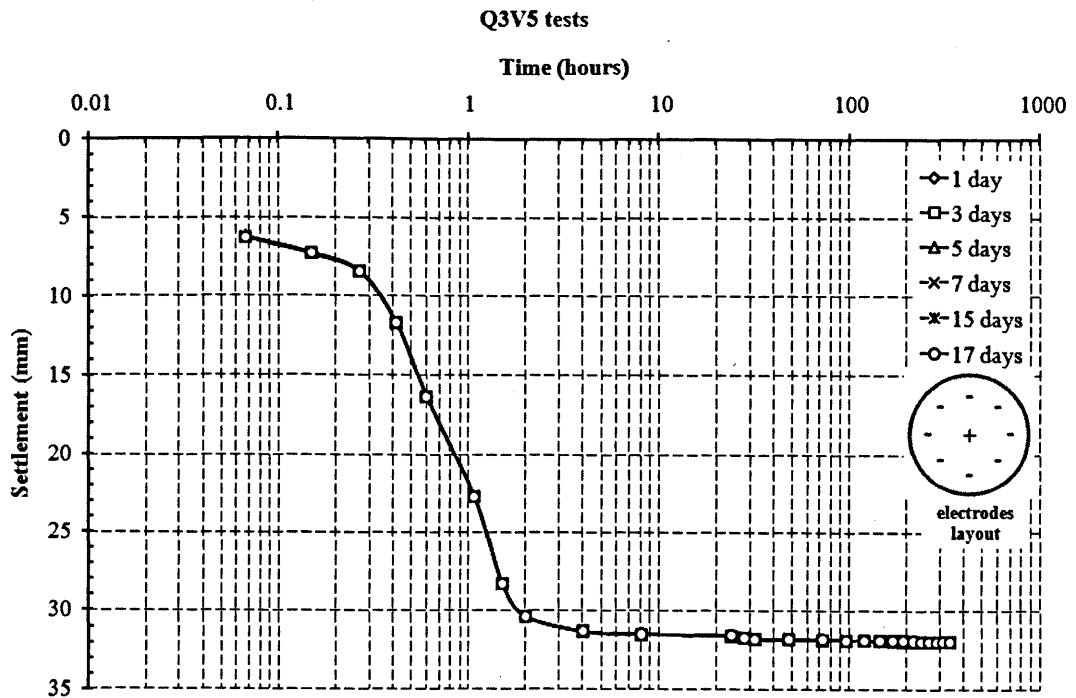


Figure 4.8 Phase 1 results of Q3V5 tests series: settlement versus time curves

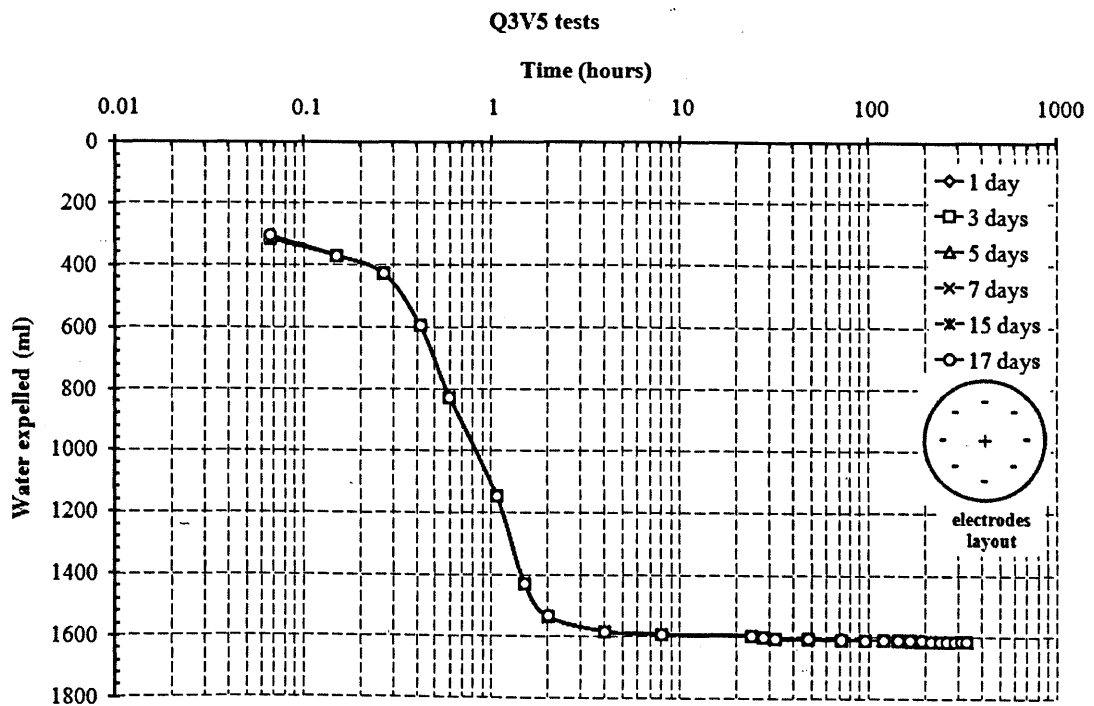


Figure 4.9 Phase 1 results of Q3V5 tests series: water expelled versus time curves

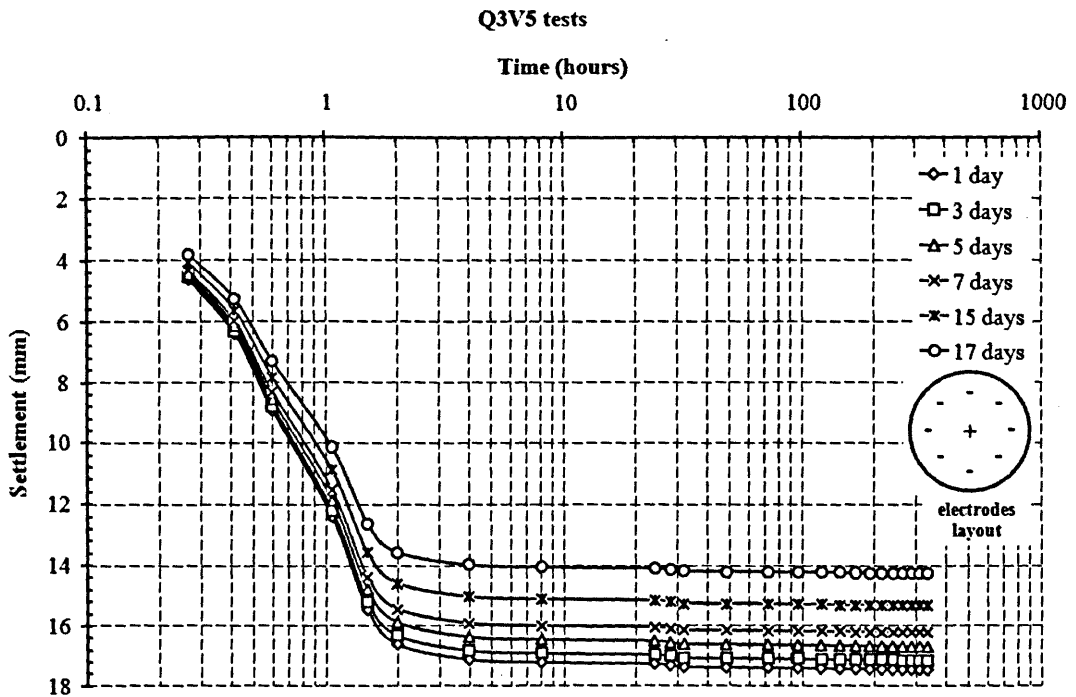


Figure 4.10 Phase 3 results of Q3V5 tests series: settlement versus time curves

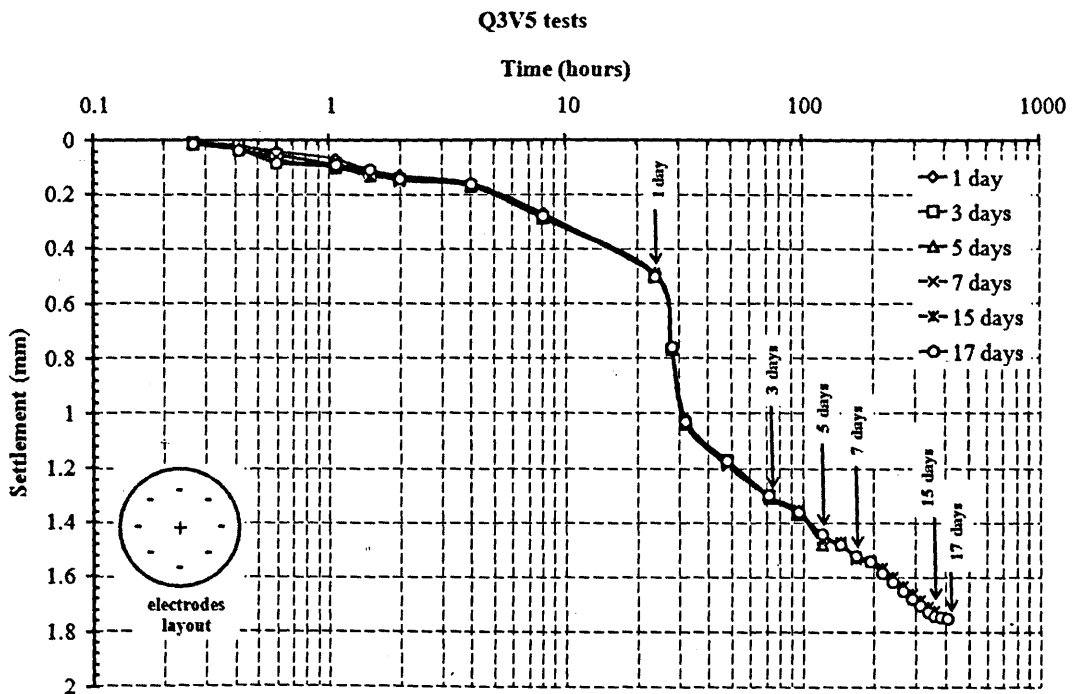


Figure 4.11 Phase 2 results of Q3V5 tests series: settlement versus time curves

4.3.1.2 Numbers of electrodes and arrangement of electrodes tests series

Six tests were carried out in this series. The tests were aimed at evaluating the effect of different numbers of electrodes and arrangement of electrodes. Table 4.1 shows the layout of the electrodes for the tests listed in Figures 4.12. to 4.14. The rest of the volume change measurement versus time graphs, from Phases 1 to 3, is shown in Figures D5 to D7 in the APPENDIX D. A constant applied voltage of 5 Volts was used in these tests.

Figure 4.6 shows the stiffness of the system after electro osmosis increased; i.e. the settlement for an increase in vertical pressure of 35 kPa (from 15kPa to 50kPa) reduced. Figure 4.10 shows that this was the case for the alternative electrode arrangement (Q3V5) as well. Note this increase in stiffness was due to electro osmosis as the consolidation due to 15 kPa was complete (Figures 4.5 and 4.8).

Figures 4.12 and 4.13 show the settlement for an applied pressure of 15 kPa. The difference in rate of settlement depends upon the number of cathodes since they acted as drains. The settlement for Q3V517d with eight cathodes was the quickest and A1V519d with two cathodes was the slowest. However, this does not explain all of the differences. For example, the test with one cathode (Q4V516d) consolidated faster than the test with two cathodes (A1V519d). This could be due to the configuration of the cathodes in relation to the boundary and the fact the settlement was measured at the centre of the cell though there was a rigid platen on top of the clay. The amount of settlement in Phase 2 depended on the number of electrodes and their relative position. The greatest settlement occurred with eight anodes and one central cathode; the least settlement with the reverse configuration.

Figure 4.13 shows two different reactions to the osmotic treatment. This is due to the number of anodes and the distance between the electrodes (see Table 4.3).

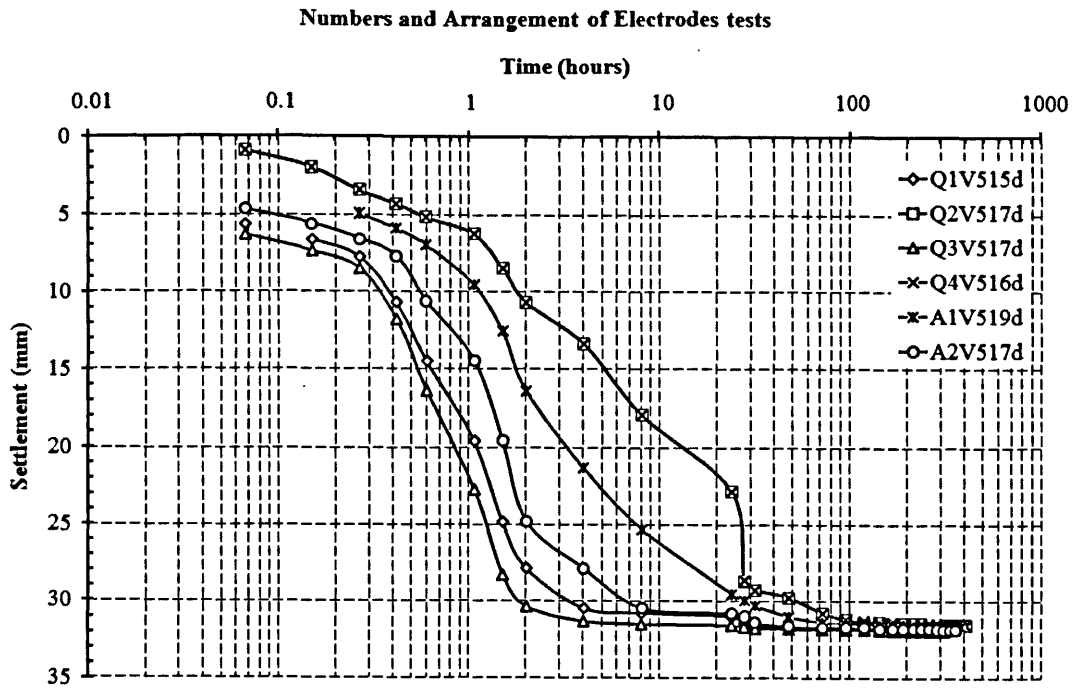


Figure 4.12 Phase 1 results for numbers and arrangement of electrodes test series: settlement versus time curves

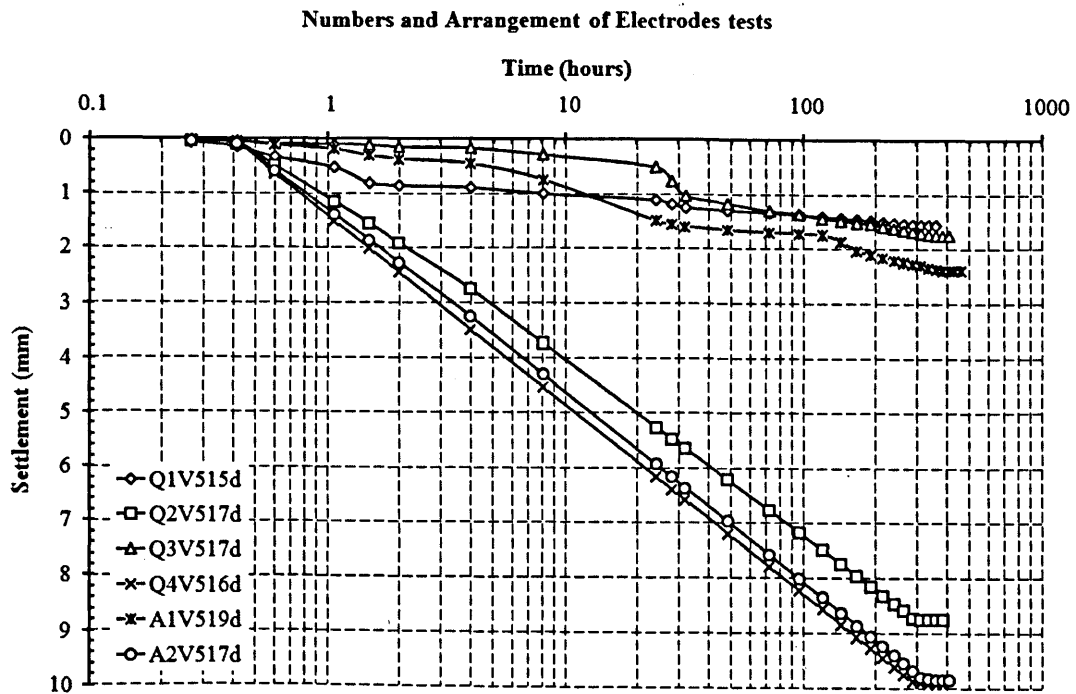


Figure 4.13 Phase 2 results for numbers and arrangement of electrodes test series: settlement versus time curves

Numbers and Arrangement of Electrodes tests

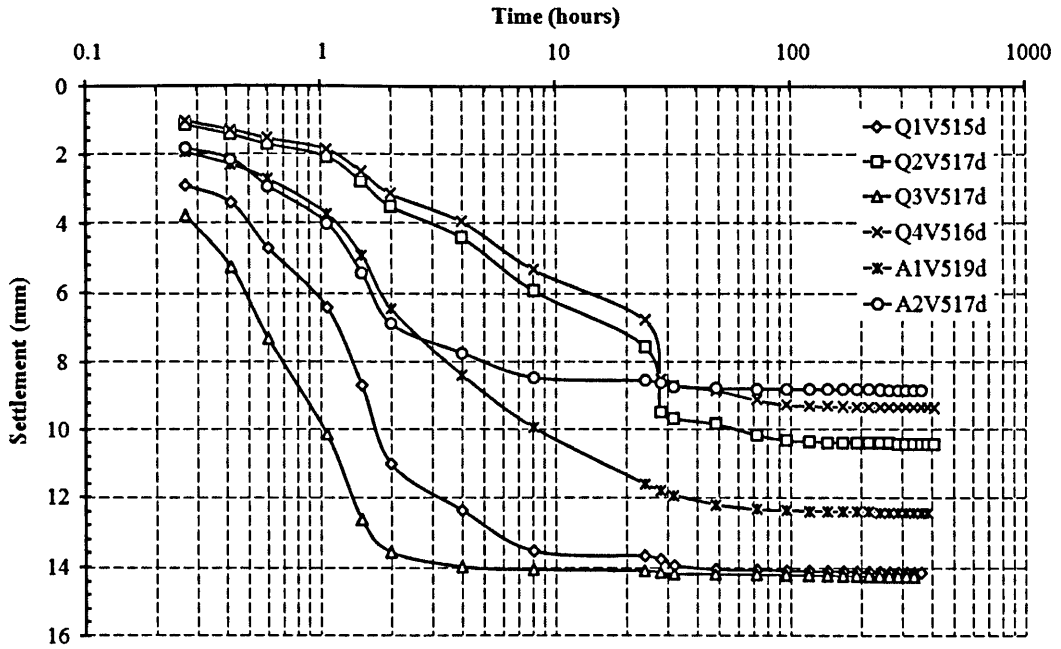


Figure 4.14 Phase 3 results for numbers and arrangement of electrodes test series: settlement versus time curves

Table 4.3 Summary of settlement for test series of number of anodes and the distance between the electrodes

Test	No of Anodes	Distance between electrodes (mm)	Settlement (mm)			Cumulative Settlement (mm)		Ratio	
			Phase 1	Phase 2	Phase 3	Phase 1 + 2	Phase 1, 2 + 3	Phase 2/Phase 1	Phase 3/Phase 3 control
Q1V515d	1	63	31.84	1.55	14.14	33.39	47.53	0.049	0.735
Q2V516d	4	63	31.56	8.76	10.43	40.32	50.75	0.278	0.542
Q3V517d	1	63	31.95	1.75	14.26	33.7	47.96	0.055	0.741
Q4V516d	8	63	31.54	9.92	9.35	41.46	50.81	0.315	0.486
A1V519d	2	124	31.65	2.40	12.45	34.05	46.50	0.076	0.647
A2V517d	4	49	31.85	9.84	8.83	41.69	50.52	0.309	0.459

Phase 3 control reading is 19.24 mm (Table E1 in the APPENDIX E).

4.3.1.3 Different applied voltage tests series

Seven tests were carried out in this series. The test was aimed at evaluating the effect of different applied voltage. The layout of the electrodes is shown in Table 4.1 for the tests listed in Figures 4.15 to 4.17. The rest of volume change measurement versus time plotted graphs, from Phases 1 to 3, are shown in Figures D8 to D10 in the APPENDIX D. Different applied voltages of 5, 10 and 20 Volts were used in these tests.

The stiffness of the system after electro osmosis increased; i.e. the settlement for an increase in vertical pressure of 35 kPa reduced (Figure 4.17), especially after 25 hours. In the same figure, it also shows that the different applied voltage with different number of anodes, and distance between the anodes and the cathodes resulted in different amounts of settlement.

Figures 4.15 and 4.16 show the settlement for an applied pressure of 15 kPa. The difference in rate of settlement depends upon the number of cathodes since they acted as drains. In Phase 1 (Figure 4.15), it can be seen that the two tests, A2V517d and A2V1016d, consolidated faster than the others. This was due to the fact there were more cathodes.

In Phase 2, the difference in rate of settlement depends upon the applied voltage in the system and also the number of cathodes since they acted as drains. With 20 V as the applied voltage, eight anodes with 63 mm distance between the anodes and the cathode, produced the most settlement in test Q4V2012d. Test Q2V516d with four anodes, 5 V and similar distance between the electrodes shoed the least settlement. Figure 4.16 shows seven different reactions to the osmotic treatment. From the same figure, it can be concluded that the fastest to slowest are Q4V2012d > Q4V1014d > A2V1016d > Q2V1015d > A2V517d > Q4V516d > Q2V516d.

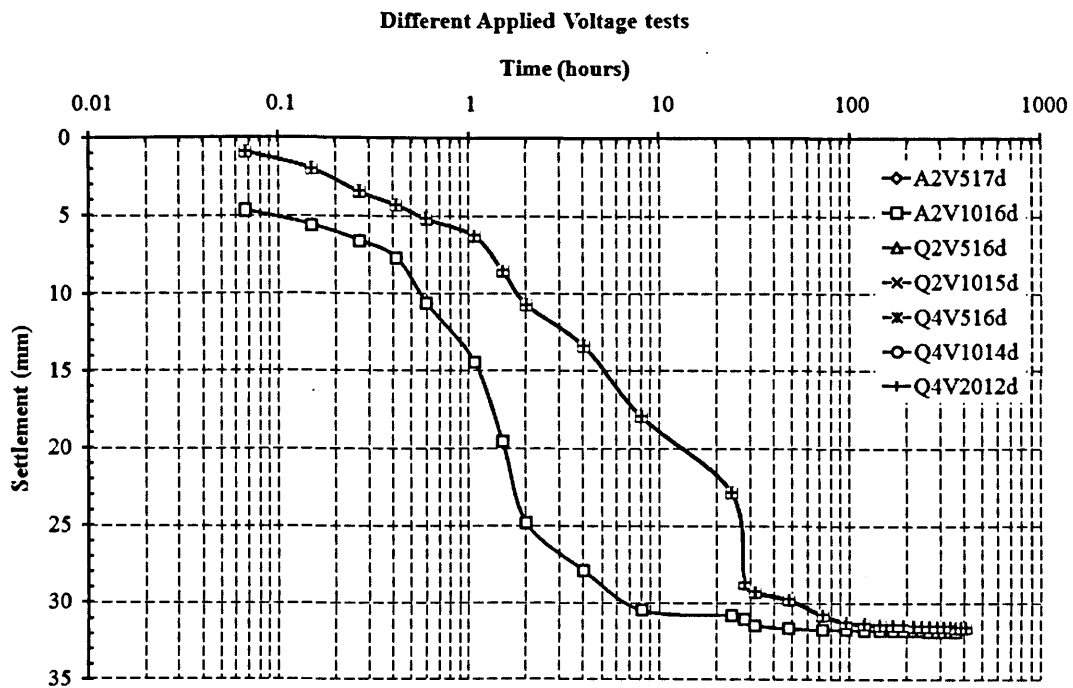


Figure 4.15 Phase 1 results for different applied voltage test series: settlement versus time curves

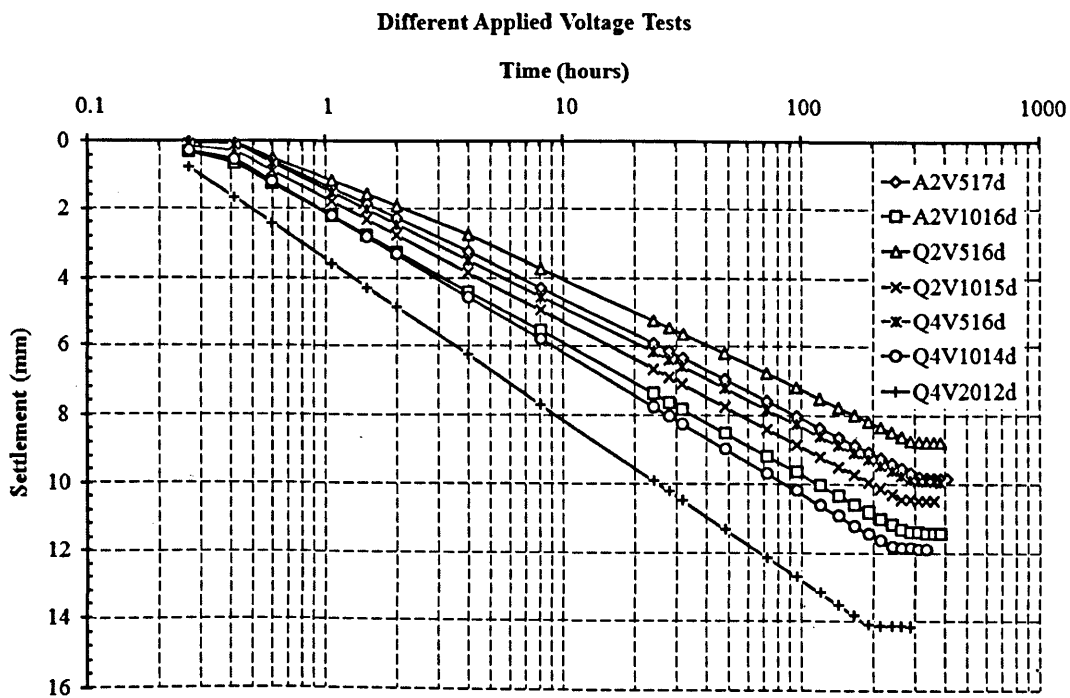


Figure 4.16 Phase 2 results for different applied voltage test series: settlement versus time curves

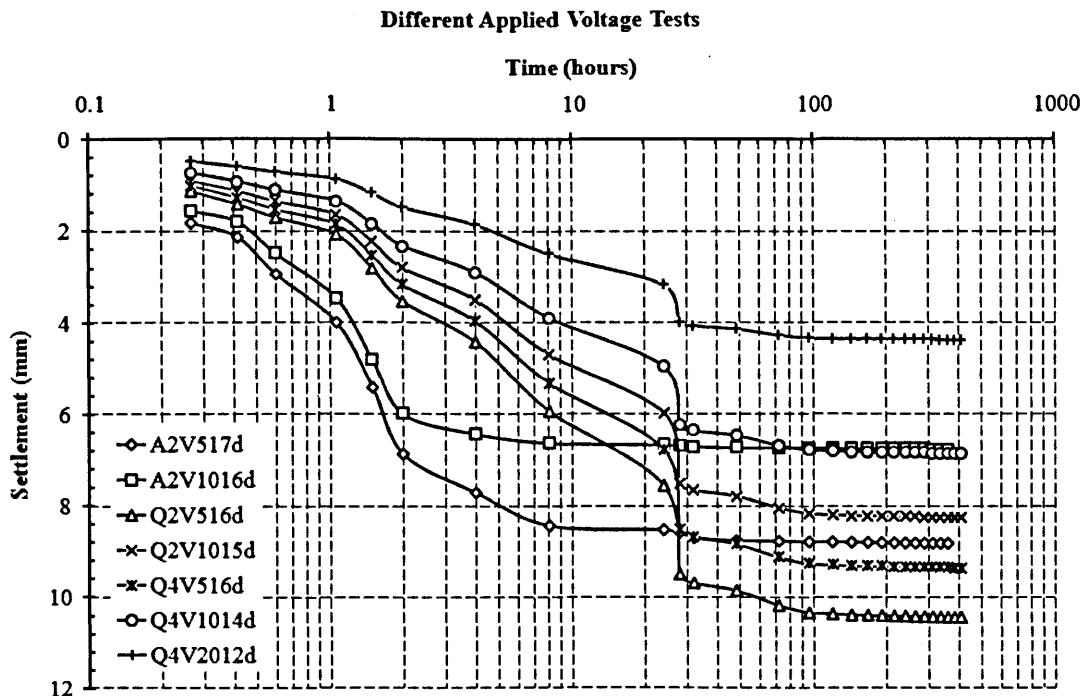


Figure 4.17 Phase 3 results for different applied voltage test series: settlement versus time curves

The configuration of the cathodes in relation to the boundary might be a factor for the difference in settlement, the fact the settlement was measured at the centre of the cell, and the value of the applied voltage through the system could be contributing factors to the amount of settlement. The amount of settlement in Phase 2 depended on the number of electrodes and their relative position. The greatest settlement occurred with the highest applied voltage, the highest number of anodes with eight anodes and one central cathode; the least settlement with the lowest number of anodes and the lowest applied voltage through the system.

Table 4.4 summarises the number of anodes, the distance between the electrodes and the measured settlements. 20 V was applied to Q4V2012d, while 10 V to Q4V1014d, Q2V1015d and A2V1016d, and the rest were 5 V.

Table 4.4 Summary of settlement for test series of different applied voltage

Test	No of Anodes	Applied Voltage (Volts)	Distance between electrodes (mm)	Settlement (mm)			Cumulative Settlement (mm)		Ratio	
				Phase 1	Phase 2	Phase 3	Phase 1 + 2	Phase 1, 2 + 3	Phase 2/Phase 1	Phase 3/Phase 3 control
A2V517d	4	5	49	31.85	9.84	8.83	41.69	50.52	0.309	0.459
A2V1016d	4	10	49	31.86	11.41	6.76	43.27	50.03	0.358	0.351
Q2V516d	4	5	63	31.56	8.76	10.43	40.32	50.75	0.278	0.542
Q2V1015d	4	10	63	31.60	10.47	8.25	42.07	50.32	0.331	0.429
Q4V516d	8	5	63	31.54	9.92	9.35	41.46	50.81	0.315	0.486
Q4V1014d	8	10	63	31.60	11.86	6.85	43.46	50.31	0.375	0.356
Q4V2012d	8	20	63	31.52	14.17	4.37	45.69	50.06	0.450	0.227

Phase 3 control reading is 19.24 mm (Table E1 in the APPENDIX E).

4.3.2 Vertical displacement multiplied by area versus water expelled lines

The settlement of the top plate was measured with a dial gauge which had an accuracy of 0.01 mm. Expelled water was measured with a measuring cylinder to an accuracy of ± 5 ml. Generally, the actual water expelled exceeded the volume change calculated from the amount of settlement.

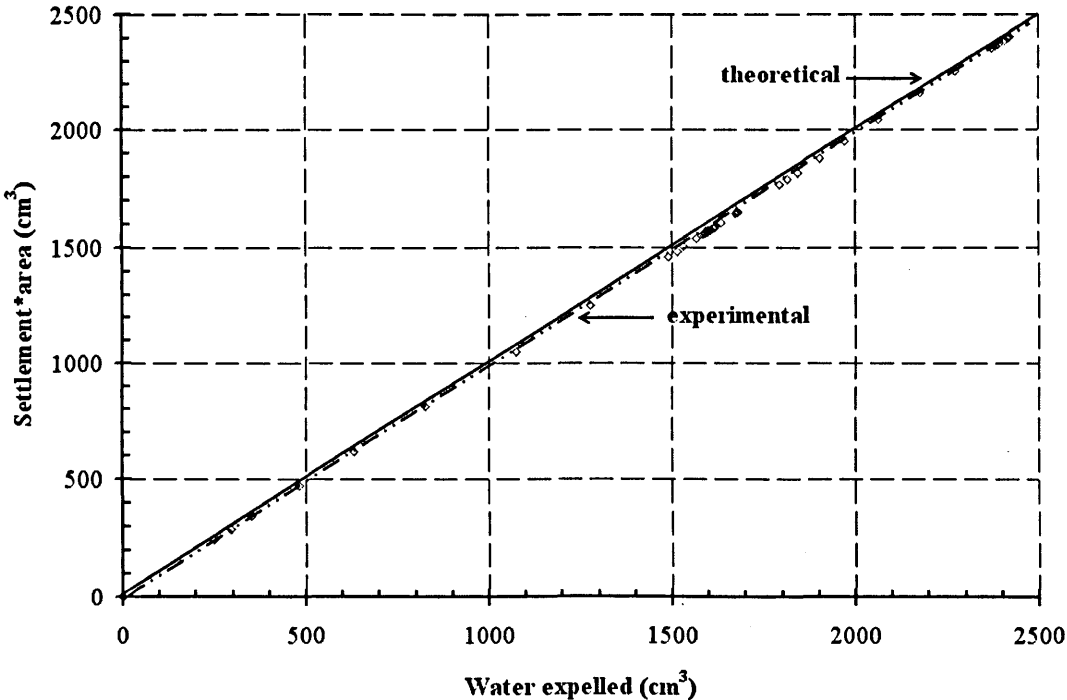


Figure 4.18 Result of A1V5 for 1 day test: settlement*area versus water expelled

4.3.3 Water expelled and current versus time curves

An example of the water expelled and current versus time curves are shown in Figure 4.19. The remainder are plotted in Figures D17 to D35 in the APPENDIX D. In general the current reduced with time. Settlement started soon after the voltage was applied and continued until the end of the experiment. Tests were stopped when the volume change reduced to less than 1.13 mm³/hour. This was taken to be the end of primary consolidation. Table 4.5 summarises volume change at the end of primary consolidation for all the tests series. It can be concluded:

- (i). Time of treatment series for A1V5 and Q3V5 tests series; increasing the time of treatment from 1 day to 3 days and more, an immediate effect of volume change was produced. And finally, increasing the time of treatment until 17 days for Q3V5 and 19 days for A1V5 days, the settlement rate and water expelled were further increased.
- (ii). Numbers and arrangement of electrodes for Q1V5515d, Q2V516d, Q2V517d, Q4V516d, A1V519d, and A2V517d tests series; the greater the numbers of electrodes installed in the system, the greater the settlement.
- (iii). Different applied voltage for A2V517d, A2V1016d, Q2V516d, Q2V1015d, Q4V516d, Q4V1014d, and Q4V2012d tests series; the greater the applied voltage applied in the system, the greater the settlement.

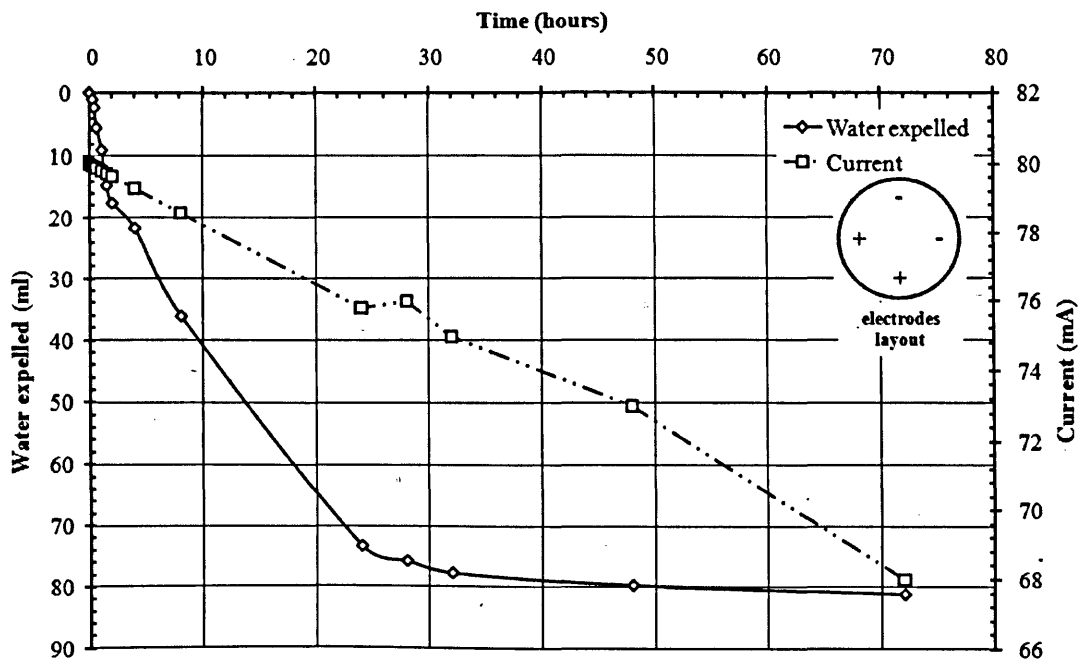


Figure 4.19 Results of A1V53d days test: water expelled and current versus time

Table 4.5 Volume changed at the end of primary consolidation on Phase 2

Test series	Volume changed (mm ³ /hour)	Total settlement (mm)
A1V51d	3.04	1.50
A1V51d	1.13	1.67
A1V51d	0.70	1.73
A1V51d	0.57	1.99
A1V51d	0.32	2.35
A1V51d	0.26	2.40
Q3V51d	1.00	0.49
Q3V51d	0.88	1.30
Q3V51d	0.60	1.48
Q3V51d	0.44	1.52
Q3V51d	0.23	1.72
Q3V51d	0.21	1.75
Q1V55d	0.21	1.55
Q2V516d	1.11	8.78
Q4V516d	1.25	9.92
A2V517d	1.17	9.84
A2V1016d	1.44	11.41
Q2V1015d	1.34	10.47
Q4V1014d	1.71	10.47
Q4V2012d	2.39	14.17

4.3.3.1 Time of treatment tests series

Figures 4.19 and D17 to D27 in the APPENDIX D show the water expelled and current versus time curves, for A1V5 and Q3V5 tests series, respectively. Test series A1V5 with four electrodes and 5 V and test series Q3V5 with one anode and eight electrodes and 5 V were used to investigate the effect of time. In the case of A1V5, there was an initial, rapid drop in current which was associated with the maximum rate of settlement. This drop in current occurred within 240 mins from the start of the test (Tables D2 to D7 in the APPENDIX D). Thereafter, the reduction in current was predominantly linear no matter the length of time. The osmotic process stopped completely after 450 hours in A1V519d and, on inspection of the electrodes, this was due to the disintegration of the electrodes. Some of the anodes were left in the other

tests through osmotic treatment effectively stopped after 20 hours. After 20 hours there appeared to be an acceleration of settlement not linked to current.

The current behaviour was different for Q3V5. In these tests, the current reduced with time in a similar manner to the rate of settlement. After 400 hours the osmotic process stopped. In this case, the settlement rate reduced with time throughout the experiment. In this case, the primary settlement due to osmosis stopped after 30 hours suggesting that the number of anodes has an effect on the time for the osmotic process to take place.

4.3.3.2 Numbers and arrangement of electrodes tests series

Table 4.6 summarises the numbers and arrangement of electrodes test series under water expelled and current versus time curves. The osmotic process stopped completely after 350 hours for all types of tests series. From the same table, it can be clearly seen where the highest to lowest numbers of anodes as the electrodes installed are Q4V516d > Q2V516d and A2V517d > A1V519d > Q1V515d and Q3V517d. In case of Q1V525d and Q2V516d, there was an initial, rapid drop in current which was associated with the maximum rate of settlement. The rapid drop occurred after 10 hours and then readings were constant until 100 hours. A similar pattern was repeated for both of these tests. The primary settlement due to osmosis for these two types effectively stopped after 40 hours and 30 hours for Q2V516d and Q1V515d, respectively. Noted that test Q2V516d was 10 hours longer than test Q1V515d, where the number of the anodes in Q2V516d is four and in Q1V515d is one. The reduction in current was not linked to the settlement as can be seen in Figures D28 and D29 in the APPENDIX D.

The current behaviour was different for Q4V516d and A2V517d. This can be clearly seen in Figures D30 and D31 in the APPENDIX D. In the case of A2V517d, it was similar to Q3V5 tests series where the current reduced with time in a similar manner to the rate of settlement. A rapid drop in current after the start of the test was noted in Q4V516d. The current rose back after 240 mins and finally it reduced after 24 hours. In these cases the settlement rate reduced with time throughout the experiment.

Table 4.6 End of time for primary consolidation and osmotic treatment under numbers and arrangement of electrodes

Types of cases	Figures in the APPENDIX	Number of anodes	Number of cathodes	Time of osmotic treatment stopped (hours)	End time of primary settlement (hours)
Q1V515d	E28	1	4	350	30
Q2V516d	E29	4	1	350	40
Q3V517d	E27	1	8	350	50
Q4V516d	E30	8	1	350	40
A1V519d	E21	2	2	350	30
A2V517d	E31	4	4	350	40

4.3.3.3 Different applied voltage tests series

Table 4.7 summarises the end of time for primary consolidation and osmotic treatment under different applied voltages. The voltage in tests A2V517d and A2V1016d with four anodes and four cathodes were 5 V and 10 V, respectively. The voltages in tests Q2V516d and Q2V1016d with four anodes and one cathode were 5 V and 10 V, respectively. The voltages in the tests Q4V516d, Q4V1014d and Q4V2012d were 5V, 10v and 20V. These remaining sets were installed with eight anodes and one cathode.

It can be clearly noted that the higher the voltage applied in the system, the shorter the time of treatment and the shorter the time of primary settlement. The trend of current for each case under different applied voltage shows that the current reduced with time in a similar manner to the rate of settlement. After 350 hours the osmotic process stopped for cases with 5 V, 300 hours with 10 V except for Q4V1014d. In the case of Q4V1014d and Q42012d, the osmotic process stopped completely after 200 hours. The figures in the APPENDIX D show that the higher the voltage, the end time of primary settlement was shorter in all those cases the primary settlement due to osmosis stopped after 40 hours with 5 V, and the other cases were 30 hours. This suggests that the number of anodes affects the time for the osmotic process to occur.

Table 4.7 End of time for primary consolidaton and osmotic treatment under different applied voltage

Types of cases	Figures in the APPENDIX	Applied voltage (Volts)	Number of anodes	Number of cathodes	Time of osmotic treatment stopped (hours)	End time of primary settlement (hours)
A2V517d	E31	5	4	4	350	40
A2V1016d	E32	10	4	4	300	30
Q2V516d	E29	5	4	1	350	40
Q2V1015d	E33	10	4	1	300	30
Q4V516d	E30	5	8	1	350	40
Q4V1014d	E34	10	8	1	250	30
Q4V2012d	E35	20	8	1	250	30

Figures 4.20 to 4.26 shows the voids ratio versus time for Phase 2 and Phase 3, and voids ratio versus current for Phase 2 only. As shown in these figures, the results of voids ratio after electro osmotic consolidation treatment show a decrease in the voids ratio of treated samples, comparing with the control test. It is because it indicated that the electro osmotic consolidation process increasing the soil stiffness. All the tested samples show similar trends (Figures 4.21, 4.23, and 4.25).

The measured current ranged from 75 mA to 2 mA for Q3V5 test series in Figure 4.21, 80 mA to 2 mA for A1V5 test series in Figure 4.23, 160 mA to 2 mA for numbers and arrangement of electrode in the test series in Figure 4.25, and 470 mA to 15 mA for different applied voltage in the test series in Figure 4.27. These figures shows the change of voids ratio with current under constant applied voltage (5 Volts).

The most noticeable difference between all the tested samples is the increase in current with reduction of voids ratio for Q3V53d, Q3V55d, Q3V57d, Q3V515d, Q3V515d, Q3V517d, Q2V1015d and Q4V516d. Figures 4.21, 4.23, 4.25 and 4.27 also show that the voids ratio is decreasing with decreasing current, and the current decreases sharply at the beginning of the test followed by a gradual reduction. This is due to the slow corrosion of the anode where it was found that the kaolin was stained in the vicinity of the anode.

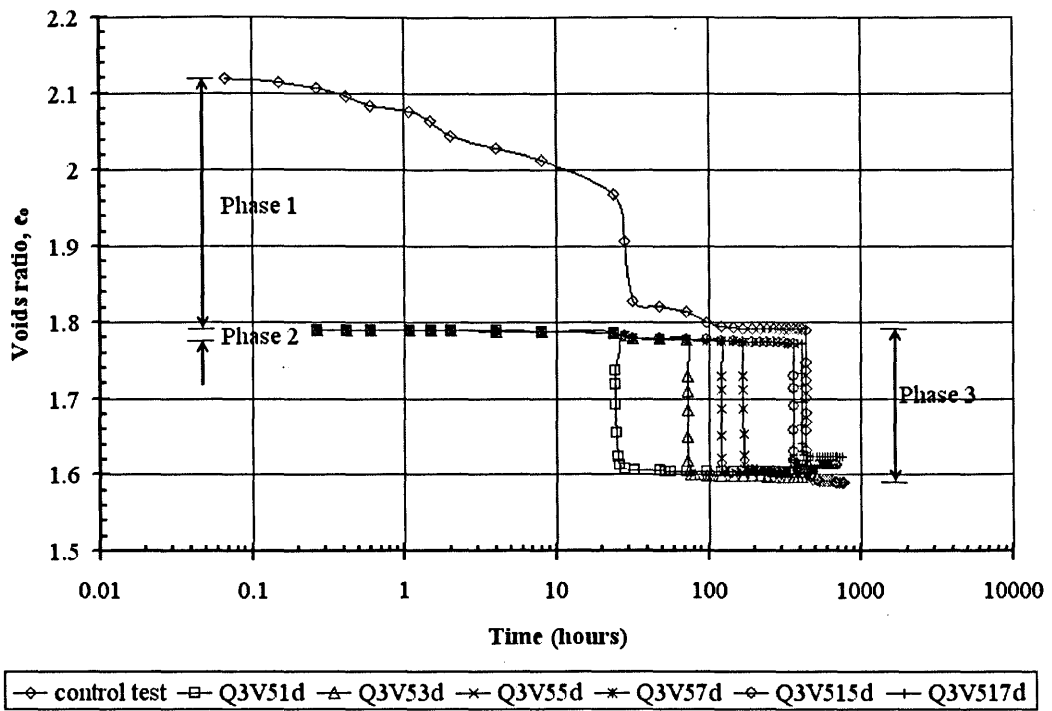


Figure 4.20 Q3V5 test series: voids ratio versus time

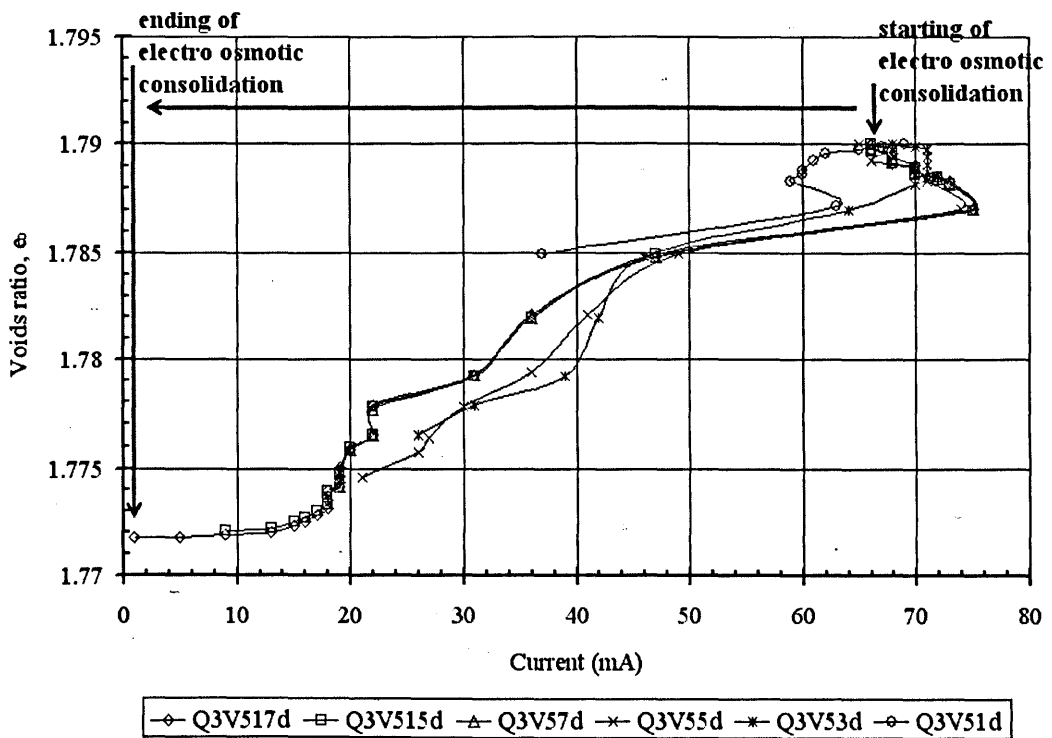


Figure 4.21 Q3V5 test series: voids ratio versus current in Phase 2

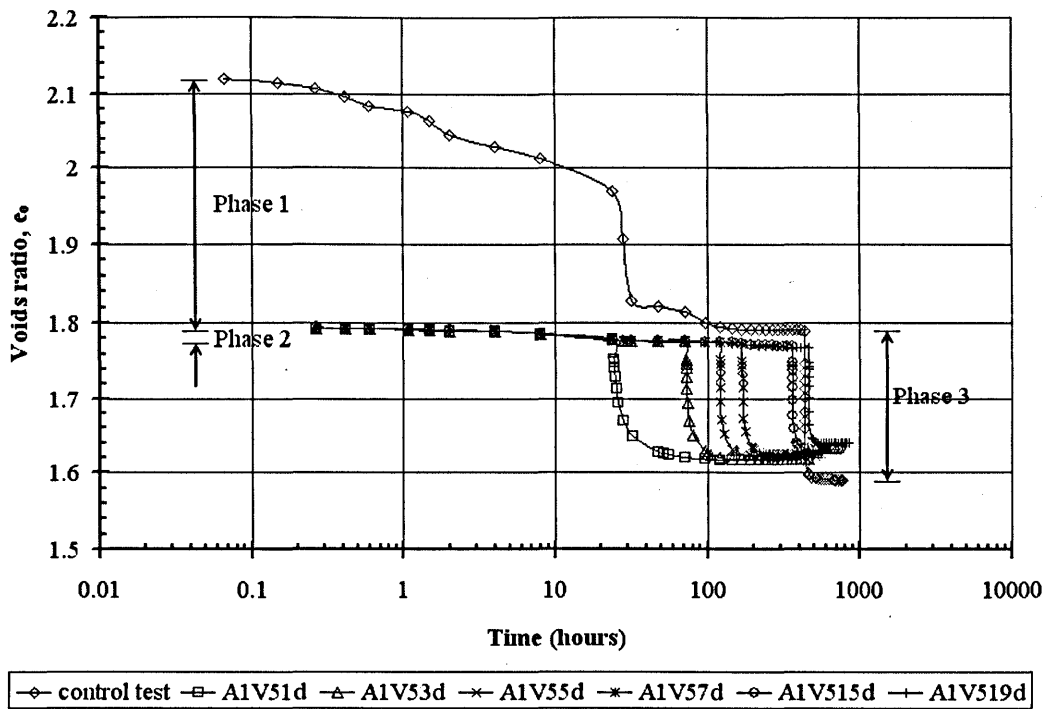


Figure 4.22 A1V5 test series: voids ratio versus time

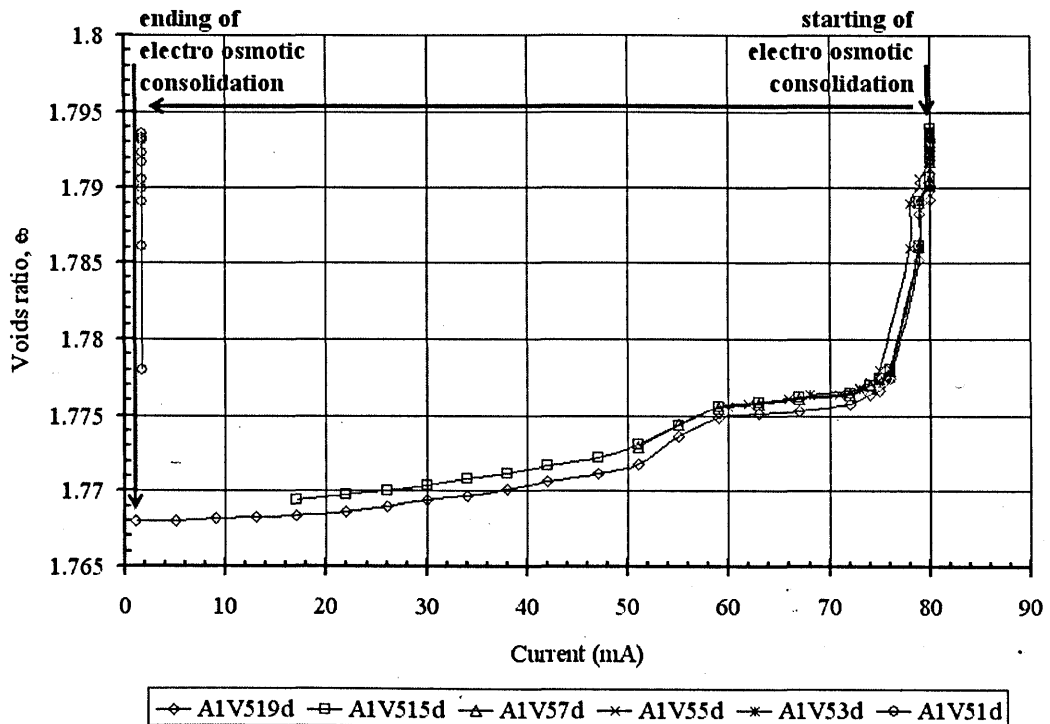


Figure 4.23 A1V5 test series: voids ratio versus current in Phase 2

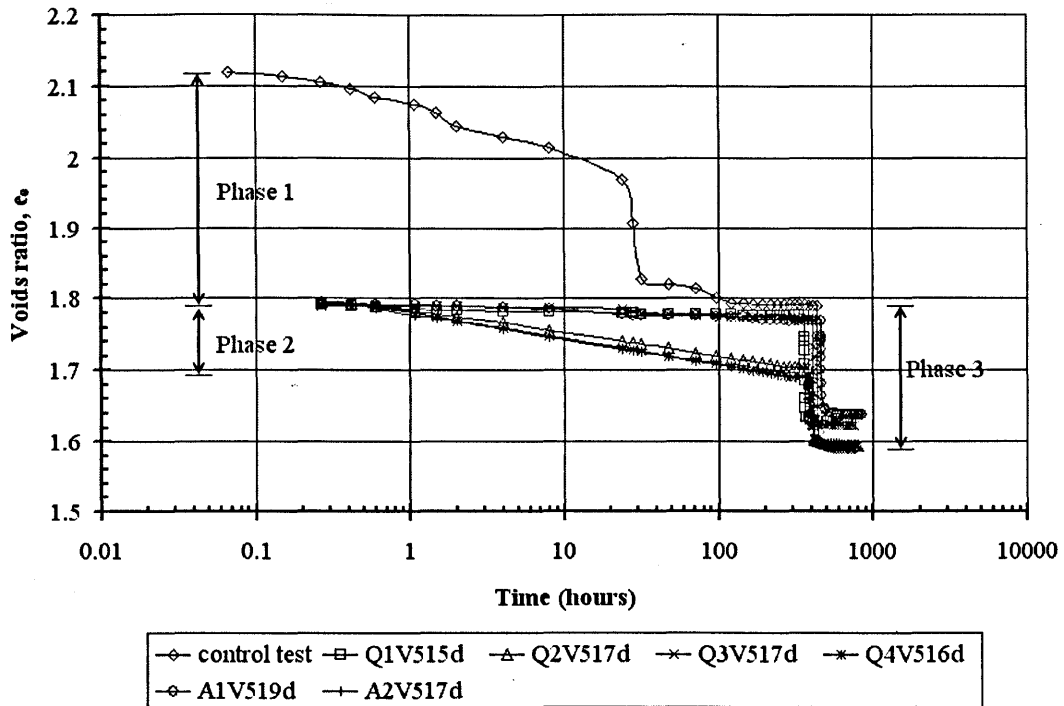


Figure 4.24 Numbers and arrangement of electrodes test series: voids ratio versus time

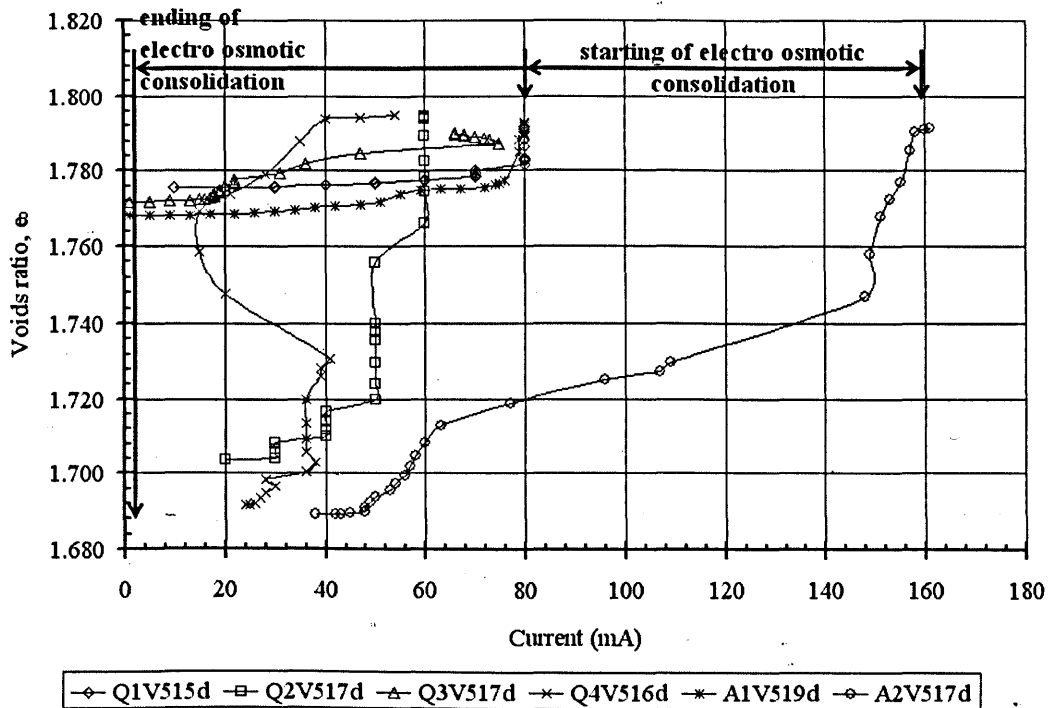


Figure 4.25 Numbers and arrangement of electrodes test series: voids ratio versus current in Phase 2

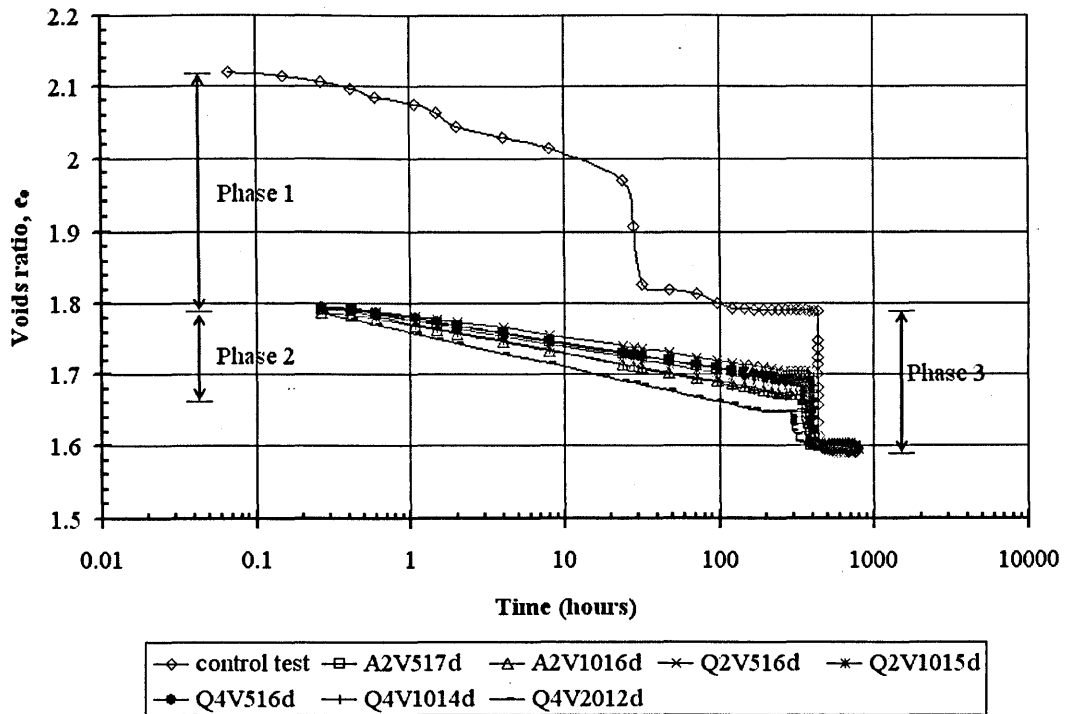


Figure 4.26 Different applied voltage test series: voids ratio versus time

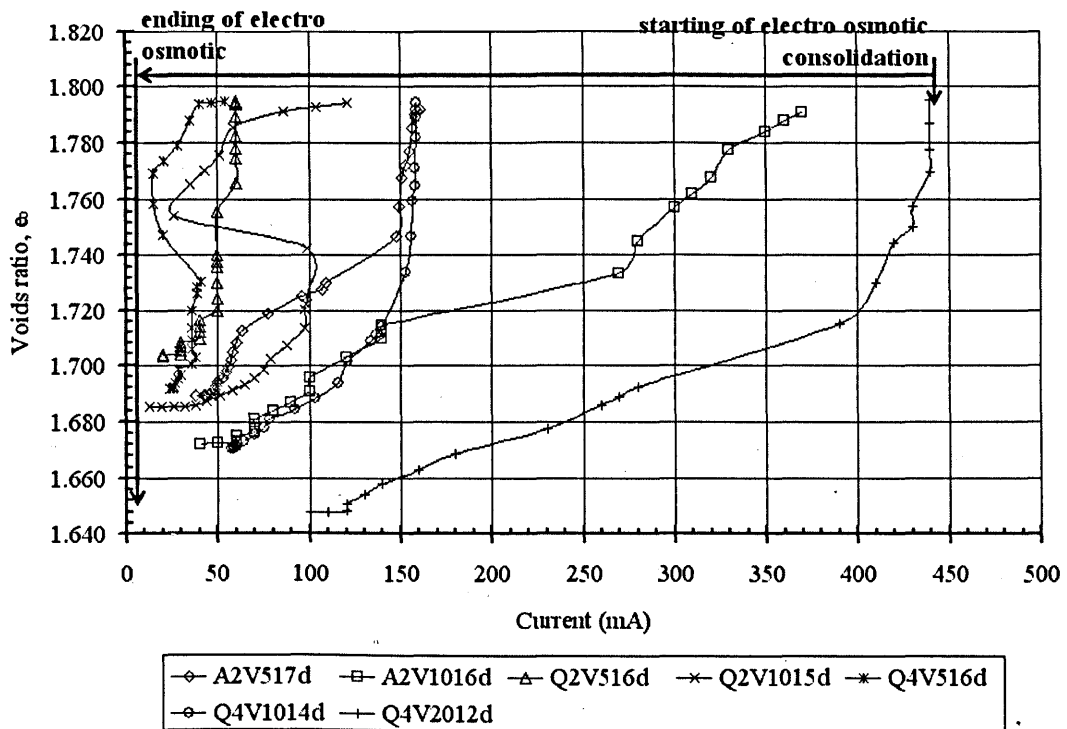


Figure 4.27 Different applied voltage test series: voids ratio versus current in Phase 2

Table 4.8 Summary of A1V5 test series: e_o , m_v , $E_{stiffness}$, $E_{pre-treatment}$ and $E_{build\ phase}$ results

Coe	e_o			$m_v (x 10^{-4})$		$E_{stiffness}$		$E_{pre-treatment}$	$E_{build\ phase}$
	Phase 1	Phase 2	Phase 3	before	after	before	after		
Control test	1.790	-	1.590	75	15	140	493*	493*	493*
Treatment of time tests series									
A1V51d	1.793	1.778	1.616	74	17	142	601	837	601
A1V53d	1.793	1.776	1.617	74	17	142	611	848	611
A1V55d	1.793	1.775	1.620	74	16	142	628	870	628
A1V57d	1.793	1.773	1.624	74	16	142	654	902	654
A1V515d	1.793	1.769	1.630	74	15	142	697	954	697
A1V519d	1.793	1.768	1.639	74	14	142	748	1019	748
Q3V51d	1.790	1.785	1.603	75	19	141	536	753	536
Q3V53d	1.790	1.776	1.598	75	19	141	544	762	544
Q3V55d	1.790	1.775	1.602	75	18	141	559	781	559
Q3V57d	1.790	1.774	1.605	75	18	141	575	801	575
Q3V515d	1.790	1.772	1.612	75	17	141	608	843	608
Q3V517d	1.790	1.772	1.623	75	15	141	654	905	654
Numbers and arrangement of electrode tests series									
Q1V515d	1.791	1.775	1.628	75	16	141	660	916	660
Q2V517d	1.794	1.703	1.595	74	12	143	871	1081	871
Q3V517d	1.790	1.772	1.623	75	16	141	654	905	654
Q4V516d	1.794	1.691	1.594	74	11	143	968	1177	968
A1V519d	1.793	1.768	1.639	74	14	142	748	1019	748
A2V517d	1.791	1.689	1.597	75	10	141	998	1211	998
Different applied voltage									
A2V517d	1.790	1.689	1.597	74	10	141	998	1211	998
A2V1016d	1.791	1.672	1.602	75	8	141	1223	1437	1223
Q2V516d	1.794	1.703	1.595	74	12	143	871	1081	871
Q2V1015d	1.794	1.685	1.599	74	9	142	1094	1309	1094
Q4V516d	1.794	1.691	1.594	74	11	143	968	1177	968
Q4V1014d	1.794	1.670	1.599	74	8	142	1311	1526	1311
Q4V2012d	1.795	1.647	1.602	74	5	143	2037	2254	2037

e_o : voids ratio; m_v : coefficient of volume compressibility (m^2/MN); $E_{stiffness}$: constrained stiffness (kPa); $E_{pre-treatment}$: constrained stiffness combining of phase 2 and phase 3; $E_{build\ phase}$: constrained stiffness at the end of phase 3; Phase 1: 15 kPa loads; Phase 2: 15 kPa + 5 V; Phase 3: 50 kPa; before: before treatment of electro osmotic consolidation; after: after treatment of electro osmotic consolidation; *without applied voltage.

4.3.5 Effect on water content, w_c

The final water content of the soil samples after treatment (at the end of 50 kPa) was measured at different locations, namely at the anode, cathode, in between electrodes, between the electrode and the cell wall. A summary of the test results is presented in Table 4.9 and in Figures D36 to ED6 in the APPENDIX D. It was found, as expected, that the water content was highest at the cathodes and lowest at the anodes. The results in Table 4.9 have been grouped according to time, electrode arrangement and voltage. Dr Murphy comments – were all tests carried out with distilled water or de-aired water? Significant difference with other clays?

From the observations it is clear that, the average water content decreases with increasing time of treatment, numbers of anode and applied voltage. The osmotically treated samples had a lower water content than the control test.

Figures 4.28 to 4.31 show the correlations between the final water content and time, number of anodes and voltages. Note that the projected water content at zero time, voltage and anodes was less than the control test suggesting that there is an initial reduction in water content which is shown in Figures D36 to D56 in the APPENDIX D. Thereafter, the correlations are linear. Thus, it is possible to predict the average water content and, possibly, the stiffness.

Figure 4.28 shows the relationship between average water content and time of treatment. From Table 4.9 and this figure, the average water content increased with treatment time. It shows the range in between 45.7% and 53.4% for A1V5 tests series, and 46.9% and 51.0% for Q3V5 tests series. The relationship obtained from this figure is:

$$w_c = 51.8 - 0.36t; \text{ for A1V5 tests series} \quad (4.1)$$

and

$$w_c = 50.3 - 0.23t; \text{ for Q3V5 tests series} \quad (4.2)$$

While in Figures 4.29 and 4.30, it shows the relationship between average water content and number of anodes, and also constant applied voltage. Clearly from table 4.9, the average water content increases with number of anodes and applied voltage. It shows the water content ranges between 39.6% and 47.3%, and 34.7% and 47.3% for the number of anodes and applied voltage, respectively. From Figures 4.29 and 4.30 it can be seen that average water content decreased with number of anodes and applied voltage with the coefficient of determination, R^2 is equal to 0.81 (very good) and 0.61 (good), respectively. The relationship is given by

$$w_c = 48.0 - 1.08(\text{nos. anode}) \quad (4.3)$$

and

$$w_c = 46.4 - 0.66V \quad (4.4)$$

Figure 4.31 shows that the voids ratio is increase with increasing of water content. Based on the values of coefficient of correlation, R^2 between voids ratio and average water content is weak.

Table 4.9 Summary of water content test, w_c (%)

Sample	Initial	at the end of 50 kPa					Average
		at Anode	at Cathode	between electrodes	Anode-wall	Cathode to wall	
Control test	79.5	nil	nil	nil	nil	nil	58.48
Time of treatment tests series							
A1V51d	79.5	49.0 – 49.2	66.4 – 66.5	49.3 – 53.6	50.1 – 50.1	52.6 – 57.2	53.4
A1V53d	79.5	46.2 – 46.5	62.7 – 62.8	46.5 – 49.7	47.2 – 47.3	49.7 – 54.0	50.4
A1V55d	79.5	45.9 – 46.1	62.2 – 62.3	46.2 – 49.3	46.9 – 47.0	49.3 – 53.6	50.0
A1V57d	79.5	43.0 – 43.3	58.4 – 58.4	43.3 – 47.1	44.0 – 44.1	46.2 – 50.3	46.9
A1V515d	79.5	42.9 – 43.1	58.2 – 58.2	43.2 – 46.9	43.8 – 43.9	46.1 – 50.1	46.7
A1V519d	79.5	42.0 – 42.2	56.9 – 57.0	42.2 – 45.9	42.9 – 43.0	45.1 – 49.1	45.7
Q3V51d	79.5	46.9	52.1 – 55.4	47.4 – 49.1	nil	50.8 – 53.6	51.0
Q3V53d	79.5	45.7	48.9 – 54.0	46.1 – 47.8	nil	48.9 – 51.6	49.6
Q3V55d	79.5	45.1	48.2 – 53.3	45.6 – 47.2	nil	48.8 – 51.0	49.0
Q3V57d	79.5	43.8	46.9 – 51.8	44.3 – 45.9	nil	48.7 – 49.6	47.6
Q3V515d	79.5	43.3	49.1 – 51.2	43.7 – 45.4	nil	46.3 – 49.0	47.0
Q3V517d	79.5	43.1	46.2 – 51.0	43.6 – 45.2	nil	46.2 – 49.3	46.9
Numbers and arrangement of electrode tests series							
Q1V515d	79.5	43.6	48.4 – 51.5	44.0 – 45.6	nil	48.41 – 49.78	47.3
Q2V516d	79.5	39.1 – 39.9	48.6	40.7 – 44.0	39.3 – 40.5	Nil	41.2
Q3V517d	79.5	43.1	46.2 – 51.0	43.6 – 45.2	Nil	46.2 – 49.3	46.9
Q4V516d	79.5	37.1 – 39.1	43.3	38.9 – 43.9	38.5 – 39.6	Nil	39.6
A1V519d	79.5	42.0 – 42.2	56.9 – 57.0	42.2 – 45.9	42.9 – 43.0	45.1 – 49.1	45.7
A2V517d	79.5	42.2 – 46.5	46.8 – 48.3	45.6 – 46.3	45.4 – 46.0	45.7 – 47.6	45.5
Different applied voltage tests series							
A2V517d	79.5	42.2 – 46.5	46.8 – 48.3	45.6 – 46.3	45.4 – 46.0	45.7 – 47.6	45.5
A2V1016d	79.5	35.8 – 39.5	39.7 – 41.0	38.7 – 39.4	38.5 – 39.2	38.8 – 40.4	38.6
Q1V515d	79.5	43.6	48.4 – 51.5	44.0 – 45.6	Nil	48.4 – 49.8	47.3
Q2V1015d	79.5	36.7 – 37.4	45.6	38.5 – 41.2	36.8 – 38.0	Nil	38.6
Q4V516d	79.5	37.1 – 39.1	43.3	38.9 – 43.9	38.5 – 39.6	Nil	39.6
Q4V1014d	79.5	34.8 – 36.6	40.6	36.5 – 41.1	36.1 – 37.2	Nil	37.2
Q4V2012d	79.5	32.5 – 34.2	37.9	34.0 – 38.4	33.7 – 34.7	Nil	34.7

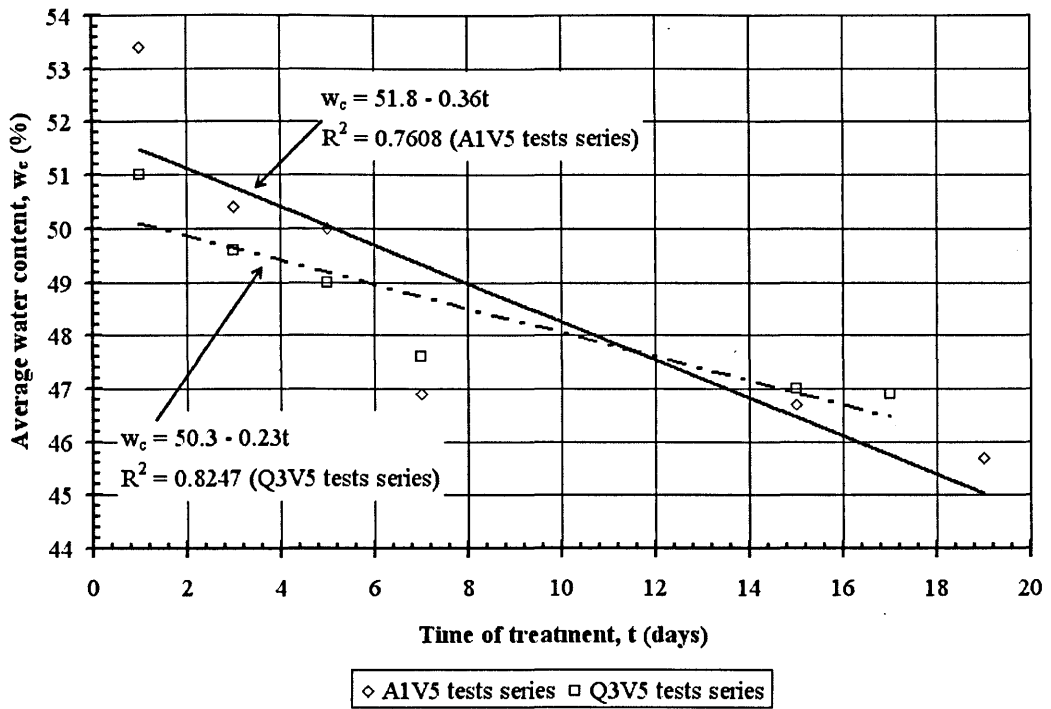


Figure 4.28: Result of treatment of time tests series: $w_{c \text{ average}}$ versus time

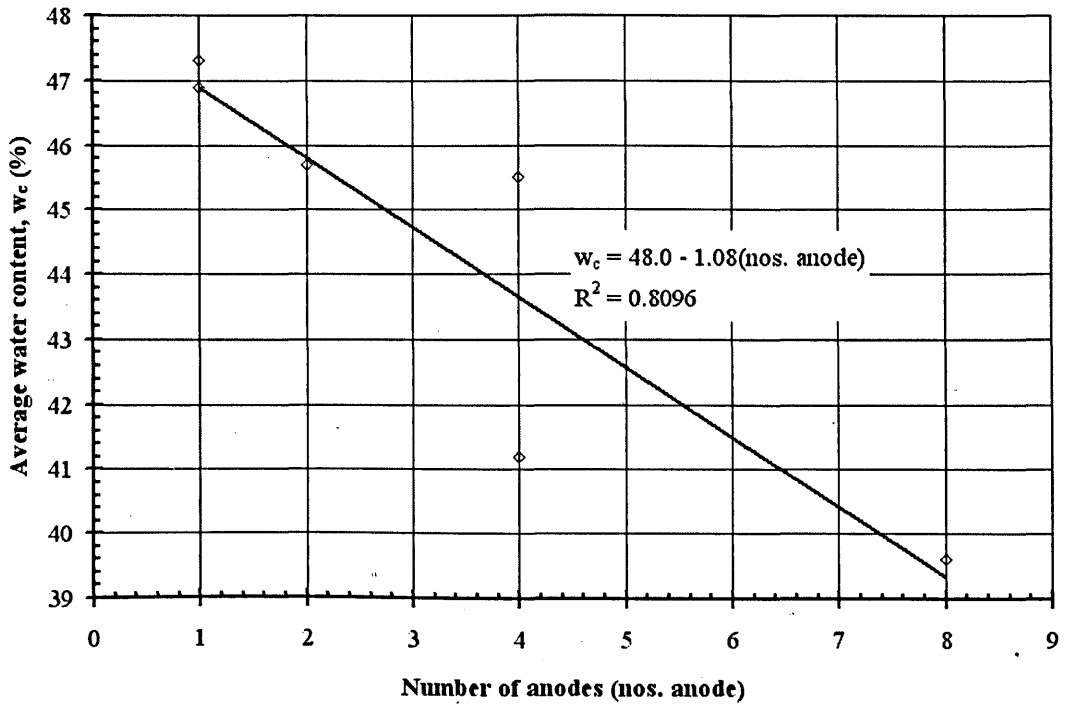


Figure 4.29: Result of numbers and arrangement of electrode tests series: $w_{c \text{ average}}$ versus number of anodes

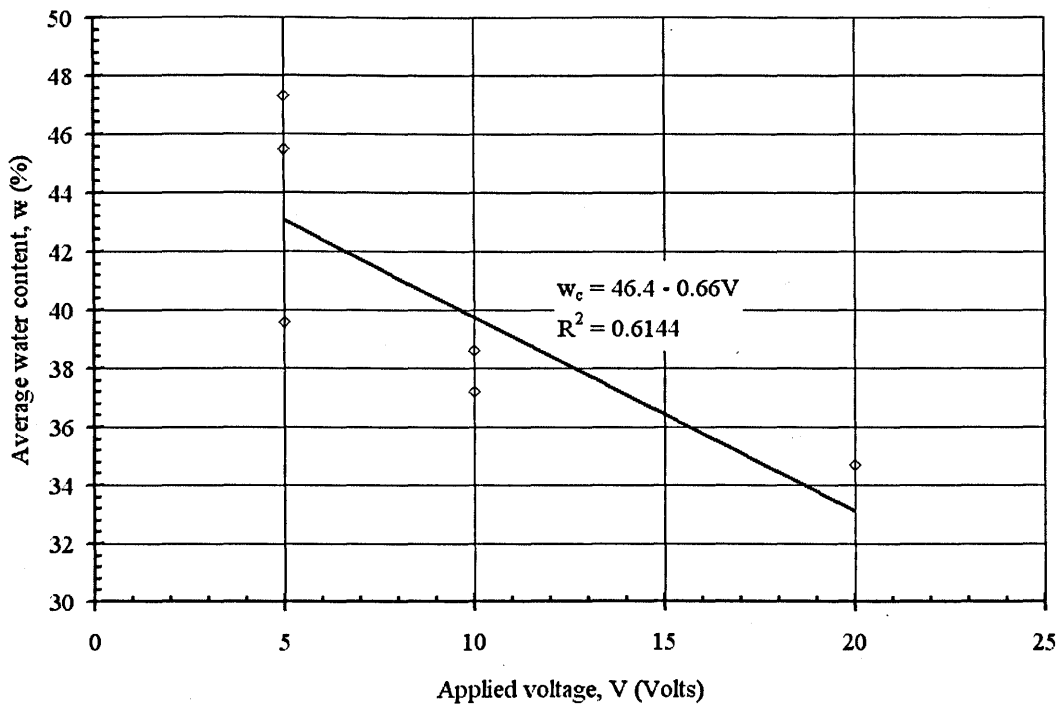


Figure 4.30: Different applied voltage tests series: w_c average versus applied voltage

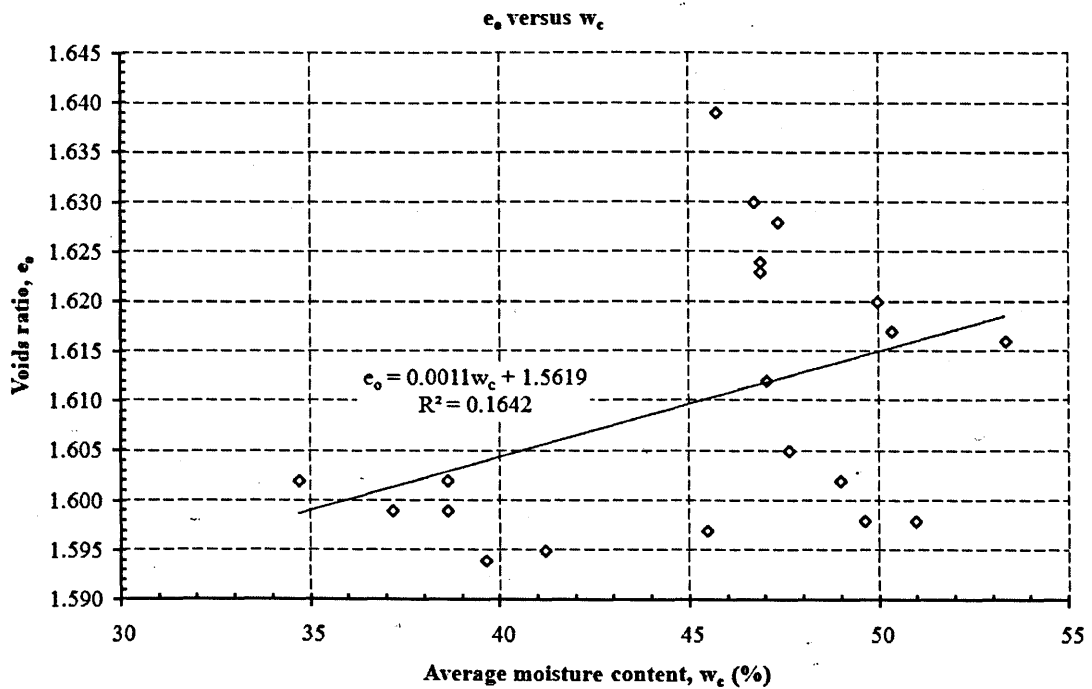


Figure 4.31 Correlation graph of all results: m_v versus e_o

4.3.6 Effect on coefficient of volume compressibility, m_v

The results of computed coefficient of volume compressibility including the result of the control test, before and after treatment, are presented in Table 4.8, as well as in Figures 4.32 to 4.35. Table 4.10 summarises the numbers of anodes, distance between electrodes, vertical displacement and water expelled at the end of electro osmotic consolidation phase, i.e., phase 2.

Table 4.10: Summary of numbers and arrangement of electrodes test series: numbers of anodes and cathodes applied voltage, distance between electrode, ΔH and W

Code	No. of anodes	No. of cathodes	Voltage (volts)	Distance (mm)	ΔH_{phase2} (mm)	W_{phase2} (mm)
Treatment of time tests series						
A1V51d	2	2	5	124	1.50	73
A1V53d	2	2	5	124	1.67	81
A1V55d	2	2	5	124	1.73	84
A1V57d	2	2	5	124	1.99	97
A1V515d	2	2	5	124	2.35	114
A1V519d	2	2	5	124	2.40	118.5
Q3V51d	1	2	5	63	0.49	24
Q3V53d	1	8	5	63	1.30	63
Q3V55d	1	8	5	63	1.48	72
Q3V57d	1	8	5	63	1.52	74
Q3V515d	1	8	5	63	1.72	83
Q3V517d	1	8	5	63	1.75	85
Numbers and arrangement of electrode tests series						
Q1V515d	1	4	5	63	1.55	75
Q2V517d	4	1	5	63	8.76	425
Q3V517d	1	8	5	63	1.75	83
Q4V516d	8	1	5	63	9.92	481
A1V519d	2	2	5	124	2.40	118.5
A2V517d	4	4	5	49	9.84	477
Different applied voltage tests series						
A2V517d	4	4	5	49	9.84	477
A2V1016d	4	4	10	49	11.41	553
Q2V516d	4	1	5	63	8.76	425
Q2V1015d	4	1	10	63	10.47	508
Q4V516d	8	1	5	63	9.92	481
Q4V1014d	8	1	10	63	11.86	575
Q4V2012d	8	1	20	63	14.17	687

Distance: distance anodes to cathodes; Voltage: applied voltage; ΔH_{phase2} : total displacement on phase 2 only; W_{phase2} : total water expelled on phase 2 only.

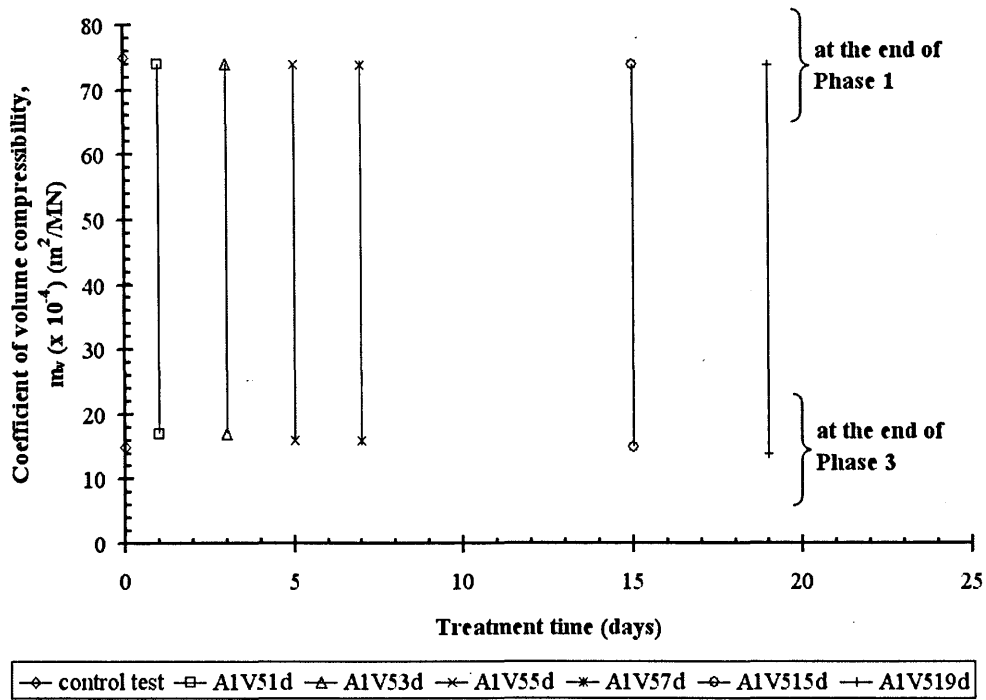


Figure 4.32 Result of A1V5 test series: m_v versus t

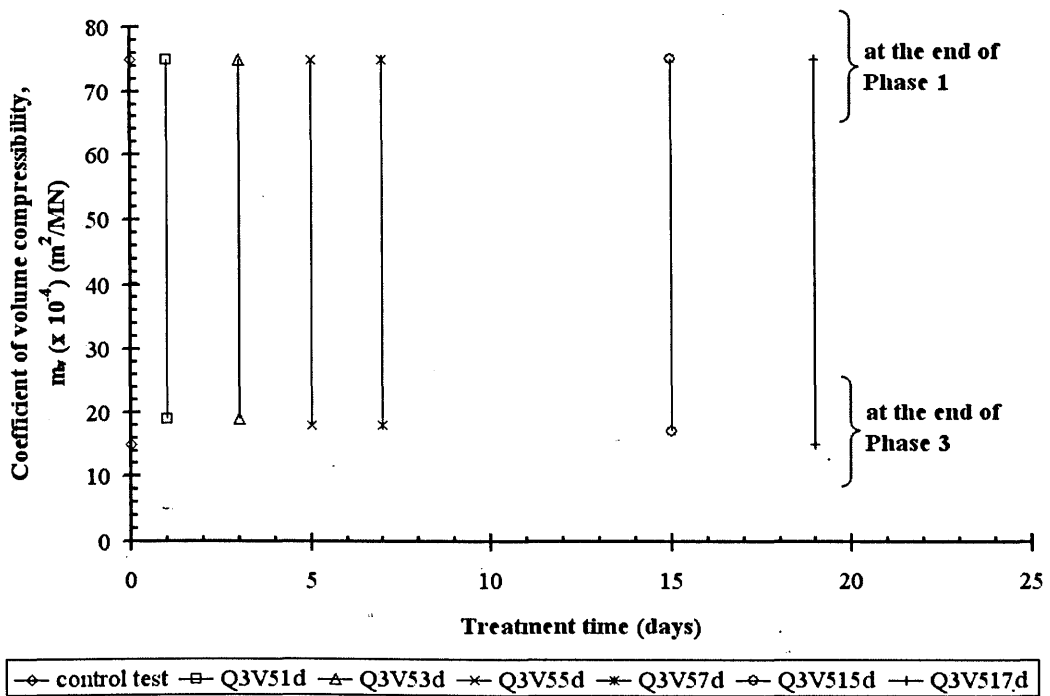


Figure 4.33 Result of Q3V5 test series: m_v versus t

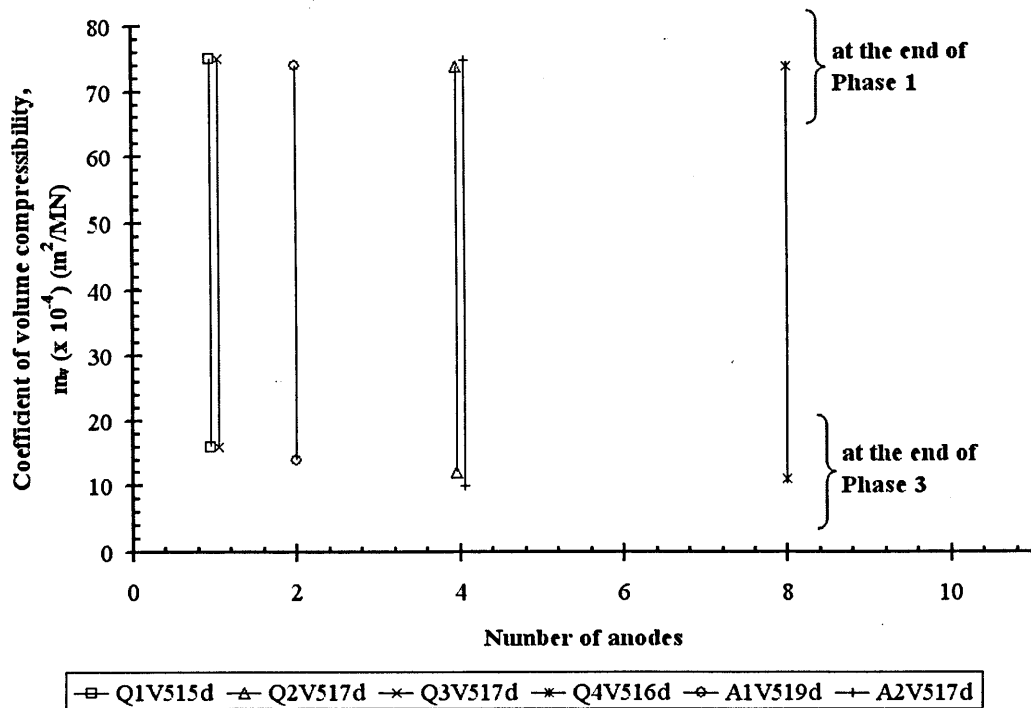


Figure 4.34 Result of numbers and arrangement of electrode test series: m_v versus number of anodes

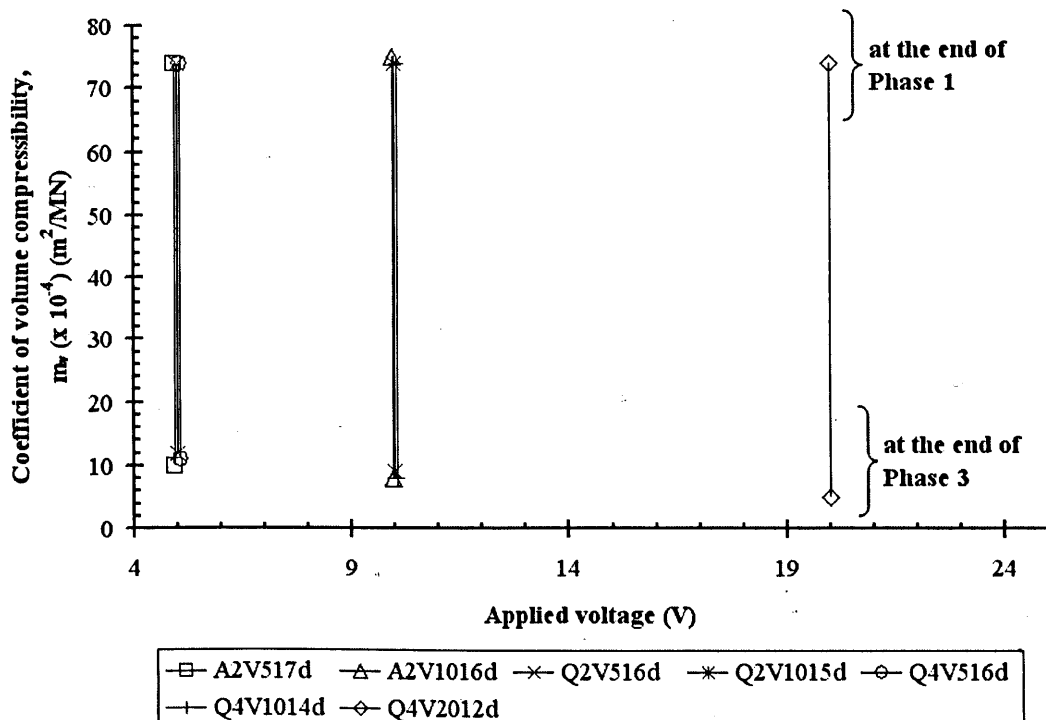


Figure 4.35 Result of different applied voltage test series: m_v versus V

4.3.7 Effect on constrained stiffness, $E_{\text{stiffness}}$

The initial constrained stiffness, $E_{\text{stiffness}}$, of the soil sample can be estimated from the applied vertical stress, $\Delta\sigma_v$, at Phase 1 which is 15 kPa. At the end of Phase 3, it can be calculated from the applied vertical stress, $\Delta\sigma_v$, at Phase 3 which was 50 kPa

$E_{\text{stiffness}}$ was divided into three parts, namely constant constrained stiffness, $E_{\text{stiffness}}$, constrained stiffness on the build phase, $E_{\text{build phase}}$, and constrained stiffness on pre-treatment, $E_{\text{pre-treatment}}$. $E_{\text{stiffness}}$ is a constrained stiffness which is calculated at the end of Phase 3 only. $E_{\text{build phase}}$ is similar to the $E_{\text{stiffness}}$ while $E_{\text{pretreatment}}$ is calculated by combining Phases 2 and 3. These three constrained stiffness are computed as average values. $E_{\text{build phase}}$ and $E_{\text{pre-treatment}}$ are used for the construction design purposes.

The results of $E_{\text{stiffness}}$, $E_{\text{build phase}}$, and $E_{\text{pre-treatment}}$ are summarised in Table 4.8, and Figures 4.36 to 4.44. As seen in these tables, the calculated $E_{\text{stiffness}}$, $E_{\text{build phase}}$, and $E_{\text{pre-treatment}}$ after treatment or at the end of 50 kPa phase, are higher than that at the end of Phase 1. Overall, compared to control test, between Phases 1 and 3, the constrained stiffness increased approximately by 3 times to 4 times.

Figures 4.36 to 4.39 show the constrained stiffness versus the time of treatment, numbers and arrangement of electrodes, and different applied voltage. The relationships in Figures 4.40 and 4.41, show the coefficient of correlation, R^2 , are 0.71 (good) with a limited data in Figure 4.40, 0.95 (very good) in Figure 4.41. Figures 4.41 to 4.44 show the average constrained stiffness for the build phase and pre-treatment. The coefficient of correlation, R^2 , in these figures are in range of 0.63 (good) to 0.98 (very good).

The computed results were consistent. The final computed average constrained stiffness were higher than the control test (Table 4.8).

It is also interesting to observe the average constrained stiffness increased more for different applied voltage compared to numbers and arrangement of electrodes. This suggests that the increase in stiffness is affected more by the voltage than the number of anodes.

Correlations of the calculated average constraint stiffness on build phase and pre-treatment are shown in Figures 4.40 to 4.45. From these figures it may be observed here that the average constrained stiffness were higher at the end of 50 kPa

mechanical loading of treated samples. The increment of the average constrained stiffness can be achieved by electro osmotic consolidation and consolidation.

The correlations (4.5) to (4.14) between the average constrained constraint stiffness, $E_{\text{stiffness}}$, constrained stiffness on build phase, $E_{\text{build phase}}$, and constrained stiffness on pre-treatment, $E_{\text{pre-treatment}}$ from Figures 4.40 to 4.45 are produced below:-

$$E_{\text{stiffness}} = 48.14 * (\text{nos. anode}) + 655.93; \\ \text{for numbers and arrangement of electrodes} \quad (4.5)$$

$$E_{\text{stiffness}} = 71.49V + 550.68; \\ \text{for different applied voltage} \quad (4.6)$$

$$E_{\text{pre-treatment}} = 9.7189t + 823.95 \quad (4.7)$$

$$E_{\text{build phase}} = 7.8868t + 590.66 \quad (4.8)$$

$$E_{\text{pre-treatment}} = 8.4985t + 739.66 \quad (4.9)$$

$$E_{\text{build phase}} = 6.606t + 526.35 \quad (4.10)$$

$$E_{\text{pre-treatment}} = 40.507(\text{nos. anode}) + 921.16 \quad (4.11)$$

$$E_{\text{build phase}} = 48.136(\text{nos. anode}) + 655.93 \quad (4.12)$$

$$E_{\text{pre-treatment}} = 71.718V + 782.22 \quad (4.13)$$

$$E_{\text{build phase}} = 71.488V + 550.68 \quad (4.14)$$

The correlations suggest that average constaned constrained stiffness, $E_{\text{stiffness}}$, constrained stiffness on build phase, $E_{\text{build phase}}$, and constrained stiffness on pre-treatment, $E_{\text{pre-treatment}}$ increases with:-

- (1) increasing number of anodes,
- (2) increasing applied voltage,

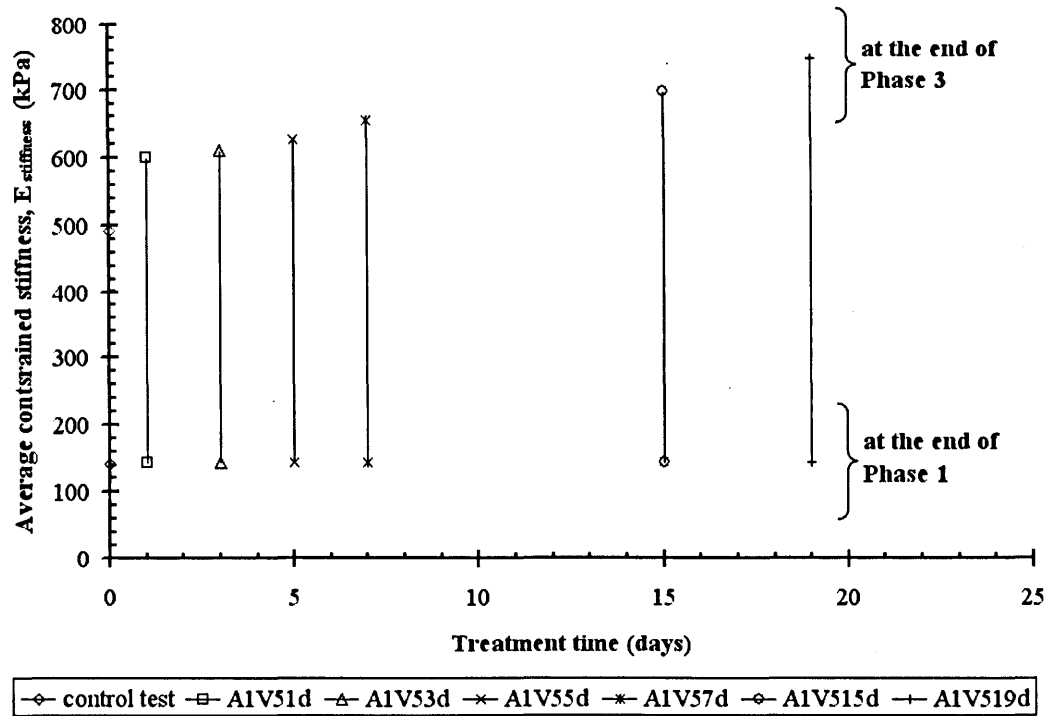


Figure 4.36 Result of A1V5 test series: $E_{stiffness}$ versus t

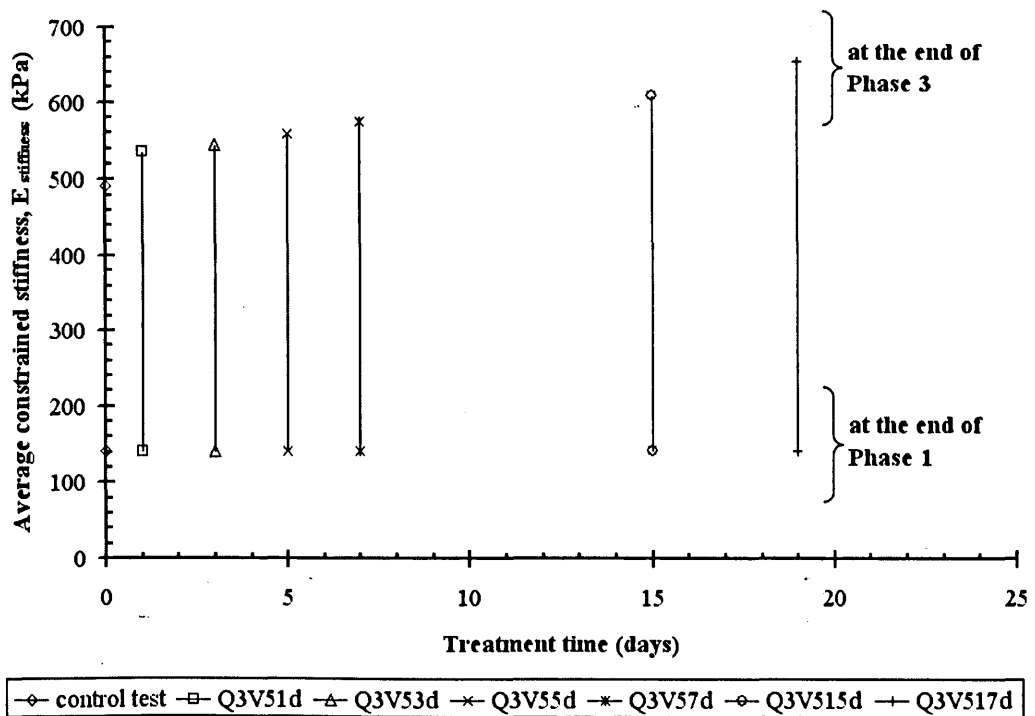


Figure 4.37 Result of Q3V5 test series: $E_{stiffness}$ versus t

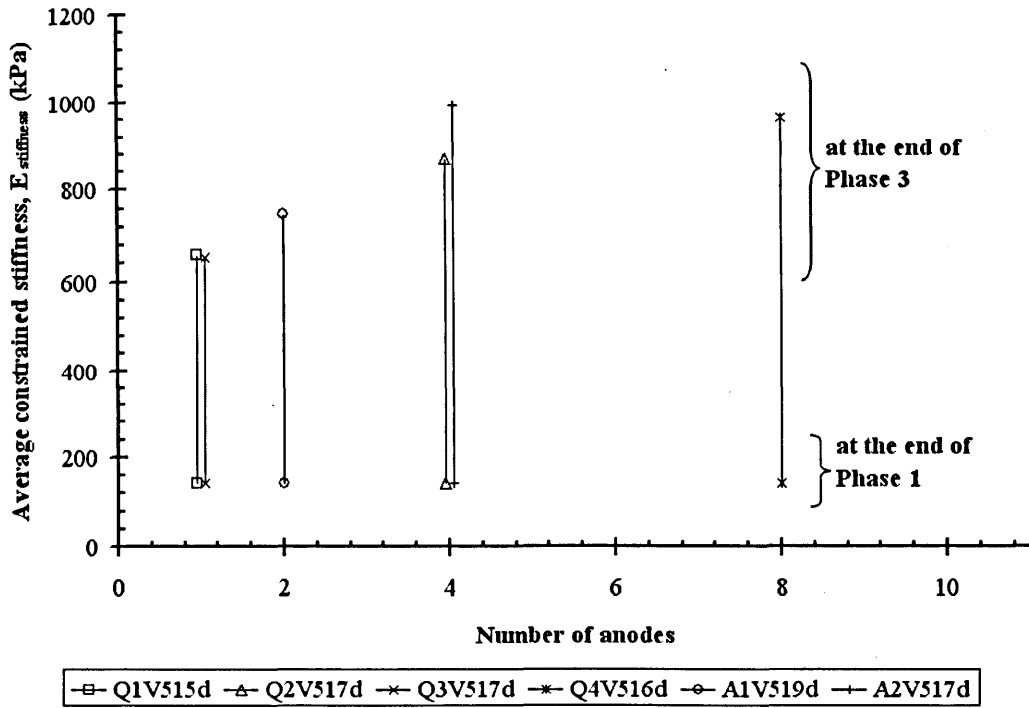


Figure 4.38 Result of numbers and arrangement of electrodes test series: $E_{stiffness}$ versus t

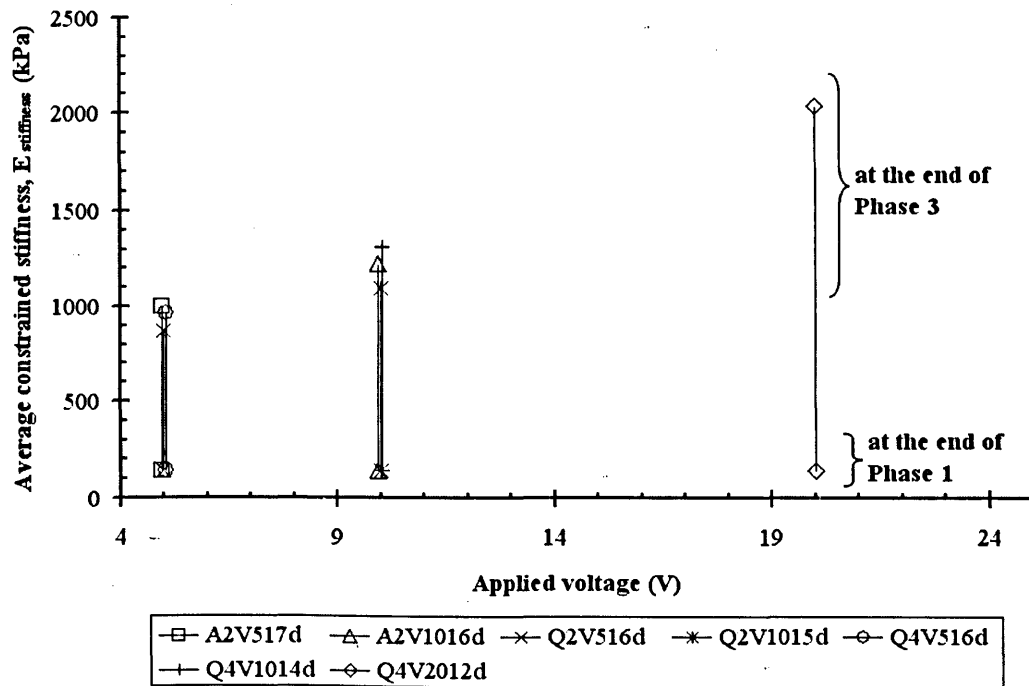


Figure 4.39 Result of different applied voltage test series: $E_{stiffness}$ versus t

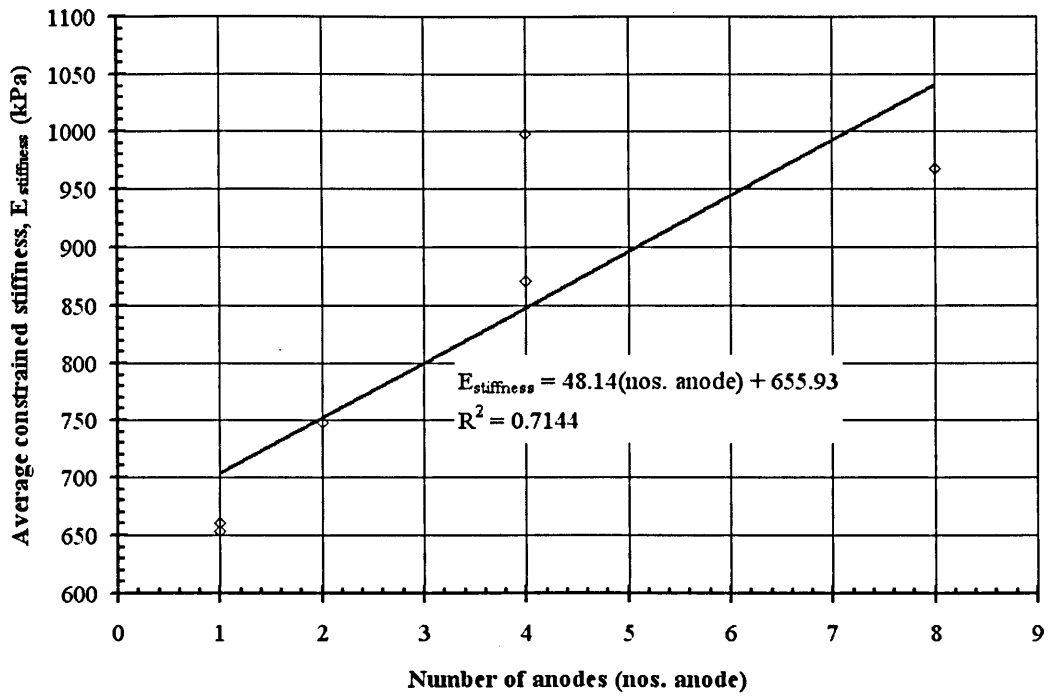


Figure 4.40 Relationship between $E_{stiffness}$ and number of anodes test series: at the end of Phase 3

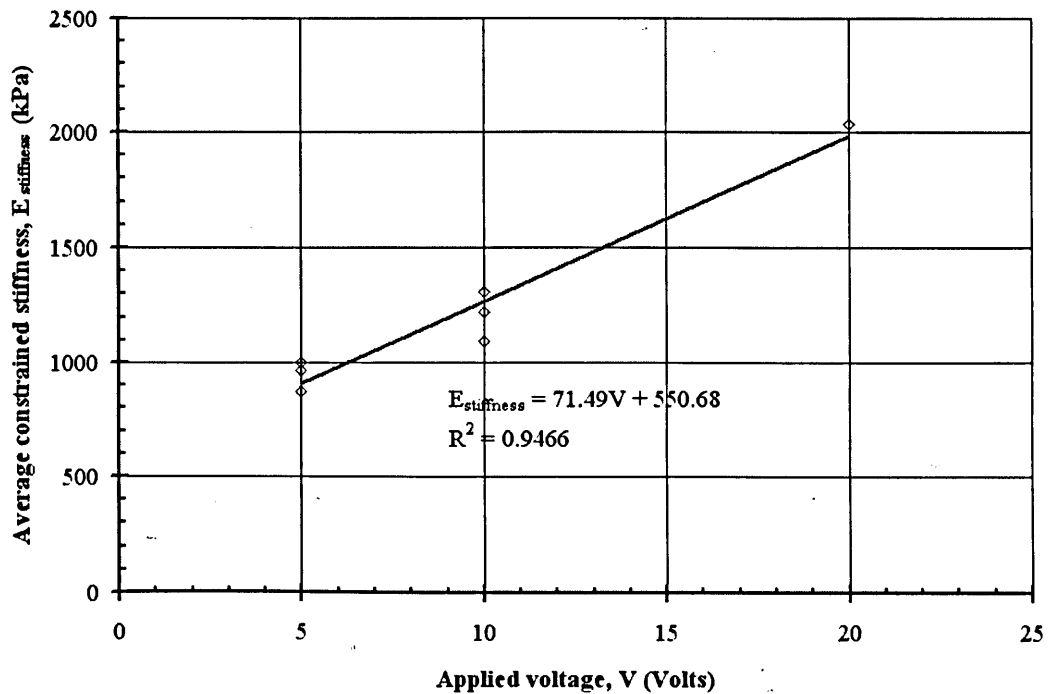


Figure 4.41 Relationship between $E_{stiffness}$ and different applied voltage test series: at the end of Phase

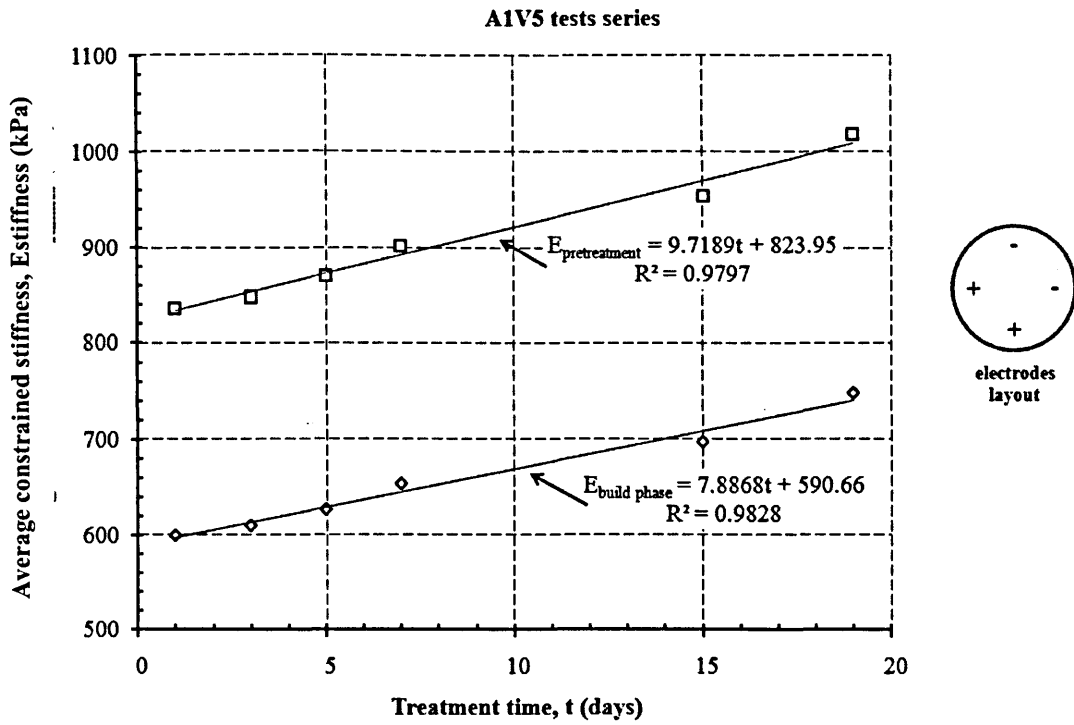


Figure 4.41 Relationship between $E_{\text{build phase}}$ and $E_{\text{pretreatment}}$ and A1V5 test series: at the end of Phase

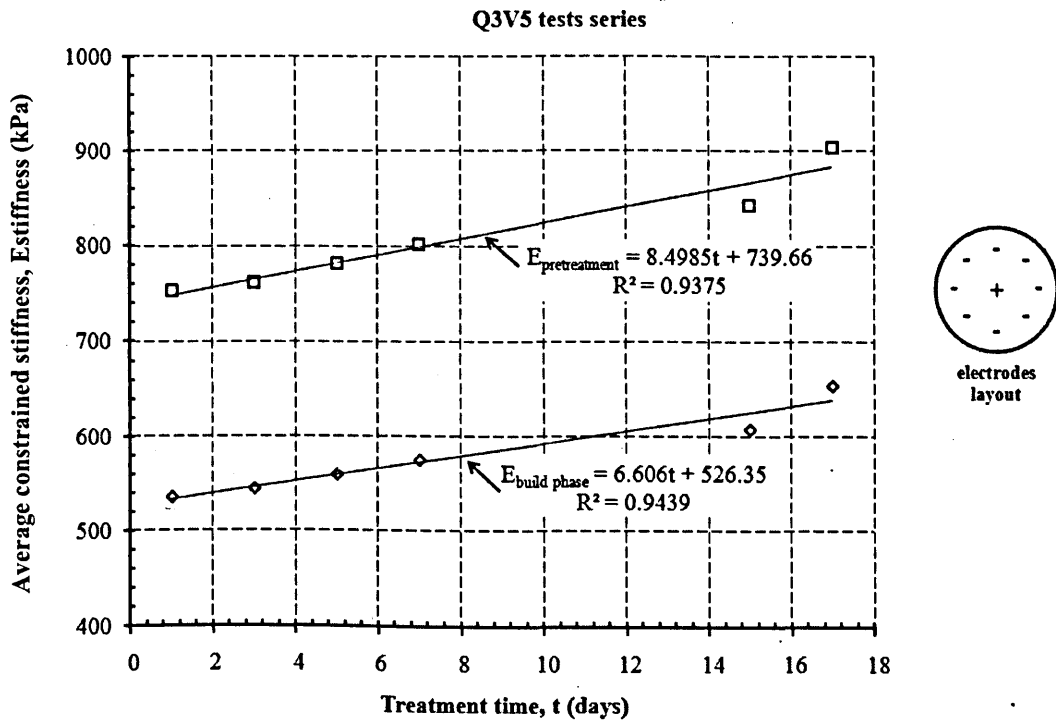


Figure 4.42 Relationship between $E_{\text{build phase}}$ and $E_{\text{pretreatment}}$ and Q3V5 test series: at the end of Phase

Numbers and arrangement of electrodes tests

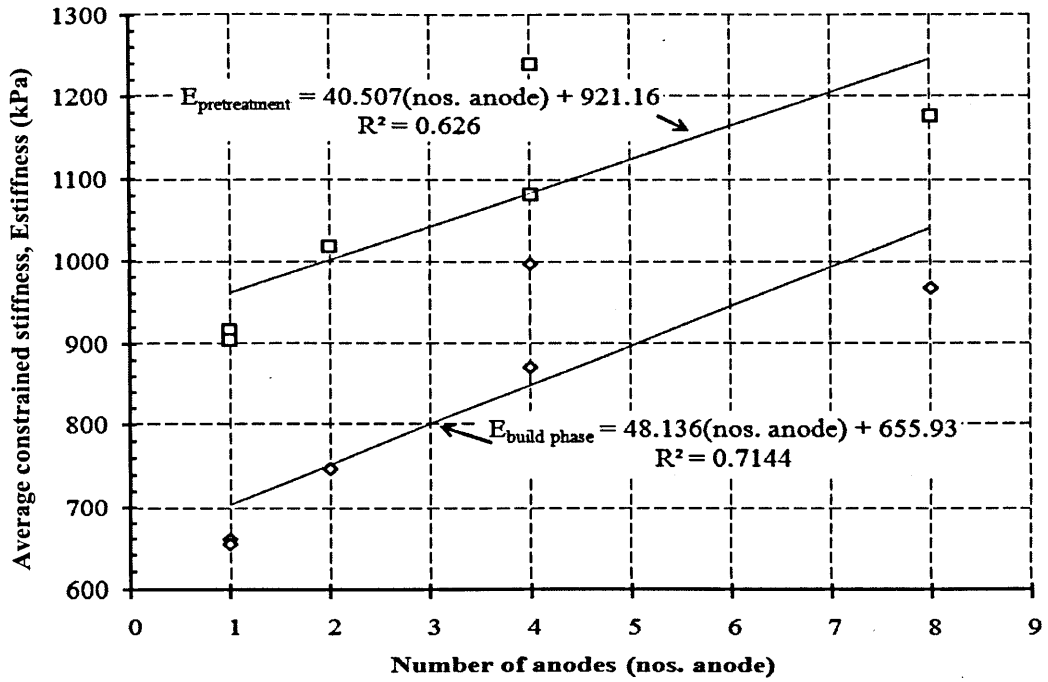


Figure 4.43 Relationship between $E_{\text{build phase}}$ and $E_{\text{pretreatment}}$ and number and arrangement of electrode test series: at the end of Phase

Different applied voltage tests

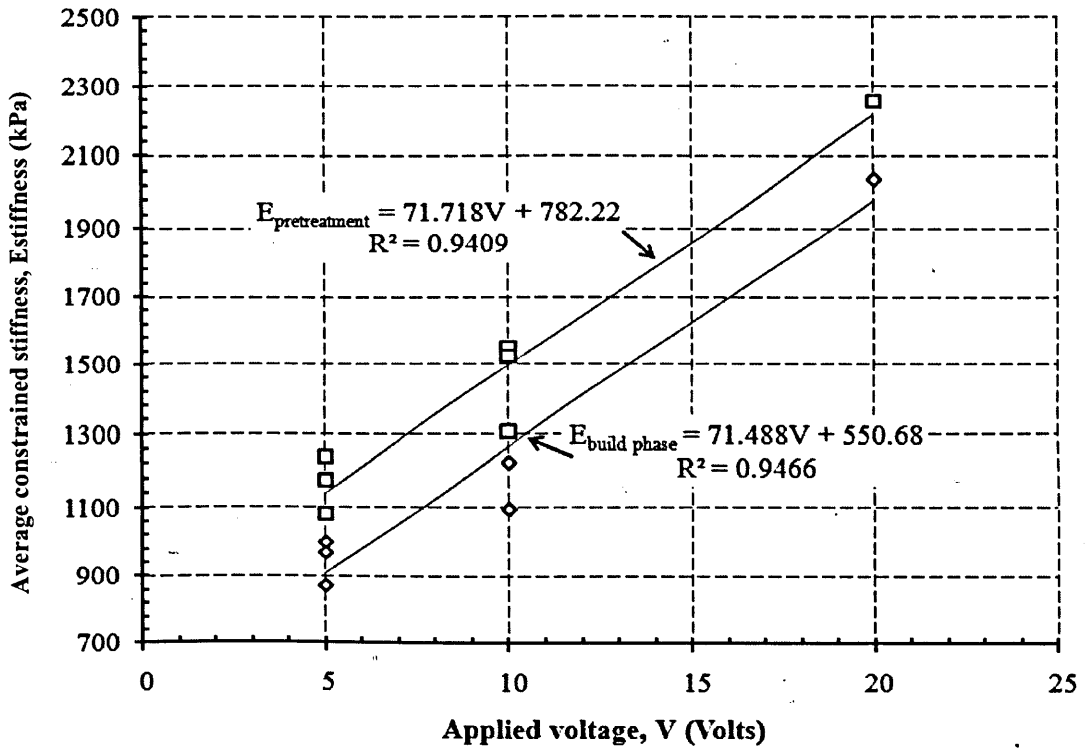


Figure 4.44 Relationship between $E_{\text{build phase}}$ and $E_{\text{pretreatment}}$ and different applied voltage test series: at the end of Phase

4.4. CONCLUSIONS

Twenty osmotic tests were performed on the China Clay Grade E kaolin in slurry form with an initial water content of 79.5%. Laboratory tests were carried out on the samples to study the effects of the electro osmotic consolidation process by 15 kPa vertical loading and consolidation process by 50 kPa vertical loading. The effects of the time of treatment, numbers and arrangement of electrodes, and applied voltage were studied. The conclusions from this investigation can be outlined as follows:

- (i). The China Clay Grade E kaolin responded well to electro osmotic consolidation treatment.
- (ii). Electro osmotic enhanced vertical loading consolidation is a feasible approach in stiffening of China Clay Grade E kaolin.
- (iii). The effectiveness of the combined electrical and mechanical consolidation treatment is significantly improved by varying the time of treatment, numbers and arrangement of electrodes, and applied voltage.
- (vi). Twelve sets of treated samples were performed for time of treatment. Longer time of treatment improves the effectiveness of the combined electro osmotic and mechanical consolidation.
- (v). Six sets of treated samples were investigated for numbers and arrangement of electrodes. Based on the experimental works, it was found that the higher numbers of the anodes installed in the system and the shorter the distance between electrodes, the greater the final total settlement.
- (vi). Seven sets of treated samples were carried out for applied voltage. The applied voltage of 20V was found to yield better results than those with a lower applied voltage. The final total settlement and volume changed readings were found to increase with increasing applied voltage.
- (vii). In addition, the final water content especially at the anodes, voids ratio and coefficient of volume compressibility were found to decrease. Meanwhile, the constrained stiffness was found to increase. All of these were found to decrease and increase with longer time of treatment, higher numbers of the anodes, the shorter distance between electrodes, higher applied voltage

CHAPTER 5

SUMMARY, CONCLUSIONS AND RECOMMENDATIONS FOR FUTURE RESEARCH

5.1 SUMMARY AND CONCLUSIONS

An extensive study on concept of the electro osmotic pile using China Clay Grade E Kaolin was carried out. The study focused on the design of an experiment to determine the relationship between the effect of osmosis and the capacity of the ground and undertake the experiments to determine the relationships between the components of the composite foundations and the improvements in the mechanical characteristics of the soft clay. The laboratory investigation was performed in a small electro osmotic consolidation chamber 345 mm high and 251 mm diameter PVC tube with 10.9 mm thick walls. 10 mm diameter vertical copper coiled springs were used as the electrodes that allowed the clay to consolidate either due to external load or osmosis. Factors, including the time of treatment, numbers of electrodes, the arrangement of electrodes and applied voltage were examined with twenty osmotic tests. A control test was used to benchmark the process.

A China Clay Grade E Kaolin slurry with a water content of 79.5% was used for all tests. 15 kPa vertical pressures were applied during Phase 1 and Phase 2 and 50 kPa in Phase 3. The 15k Pa was applied to simulate a working platform and to limit potential cracking at the surface. The 50 kPa was used to stimulate a surcharge such as that due to a shallow foundation or raising the ground level by about 3.0 m.

The properties of China Clay Grade E Kaolin, including water content, void ratio, coefficient of volume compressibility, average constrained stiffness and constrained stiffness in build phase and pre-treatment were determined before and after the treatment. Analysis of changes in soil properties provided important information about the effectiveness of electro osmotic consolidation approaches for soil stabilisation. The major findings can be summarised as follows:

- (i) There was 32 mm of settlement in Phase 1 of the control test and 19 mm further settlement in Phase 3. There was no Phase 2 in the control test. The further settlement in those tests with osmotic treatment varied between 12.45 mm and 17.47 mm for time of treatment test series, 8.83 mm and 14.26 mm for numbers of anodes and the distance between the electrodes, and 4.37 mm and 10.43 mm for different applied voltage test series.
- (ii) Twelve tests, series A1V5 and Q3V5, were used to evaluate the effect of time of osmotic treatment. The longer the time of treatment, the greater the settlement occurs. The current gradually reduced to zero at which time settlement stopped.
- (iii) Six tests series, Q1V515d, Q2V517d, Q3V517d, Q4V516d, A1V519d and A2V517d, were used to investigate the numbers of electrodes and arrangement of electrodes. Q3V517d showed the most amount of settlement. It had eight anodes and one central cathode. It can be concluded that increasing the number of anodes increased the settlement.
- (iv) Different applied voltage tests series are namely A2V517d, A2V1016d, Q2V516d, Q2V1015d, Q4V516d, Q4V1014d, and Q4V2012d. There were carried out to determine the effect of the applied voltage. Q4V2012d with 20 V gave the most settlement; that is increasing the voltage increased the settlement.
- (v) The tests clearly showed that the time of treatment, numbers of electrodes, arrangement of electrodes and applied voltage affected the electro osmotic processes. The stiffness of the system at the end of Phase 2 increased due to electro osmosis.

- (vi) Electro osmosis as preloading is an effective process for consolidating and strengthening China Clay Grade E Kaolin. Electro osmosis treatment reduced the water content at the anodes resulting in a reduction in voids ratio. This meant that there was a variation in stiffness across the sample but the overall stiffness of the samples increased resulting in ground improvement. Hence the principle of an electro osmotic pile was proven.

5.2 RECOMMENDATIONS FOR FURTHER RESEARCH

This study demonstrated that the combined electro osmotic and preloading approach can be utilised as a successful soil improvement technique for soft clay soil. Low voltage direct current was effective for this soil. The effects are illustrated by an increase of soil settlement, decrease of soil water content, decrease of voids ratio, decrease of coefficient of volume compressibility, and increase of average constrained stiffness, and constrained stiffness in build phase and pre-treatment. With the understanding obtained in this study, the following recommendations for further research may be made:

- (i) A field test should be conducted as the next stage of investigation. The applied voltage, electrical field configuration, electrodes spacing and arrangement should be carefully designed to determine the optimum layout.
- (ii) Application of high voltage electro osmotic consolidation should be further investigated as a possible technique for soil stabilisation merged with vertical loading.
- (iii) Further investigations on the use of other materials, such as iron, aluminium, steel or zinc, as electrodes. While different clay, different pore fluid chemistries and different structural clay soil can be further investigates.
- (iv) An analytical model of three dimensional electro osmotic consolidations should be developed and evaluated against the results obtained in this study.
- (v) Design guidelines should be prepared.

REFERENCES

- Abdullah, A.M.L.B. and Chandra, P. (1987) *Engineering Properties of Coastal Subsoils in Peninsular Malaysia*, Proceedings of the 9th Southeast Asia Geotechnical Conference, Volume 1, Bangkok, Thailand, page 127 – 138.
- Acar, Y.B., Gale, R.J., Hamed, J. and Putnam, G. (1990) *Acid/Base Distributions in Electrokinetic Soil Processing*, Journal of Transportation Research Record 1288, page 23 – 34.
- Alshawabkeh, A.N., Sheahan, T.C. and Wu, X. (2004) *Coupling of Electrochemical and Mechanical Processes in Soils Under DC Fields*, Journal of Mechanics of Materials, Volume 36, pp 453 – 465.
- Alshawabkeh, A.N., Yeung, A.T. and Bricka, M.R. (1999b) *Practical Aspects of In-Situ Electrokinetic Extraction*, Journal of Environmental Engineering, Volume 125, Number 1, page 27 – 35.
- Alshawabkeh, A.N., Gale, R.J., Ozsu-Acar, E. and Bricka, R.M. (1999a) *Optimization of 2-D Electrode Configuration for Electrokinetic Remediation*, Journal of Soil Contamination, Volume 8, Number 6, page 617 – 635.
- Aziz, S. (1993) *Engineering Characteristics of the Coastal Soft Soils of West Peninsular Malaysia*, M. Phil. Thesis, University of Strathclyde, United Kingdom.
- Balasubramaniam, A.S., Bergado, D.T. and Chandra, S. (1985) *Geotechnical Engineering in Southeast Asia – A Commemorative Volume of the Southeast Asia Geotechnical Society*, A.A. Balkema, Rotterdam, Boston.
- Ballou, E.V. (1955) *Electroosmotic Flow in Homoionic Kaolinite*, Journal of Colloid Science, Volume 10, page 450 – 460.
- Barker, J.E., Rogers, C.D.F., Boardman, D.I., and Peterson, J. (2004) *Electrokinetic Stabilisation: Overview and Case*, Ground Improvement, Vol. 8, No. 2, page 47 – 58.

- Bazozuk, M. and Labrecque, A. (1969) *Downdrag Measurements on 270-ft Composite Piles*, ASTM Special Technical Publications, No. 444, Research Paper No. 395, page 15 – 19.
- Bergado, D.T., Sasanakul, I., and Horpibulsuk, S. (2003) *Electro-Osmotic Consolidation of Soft Bangkok Clay using Copper and Carbon Electrodes with PVD*, Geotechnical Testing Journal, Vol. 26, No. 3, page 1 – 12.
- Bergado, D.T., Chai, J.C., Alfaro, M.C. and Balasubramaniam, A.S. (1994) *Improvement Techniques of Soft Ground in Subsiding and Lowland Environment*, A.A. Balkema, Rotterdam, Brookfield, Netherlands.
- Bjerrum, L., Moum, J. and Eide, O. (1967) *Application of Electro-Osmosis to a Foundation Problem in a Norwegian Quick Clay*, Géotechnique, Issue. 17, page 214 – 235.
- Brand, E.W. and Brenner, R.P. (1981) *Soft Clay Engineering*, Elsevier Scientific Publishing Company, Amsterdam, 1981.
- Bergado, D.T., Chai, J.C., Alfaro, M.C. and Balasubramaniam, A.S. (1994) *Improvement Techniques of Soft Ground in Subsiding and Lowland Environment*, A.A. Balkema, Rotterdam, Brookfield, Netherlands.
- Burnotte, F., Lefebvre, G. and Grondin, G. (2004) *A Case Record of Electroosmotic Consolidation Soft Clay with Improved Soil-Electrode Contact*, Canadian Geotechnical Journal, Volume 41, page 1038 – 1053.
- Bergado, D.T., Sasanakul, I., and Horpibulsuk, S. (2003) *Electro-Osmotic Consolidation of Soft Bangkok Clay using Copper and Carbon Electrodes with PVD*, Geotechnical Testing Journal, Vol. 26, No. 3, page 1 – 12.
- Butterfield, R. and Johnston, I.W. (1980) *The Influence of Electro-Osmosis on Metallic Piles in Clay*, Géotechnique, Number 1, Issue 30, page 17 – 38.
- Casagrande, L., Loughney, R.W. and Matich, M.A.J. (1961) *Electro-Osmotic Stabilization of High Slope in Loose Saturated Silt*, 5th International Conference on Soil Mechanics, Paris, Volume II, page 555 – 561.

- Casagrande, L. (1952b) *Electro-Osmotic Stabilization of Soils*, Journal of Boston Society of Civil Engineers, Volume 34, Number 1, pp 285 – 317.
- Casagrande, L (1952a) *Electrical Stabilization in Earthwork and Foundation Engineering*, Proceedings of Conference on Soil Stabilization, Massachusetts, pp 84 – 106.
- Casagrande, L. (1949) *Electro-Osmosis in Soils*, Géotechnique, Volume 1, Number 2, page 159 – 177.
- Chappell, B.A. and Burton, P.L. (1975) *Electro-Osmosis Applied to Unstable Embankment*, Journal of Geotechnical Engineering Division, Issue. 11495, page 733 – 740.
- Chen, J.-L. and Murdoch, L. (2002) *Effects of Electroosmosis on Natural Soil*, Journal of Geotechnical and Geoenvironmental Engineering, ASCE, Volume 125, Number 12, page 1090 – 1098.
- Das, B.M. (2010) *Principles of Geotechnical Engineering*, Cengage Learning, Stamford, USA.
- Eggstad, Å. (1983) *Improvement of Cohesive Soils*, Proceedings of the Eight European Conference on Soil Mechanics and Foundation Engineering, Volume 3, pp 991 – 1007.
- Eggstad, Å. And Føyn, T. (1983) *Electro-Osmotic Improvement of a Soft Sensitive Clay*, Proceedings of the 8th European Conference on Soil Mechanics and Foundation Engineering – Improvement of Ground, page 597 – 603.
- Esrig, M.I. (1968) *Pore Pressures, Consolidation, and Electrokinetics*, Journal of Soil Mechanics and Foundations Division, Proceedings of the American Society of Civil Engineers, Volume 94, Number SM4, page 899 – 921.
- Eykholt, G.R. and Daniel, D.E. (1994) *Impact of System Chemistry on Electroosmosis in Contaminated Soil*, Journal of Geotechnical Engineering, ASCE, Vol. 120, No. 5, page 797 – 815.

- Fetzer, C.A. (1967) *Electro-Osmotic Stabilization of West Branch Dam*, Journal of the Soil Mechanics and Foundations Division, Proceedings of the American Society of Civil Engineers, Volume 93, SM4, page 85 – 106.
- Gray, D.H. (1970) *Electrochemical Hardening of Clay Soils*, Géotechnique, Volume 20, Number 1, page 81 – 93.
- Gray, D.H. and Mitchell, J.K. (1967) *Fundamental Aspects of Electro-Osmosis in Soils*, Journal of the Soil Mechanics and Foundations Division, Proceedings of the American Society of Civil Engineers, Volume 93, SM6, page 209 – 236.
- Hamir, R. (1997) *Some Aspects and Applications of Electrically Conductive Geosynthetic Materials*, Doctor of Philosophy Thesis, University of Newcastle Upon Tyne, U.K.
- Hamir, R., Jones, C.J.F.P. and Clarke, B.G. (2001) *Electrically Conductive Geosynthetics for Consolidation and Reinforced Soil*, Geotextiles and Geomembranes, Volume 19, page 455 – 482.
- Hausmann, M. R (1990) *Engineering Principles of Ground Modification*, McGraw-Hill, Singapore.
- Head, K.H. (1994) *Manual of Soil Laboratory Testing, Volume 2: Permeability, Shear Strength and Compressibility Tests*, London: Pentech Press Limited Graham Lodge.
- Howell, A.E. (1970) *Construction of the Main Canals on the Muda Irrigation Project*, Proceedings 2nd Southeast Asian Conference on Soil Engineering, Singapore, page 149 – 161.
- Kalumba, D. (2006) *Remediation of Heavy Metal Contaminated Fine Grained Soils using Electrokinetic Geosynthetics*, Doctor of Philosophy Thesis, University of Newcastle Upon Tyne, U.K.
- Kamarudin, A., Khairul Anuar, K. and Mohd Raihan, T. (2006) *Electroosmotic Flows and Electromigrations during Electrokinetic Processing of Tropical Residual Soils*, Malaysian Journal of Civil Engineering, 18(2), page 74 – 88 .

- Kobayashi, Y., Todo, H., Weerasinghe, W.A.Y. and Chandra, P. (1990) *Comparison of Coastal Clay found in Singapore, Malaysia and Indonesia*, 10th Southeast Asian Geotechnical Conference, 16th – 20th April 1990, Taipei, Taiwan.
- Lambe, T.W. (1958) *The Structure of Compacted Clay*, Journal of the Soil Mechanics and Foundations Division, Proceedings of the American Society and Civil Engineers, Volume 84, Number 2, pp 1 – 34.
- Lee, S.L., Ramaswamy, S.D., Karunaratne, G.P., Lo, K.W., Yong, K.Y. and Moh, Z.C. (1985) *Ground Improvement Works in South-East Asia*, Geotechnical Engineering in Southeast Asia, A.A. Balkema/Rotterdam/Boston, page 97 – 110.
- Lefebvre, G. and Burnotte, F. (2002) *Improvements of Electroosmotic Consolidation of Soft Clays by Minimizing Power Loss at Electrodes*, Canadian Geotechnical Journal, Volume 39, page 399 – 408.
- Ledgerwood, E. (1990) *Short Geological Report on the Muda River Project, (Irrigation)*, Depth of Geology Survey, Min. of Rural Dev. Report.
- Lo, K.Y. and Shang, J.Q. (1994) *Effects of Intervening Media on Dielectrophoretic Strengthening of Soft Clays*, Canadian Geotechnical Journal, Volume 31, page 607 – 613.
- Lo, K.Y., Shang, J.Q. and Incullet, I.I. (1994) *Electrical Strengthening of Clays by Dielectrophoresis*, Canadian Geotechnical Journal, Volume 31, page 192 – 203.
- Lo, K.Y., Ho, K.S. and Incullet, I.I. (1992) *A Novel Technique of Electrical Strengthening of Soft Sensitive Clays by Dielectrophoresis*, Canadian Geotechnical Journal, Volume 29, page 599 – 608.
- Lo, K.Y., Incullet, I.I. and Ho, K.S. (1991a) *Electroosmotic Strengthening of Soft Sensitive Clays*, Canadian Geotechnical Journal, Volume 28, page 62 – 73.
- Lo, K.Y., Ho, K.S. and Incullet, I.I. (1991b) *Field Test of Electroosmotic Strengthening of Soft Sensitive Clays*, Canadian Geotechnical Journal, Volume 28, page 74 – 83.

- Lo, K.Y., Ho, K.S. and Incullet, I.I. (1991c) *The Effects of Electroosmotic Field Treatment on The Soil Properties of a Soft Sensitive Clays*, Canadian Geotechnical Journal, Volume 28, page 763 – 770.
- Lockhart, N.C. (1983c) *Electroosmotic Dewatering of Clays. III. Influence of Clay Type, Exchangeable Cations and Electrode Materials*, Journal of Colloids and Surfaces, Volume 6, Number 3, page 253 – 269.
- Lockhart, N.C. (1983b) *Electroosmotic Dewatering of Clays. II. Influence of Salt, Acid and Flocculants*, Journal of Colloids and Surfaces, Volume 6, Number 3, page 239 – 251.
- Lockhart, N.C. (1983a) *Electroosmotic Dewatering of Clays. I. Influence of Voltage*, Journal of Colloids and Surfaces, Volume 6, Number 3, page 229 – 238.
- Malaysian Highway Authority (1989) *Proceeding of the International Symposium on Trial Embankment on Malaysian Marine Clay*, Kuala Lumpur, Volume 1.
- Malusis, M.A. and Shackelford, C.D. (2002) *Chemico-Osmotic Efficiency of a Geosynthetic Clay Liner*, Journal of Geotechnical and Geoenvironmental Engineering, Volume 128, Number 2, page 97 – 106.
- Micic, S., Shang, J.Q. and Lo, K.Y. (2003a) *Improvement of the Load-Carrying Capacity of Offshore Skirted Foundations by Electrokinetics*, Canadian Geotechnical Journal, Volume 40, page 949 – 963.
- Micic, S., Shang, J.Q. and Lo, K.Y. (2003b) *Electrokinetics Strengthening of Soil Surrounding Offshore Skirted Foundations*, in Proceedings of the 13th International Offshore and Polar Engineering Conference, Honolulu, Hawaii, USA, 25 – 30 May 2003, ISOPE, Cupertino, California, page 665 – 672.
- Micic, S., Shang, J.Q. and Lo, K.Y. (2002c) *Bearing Capacity Enhancement of Skirted Foundation Element by Electrokinetics*, in Proceedings of the 12th International Offshore and Polar Engineering Conference, Kitakyushu, Japan, ISOPE, 25 – 31 May 2001, Volume 2, Cupertino, California, page 569 – 577.

- Micic, S., Shang, J.Q. and Lo, K.Y. (2002b) *Electro-Cementation of a Marine Clay Induced by Electrokinetics*, in Proceedings of the 12th International Offshore and Polar Engineering Conference, Kitakyushu, Japan, ISOPE, 25 – 31 May 2001, Volume 2, Cupertino, California, page 569 – 577.
- Micic, S., Shang, J.Q. and Mohamedelhassan, E., (2002a) *Bearing Capacity Enhancement of Skirted Foundation Element by Electrokinetics*, JSC, page 174 – 182.
- Micic, S., Shang, J.Q., Lo, K.Y., Lee, Y.N. and Lee, S.W. (2001) *Electrokinetic Strengthening of a Marine Sediment using Intermittent Current*, Canadian Geotechnical Journal, Volume 38, page 287 – 302.
- Mitchell, J.K. (1993) *Fundamentals of Soil Behaviour*, 2nd Edition, John Wiley and Sons, Inc., United States of America.
- Mitchell, J.K. (1991) *Conduction Phenomena: from Theory to Geotechnical Practice*, Géotechnique, Volume 41, Number 3, page 299 – 340.
- Mitchell, J.K. and Soga, K. (2005) *Fundamentals of Soil Behaviour*, 3rd Edition, John Wiley and Sons, Inc., United States of America.
- Mitchell, J.K. and Wan, T.-Y. (1977) *Electro-Osmotic Consolidation – Its Effects on Soft Soils*, Proceedings of the 9th International Conference on Soil Mechanics and Foundation Engineering, Volume 1, page 219 – 224.
- Mohamedelhassan, E.E. (2011) *Laboratory Model Test on Improving the Properties of Soft Clay by Electrokinetics*, International Scholarly Research Network, ISRN Civil Engineering, Volume 2011.
- Mohamedelhassan, E.E. (1998) *Electroosmotic Permeability of a Marine Sediment*, Master Thesis, The University of Western Ontario, London, Ontario.
- Morris, D.V., Hillis, S.F. and Caldwell, J.A. (1985) *Improvement of Sensitive Silty Clay by Electroosmosis*, Journal of Canadian Geotechnical, Issue 22, page 17 – 24.
- Murayama, S., and Mise, T. (1953) *On the Electrochemical Consolidation of Soil using Aluminium Electrodes*, Proceedings of the 3rd International Conference on Soil Mechanics and Foundation Engineering, Switzerland, Vol. 1, page 156 – 159.

- Nagaraj, T.S. and Miura, N. (2001) *Soft Clay Behaviour Analysis and Assessment*, Netherlands, A.A. Balkema.
- Pączkowska, B. (2005) *Electroosmotic Introduction of Methacrylate Polycations to Dehydrate Clayey Soil*, Canadian Geotechnical Journal, Volume 42, page 780 – 786.
- Pamukcu, S. (1997) *Electro-Chemical Technologies for In-Situ Restoration of Contaminated Subsurface Soils*, EJGE Paper 1997-04, page 1 – 37.
<http://ejge.com/1997/Ppr9704/Ppr9704.htm> on 25.04.2007.
- Pugh, R.C. (2002) *The Application of Electrokinetic Geosynthetic Materials to Uses in The Construction Industry*, PhD Thesis, School of Civil Engineering and Geosciences, University of Newcastle Upon Tyne, U.K.
- Rittirong, A., Shang, J.Q., Mohamedelhassan, E., Ismail, M.A., and Randolph, M.F. (2008) *Effect of Electrode Configuration on Electrokinetic Stabilization for Caissons in Calcareous Sand*, Journal of Geotechnical and Geoenvironmental Engineering, ASCE, Vol. 134, No. 3, page 352 – 365.
- Rittirong, A., Shang, J.Q., Ismail, M.A. and Randolph, M.F. (2006) *Effect of Electric Field Intensity on Electro-Cementation of Caissons in Calcareous Sand*, in Proceedings of the 16th International Offshore and Polar Engineering Conference, San Francisco, California, USA, ISOPE, May 28 – June 2, Cupertino, California, page 408 – 415.
- Schultz, D.S. (1997) *Electroosmosis Technology for Soil Remediation: Laboratory Results, Field Trial and Economic Modeling*, Journal of Hazardous Materials, Volume 55, page 81 – 91.
- Segall, B.A. and Bruell, C.J. (1992) *Electroosmotic Contaminant-Removal Process*, Journal of Environmental Engineering, ASCE, Volume 118, Number 1, pp 84 – 100.
- Shang, J.Q., Mohamedelhassan, E. and Ismail, M.A. (2004a) *Electrochemical Cementation of Offshore Calcareous Soil*, Canadian Geotechnical Journal, Vol. 41, No. 5, page 877 – 893.

- Shang, J.Q., Mohamedelhassan, E., Ismail, M.A. and Randolph, M.F. (2004b) *Electrochemical Cementation of Calcareous Sand for Offshore Foundations*, JSC, page 170 – 177.
- Shang, J.Q. (1997a) *Electrokinetic Sedimentation: A Theoretical and Experimental Study*, Journal of Canadian Geotechnical, Vol. 34, pp 305 – 314.
- Shang, J.Q. (1997b) *Zeta Potential and Electroosmotic Permeability of Clay Soils*, Canadian Geotechnical Journal, Volume 34, pp 627 – 631.
- Shang, J.Q. (1997c) *Electrokinetic Dewatering of Clay Slurries as Engineered Soil Covers*, Canadian Geotechnical Journal, Volume 34, pp 78 – 86.
- Shang, J.Q. and Lo, K.Y. (1997) *Electrokinetic Dewatering of a Phosphate Clay*, Journal of Hazardous Materials, Volume 55, pp 117 – 133.
- Shang, J.Q. and Dunlap, W.A. (1996) *Improvement of Soft Clays by High-Voltage Electrokinetics*, Journal of Geotechnical Engineering, ASCE, Volume 122, Number 4, page 274 – 280.
- Shukla, K.P. (1953) *Electro-Chemical Treatment of Clays*, Proceedings of the 3rd International Conference on Soil Mechanics and Foundation Engineering, Switzerland, Vol. 1, page 199 – 202.
- Soderman, L.G. and Milligan, V. (1961) *Capacity of Friction Piles in Varved Clay Increased by Electro-Osmosis*, 5th International Conference on Soil Mechanics, Paris, Volume II, page 143 – 147.
- Soo, S.S., Jeong, S.Y., Koh, K.H., Kim, J.Y. and Jang, Y.S. (2006) *A Study on Improvement on Marine Clay through the Electrolytic Leaching Effect in an Electrode*, Proceedings of the 16th (2006) International Offshore and Polar Engineering Conference, San Francisco, California, USA, page 540 – 545.
- Suter, S. (2008) *Development of a Composite Foundation Using Electrokinetic Dewatering*, Master of Engineering Thesis, University of Newcastle Upon Tyne, U.K.
- Taylor, R.G. and James, P.G. (1967) *Geotechnical Aspects of the Muda Irrigation Project*, Proceedings 1st Southeast Asian Conference on Soil Engineering, Bangkok, page 33 – 42.

- Terzhagi, K., Peck, R.B. and Mesri, G. (1996) *Soil Mechanics in Engineering Practice*, 3rd Edition, New York, Wiley.
- Ting, W.H. and Chan, S.F. (1971) *Bearing Capacity of Bakau Timber Piles in the Coastal Alluvium of West Malaysia*, Proceedings 4th Asian Regional Conference on Soil Mechanic and Foundation Engineering, Bangkok, Volume 1, page 317 – 322.
- Ting, W.H., Ooi, T.A. and Chong, S.M. (1975) *An Analysis of Pile Behaviour in Prai Area*, Proceedings 4th Asian Regional Conference on Soil Mechanic and Foundation Engineering, Bangkok, Volume 1, page 328 – 334.
- Ting, W.H. and Ooi, T.A. (1977) *Some Properties of the Coastal Alluvia of Peninsular Malaysia*, Proceedings of the International Symposium on Soft Clay, Bangkok, page 89 – 101.
- Wan, T.-Y. & Mitchell, J.K. (1976) *Electro-Osmotic Consolidation of Soils*, Journal of the Geotechnical Engineering Division, ASCE, Volume 102, GT5, page 473 – 491.
- Yee, K. and Ong, R. (2006) *Ground Improvement Techniques Concepts and Applications*, 2 Day Technical Course on Geotechnical Engineering, The Institution of Engineers, Malaysia, Lecture: 8, pp 1 – 25.
- Yodsudjai, W., Otsuki, N. and Nishida, T. (2006) *Feasibility Study on Soil Improvement using Electrochemical Technique*, Technology and Innovation for Sustainable Development Conference (TISD2006), Thailand, page 117 – 121.

APPENDIX A

Soil improvement approaches (reproduced from Hausmann, 1990, Lee *et al.*, 1985)

Approach	Improvement Type	Principle	Most suitable soils and types	Depth (m)	Advantages and Limitations
Blasting	Vibrocompaction	Shock waves lead liquefaction, displacement and remoulding	Saturated, clean sands, partly saturated sands and silts after flooding	18.3	speedy, cost-cutting, treat small areas, no improvement near surface, unsafe (refer to Figure 2.3)
Terra probe		Densify by vertical vibration, liquefaction induced displacement under overburden	Saturated or dry clean sand (less effective in finer sand)	18.3 (ineffective above 3.66 m depth)	speedy, easy, excellent under water, soft under layers may damp vibrations, difficult to penetrate over layers (refer to Figure 2.4)
Vibratory rollers		Densify by vibration, liquefaction induced displacement under roller weight	Cohesionless soils	1.80 to 2.75	finest approach for thin layers or lifts (refer to Figure 2.5)

depth: the maximum depth of treatment for effective treatment.

Approach	Improvement Type	Principle	Most suitable soils and types	Depth (m)	Advantages and Limitations
Dynamic compaction (consolidation) or heavy tamping		Duplicated high intensity impacts at the surface gives instant displacement	Cohesionless soils best, other soils can be improved	13.73 to 18.30	Easy, speedy, have to look after from personal injury and goods damage from airborne debris; groundwater have to be more than 1.83 m

		soil			sands
--	--	------	--	--	-------

depth: the maximum depth of treatment for effective treatment.

Approach	Improvement Type	Principle	Most suitable soils and types	Depth (m)	Advantages and Limitations
Compaction piles	Compaction piles	Densify by displacement of pile volume and by vibration during driving	Loose sandy soils, partly saturated clayey soils, loess	18.3 (limited improvement above 0.92 to 1.83)	helpful in soils with fines, consistent compaction, simple to verify results, time-consuming
Sand compaction piles		Sand installed in driven pipe, pipe partially withdrawn and redriven with vibratory hammer	all	nil	Compressed air may be employed to maintain hole open as casing partially withdrawn (refer to Figure 2.8)
Preloading	Precompression	Load applied adequately in advance of construction to precompress soil	Normally consolidated soft clays, silts, organic deposits, landfills	nil	Simple, consistent, extensive time requisite (apply sand drains or strip drains to lessen time)
Surcharge fills		Fill exceeding that required to achieve a		nil	quicker than preloading exclusive of

		given displacement; shorter time; excess fill removed			surcharge (apply sand or strip drains to lessen time)
--	--	---	--	--	---

depth: the maximum depth of treatment for effective treatment.

Approach	Improvement Type	Principle	Most suitable soils and types	Depth (m)	Advantages and Limitations
Electro osmosis	Precompression	Direct current causes water flow from anode towards cathode where it is removed	Normally consolidated silts and clays	9.15 to 18.3	No fill loading necessary; apply in small areas; speedy; non consistent properties between electrodes; ineffective in extremely pervious soil
Mix-in-place Piles and Walls	Reinforcement	Lime, cement or asphalt mixed by rotating auger or in place mixer	All soft or loose inorganic soils	More than 18.3	Applies native soil; diminished lateral sustain necessitated during excavation; complicated quality control
Strips and membranes		Horizontal tensile strips or membranes buried in soil under footings	All	Less than 3.05	Increased allowable bearing capacity; diminished deformations

Vibroreplacement stone		Hole jetted in soft, fine grain soil and back filled with densely compacted gravel	Very soft to firm soils (undrained strength 19.15 kPa to 47.88 kPa)	18.3	Quicker than precompression; evades dewatering necessitated for eliminate and restore; restricted bearing capacity
------------------------	--	--	---	------	--

depth: the maximum depth of treatment for effective treatment.

Approach	Improvement Type	Principle	Most suitable soils and types	Depth (m)	Advantages and Limitations
Vibrodisplacement stone	Reinforcement	Probe displaces soil laterally; backfill discharged via probe or placed in layers after probe removed	Soft to firm soils (undrained strength 28.73 kPa to 57.46 kPa)	15.25	Best in low sensitivity soils with low groundwater
Particulate grouting	Grouting and Injection	Penetration grout fills soil voids	Medium to coarse sand and gravel	Unlimited	Cost cutting; grout high strength
Chemical grouting		Solutions of two or more chemical react in soil pores to form gel or soil precipitate	Medium silts and coarser	Unlimited	Low viscosity; handy gel time; excellent water shut off; high cost; difficult to assess
Pressure injected lime and lime-flyash		Lime slurry and lime-flyash slurry injected to shallow depths under pressure	Expansive clays, silts and loose sands	Unlimited (usually 1.83 to 2.75)	Rapid and cost cutting for foundations under light structures; flyash with lime may rise cementation and strength and reduce

					permeability
Displacement or compaction grout		Highly viscous grout acts as radial hydraulic jack when pumped under high pressure	Soft, fine grained soils; soils with large voids or cavities	12.20	accurates differential displacement; fills large voids; necessitates cautious control

depth: the maximum depth of treatment for effective treatment.

Approach	Improvement Type	Principle	Most suitable soils and types	Depth (m)	Advantages and Limitations
Jet grouting	Grouting and Injection	Cement grouts injected to substitute and blend with soils eroded by high pressure water jet	Alluvial, cohesive, sandy, gravelly soils, miscellaneous fill and others	Unlimited	Rises soil strength and lessens permeability; broad application
Electro kinetic injection		Stabilizing chemical moved into soil by electro osmosis	Saturated silts; silt clays	Unknown	Soil and structure not subject to high pressures; ineffective in pervious soil
Remove and replace	Miscellaneous	Soil excavated, substituted with competent matter or improved by drying or admixture and recompacted	Inorganic soil	Less than 9.15	Consistent; controlled when substituted; may necessitate huge area dewatering
Moisture barriers		Water access to foundation soil is minimized and more	Expansive soil	4.58	Most excellent for undersized structures and pavements; may

		consistent			not be 100% effective
Prewetting		Soil is brought to approximated final water content prior to construction		1.83	Cost cutting; most excellent for undersized; light structures; soil may still shrink and swell

depth: the maximum depth of treatment for effective treatment.

Approach	Improvement Type	Principle	Most suitable soils and types	Depth (m)	Advantages and Limitations
Structural fills	Miscellaneous	Structural fill distributes loads to underlying soft soils	Soft clays or organic soils; marsh deposits	nil	High strength; good distribution to underlying soft soils

depth: the maximum depth of treatment for effective treatment.

APPENDIX B

Outline of several of the earlier electro osmosis experiments

Voltage: applied voltage (unit volts); voltage gradient: volts/cm; current densities (Amp/m²); *.: not applicable; ✓: applicable; C-EO: consolidation by electro osmosis; EO-DL: electro osmosis combined with direct loading consolidation; n.m.: not mentioned; rod or plate: type of electrodes applied in the experiments; h: height of tank model; L: length of tank model; D: diameter of tank model; W: width of tank model; d: diameter of electrode; l: length of electrode.

Reference	Description	Voltage	Voltage Gradient	Current Density	Electrodes	Field/Lab Test	Series of Test	
							C-EO	EO-DL
Rittirong <i>et al.</i> (2008)	To study the effects of the electrodes configuration on the electric field on model caissons embedded in calcareous sand	6, 13	n.m.	n.m.	Ferum	*lab test *cylinder tank model with D = 575 mm; h = 575 mm *electrode states = rod with d = 14 mm, 50 mm; l = 140 mm, 240 mm, 250 mm, 450 mm and its vertically installed		✓
Suter (2008)	To study use of MMO as electrodes in electro osmotic consolidation.	20	25	n.m.	Netlon electrokinetic geosynthetics	*lab test *cylinder tank model with D = 322 mm; h = 250 mm * electrode states = rod and its vertically installed	✓	✓
Kalumba (2006)	To determine the feasibility study of extracting heavy metals from contaminated fine soils using electrokinetic technology with electrokinetic geosynthetics	18	0.5	1 – 10	Netlon electrokinetic geosynthetics	*lab test *rectangular tank model with L = 500 mm; W = h = 250 mm * electrode states = rod with d = 65 mm, l = 250 mm and its vertically installed	✓	

Reference	Description	Voltage	Voltage Gradient	Current Density	Electrodes	Field/Lab Test	Series of Test	
							C-EO	EO-DL
Kamarudin <i>et al.</i> (2006)	To investigate the changes in strength, compressibility and hydraulic conductivity of a tropical residual soil after treated by EK processing using different concentrations of a selected electrolyte.	30	0.06 – 4.29	0.01 – 3.13	Titanium mesh	*lab test *cylinder tank model with D = 100 mm; L = 230 mm * electrode states = plate and its vertically installed	✓	
Rittirong <i>et al.</i> (2006)	To investigates the effects of the electric field intensity on the electrocementation	13	n.m.	n.m.	Perforated steel pipe	*lab test *rectangular tank model with L = 575 mm; h = 890 mm * electrode states = rod with d = 65 mm, l = 250 mm and its vertically installed		✓
Soo <i>et al.</i> (2006)	To suggest a new method to increase the shear strength in marine clay using an electric decomposition reaction of ferum and aluminium electrode inserted in marine clay.	n.m.	n.m.	n.m.	Ferum and aluminium	*lab test *rectangular tank model with L = 500 mm, W = 400 mm; h = 500 mm * electrode states = rod	✓	
Yodsujai <i>et al.</i> (2006)	To study the feasibility of using an electrochemical technique to improve the soil mechanics properties	n.m.	n.m.	n.m.	Titanium mesh	*lab test *cylinder tank model 1 with D = 25 mm; L = 115 mm *cylinder tank model 2 with D = 100 mm; L = 200 mm * electrode states = plate and its vertically installed	✓	

Reference	Description	Voltage	Voltage Gradient	Current Density	Electrodes	Field/Lab Test	Series of Test	
							C-EO	EO-DL
Pączkowska (2005)	To present the results of research on the modification of highly swelling and contractible Pliocene clays.	n.m.	0.5	n.m.	Stainless steel sheet	*lab test *rectangular tank model with L = 360 mm; W = 200 mm; h = 200 mm * electrode states = plate		✓
Alshwabkeh <i>et al.</i> (2004)	To covers the fundamentals of this three-way coupling and presents specific case studies on its applications and modelling the effects.	n.m.	1	1.33	analyte	*lab test *rectangular tank model with L = 400 mm; W = 50; h = 150 cm *electrode installed vertically	✓	
Barker <i>et al.</i> (2004)	To provide an overview of the electrokinetic process and to describe a field trial	8, 20, 50	n.m.	n.m.	Mild steel tube	*field work * electrode states = rod with L = 1 m; d = 65 mm and its vertically installed	✓	
Burnotte <i>et al.</i> (2004)	Describe the site and the site field setup for electro osmotic consolidation	93	0.31	n.m.	Cylinder steel pipe	*field work *piles with D = 300 mm; L = 14.5 m and its vertically installed		✓
Bergado <i>et al.</i> (2003)	To evaluate the electro osmotic effects generated on both undisturbed and reconstituted Bangkok clay using the combination of electrodes with PVD and to compare the efficiency of using copper and carbon	n.m.	60 – 120	n.m.	Copper and carbon	*lab test *square tank model 1 with D = 300 mm; h = 300 mm *square tank model 2 with D = 450 mm; h = 950 mm * electrode states = rod with d = 13.6 mm and its vertically installed		✓

Reference	Description	Voltage	Voltage Gradient	Current Density	Electrodes	Field/Lab Test	Series of Test	
							C-EO	EO-DL
Shang <i>et al.</i> (2004b, 2004a)	To explore the feasibility of applying electrokinetic and electrochemical techniques in the improvement of offshore calcareous soils.	4	15.7 – 24.1	n.m.	Stainless steel for anode; perforated steel for cathode	*lab test *rectangular tank model with L = 350 mm; W = 100 mm; h = 240 mm * electrode states = plate and its vertically installed		✓
Bergado <i>et al.</i> (2003)	To evaluate the electroosmotic effects generated on both undisturbed and reconstituted Bangkok clay using the combination of electrodes with PVD and to compare the efficiency of using copper and carbon as electrodes	n.m.	60, 120	n.m.	Copper and carbon	*lab test *cylinder tank model 1 with D = 300 mm; h = 300 mm *cylinder model 2 with D = 450 mm; h = 950 mm * electrode states = rod with d = 13.6 mm and its vertically installed		✓
Micic <i>et al.</i> (2003b)	To presents the results of soil laboratory tests carried out on simulated marine sediment adjacent to skirted foundation models placed in a model tank after electrokinetic treatment.	5, 5.2	n.m.	n.m.	Stainless steel for anode; perforated steel for cathode	*lab test *rectangular tank model with L = 750 mm; W = 730 mm; h = 650 mm * electrode states = rod with d = 10 mm, 16 mm and its vertically installed		✓
Micic <i>et al.</i> (2003a; 2002b; 2002a)	To examine (i) the effect of combined electrokinetics and surcharge, (ii) the effect of electric field parameters including current intermittence and electric field intensity, (iii) the role of electrochemical reactions.	5, 6.2	n.m.	n.m.	Steel mesh	*lab test *rectangular tank model with L = 750 mm; W = 730 mm; h = 650 mm * electrode states = rod with d = 10 mm, 16 mm and its vertically installed		✓
Lefebvre and Burnotte (2002)	To investigate the feasibility of using electro osmosis to consolidate the clay foundation of existing embankments to solve the problem of continuous long-term settlements.	5.2	0.35	n.m.	Perforated steel tube	*lab test *cylinder tank model with D = 254 mm; h = 90 - 130 mm * electrode states = rod with d = 10 mm and its vertically installed		✓

Reference	Description	Voltage	Voltage Gradient	Current Density	Electrodes	Field/Lab Test	Series of Test	
							C-EO	EO-DL
Malusis and Shackelford (2002)	To evaluate the potential for membrane behaviour of a GCL by measuring the chemico-osmotic efficiency of the GCL in the presence of kalium chloride solutions.	n.m.	n.m.	n.m.	Analyte	*lab test *cylinder tank model with d = 71.1 mm		✓
Micic <i>et al.</i> (2001)	To examine the effect of electrokinetics on the shear strength of the foundation.	3.2, 6.6	12.8, 25.6	15, 30	Steel mesh	*lab test *rectangular tank model with L = 306 mm; W = 119 mm; h = 254 mm * electrode states = plate with L = 200; W = 110 mm and its horizontally installed		✓
Hamir <i>et al.</i> (2001)	Describes the laboratory assessment of the performance of prototype EKG materials which can be used in civil engineering applications.	5 – 30	0.4 – 2.5	0.3 – 5.9	Copper wire stringer, stainless steel fibres, polypropylene and carbon fibre non-woven sheet, copper disk	*lab test *cylinder tank model with D = 150 mm; H = 230 mm * electrode states = plate with d = 150 mm and its horizontally installed	✓	✓
Chen and Murdoch (1999)	To characterise the changes of in situ electrical conductivity and pH of a natural soil during electro osmotic	25	20 – 31	n.m.	Titanium mesh as anode, granular graphite as cathode	*field work *anode with L = 3.4 m; W = 3.1 m and its horizontally installed	✓	

Reference	Description	Voltage	Voltage Gradient	Current Density	Electrodes	Field/Lab Test	Series of Test	
							C-EO	EO-DL
Shang and Dunlap (1996)	The pullout resistance of ground anchor models as affected by the intensity and configuration of high voltage electric fields is further investigated	7000, 15 000, 30 000	n.m.	n.m.	Steel plates	*lab test *cylinder tank model with D = 300 mm; h = 370 mm * electrode states = plate with d = 152 mm and its vertically installed		✓
Hamir (1997)	To study use of conductive geosynthetics as electrodes in electro osmotic consolidation.	5 – 30	0.4 – 2.5	0.3 – 5.9	Copper wire stringer, stainless steel fibres, polypropylene and carbon fibre non-woven sheet, copper disk	*lab test *cylinder tank model with D = 150 mm; H = 230 mm * electrode states = plate with d = 150 mm and its horizontally installed	✓	✓
Schultz (1997)	To determine whether electro osmosis might be a practical means of in situ treatment by carried out a laboratory and engineering analysis program.	40 – 150	1 – 4	3	Analyte	*lab test *rectangular tank model with L = 410 mm; h = 90 mm; W = 150 mm * electrode states = plate and its vertically installed	✓	
Shang (1997a; 1997c)	To study the theoretical and experimental aspects of electrokinetic sedimentation in clay suspensions.	n.m.	n.m.	5	Steel mesh	*lab test *cylinder tank model with D = 90 mm; h = 200 mm * electrode states = plate and its horizontally installed	✓	

Reference	Description	Voltage	Voltage Gradient	Current Density	Electrodes	Field/Lab Test	Series of Test	
							C-EO	EO-DL
Shang and Lo (1997)	To investigate the factors influencing the effectiveness of electrokinetic dewatering of a phosphate clay suspension from a waste disposal pond in Florida.	3, 6, 10, 15, 16, 19.5, 20	n.m.	1, 3.7, 5	Steel mesh, copper rod	*lab test *cylinder tank model with D = 90 mm; h = 200 mm * electrode states = plate and its horizontally installed		✓
Eykholt and Daniel (1994)	To show the chemical affects on electro osmosis and the implications on electrokinetic remediation schemes in general.	5.0 ± 0.2, 5.5 ± 0.2	0.25, 0.275	n.m.	Platinum	*lab test *cylinder tank model with D = 51 mm; L = 200 mm * electrode states = plate and its vertically installed	✓	
Lo and Shang (1994)	To demonstrate the function of the intervening medium filling the space between the electrode and soil.	18000	n.m.	n.m.	Copper bars	*lab test *cylinder tank model with D = 127 mm; L = 203 mm * electrode states = rod with d = 2 mm and its vertically installed		✓
Lo <i>et al.</i> (1992; 1991a)	To explore the phenomenon of dielectrophoresis for possible applications in soil strengthening, and to study the effects of applied potential and electrode depth on the shear strength, water content and compression of clays.	3 - 6	0.15 – 0.30	1.27 – 3.80	Copper	*lab test *cylinder tank model with D = 300 mm; L = 300 mm * electrode states = rod with d = 16 mm; h = 250 mm and its vertically installed		✓
Lo <i>et al.</i> (1991c)	To investigate the change in stress-strain and strength behaviour, compressibility, preconsolidation pressure and accompanying physicochemical changes.	n.m.	n.m.	n.m.	n.m.	*field work *other description is n.m.	✓	

Reference	Description	Voltage	Voltage Gradient	Current Density	Electrodes	Field/Lab Test	Series of Test	
							C-EO	EO-DL
Lo <i>et al.</i> (1991b)	To verify the applicability of the process for strengthening of Leda clay in the field; to develop an efficient and economical version of electro osmosis for engineering practice; and to assess the limitations of the process.	25	n.m.	n.m.	Copper pipe	*field work *anode rod with d = 50.8 mm; L = 6.1 m and its vertically installed	✓	
Morris <i>et al.</i> (1985)	To evaluate the possible degree of improvement in the most accurate way possible, to perform on both treated and untreated electro osmotic sample on index tests, monotonic and mechanical tests.	n.m.	0.40 – 0.60	n.m.	Stainless steel wool as anode, galvanized wire mesh as cathode	*lab test *cylinder tank model with D = 75 mm; h = 550 mm		✓
Eggestad and Føyn (1983)	To reduce the water content and to increase the shear strength of a soft marine silty clay by applying electro osmosis	18, 43	n.m.	n.m.	Reinforcing rod as anode, sheet pile wall as cathode	*field work *anode rod with d = 20 mm, L = 3 m, 6 m and its vertically installed	✓	
Lockhart (1983c)	To study the effects of different clays, exchangeable cations, and electrode materials.	1 - 4, 10, 50	n.m.	n.m.	Magnesium ribbon as anode, gold-plated as cathode	*lab test *cylinder tank model n.m. * electrode states = plate and its horizontally installed	✓	
Lockhart (1983b)	To study the relationship between electro osmotic dewatering and the influence of salt, acid and flocculants.	1-3, 5.5, 10, 25, 50, 72	n.m.	n.m.	Magnesium ribbon as anode, gold-plated as cathode	*lab test *cylinder tank model n.m. * electrode states = plate and its horizontally installed	✓	

Reference	Description	Voltage	Voltage Gradient	Current Density	Electrodes	Field/Lab Test	Series of Test	
							C-EO	EO-DL
Lockhart (1983a)	To study the relationship between electro osmotic dewatering and the voltage applied.	1-3, 5.5, 10, 25, 50, 150, 240	n.m.	n.m.	Stainless steel, carbon-coated stainless steel, carbon-mild steel-copper, carbon-aluminium	*lab test *cylinder tank model n.m. * electrode states = plate and its horizontally installed	✓	
Butterfield and Johnston (1980)	To investigate the effect of electro osmotic consolidation during pile driving	25 to 95	n.m.	n.m.	Steel piles	*field work *piles with D = 100 mm and its vertically installed	✓	
Mitchell and Wan (1977)	To evaluate the stress-strain and strength changes caused by electro osmotic consolidation.	n.m.	2.5, 3.0	n.m.	n.m.	*lab test *square tank model with L = W = 200 mm; h = 200 mm * electrode states = plate and its vertically installed		✓
Wan and Mitchell (1976)	To evaluate the stress-strain and strength changes caused by electro osmotic consolidation.	n.m.	1.25	1.0 – 1.5	Silver chloride with porous disc	*lab test *square tank model with L = W = 200 mm; h = 200 mm * electrode states = plate and its vertically installed		✓

Reference	Description	Voltage	Voltage Gradient	Current Density	Electrodes	Field/Lab Test	Series of Test	
							C-EO	EO-DL
Chapel and Burton (1975)	To apply electro osmosis as minimising the treating time on unstable embankment	40	n.m.	n.m.	Reinforcing bar	*field work *piles with d = 25 mm and its vertically installed	✓	
Gray (1970)	To study the changes in the composition and mineralogy of electrically treated clay soils.	30 – 190	1	0.001 – 0.005	Copper as cathode, aluminium and graphite as anode	*lab test *square tank model * electrode states = plate and its vertically installed	✓	
Bjerrum <i>et al.</i> (1967)	To observe the settlements and pore pressures at various depths and studies of the change in properties of the clay resulting from the treatment	10 – 40	n.m.	n.m.	Reinforcing bar	*field work *anode rod with d = 19 mm; L = 10 m and its vertically installed	✓	
Fetzer (1967)	To reduce the pore water pressure thus enabling completion of the embankment with application of electro osmosis	50 – 70, 140, 150	n.m.	n.m.	Black steel pipe	*field work *anode rod with d = 191 mm, 203 mm; cathode rod with d = 356 mm L = 3 m, 6 m and its vertically installed	✓	
Casagrande <i>et al.</i> (1961)	To stabilise unstable embankment by electro osmosis approach	100	0.3	n.m.	n.m.	*field work *electrode states with L = 3.05 m and its vertically installed	✓	

Reference	Description	Voltage	Voltage Gradient	Current Density	Electrodes	Field/Lab Test	Series of Test	
							C-EO	EO-DL
Soderman and Milligan (1961)	Describes the solution adopted for substructure support at the Big Pic River Bridge	70 - 120	n.m.	n.m.	Steel H piles	*field work *piles with H = W = 305 mm; L = 16.8 m, 50.6 m and its vertically installed	✓	
Murayama and Mise (1953)	To make clear the mechanism of electrochemical consolidation and its practical application	50	n.m.	n.m.	n.m.	*lab test *rectangular tank model with L = 150; W = 70 mm; h = 35 mm * electrode states = plate and its vertically installed	✓	
Shukla (1953)	To investigate the influence of electric current on the common physical properties and the chemical changes	n.m.	n.m.	n.m.	Aluminium and copper	*lab test *cylinder tank model with D = 100 mm; h = 25 mm * electrode states = plate and its horizontally installed	✓	✓
Casagrande (1952b)	To discuss the possible applications of a new method for stabilizing fine grained soils in foundation construction by means of electro osmosis	90, 180	n.m.	n.m.	Steel pile as cathode, gas pipe as anode	*field work *cathode rod with d = 102 mm, l = 6.9 m and its horizontally installed	✓	
Casagrande (1952a)	To study the effect of electro osmosis on compressible fine grained soil.	n.m.	1.6	n.m.	Platinum wire mesh	*lab test *tank model is n.m.		✓



IMAGING SERVICES NORTH

Boston Spa, Wetherby
West Yorkshire, LS23 7BQ
www.bl.uk

**PAGE MISSING IN
ORIGINAL**

APPENDIX C

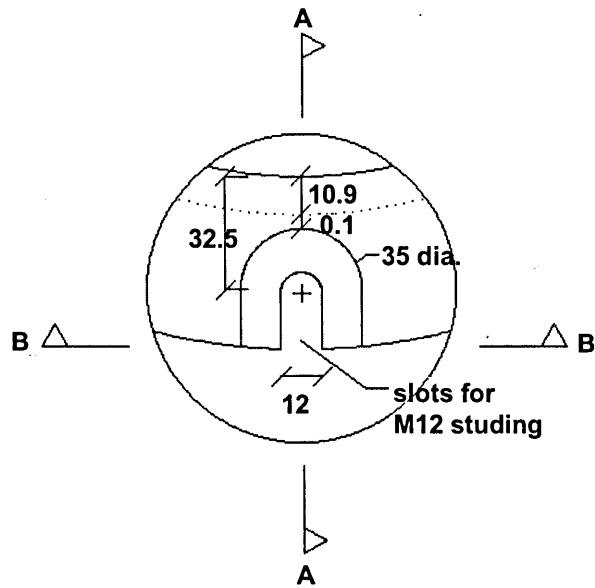


Figure C1 Plan of slot for clamping bolt type 1 (A) (all dimensions in mm, not to scale)

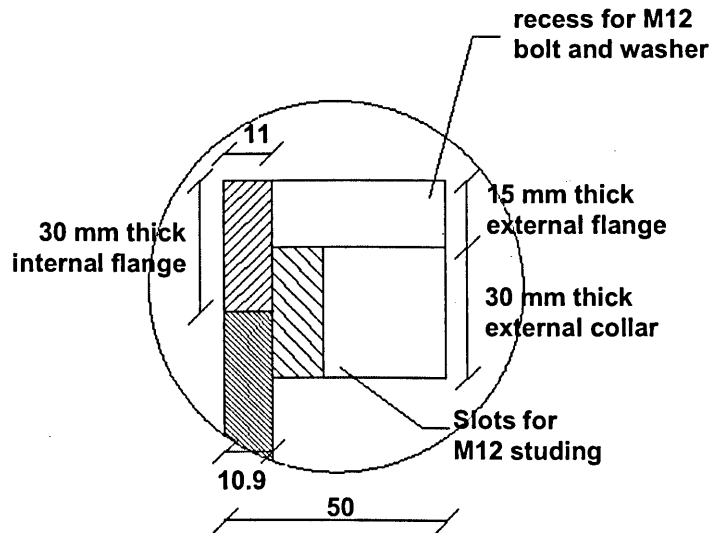


Figure C2 Elevation view for clamping bolt type 1 (A) from Section AA (all dimensions in mm, not to scale)

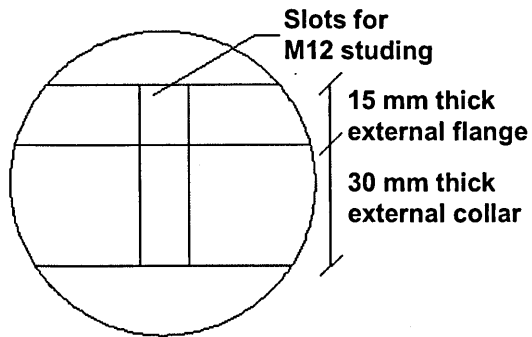


Figure C3 Elevation view of slot clamping bolt type 1 (A) from Section BB (all dimensions in mm, not to scale)

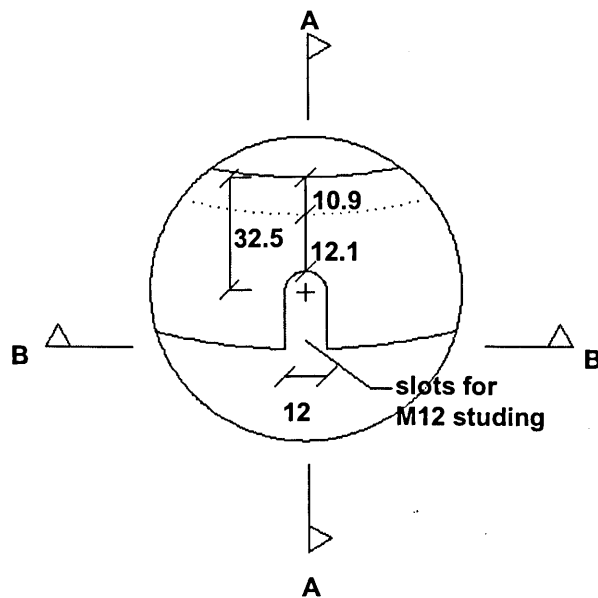


Figure C4 Plan of slot for clamping down bolt type 2 (B) (all dimensions in mm, not to scale)

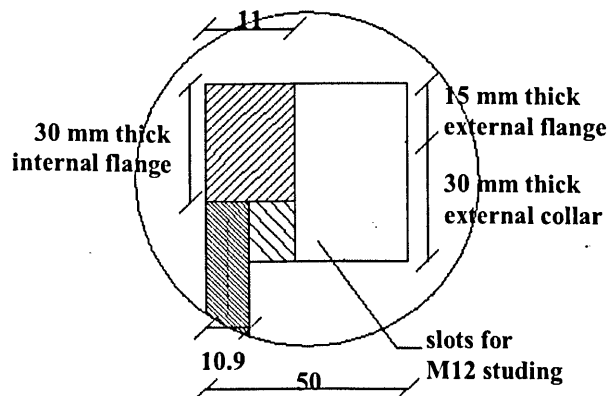


Figure C5 Elevation view for clamping bolt type 2 (B) from Section AA (all dimensions in mm, not to scale)

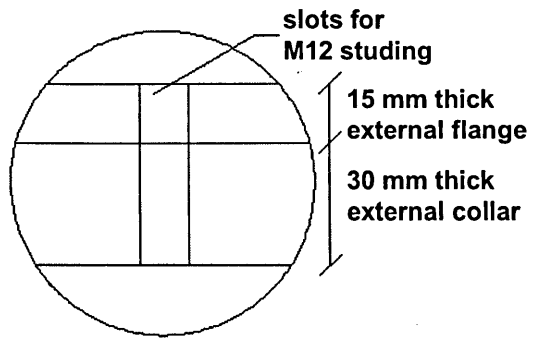


Figure C6 Elevation view of slot clamping bolt type 2 (B) from Section BB (all dimensions in mm, not to scale)

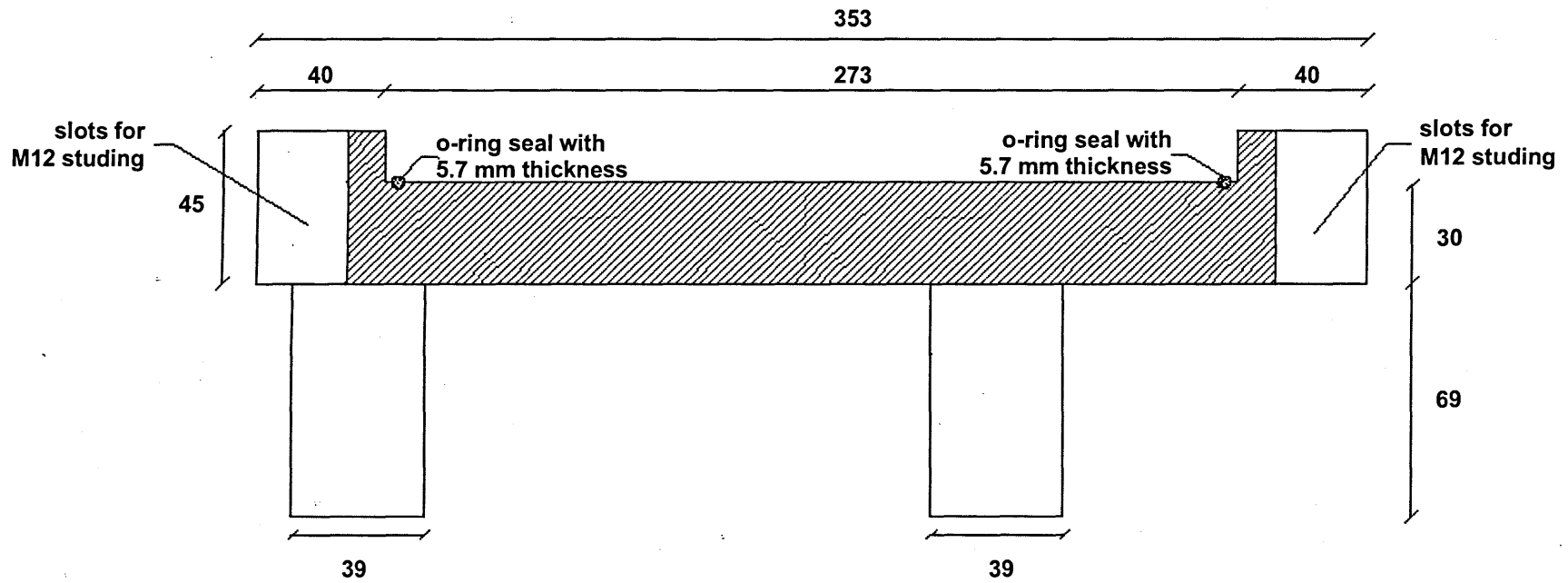


Figure C7 Elevation view for bottom base (sockets, ports and locating sockets not shown; all dimensions in mm, not to scale)

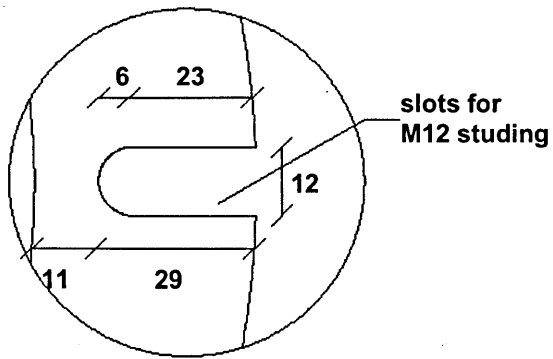


Figure C8 Plan view of slot for clamping bolts and holding down (all dimensions in mm, not to scale)

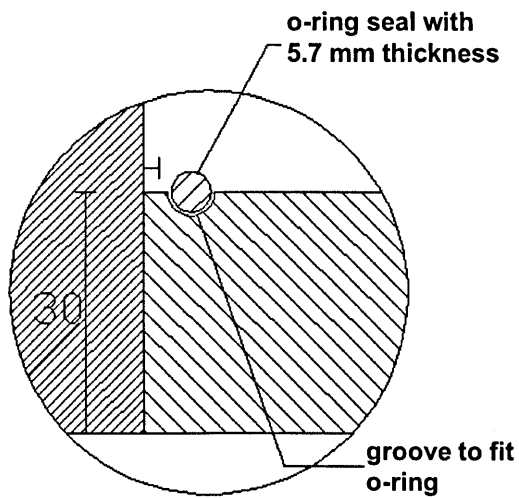


Figure C9 Elevation view (all dimensions in mm, not to scale)

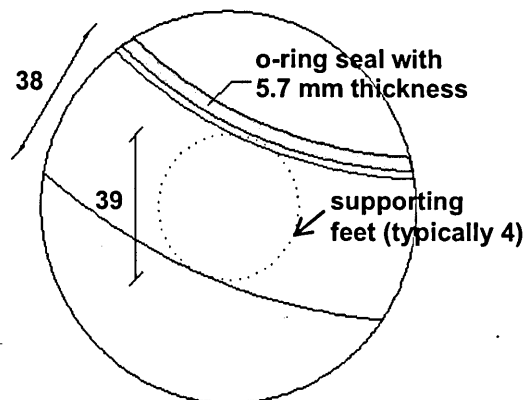


Figure C10 Plan view (all dimensions in mm, not to scale)

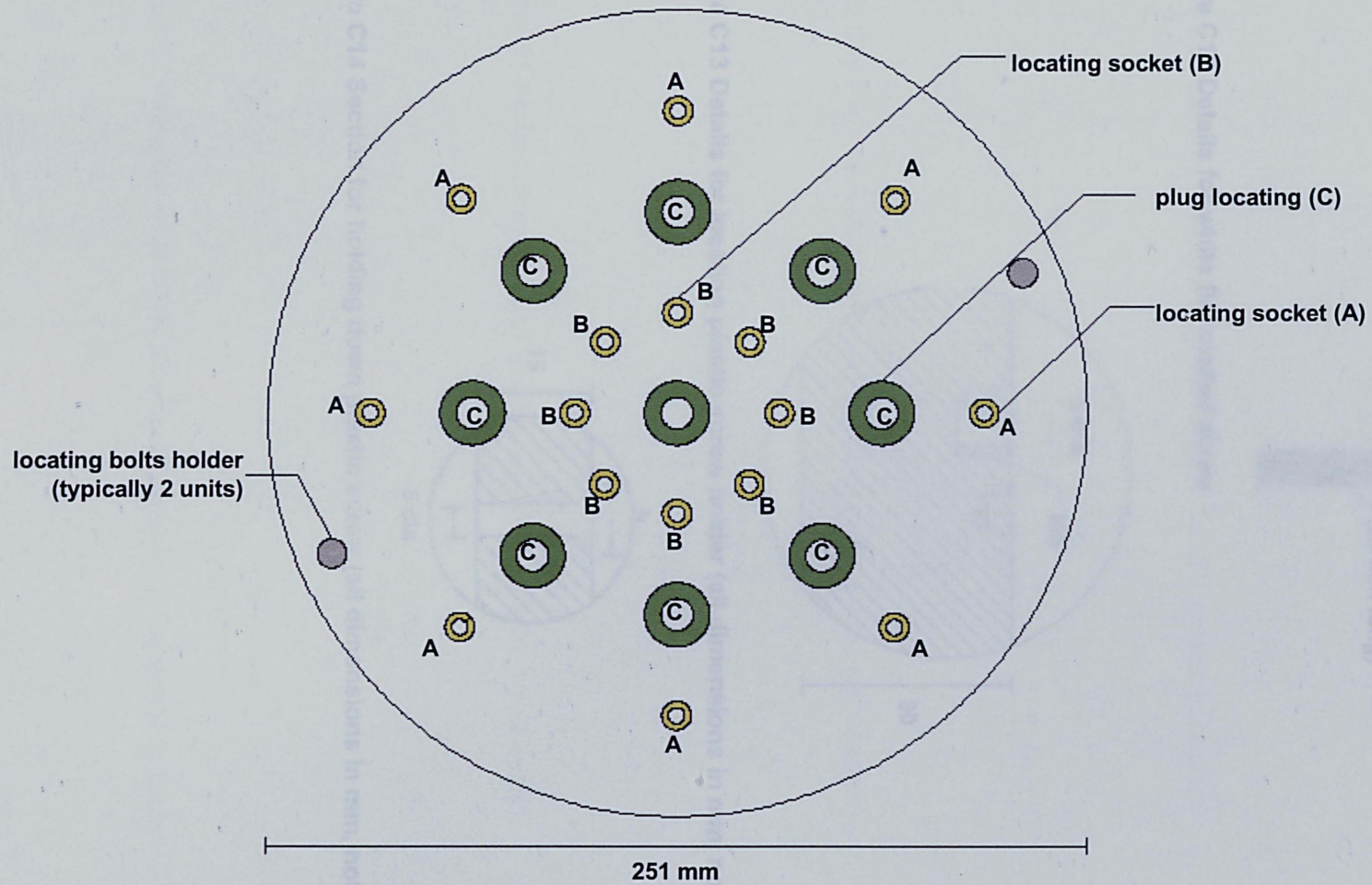


Figure C11 Plan view of bottom plate (not to scale)

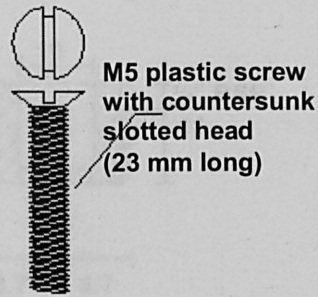


Figure C12 Details for white flat slotted screw

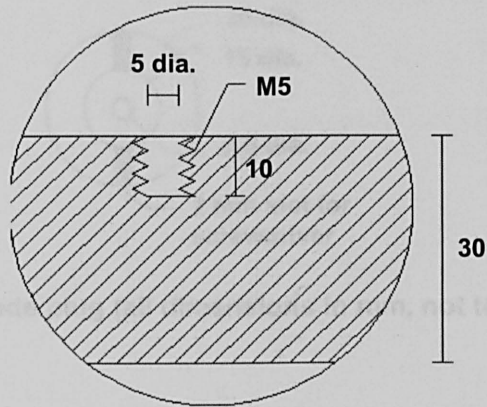


Figure C13 Details for locating plastic screw holder (all dimensions in mm, not to scale)

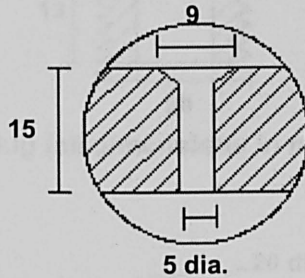


Figure C14 Section for holding down plastic screw (all dimensions in mm, not to scale)

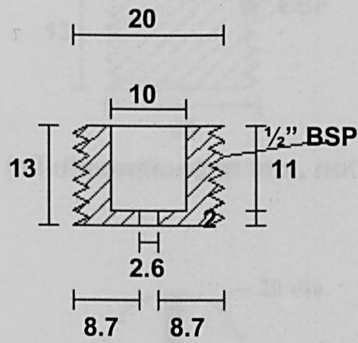


Figure C15 Section of anode plug (all dimensions in mm, not to scale)

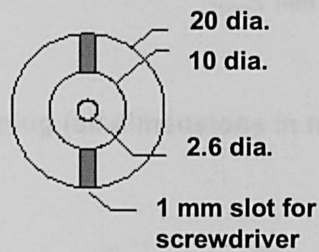


Figure C16 Plan view of anode plug (all dimensions in mm, not to scale)

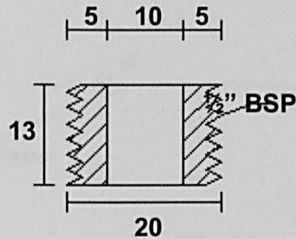


Figure C17 Section of cathode plug (all dimensions in mm, not to scale)

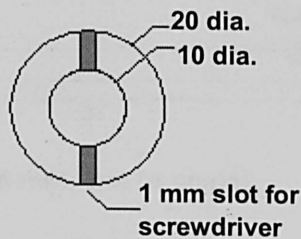


Figure C18 Plan view of cathode plug (all dimensions in mm, not to scale)

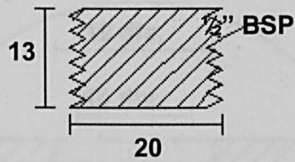


Figure C19 Section of solid plug (all dimensions in mm, not to scale)

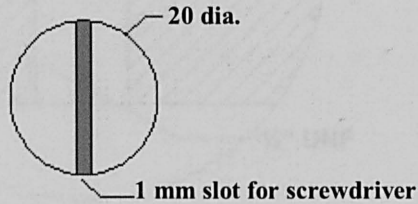


Figure C22 Details for gland locations (all dimensions in mm, not to scale)

Figure C20 Plan view of solid plug (all dimensions in mm, not to scale)

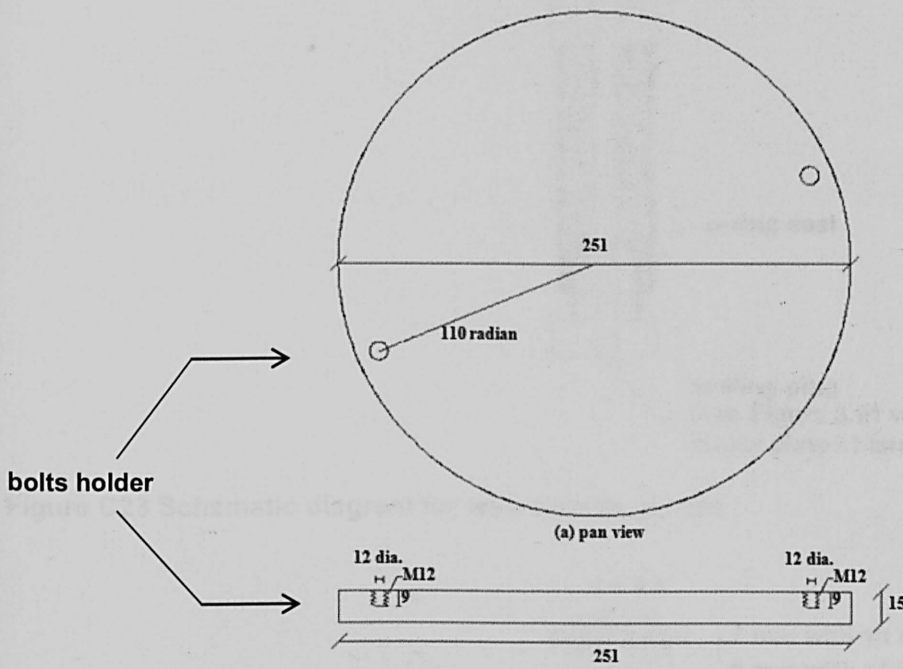


Figure C21 Top plate (all dimensions in mm, not to scale)

Figure C24 Elevation view for wire access (all dimensions in mm, not to scale)

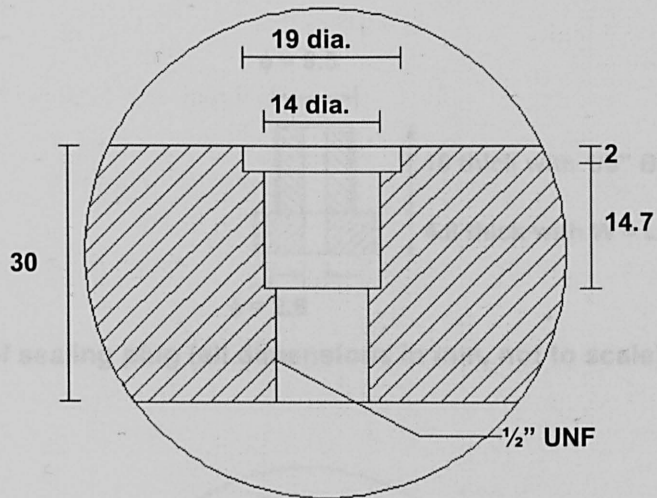


Figure C22 Details for gland locations (all dimensions in mm, not to scale)

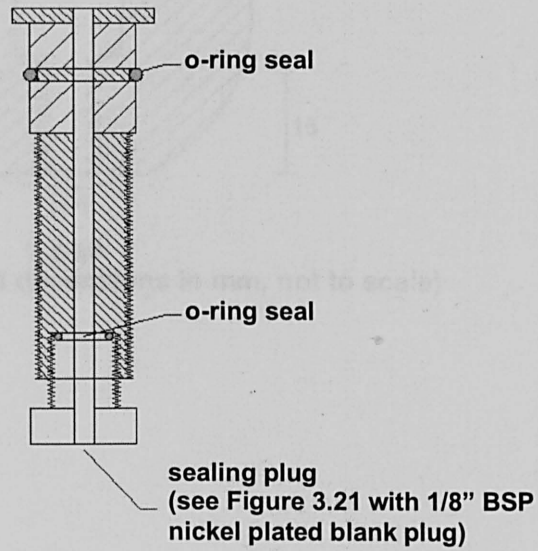


Figure C23 Schematic diagram for wire access glands

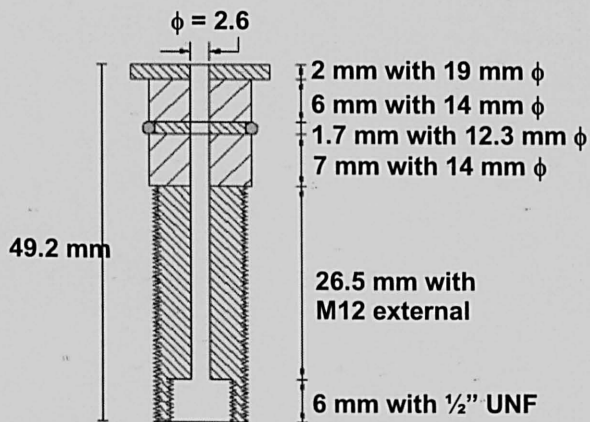


Figure C24 Elevation view for wire access glands (all dimensions in mm, not to scale)

APPENDIX D

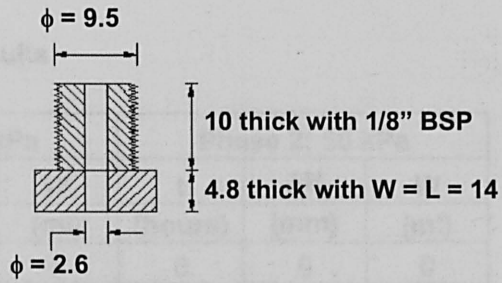


Figure C25 Section of sealing plug (all dimensions in mm, not to scale)

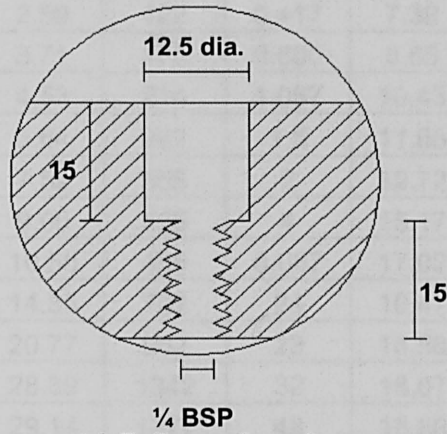


Figure C26 Details for drainage port (all dimensions in mm, not to scale)

APPENDIX D

Table D1 Summary of control test results

Phase 1: 15 kPa			Phase 2: 50 kPa		
t	ΔH	W	t	ΔH	W
(hours)	(mm)	(ml)	(hours)	(mm)	(ml)
0	0.00	0	0	0	0
0.067	0.42	20	0.067	4.15	209
0.150	0.93	44	0.150	5.23	264
0.267	1.65	78	0.267	6.42	324
0.417	2.59	122	0.417	7.39	373
0.600	3.71	175	0.600	8.65	437
1.067	4.53	214	1.067	10.43	527
1.5	5.64	267	1.5	11.60	586
2	7.59	358	2	12.72	642
4	9.00	425	4	15.17	766
8.067	10.50	496	8.067	17.02	860
24	14.83	701	24	18.47	933
28	20.77	982	28	18.58	939
32	28.39	1342	32	18.67	943
48	29.14	1377	48	18.86	952
72	29.79	1408	72	18.99	959
96	31.10	1469	96	19.06	962
120	31.70	1498	120	19.10	964
144	31.80	1503	144	19.12	966
168	31.91	1508	168	19.14	967
192	31.93	1509	192	19.16	967
216	31.95	1510	216	19.17	968
240	31.96	1511	240	19.19	969
264	32.00	1512	264	19.20	970
288	32.00	1512	288	19.22	970
312	32.01	1513	312	19.23	971
336	32.02	1513	336	19.24	972
360	32.03	1514			
384	32.04	1514			
408	32.05	1515			
432	32.07	1516			

t: total time; ΔH: settlement; W: water expelled.

Table D2 Summary of A1V51d test results

Phase 1: 15 kPa			Phase 2: 15 kPa + 5 V					Phase 3: 50 kPa		
t	W	ΔH	t	ΔH	W	Voltage	Current	t	W	ΔH
(hours)	(ml)	(mm)	(hours)	(mm)	(ml)	(volts)	(mA)	(hours)	(ml)	(mm)
0	0	0	0	0.00	0	5	81	0	0	0
0.267	249	4.93	0.267	0.03	1	5	81	0.267	117	2.42
0.417	296	5.86	0.417	0.04	2	5	81	0.417	140	2.88
0.6	352	6.97	0.6	0.12	6	5	81	0.6	166	3.42
1.067	482	9.54	1.067	0.18	9	5	81	1.067	227	4.69
1.5	633	12.53	1.5	0.29	14	5	81	1.5	298	6.15
2	829	16.41	2	0.35	17	5	81	2	391	8.06
4	1076	21.31	4	0.43	21	5	80	4	508	10.47
8.067	1277	25.29	8.067	0.72	35	5	80	8.067	602	12.42
24	1491	29.52	24	1.50	73	5	77	24	703	14.50
28	1514	29.98						28	714	14.73
32	1532	30.34						32	723	14.90
48	1568	31.04						48	739	15.25
72	1585	31.39						72	748	15.42
96	1589	31.46						96	749	15.45
120	1592	31.52						120	751	15.48
144	1593	31.54						144	751	15.49
168	1594	31.56						168	752	15.50
192	1595	31.58						192	752	15.51
216	1595	31.59						216	753	15.52
240	1596	31.61						240	753	15.52
264	1597	31.62						264	753	15.53
288	1597	31.63						288	753	15.53
312	1598	31.64						312	754	15.54
336	1598	31.65						336	754	15.54
360	1599	31.66						360	754	15.55
384	1599	31.66						384	754	15.55

t: total time; ΔH: settlement; W: water expelled.

Table D3 Summary of A1V53d test results

Phase 1: 15 kPa			Phase 2: 15 kPa + 5 V					Phase 3: 50 kPa		
t	W	ΔH	t	ΔH	W	Voltage	Current	t	W	ΔH
(hours)	(ml)	(mm)	(hours)	(ml)	(mm)	(volts)	(mA)	(hours)	(ml)	(mm)
0	0	0	0	0	0.00	5	80	0	0	0
0.267	249	4.93	0.267	1	0.02	5	80	0.267	115	2.38
0.417	296	5.86	0.417	2	0.05	5	80	0.417	137	2.83
0.6	352	6.97	0.6	6	0.11	5	80	0.6	163	3.36
1.067	482	9.54	1.067	9	0.19	5	80	1.067	223	4.61
1.5	632	12.52	1.5	15	0.30	5	80	1.5	293	6.05
2	828	16.40	2	18	0.36	5	80	2	384	7.92
4	1076	21.30	4	22	0.45	5	79	4	499	10.29
8.067	1276	25.27	8.067	36	0.74	5	79	8.067	592	12.20
24	1490	29.50	24	73	1.51	5	76	24	691	14.25
28	1513	29.96	28	76	1.56	5	76	28	702	14.47
32	1531	30.32	32	78	1.60	5	75	32	710	14.64
48	1567	31.02	48	80	1.64	5	73	48	727	14.98
72	1584	31.37	72	81	1.67	5	68	72	735	15.15
96	1588	31.44						96	736	15.18
120	1591	31.50						120	738	15.21
144	1592	31.52						144	738	15.22
168	1593	31.54						168	739	15.23
192	1594	31.56						192	739	15.24
216	1594	31.57						216	739	15.25
240	1595	31.59						240	740	15.25
264	1596	31.60						264	740	15.26
288	1596	31.61						288	740	15.26
312	1597	31.62						312	741	15.27
336	1597	31.63						336	741	15.27
360	1598	31.64						360	741	15.28
384	1598	31.64						384	741	15.28

t: total time; ΔH: settlement; W: water expelled.

Table D4 Summary of A1V55d test results

Phase 1: 15 kPa			Phase 2: 15 kPa + 5 V					Phase 3: 50 kPa		
t	W	ΔH	t	ΔH	W	Voltage	Current	t	W	ΔH
(hours)	(ml)	(mm)	(hours)	(ml)	(mm)	(volts)	(mA)	(hours)	(ml)	(mm)
0	0	0	0	0	0.00	5	80	0	0	0
0.267	249	4.93	0.267	1	0.02	5	80	0.267	112	2.31
0.417	296	5.86	0.417	2	0.04	5	80	0.417	134	2.75
0.6	352	6.97	0.6	5	0.10	5	80	0.6	159	3.27
1.067	482	9.54	1.067	8	0.17	5	80	1.067	217	4.48
1.5	633	12.53	1.5	13	0.28	5	79	1.5	285	5.89
2	829	16.41	2	16	0.33	5	79	2	374	7.71
4	1076	21.31	4	22	0.44	5	78	4	486	10.01
8.067	1277	25.29	8.067	35	0.73	5	78	8.067	576	11.88
24	1491	29.52	24	73	1.50	5	75	24	673	13.87
28	1514	29.98	28	77	1.58	5	74	28	683	14.08
32	1532	30.34	32	78	1.61	5	73	32	691	14.25
48	1568	31.04	48	80	1.65	5	71	48	707	14.58
72	1585	31.39	72	81	1.68	5	66	72	715	14.74
96	1589	31.46	96	83	1.71	5	62	96	717	14.77
120	1592	31.52	120	84	1.73	5	60	120	718	14.80
144	1593	31.54						144	718	14.81
168	1594	31.56						168	719	14.82
192	1595	31.58						192	719	14.83
216	1595	31.59						216	720	14.84
240	1596	31.61						240	720	14.84
264	1597	31.62						264	720	14.85
288	1597	31.63						288	720	14.85
312	1598	31.64						312	721	14.86
336	1598	31.65						336	721	14.86
360	1599	31.66						360	721	14.87
384	1599	31.66						384	721	14.87

t: total time; ΔH: settlement; W: water expelled.

Table D5 Summary of A1V57d test results

Phase 1: 15 kPa			Phase 2: 15 kPa + 5 V					Phase 3: 50 kPa		
t	W	ΔH	t	ΔH	W	Voltage	Current	t	W	ΔH
(hours)	(ml)	(mm)	(hours)	(ml)	(mm)	(volts)	(mA)	(hours)	(ml)	(mm)
0	0	0	0	0	0.00	5	80	0	0	0
0.267	249	4.93	0.267	1	0.02	5	80	0.267	108	2.22
0.417	296	5.86	0.417	2	0.05	5	80	0.417	128	2.64
0.6	352	6.97	0.6	5	0.11	5	80	0.6	152	3.14
1.067	482	9.54	1.067	9	0.18	5	80	1.067	208	4.30
1.5	633	12.53	1.5	14	0.30	5	80	1.5	274	5.64
2	829	16.41	2	15	0.31	5	80	2	358	7.39
4	1076	21.31	4	21	0.44	5	79	4	465	9.59
8.067	1277	25.28	8.067	35	0.73	5	79	8.067	552	11.38
24	1490	29.51	24	73	1.51	5	76	24	644	13.29
28	1514	29.97	28	76	1.56	5	75	28	654	13.49
32	1532	30.33	32	78	1.60	5	74	32	662	13.66
48	1567	31.03	48	81	1.66	5	72	48	678	13.97
72	1585	31.38	72	82	1.69	5	67	72	685	14.13
96	1588	31.45	96	83	1.72	5	63	96	687	14.16
120	1591	31.51	120	85	1.75	5	59	120	688	14.19
144	1592	31.53	144	90	1.85	5	55	144	688	14.19
168	1593	31.55	168	97	1.99	5	51	168	689	14.20
192	1594	31.57						192	689	14.21
216	1595	31.58						216	690	14.22
240	1596	31.60						240	690	14.23
264	1596	31.61						264	690	14.23
288	1597	31.62						288	690	14.23
312	1597	31.63						312	691	14.24
336	1598	31.64						336	691	14.24
360	1598	31.65						360	691	14.25
384	1598	31.65						384	691	14.25

t: total time; ΔH: settlement; W: water expelled.

Table D6 Summary of A1V515d test results

Phase 1: 15 kPa			Phase 2: 15 kPa + 5 V					Phase 3: 50 kPa		
t	W	ΔH	t	ΔH	W	Voltage	Current	t	W	ΔH
(hours)	(ml)	(mm)	(hours)	(ml)	(mm)	(volts)	(mA)	(hours)	(ml)	(mm)
0	0	0	0	0	0.00	5	80	0	0	0
0.267	249	4.92	0.267	1	0.02	5	80	0.267	105	2.08
0.417	296	5.86	0.417	2	0.05	5	80	0.417	125	2.47
0.6	352	6.96	0.6	5	0.11	5	80	0.6	148	2.94
1.067	482	9.54	1.067	9	0.18	5	80	1.067	203	4.02
1.5	632	12.52	1.5	15	0.30	5	80	1.5	267	5.28
2	828	16.40	2	18	0.36	5	80	2	349	6.92
4	1075	21.29	4	22	0.45	5	79	4	454	8.99
8.067	1276	25.26	8.067	36	0.74	5	79	8.067	538	10.66
24	1490	29.50	24	74	1.52	5	76	24	629	12.45
28	1513	29.95	28	77	1.58	5	75	28	638	12.64
32	1531	30.31	32	79	1.62	5	74	32	646	12.79
48	1566	31.01	48	81	1.67	5	72	48	661	13.09
72	1584	31.36	72	82	1.70	5	67	72	668	13.24
96	1587	31.43	96	84	1.73	5	63	96	670	13.26
120	1590	31.49	120	85	1.76	5	59	120	671	13.29
144	1591	31.51	144	91	1.88	5	55	144	672	13.30
168	1592	31.53	168	97	2.00	5	51	168	672	13.31
192	1593	31.55	192	101	2.08	5	47	192	672	13.31
216	1594	31.56	216	103	2.13	5	42	216	673	13.32
240	1595	31.58	240	106	2.18	5	38	240	673	13.33
264	1595	31.59	264	108	2.22	5	34	264	673	13.33
288	1596	31.60	288	109	2.26	5	30	288	673	13.34
312	1596	31.61	312	111	2.29	5	26	312	674	13.34
336	1597	31.62	336	112	2.32	5	22	336	674	13.34
360	1597	31.63	360	114	2.35	5	17	360	674	13.35
384	1597	31.63						384	674	13.35

t: total time; ΔH: settlement; W: water expelled.

Table D7 Summary of A1V519d test results

Phase 1: 15 kPa			Phase 2: 15 kPa + 5 V					Phase 3: 50 kPa		
t	W	ΔH	t	ΔH	W	Voltage	Current	t	W	ΔH
(hours)	(ml)	(mm)	(hours)	(ml)	(mm)	(volts)	(mA)	(hours)	(ml)	(mm)
0	0	0	0	0	0.00	5	80	0	0	0
0.267	249	4.93	0.267	1	0.02	5	80	0.267	94	1.94
0.417	296	5.86	0.417	2	0.05	5	80	0.417	112	2.31
0.6	352	6.97	0.6	6	0.11	5	80	0.6	133	2.74
1.067	482	9.54	1.067	9	0.19	5	80	1.067	182	3.75
1.5	633	12.53	1.5	15	0.30	5	80	1.5	239	4.93
2	829	16.41	2	18	0.36	5	80	2	313	6.45
4	1076	21.31	4	22	0.45	5	79	4	407	8.38
8.067	1277	25.28	8.067	36	0.75	5	79	8.067	482	9.94
24	1490	29.51	24	73	1.50	5	76	24	563	11.61
28	1514	29.97	28	76	1.57	5	75	28	572	11.79
32	1532	30.33	32	78	1.60	5	74	32	579	11.93
48	1567	31.03	48	81	1.66	5	72	48	592	12.21
72	1585	31.38	72	82	1.70	5	67	72	599	12.34
96	1588	31.45	96	83	1.72	5	63	96	600	12.37
120	1591	31.51	120	84	1.74	5	59	120	601	12.39
144	1592	31.53	144	90	1.86	5	55	144	601	12.40
168	1593	31.55	168	99	2.04	5	51	168	602	12.41
192	1594	31.57	192	102	2.10	5	47	192	602	12.42
216	1595	31.58	216	104	2.15	5	42	216	603	12.42
240	1596	31.60	240	106	2.20	5	38	240	603	12.43
264	1596	31.61	264	109	2.24	5	34	264	603	12.43
288	1597	31.62	288	112	2.27	5	30	288	603	12.44
312	1597	31.63	312	113	2.31	5	26	312	603	12.44
336	1598	31.64	336	114	2.34	5	22	336	604	12.44
360	1598	31.65	360	115	2.37	5	17	360	604	12.45
384	1598	31.65	384	116	2.38	5	13	384	604	12.45
			408	117	2.39	5	9			
			432	118	2.40	5	5			
			456	118.5	2.40	5	1			

t: total time; ΔH: settlement; W: water expelled.

Table D8 Summary of Q3V51d test results

Phase 1: 15 kPa			Phase 2: 15 kPa + 5 V					Phase 3: 50 kPa		
t	W	ΔH	t	ΔH	W	Voltage	Current	t	W	ΔH
(hours)	(ml)	(mm)	(hours)	(mm)	(ml)	(volts)	(mA)	(hours)	(ml)	(mm)
0	0	0.00	0	0	0	5	69	0	0	0
0.067	316	6.25	0.267	0.01	0	5	67	0.267	224	4.62
0.150	370	7.32	0.417	0.02	1	5	65	0.417	311	6.41
0.267	427	8.45	0.6	0.04	2	5	62	0.6	434	8.94
0.417	592	11.72	1.067	0.07	3	5	61	1.067	602	12.41
0.6	826	16.35	1.5	0.11	5	5	60	1.5	750	15.46
1.067	1146	22.70	2	0.13	6	5	60	2	805	16.60
1.5	1428	28.27	4	0.16	8	5	59	4	830	17.12
2	1533	30.37	8.067	0.27	13	5	63	8.067	835	17.22
4	1581	31.30	24	0.49	24	5	37	24	837	17.26
8.067	1590	31.49						28	840	17.32
24	1594	31.56						32	843	17.37
28	1599	31.67						48	843	17.38
32	1604	31.77						72	844	17.39
48	1605	31.79						96	844	17.41
72	1606	31.81						120	845	17.42
96	1607	31.83						144	845	17.43
120	1608	31.85						168	845	17.43
144	1609	31.87						192	846	17.44
168	1610	31.88						216	846	17.44
192	1610	31.89						240	846	17.45
216	1611	31.90						264	847	17.45
240	1611	31.91						288	847	17.46
264	1612	31.92						312	847	17.47
288	1612	31.93						336	847	17.47
312	1613	31.94								
336	1613	31.94								

t: total time; ΔH: settlement; W: water expelled.

Table D9 Summary of Q3V53d test results

Phase 1: 15 kPa			Phase 2: 15 kPa + 5 V				Phase 3: 50 kPa			
t	W	ΔH	t	ΔH	W	Voltage	Current	t	W	ΔH
(hours)	(ml)	(mm)	(hours)	(mm)	(ml)	(volts)	(mA)	(hours)	(ml)	(mm)
0	0	0	0	0	0	5	68	0	0	0
0.067	316	6.26	0.267	0.01	0	5	70	0.267	220	4.54
0.150	370	7.33	0.417	0.02	1	5	71	0.417	305	6.29
0.267	427	8.46	0.6	0.05	2	5	71	0.6	426	8.78
0.417	592	11.73	1.067	0.09	4	5	71	1.067	591	12.19
0.6	826	16.36	1.5	0.12	6	5	71	1.5	736	15.18
1.067	1147	22.71	2	0.14	7	5	72	2	791	16.30
1.5	1429	28.29	4	0.17	8	5	70	4	815	16.81
2	1534	30.39	8.067	0.29	14	5	64	8.067	820	16.91
4	1582	31.32	24	0.5	24	5	46	24	822	16.95
8.067	1591	31.51	28	0.77	37	5	42	28	825	17.01
24	1595	31.58	32	1.04	50	5	39	32	827	17.06
28	1600	31.69	48	1.17	57	5	31	48	828	17.07
32	1605	31.79	72	1.3	63	5	26	72	828	17.08
48	1606	31.81						96	829	17.09
72	1607	31.83						120	829	17.10
96	1608	31.85						144	830	17.11
120	1609	31.87						168	830	17.12
144	1610	31.89						192	830	17.12
168	1611	31.90						216	831	17.13
192	1611	31.91						240	831	17.13
216	1612	31.92						264	831	17.14
240	1612	31.93						288	832	17.14
264	1613	31.94						312	832	17.15
288	1613	31.95						336	832	17.15
312	1614	31.96								
336	1614	31.96								

t: total time; ΔH: settlement; W: water expelled.

Table D10 Summary of Q3V55d test results

Phase 1: 15 kPa			Phase 2: 15 kPa + 5 V					Phase 3: 50 kPa		
t	W	ΔH	t	ΔH	W	Voltage	Current	t	W	ΔH
(hours)	(ml)	(mm)	(hours)	(mm)	(ml)	(volts)	(mA)	(hours)	(ml)	(mm)
0	0	0	0	0	0	5	65	0	0	0
0.067	316	6.25	0.267	0.01	1	5	67	0.267	214	4.41
0.150	370	7.32	0.417	0.03	1	5	68	0.417	297	6.12
0.267	427	8.45	0.6	0.07	3	5	66	0.6	414	8.54
0.417	592	11.72	1.067	0.10	5	5	70	1.067	575	11.85
0.6	826	16.35	1.5	0.13	6	5	70	1.5	716	14.77
1.067	1146	22.70	2	0.14	7	5	71	2	769	15.86
1.5	1428	28.27	4	0.16	8	5	71	4	793	16.35
2	1533	30.37	8.067	0.28	14	5	74	8.067	797	16.44
4	1581	31.30	24	0.49	24	5	49	24	799	16.48
8.067	1590	31.49	28	0.76	37	5	41	28	802	16.54
24	1594	31.56	32	1.02	49	5	36	32	805	16.59
28	1599	31.67	48	1.18	57	5	30	48	805	16.60
32	1604	31.77	72	1.31	64	5	27	72	806	16.61
48	1605	31.79	96	1.37	66	5	26	96	806	16.62
72	1606	31.81	120	1.48	72	5	21	120	807	16.63
96	1607	31.83						144	807	16.64
120	1608	31.85						168	807	16.65
144	1609	31.87						192	808	16.65
168	1610	31.88						216	808	16.66
192	1610	31.89						240	808	16.66
216	1611	31.90						264	808	16.67
240	1611	31.91						288	809	16.67
264	1612	31.92						312	809	16.68
288	1612	31.93						336	809	16.68
312	1613	31.94								
336	1613	31.94								

t: total time; ΔH: settlement; W: water expelled.

Table D11 Summary of Q3V57d test results

Phase 1: 15 kPa			Phase 2: 15 kPa + 5 V					Phase 3: 50 kPa		
t	W	ΔH	t	ΔH	W	Voltage	Current	t	W	ΔH
(hours)	(ml)	(mm)	(hours)	(mm)	(ml)	(volts)	(mA)	(hours)	(ml)	(mm)
0	0	0	0	0	0	5	66	0	0	0
0.067	316	6.25	0.267	0.02	1	5	66	0.267	208	4.30
0.150	370	7.32	0.417	0.04	2	5	68	0.417	289	5.96
0.267	427	8.45	0.6	0.06	3	5	68	0.6	403	8.31
0.417	592	11.72	1.067	0.09	4	5	70	1.067	559	11.53
0.6	826	16.35	1.5	0.12	6	5	70	1.5	697	14.37
1.067	1146	22.69	2	0.15	7	5	72	2	748	15.43
1.5	1427	28.27	4	0.17	8	5	73	4	771	15.91
2	1533	30.36	8.067	0.28	14	5	75	8.067	776	16.00
4	1580	31.29	24	0.50	24	5	47	24	778	16.04
8.067	1590	31.48	28	0.77	37	5	36	28	781	16.09
24	1593	31.55	32	1.03	50	5	31	32	783	16.14
28	1599	31.66	48	1.19	58	5	22	48	783	16.15
32	1604	31.76	72	1.30	63	5	22	72	784	16.16
48	1605	31.78	96	1.36	66	5	20	96	784	16.17
72	1606	31.80	120	1.45	70	5	19	120	785	16.18
96	1607	31.82	144	1.48	72	5	19	144	785	16.19
120	1608	31.84	168	1.52	74	5	19	168	786	16.20
144	1609	31.86						192	786	16.20
168	1609	31.87						216	786	16.21
192	1610	31.88						240	786	16.21
216	1610	31.89						264	787	16.22
240	1611	31.90						288	787	16.22
264	1611	31.91						312	787	16.23
288	1612	31.92						336	787	16.23
312	1612	31.93								
336	1612	31.93								

t: total time; ΔH: settlement; W: water expelled.

Table D12 Summary of Q3V515d test results

Phase 1: 15 kPa			Phase 2: 15 kPa + 5 V					Phase 3: 50 kPa		
t	W	ΔH	t	ΔH	W	Voltage	Current	t	W	ΔH
(hours)	(ml)	(mm)	(hours)	(mm)	(ml)	(volts)	(mA)	(hours)	(ml)	(mm)
0	0	0	0	0	0	5	66	0	0	0
0.067	316	6.26	0.267	0.02	1	5	66	0.267	197	4.06
0.150	370	7.33	0.417	0.04	2	5	68	0.417	273	5.63
0.267	427	8.46	0.6	0.08	4	5	68	0.6	381	7.85
0.417	593	11.73	1.067	0.10	5	5	70	1.067	529	10.90
0.6	827	16.37	1.5	0.13	6	5	70	1.5	659	13.58
1.067	1147	22.72	2	0.14	7	5	72	2	707	14.58
1.5	1429	28.30	4	0.17	8	5	73	4	729	15.03
2	1535	30.39	8.067	0.29	14	5	75	8.067	733	15.12
4	1582	31.33	24	0.49	24	5	47	24	735	15.16
8.067	1592	31.52	28	0.77	37	5	36	28	738	15.21
24	1595	31.59	32	1.04	50	5	31	32	740	15.26
28	1601	31.70	48	1.18	57	5	22	48	741	15.27
32	1606	31.80	72	1.30	63	5	22	72	741	15.28
48	1607	31.82	96	1.35	65	5	20	96	741	15.29
72	1608	31.84	120	1.46	71	5	19	120	742	15.30
96	1609	31.86	144	1.47	71	5	19	144	742	15.31
120	1610	31.88	168	1.53	74	5	19	168	743	15.31
144	1611	31.90	192	1.54	75	5	18	192	743	15.32
168	1611	31.91	216	1.57	76	5	18	216	743	15.32
192	1612	31.92	240	1.60	78	5	18	240	743	15.33
216	1612	31.93	264	1.63	79	5	17	264	744	15.33
240	1613	31.94	288	1.66	80	5	16	288	744	15.34
264	1613	31.95	312	1.68	82	5	15	312	744	15.34
288	1614	31.96	336	1.71	83	5	13	336	744	15.34
312	1614	31.97	360	1.72	83	5	9			
336	1614	31.97								

t: total time; ΔH: settlement; W: water expelled.

Table D13 Summary of Q3V517d test results

Phase 1: 15 kPa			Phase 2: 15 kPa + 5 V					Phase 3: 50 kPa		
t	W	ΔH	t	ΔH	W	Voltage	Current	t	W	ΔH
(hours)	(ml)	(mm)	(hours)	(mm)	(ml)	(volts)	(mA)	(hours)	(ml)	(mm)
0	0	0.00	0	0	0	5	66	0	0	0
0.067	303	6.26	0.267	0.02	1	5	66	0.267	183	3.77
0.150	370	7.33	0.417	0.04	2	5	68	0.417	254	5.23
0.267	427	8.46	0.6	0.08	4	5	68	0.6	354	7.30
0.417	592	11.73	1.067	0.09	4	5	70	1.067	492	10.13
0.6	826	16.36	1.5	0.11	5	5	70	1.5	612	12.62
1.067	1147	22.71	2	0.14	7	5	72	2	658	13.56
1.5	1428	28.28	4	0.16	8	5	73	4	678	13.98
2	1534	30.38	8.067	0.28	14	5	75	8.067	682	14.06
4	1581	31.31	24	0.50	24	5	47	24	683	14.09
8.067	1591	31.50	28	0.76	37	5	36	28	686	14.14
24	1594	31.57	32	1.03	50	5	31	32	688	14.18
28	1600	31.68	48	1.17	57	5	22	48	688	14.19
32	1605	31.78	72	1.30	63	5	22	72	689	14.20
48	1606	31.80	96	1.36	66	5	20	96	689	14.21
72	1607	31.82	120	1.44	70	5	19	120	690	14.22
96	1608	31.84	144	1.48	72	5	19	144	690	14.23
120	1609	31.86	168	1.52	74	5	19	168	690	14.23
144	1610	31.88	192	1.54	75	5	18	192	691	14.24
168	1610	31.89	216	1.58	77	5	18	216	691	14.24
192	1611	31.90	240	1.62	78	5	18	240	691	14.25
216	1611	31.91	264	1.65	80	5	17	264	691	14.25
240	1612	31.92	288	1.68	81	5	16	288	691	14.26
264	1612	31.93	312	1.70	82	5	15	312	692	14.26
288	1613	31.94	336	1.73	83	5	13	336	692	14.26
312	1613	31.95	360	1.74	84	5	9			
336	1613	31.95	384	1.75	85	5	5			
			408	1.75	85	5	1			

t: total time; ΔH: settlement; W: water expelled.

Table D14 Summary of Q1V515d test results

Phase 1: 15 kPa			Phase 2: 15 kPa + 5 V					Phase 3: 50 kPa		
t	W	ΔH	t	ΔH	W	Voltage	Current	t	W	ΔH
(hours)	(ml)	(mm)	(hours)	(mm)	(ml)	(volts)	(mA)	(hours)	(ml)	(mm)
0	0	0.00	0	0.00	0	5	80	0	0	0.00
0.067	227	4.67	0.267	0.06	3	5	80	0.267	142	2.93
0.150	282	5.59	0.417	0.13	6	5	80	0.417	166	3.43
0.267	333	6.60	0.6	0.32	16	5	80	0.6	229	4.72
0.417	390	7.72	1.067	0.51	25	5	80	1.067	311	6.42
0.6	537	10.64	1.5	0.80	39	5	80	1.5	421	8.69
1.067	730	14.45	2	0.84	41	5	80	2	534	11.01
1.5	988	19.56	4	0.88	43	5	80	4	600	12.36
2	1252	24.80	8.067	0.99	48	5	80	8.067	656	13.52
4	1406	27.84	24	1.10	53	5	70	24	663	13.66
8.067	1538	30.45	28	1.18	57	5	70	28	667	13.76
24	1554	30.77	32	1.24	60	5	70	32	676	13.94
28	1565	30.99	48	1.28	62	5	70	48	681	14.04
32	1585	31.39	72	1.33	64	5	60	72	682	14.06
48	1597	31.62	96	1.36	65	5	60	96	683	14.08
72	1599	31.66	120	1.39	66	5	60	120	683	14.09
96	1601	31.70	144	1.42	67	5	50	144	684	14.10
120	1602	31.72	168	1.45	68	5	50	168	684	14.11
144	1603	31.74	192	1.47	69	5	40	192	684	14.11
168	1604	31.76	216	1.49	70	5	40	216	685	14.12
192	1605	31.78	240	1.51	71	5	30	240	685	14.12
216	1605	31.79	264	1.53	72	5	30	264	685	14.13
240	1606	31.80	288	1.54	73	5	30	288	685	14.13
264	1606	31.81	312	1.55	74	5	20	312	686	14.13
288	1607	31.82	336	1.55	75	5	10	336	686	14.14
312	1607	31.83	360	1.55	75	5	10	360	686	14.14
336	1608	31.84								
360	1608	31.84								

t: total time; ΔH: settlement; W: water expelled.

Table D15 Summary of Q2V516d test results

Phase 1: 15 kPa			Phase 2: 15 kPa + 5 V					Phase 3: 50 kPa		
t	W	ΔH	t	ΔH	W	Voltage	Current	t	W	ΔH
(hours)	(ml)	(mm)	(hours)	(mm)	(ml)	(volts)	(mA)	(hours)	(ml)	(mm)
0	0	0.00	0	0.00	0	5	60	0	0	0
0.067	42	0.87	0.267	0.04	2	5	60	0.267	55	1.13
0.150	98	1.95	0.417	0.08	4	5	60	0.417	69	1.42
0.267	173	3.42	0.6	0.50	24	5	60	0.6	83	1.70
0.417	216	4.29	1.067	1.16	56	5	60	1.067	100	2.07
0.6	260	5.15	1.5	1.56	76	5	60	1.5	136	2.81
1.067	316	6.25	2	1.92	93	5	60	2	171	3.53
1.5	429	8.49	4	2.75	134	5	60	4	214	4.41
2	539	10.67	8.067	3.73	181	5	50	8.067	287	5.93
4	674	13.35	24	5.25	255	5	50	24	366	7.54
8.067	906	17.93	28	5.47	265	5	50	28	460	9.48
24	1153	22.83	32	5.65	274	5	50	32	469	9.68
28	1449	28.69	48	6.22	302	5	50	48	477	9.84
32	1479	29.28	72	6.78	329	5	50	72	493	10.17
48	1504	29.78	96	7.18	348	5	50	96	501	10.33
72	1554	30.77	120	7.50	364	5	40	120	502	10.35
96	1578	31.24	144	7.75	376	5	40	144	503	10.38
120	1582	31.33	168	7.96	386	5	40	168	504	10.39
144	1586	31.41	192	8.15	395	5	40	192	504	10.39
168	1587	31.43	216	8.31	403	5	30	216	504	10.40
192	1588	31.45	240	8.46	410	5	30	240	505	10.41
216	1589	31.47	264	8.59	417	5	30	264	505	10.41
240	1590	31.49	288	8.72	420	5	30	288	505	10.41
264	1591	31.50	312	8.74	423	5	20	312	505	10.42
288	1591	31.51	336	8.75	424	5	20	336	505	10.42
312	1592	31.52	360	8.76	425	5	20	360	506	10.42
336	1592	31.53	384	8.76	425	5	20	384	506	10.43
360	1593	31.54						408	506	10.43
384	1593	31.55								
408	1594	31.56								

t: total time; ΔH: settlement; W: water expelled.

Table D16 Summary of Q4V516d test results

Phase 1: 15 kPa			Phase 2: 15 kPa + 5 V					Phase 3: 50 kPa		
t	W	ΔH	t	ΔH	W	Voltage	Current	t	W	ΔH
(hours)	(ml)	(mm)	(hours)	(mm)	(ml)	(volts)	(mA)	(hours)	(ml)	(mm)
0	0	0.00	0	0.00	0	5	54	0	0	0
0.067	44	0.87	0.267	0.05	3	5	47	0.267	49	1.01
0.150	98	1.95	0.417	0.10	5	5	40	0.417	62	1.27
0.267	173	3.42	0.6	0.65	31	5	35	0.6	74	1.53
0.417	216	4.28	1.067	1.51	73	5	28	1.067	90	1.85
0.6	260	5.15	1.5	2.02	98	5	21	1.5	122	2.52
1.067	316	6.25	2	2.45	119	5	15	2	153	3.16
1.5	428	8.48	4	3.48	169	5	15	4	192	3.96
2	539	10.67	8.067	4.53	220	5	20	8.067	258	5.31
4	674	13.34	24	6.16	299	5	41	24	328	6.76
8.067	905	17.92	28	6.39	310	5	39	28	412	8.50
24	1152	22.81	32	6.59	320	5	39	32	421	8.67
28	1448	28.67	48	7.20	349	5	36	48	428	8.82
32	1478	29.26	72	7.80	378	5	36	72	442	9.12
48	1503	29.76	96	8.23	399	5	36	96	449	9.26
72	1553	30.75	120	8.57	415	5	36	120	450	9.28
96	1577	31.22	144	8.84	429	5	38	144	451	9.31
120	1581	31.31	168	9.07	440	5	36	168	452	9.31
144	1585	31.39	192	9.27	450	5	28	192	452	9.32
168	1586	31.41	216	9.45	458	5	30	216	452	9.32
192	1587	31.43	240	9.60	466	5	28	240	452	9.33
216	1588	31.45	264	9.75	473	5	27	264	453	9.33
240	1589	31.47	288	9.88	476	5	26	288	453	9.34
264	1590	31.48	312	9.90	478	5	25	312	453	9.34
288	1590	31.49	336	9.91	479	5	24	336	453	9.34
312	1591	31.50	360	9.92	480	5	24	360	453	9.34
336	1591	31.51	384	9.92	481	5	24	384	453	9.35
360	1592	31.52						408	453	9.35
384	1592	31.53								
408	1593	31.54								

t: total time; ΔH: settlement; W: water expelled.

Table D17 Summary of A2V517d test results

Phase 1: 15 kPa			Phase 2: 15 kPa + 5 V					Phase 3: 50 kPa		
t	W	ΔH	t	ΔH	W	Voltage	Current	t	W	ΔH
(hours)	(ml)	(mm)	(hours)	(mm)	(ml)	(volts)	(mA)	(hours)	(ml)	(mm)
0	0	0.00	0	0.00	0	5	161	0	0	0
0.067	236	4.68	0.267	0.05	2	5	160	0.267	89	1.83
0.150	283	5.60	0.417	0.10	5	5	158	0.417	104	2.14
0.267	333	6.60	0.6	0.60	29	5	157	0.6	143	2.95
0.417	390	7.72	1.067	1.39	67	5	155	1.067	194	4.01
0.6	537	10.64	1.5	1.86	90	5	153	1.5	263	5.42
1.067	730	14.45	2	2.27	110	5	151	2	334	6.88
1.5	988	19.56	4	3.24	157	5	149	4	374	7.72
2	1253	24.81	8.067	4.30	208	5	148	8.067	410	8.44
4	1406	27.85	24	5.94	288	5	109	24	414	8.53
8.067	1538	30.46	28	6.17	299	5	107	28	417	8.59
24	1554	30.78	32	6.37	309	5	96	32	422	8.71
28	1565	31.00	48	6.98	338	5	77	48	425	8.77
32	1586	31.40	72	7.58	368	5	63	72	426	8.78
48	1597	31.63	96	8.02	389	5	60	96	426	8.79
72	1600	31.67	120	8.35	405	5	58	120	427	8.80
96	1602	31.71	144	8.63	418	5	57	144	427	8.80
120	1603	31.73	168	8.86	430	5	56	168	427	8.81
144	1604	31.75	192	9.06	439	5	54	192	427	8.81
168	1605	31.77	216	9.23	448	5	53	216	428	8.82
192	1605	31.79	240	9.39	456	5	50	240	428	8.82
216	1606	31.80	264	9.54	462	5	49	264	428	8.82
240	1606	31.81	288	9.67	469	5	48	288	428	8.82
264	1607	31.82	312	9.79	472	5	48	312	428	8.83
288	1607	31.83	336	9.82	475	5	45	336	428	8.83
312	1608	31.84	360	9.83	476	5	43	360	428	8.83
336	1608	31.85	384	9.84	477	5	42			
360	1608	31.85	408	9.84	477	5	38			

t: total time; ΔH: settlement; W: water expelled.

Table D18 Summary of A2V1016d test results

Phase 1: 15 kPa			Phase 2: 15 kPa + 10 V					Phase 3: 50 kPa		
t	W	ΔH	t	ΔH	W	Voltage	Current	t	W	ΔH
(hours)	(ml)	(mm)	(hours)	(mm)	(ml)	(volts)	(mA)	(hours)	(ml)	(mm)
0	0	0.00	0	0.00	0	10	370	0	0	0
0.067	236	4.68	0.267	0.31	15	10	360	0.267	75	1.55
0.150	283	5.60	0.417	0.66	32	10	350	0.417	87	1.79
0.267	333	6.60	0.6	1.26	61	10	330	0.6	120	2.48
0.417	390	7.72	1.067	2.21	107	10	320	1.067	168	3.46
0.6	538	10.65	1.5	2.77	135	10	310	1.5	233	4.80
1.067	730	14.46	2	3.25	158	10	300	2	290	5.98
1.5	988	19.57	4	4.39	213	10	280	4	312	6.43
2	1253	24.82	8.067	5.55	269	10	270	8.067	321	6.63
4	1407	27.86	24	7.36	357	10	140	24	323	6.66
8.067	1539	30.47	28	7.61	369	10	140	28	324	6.68
24	1555	30.79	32	7.83	380	10	140	32	325	6.70
28	1566	31.01	48	8.50	412	10	120	48	326	6.72
32	1586	31.41	72	9.17	445	10	100	72	326	6.73
48	1598	31.64	96	9.65	468	10	100	96	327	6.73
72	1600	31.68	120	10.02	486	10	90	120	327	6.74
96	1602	31.72	144	10.32	500	10	80	144	327	6.74
120	1603	31.74	168	10.57	513	10	70	168	327	6.75
144	1604	31.76	192	10.79	523	10	70	192	327	6.75
168	1605	31.78	216	10.99	533	10	70	216	327	6.75
192	1606	31.80	240	11.16	541	10	60	240	327	6.75
216	1606	31.81	264	11.32	545	10	60	264	328	6.75
240	1607	31.82	288	11.37	550	10	60	288	328	6.76
264	1607	31.83	312	11.39	551	10	50	312	328	6.76
288	1608	31.84	336	11.40	552	10	50	336	328	6.76
312	1608	31.85	360	11.41	553	10	40	360	328	6.76
336	1609	31.86	384	11.41	553	10	40			
360	1609	31.86								

t: total time; ΔH: settlement; W: water expelled.

Table D19 Summary of Q2V1015d test results

Phase 1: 15 kPa			Phase 2: 15 kPa + 10 V					Phase 3: 50 kPa		
t	W	ΔH	t	ΔH	W	Voltage	Current	t	W	ΔH
(hours)	(ml)	(mm)	(hours)	(mm)	(ml)	(volts)	(mA)	(hours)	(ml)	(mm)
0	0	0.00	0	0	0	5	121	0	0	0.00
0.067	42	0.87	0.267	0.14	7	5	104	0.267	43	0.90
0.150	98	1.95	0.417	0.29	14	5	86	0.417	54	1.12
0.267	173	3.43	0.6	0.86	42	5	59	0.6	65	1.35
0.417	217	4.29	1.067	1.77	86	5	51	1.067	79	1.63
0.6	261	5.16	1.5	2.30	112	5	43	1.5	108	2.22
1.067	316	6.26	2	2.76	134	5	35	2	135	2.79
1.5	429	8.50	4	3.84	186	5	26	4	169	3.49
2	540	10.69	8.067	4.95	240	5	99	8.067	227	4.69
4	675	13.37	24	6.66	323	5	99	24	289	5.97
8.067	907	17.95	28	6.90	335	5	98	28	364	7.50
24	1154	22.86	32	7.11	345	5	97	32	371	7.65
28	1451	28.72	48	7.75	376	5	97	48	378	7.78
32	1480	29.32	72	8.38	407	5	88	72	390	8.04
48	1506	29.82	96	8.84	429	5	79	96	396	8.17
72	1556	30.81	120	9.19	446	5	75	120	397	8.19
96	1580	31.28	144	9.47	459	5	70	144	398	8.21
120	1584	31.37	168	9.71	471	5	65	168	398	8.22
144	1588	31.45	192	9.92	481	5	58	192	399	8.22
168	1589	31.47	216	10.11	490	5	51	216	399	8.23
192	1590	31.49	240	10.27	498	5	44	240	399	8.23
216	1591	31.51	264	10.42	502	5	38	264	399	8.24
240	1592	31.53	288	10.45	506	5	32	288	400	8.24
264	1593	31.54	312	10.46	507	5	26	312	400	8.24
288	1593	31.55	336	10.47	508	5	19	336	400	8.24
312	1594	31.56	360	10.47	508	5	13	360	400	8.25
336	1594	31.57						384	400	8.25
360	1595	31.58						408	400	8.25
384	1595	31.59								
408	1596	31.60								

t: total time; ΔH: settlement; W: water expelled.

Table D20 Summary of Q4V1014d test results

Phase 1: 15 kPa			Phase 2: 15 kPa + 10 V					Phase 3: 50 kPa		
t	W	ΔH	t	ΔH	W	Voltage	Current	t	W	ΔH
(hours)	(ml)	(mm)	(hours)	(mm)	(ml)	(volts)	(mA)	(hours)	(ml)	(mm)
0	0	0.00	0	0.00	0	10	159	0	0	0
0.06667	44	0.87	0.26667	0.25	12	10	159	0.26667	37	0.74
0.15	98	1.95	0.41667	0.52	25	10	159	0.41667	47	0.93
0.26667	173	3.43	0.6	1.17	57	10	159	0.6	56	1.12
0.41667	216	4.29	1.06667	2.19	106	10	158	1.06667	68	1.36
0.6	260	5.16	1.5	2.80	136	10	158	1.5	92	1.84
1.06667	316	6.26	2	3.31	160	10	157	2	116	2.32
1.5	428	8.50	4	4.54	220	10	156	4	145	2.90
2	539	10.69	8.06667	5.79	281	10	153	8.06667	195	3.89
4	674	13.37	24	7.72	374	10	140	24	248	4.95
8.06667	905	17.95	28	8.00	388	10	137	28	311	6.23
24	1152	22.86	32	8.23	399	10	134	32	318	6.35
28	1448	28.72	48	8.95	434	10	121	48	323	6.46
32	1478	29.32	72	9.67	469	10	116	72	334	6.68
48	1503	29.82	96	10.18	494	10	103	96	339	6.78
72	1553	30.81	120	10.58	513	10	92	120	340	6.80
96	1577	31.28	144	10.90	529	10	78	144	341	6.82
120	1581	31.37	168	11.18	542	10	75	168	341	6.82
144	1585	31.45	192	11.41	554	10	70	192	341	6.83
168	1586	31.47	216	11.62	564	10	64	216	342	6.83
192	1587	31.49	240	11.81	569	10	60	240	342	6.83
216	1588	31.51	264	11.84	573	10	59	264	342	6.84
240	1589	31.53	288	11.85	574	10	59	288	342	6.84
264	1590	31.54	312	11.86	575	10	57	312	342	6.84
288	1590	31.55	336	11.86	575	10	57	336	342	6.84
312	1591	31.56						360	342	6.85
336	1591	31.57						384	342	6.85
360	1592	31.58						408	343	6.85
384	1592	31.59								
408	1593	31.60								

t: total time; ΔH: settlement; W: water expelled.

Table D21 Summary of Q4V2012d test results

Phase 1: 15 kPa			Phase 2: 15 kPa + 20 V					Phase 3: 50 kPa		
t	W	ΔH	t	ΔH	W	Voltage	Current	t	W	ΔH
(hours)	(ml)	(mm)	(hours)	(mm)	(ml)	(volts)	(mA)	(hours)	(ml)	(mm)
0	0	0.00	0	0	0	20	440	0	0	0
0.06667	44	0.87	0.26667	0.77	37	20	440	0.26667	24	0.47
0.15	98	1.95	0.41667	1.68	81	20	440	0.41667	30	0.59
0.26667	173	3.42	0.6	2.42	117	20	440	0.6	36	0.71
0.41667	216	4.28	1.06667	3.58	174	20	430	1.06667	43	0.87
0.6	260	5.15	1.5	4.28	207	20	430	1.5	59	1.18
1.06667	315	6.25	2	4.86	236	20	420	2	74	1.48
1.5	428	8.48	4	6.27	304	20	410	4	92	1.85
2	538	10.66	8.06667	7.69	373	20	390	8.06667	124	2.48
4	673	13.34	24	9.90	480	20	280	24	158	3.16
8.06667	904	17.91	28	10.22	495	20	270	28	199	3.97
24	1151	22.80	32	10.49	509	20	260	32	203	4.05
28	1447	28.65	48	11.31	549	20	230	48	206	4.12
32	1477	29.24	72	12.13	588	20	180	72	213	4.26
48	1502	29.74	96	12.72	617	20	160	96	216	4.33
72	1552	30.73	120	13.17	639	20	140	120	217	4.34
96	1576	31.20	144	13.54	657	20	130	144	217	4.35
120	1580	31.29	168	13.85	672	20	120	168	218	4.35
144	1584	31.37	192	14.12	679	20	120	192	218	4.35
168	1585	31.39	216	14.15	685	20	110	216	218	4.36
192	1586	31.41	240	14.16	686	20	110	240	218	4.36
216	1587	31.43	264	14.17	687	20	100	264	218	4.36
240	1588	31.45	288	14.17	687	20	100	288	218	4.36
264	1589	31.46						312	218	4.36
288	1589	31.47						336	218	4.37
312	1590	31.48						360	218	4.37
336	1590	31.49						384	218	4.37
360	1591	31.50						408	219	4.37
384	1591	31.51								
408	1592	31.52								

t: total time; ΔH: settlement; W: water expelled.

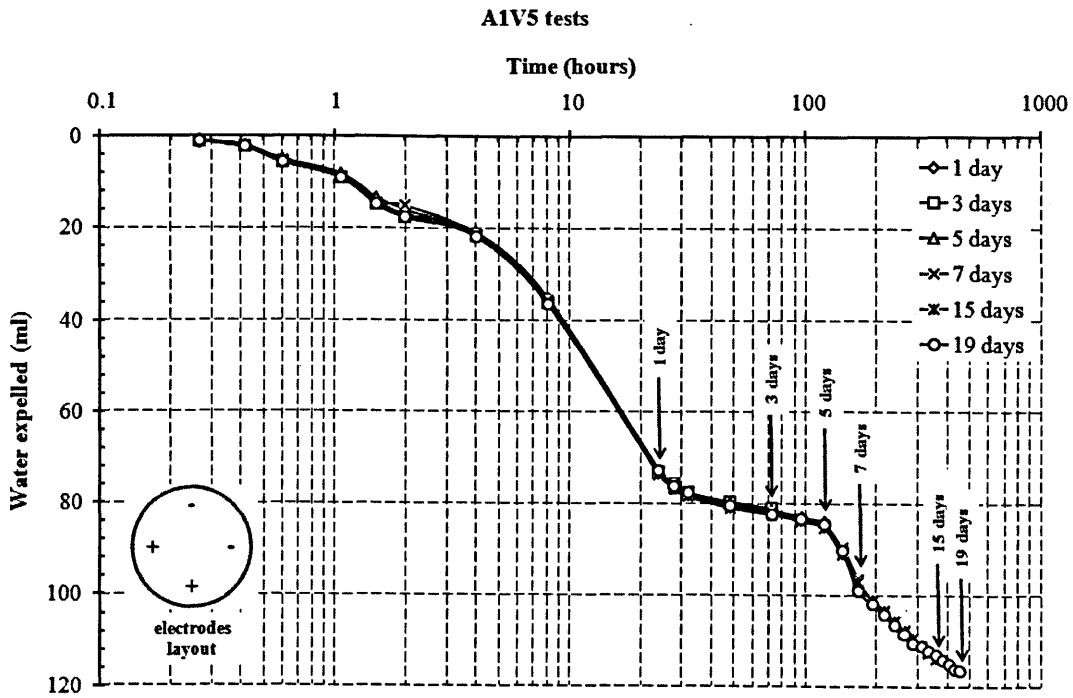


Figure D1 Phase 2 results of A1V5 tests series: water expelled versus time curves

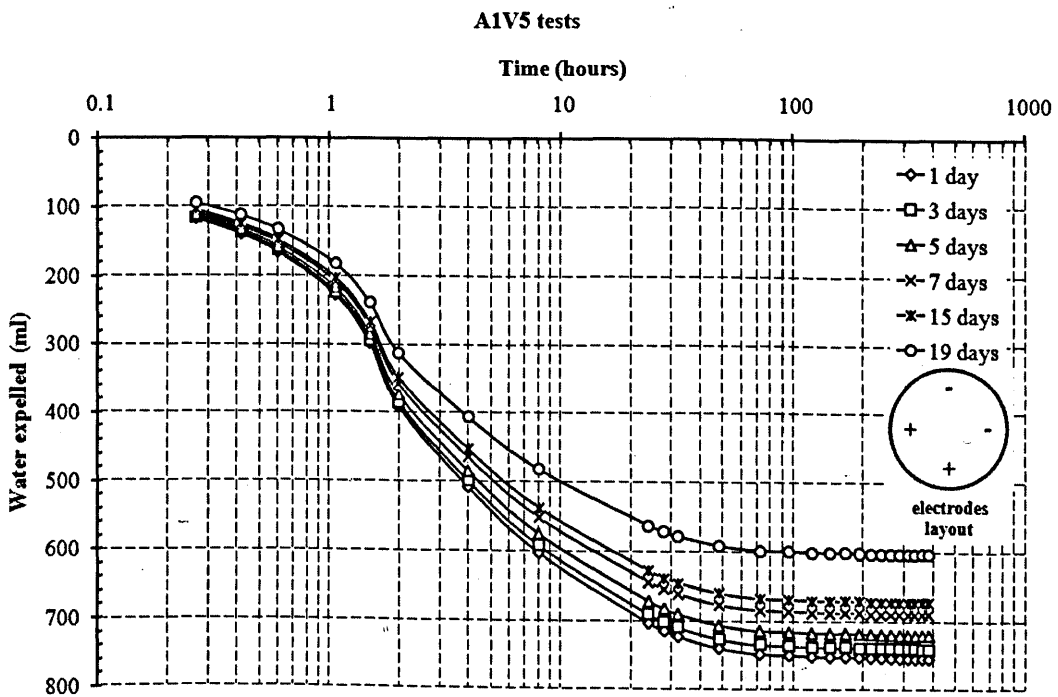


Figure D2 Phase 3 results of A1V5 tests series: water expelled versus time curves

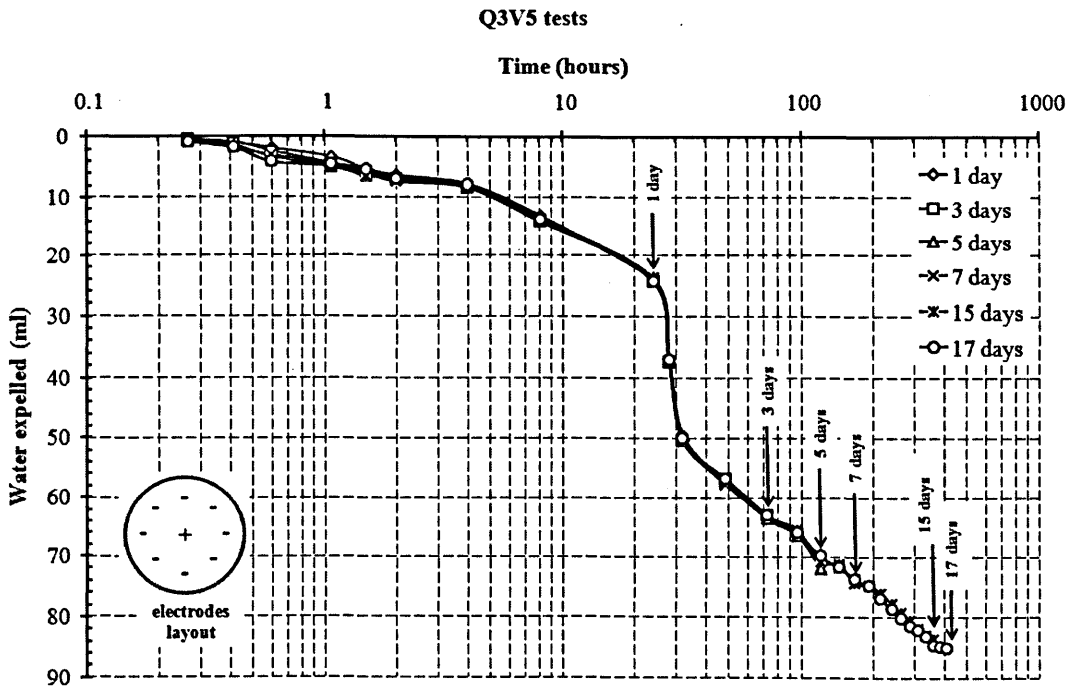


Figure D3 Phase 2 results of Q3V5 tests series: water expelled versus time curves

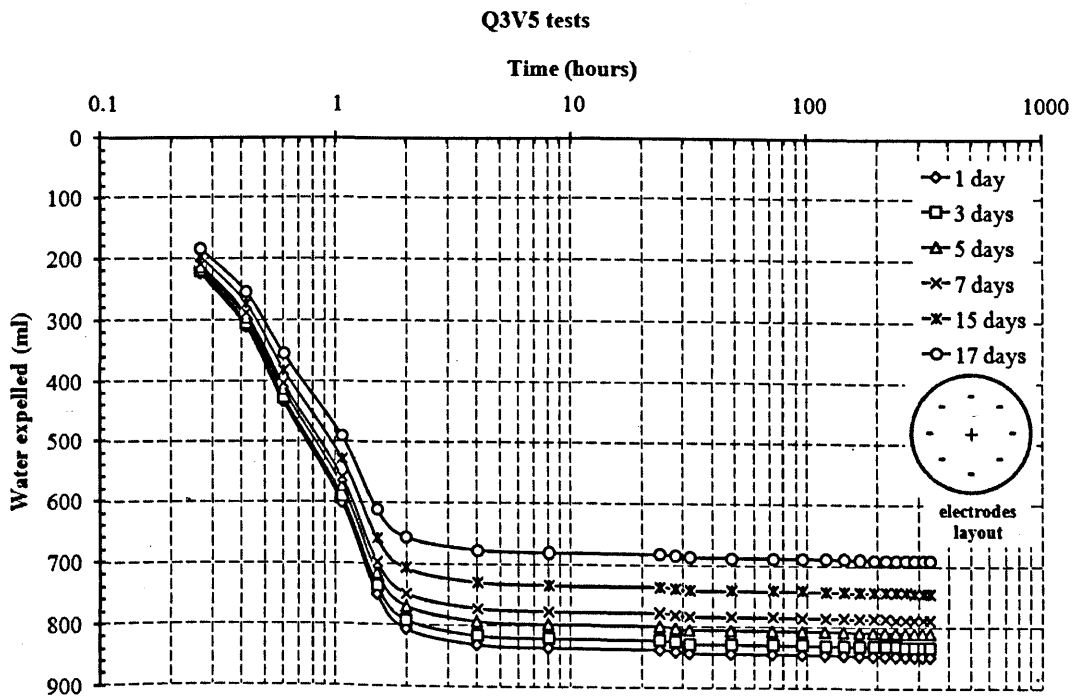


Figure D4 Phase 3 results of Q3V5 tests series: water expelled versus time curves

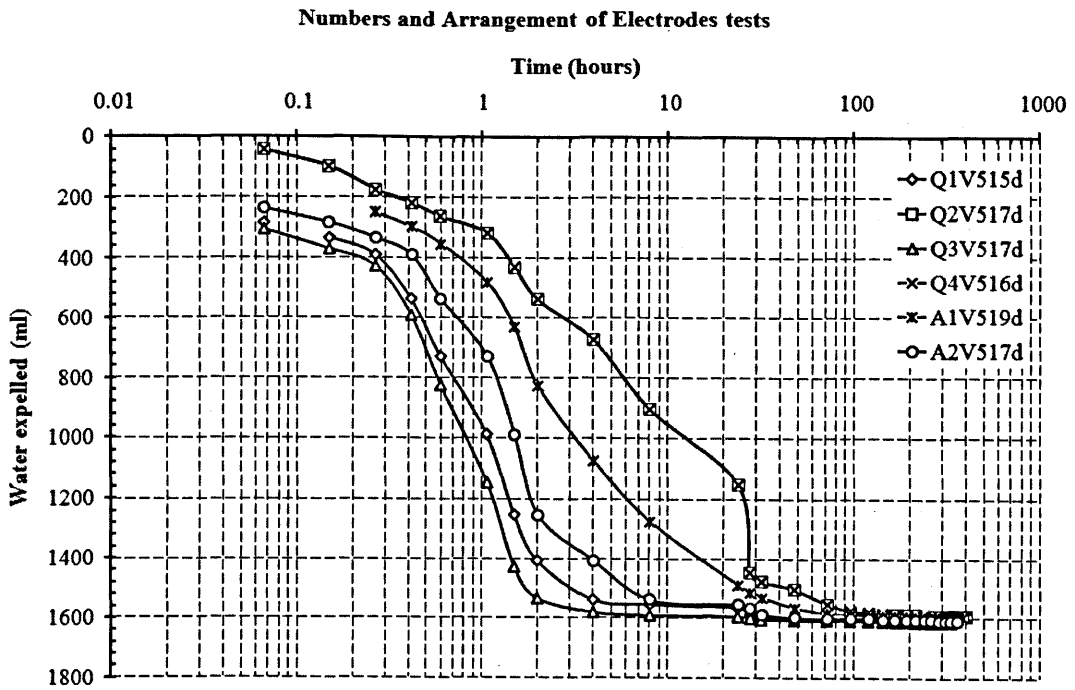


Figure D5 Phase 1 results for numbers and arrangement of electrodes test series: water expelled versus time curves

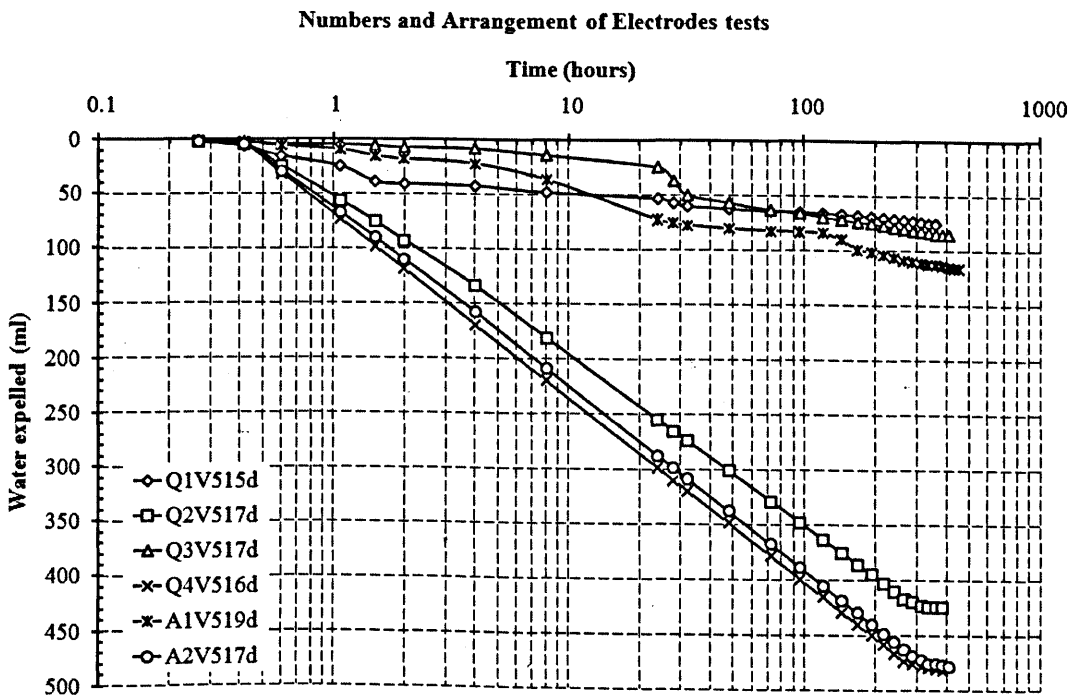


Figure D6 Phase 2 results for numbers and arrangement of electrodes test series: water expelled versus time curves

Numbers and Arrangement of Electrodes tests

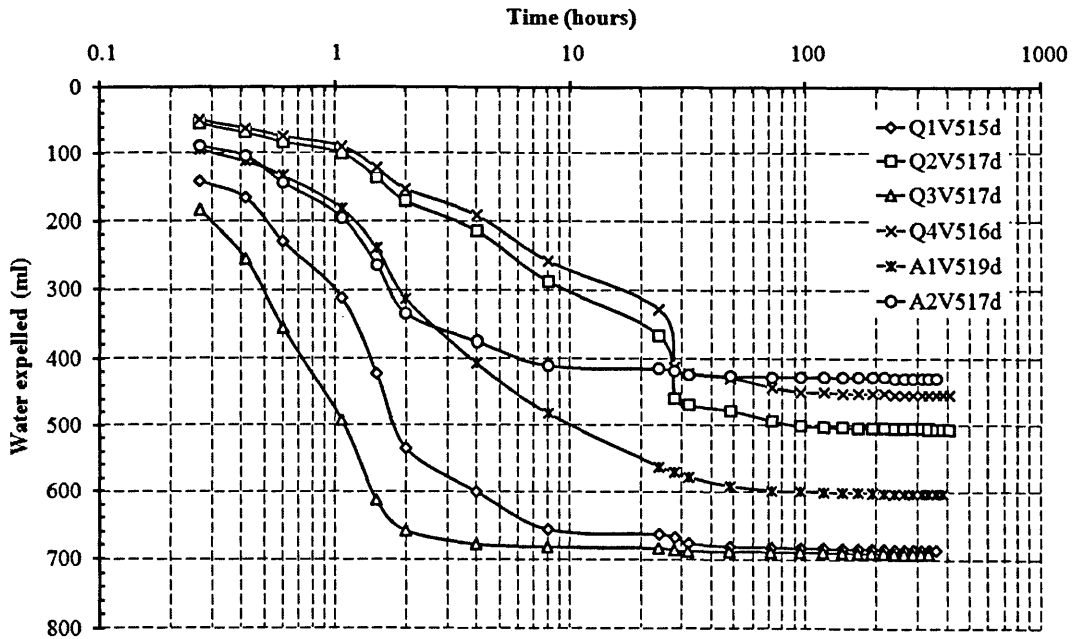


Figure D7 Phase 3 results for numbers and arrangement of electrodes test series: water expelled versus time curves

Different Applied Voltage tests

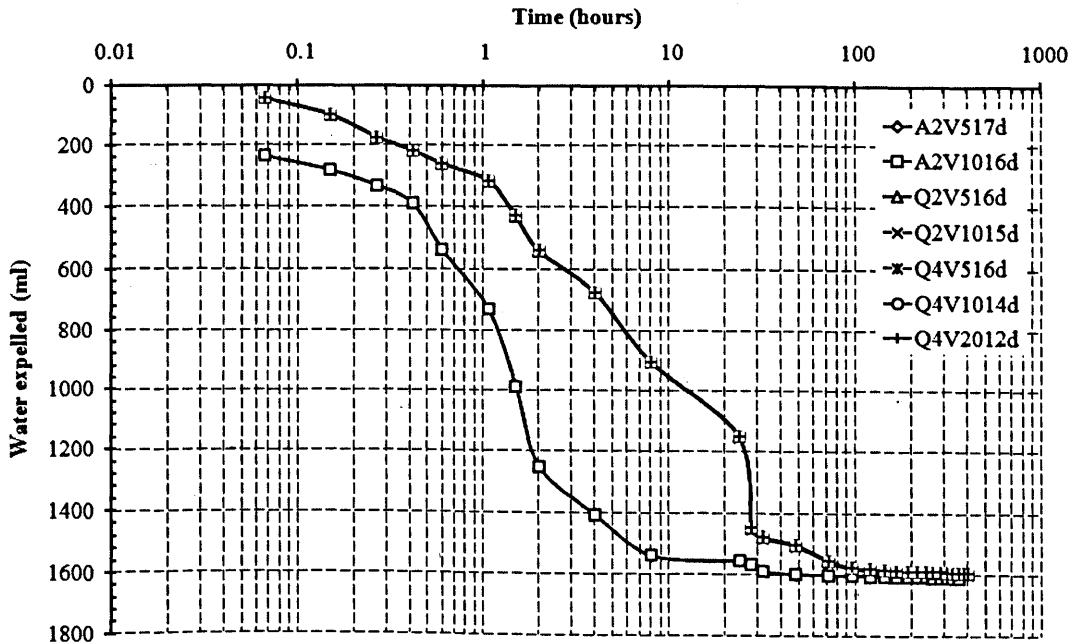


Figure D8 Phase 1 results for different applied voltage test series: water expelled versus time curves

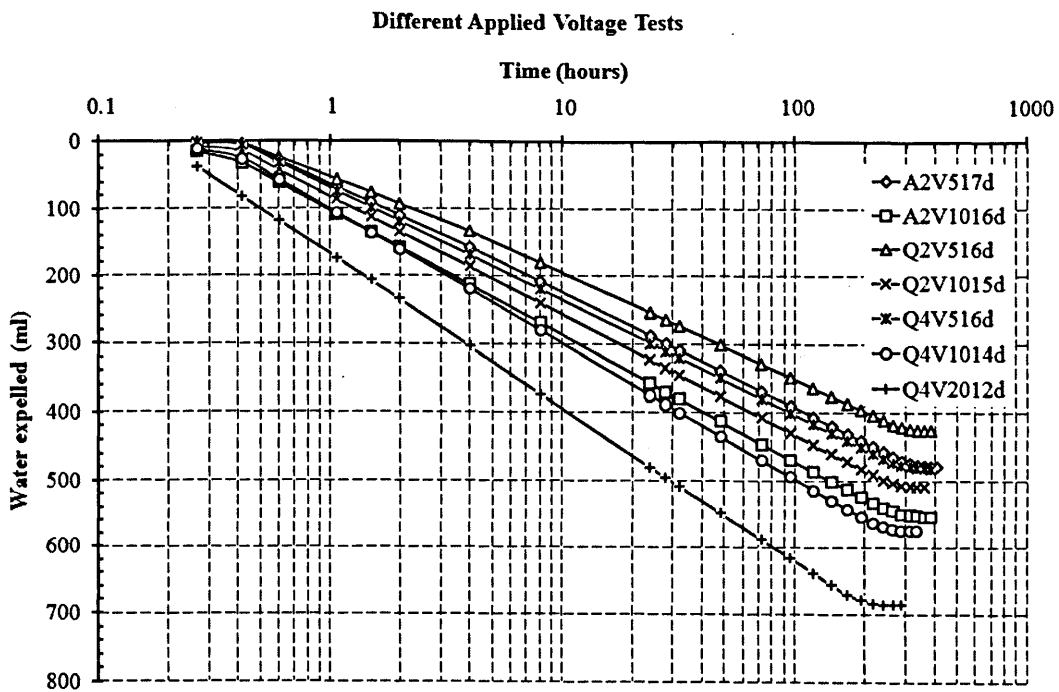


Figure D9 Phase 2 results for different applied voltage test series: water expelled versus time curves

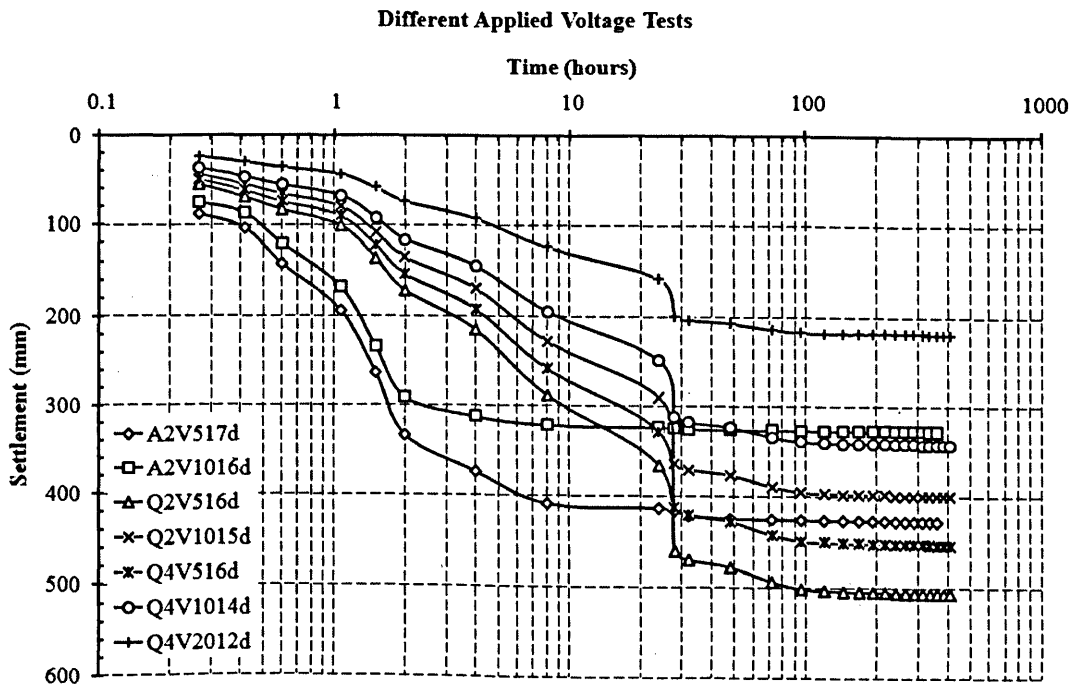


Figure D10 Phase 3 results for different applied voltage test series: water expelled versus time curves

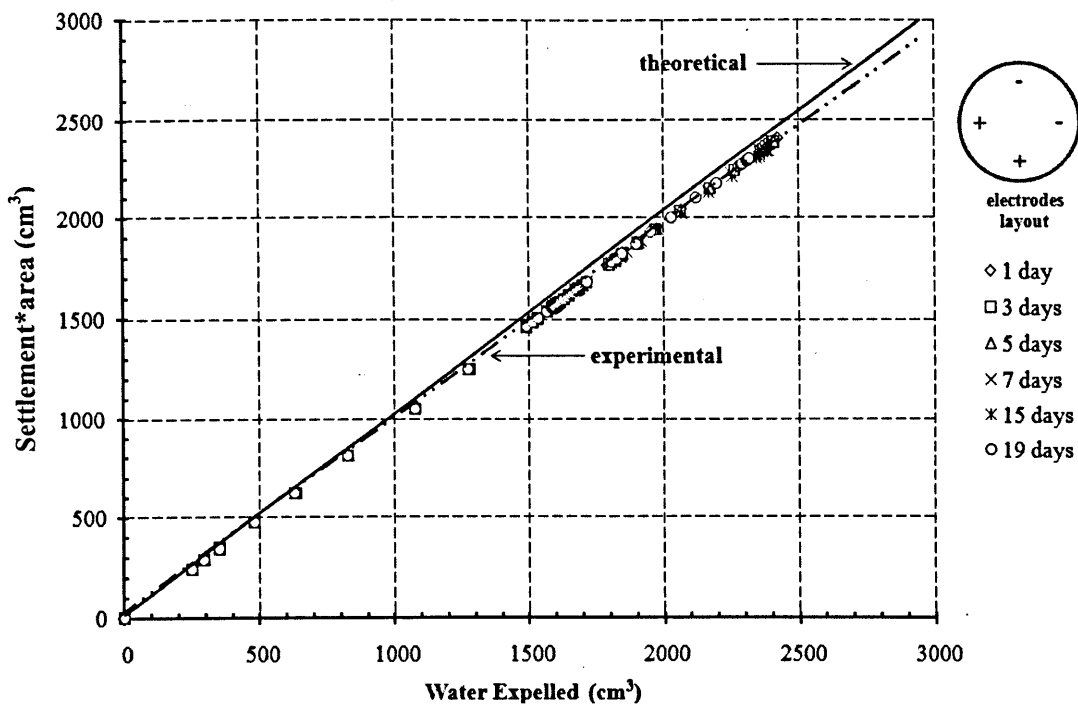


Figure D11 Result of A1V5 test series: settlement*area versus water expelled

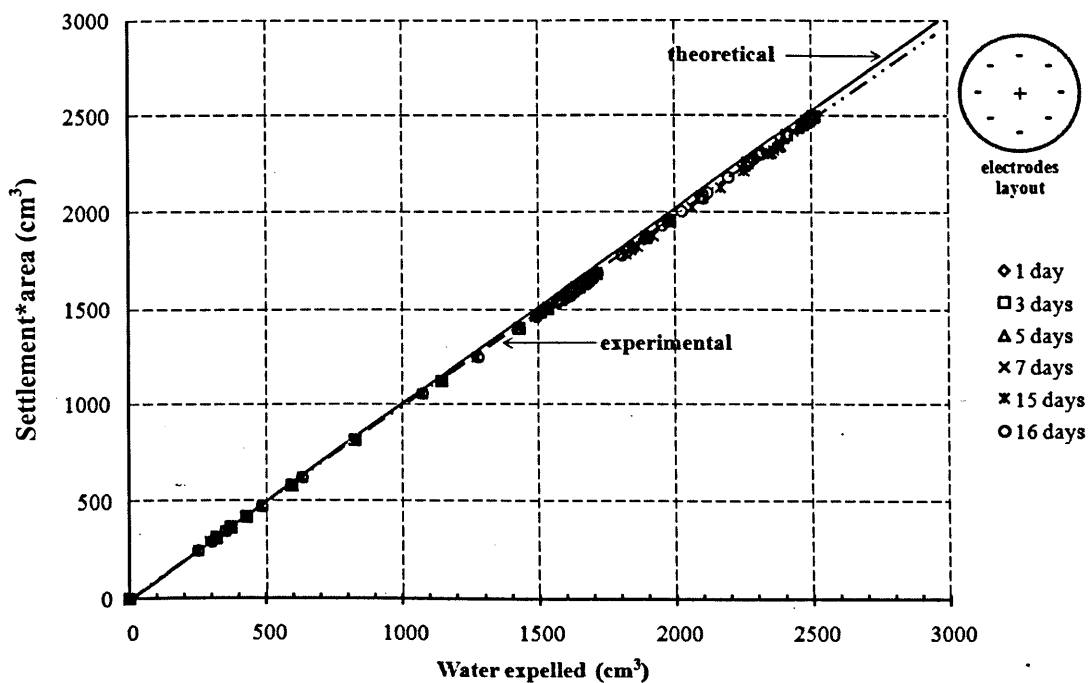
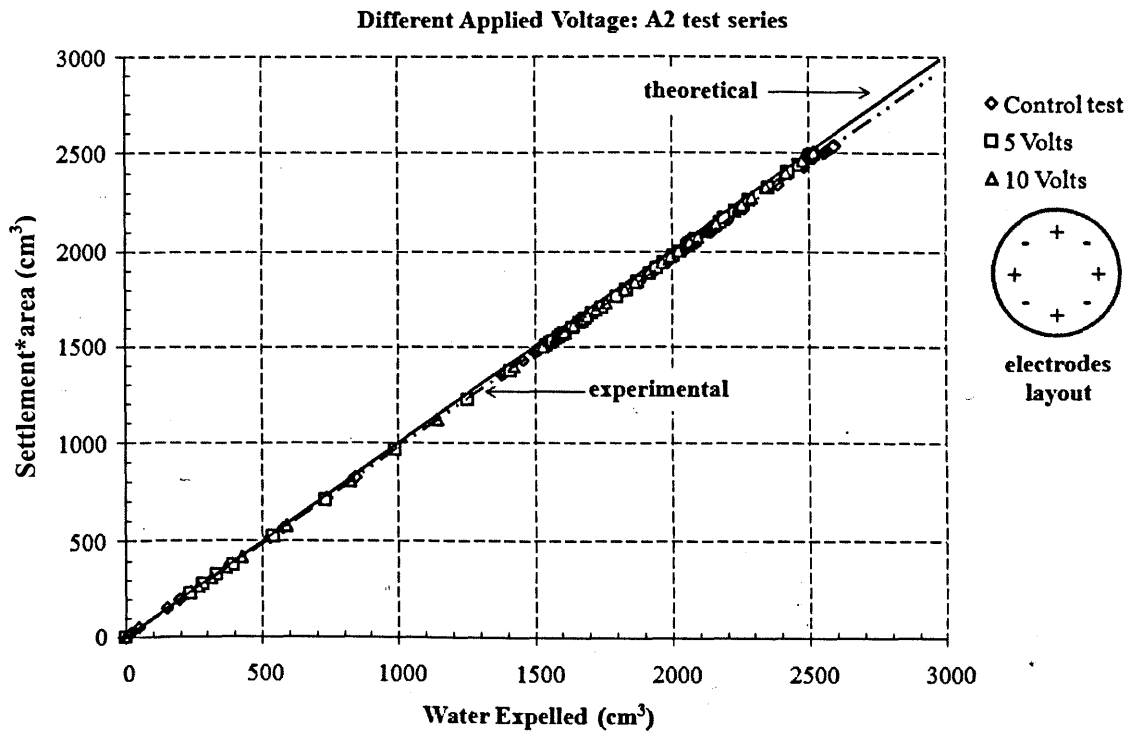
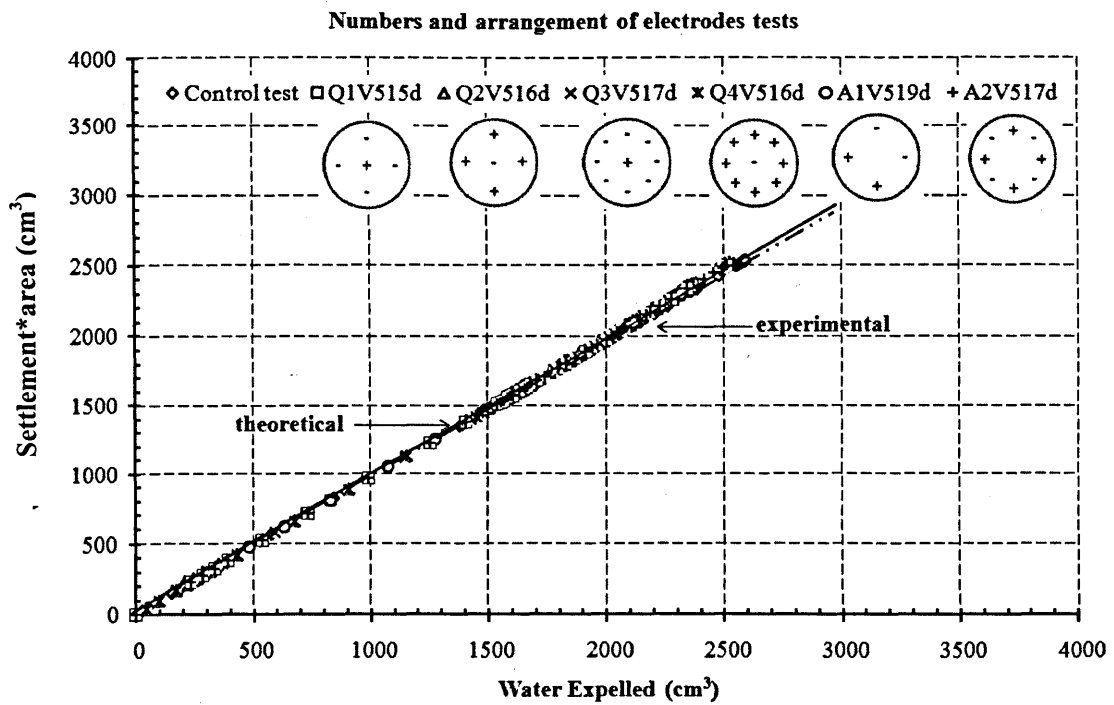


Figure D12 Result of Q3V5 test series: settlement*area versus water expelled



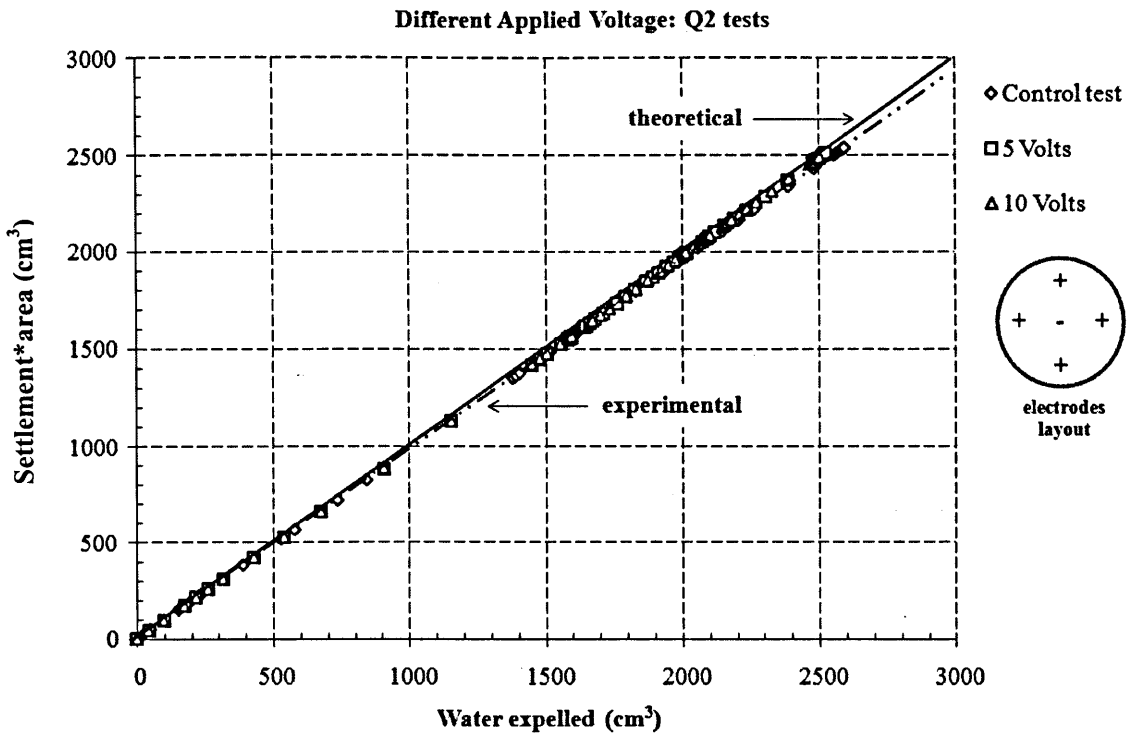


Figure D15 Result of different applied voltage on Q2 test series: settlement *area versus water expelled

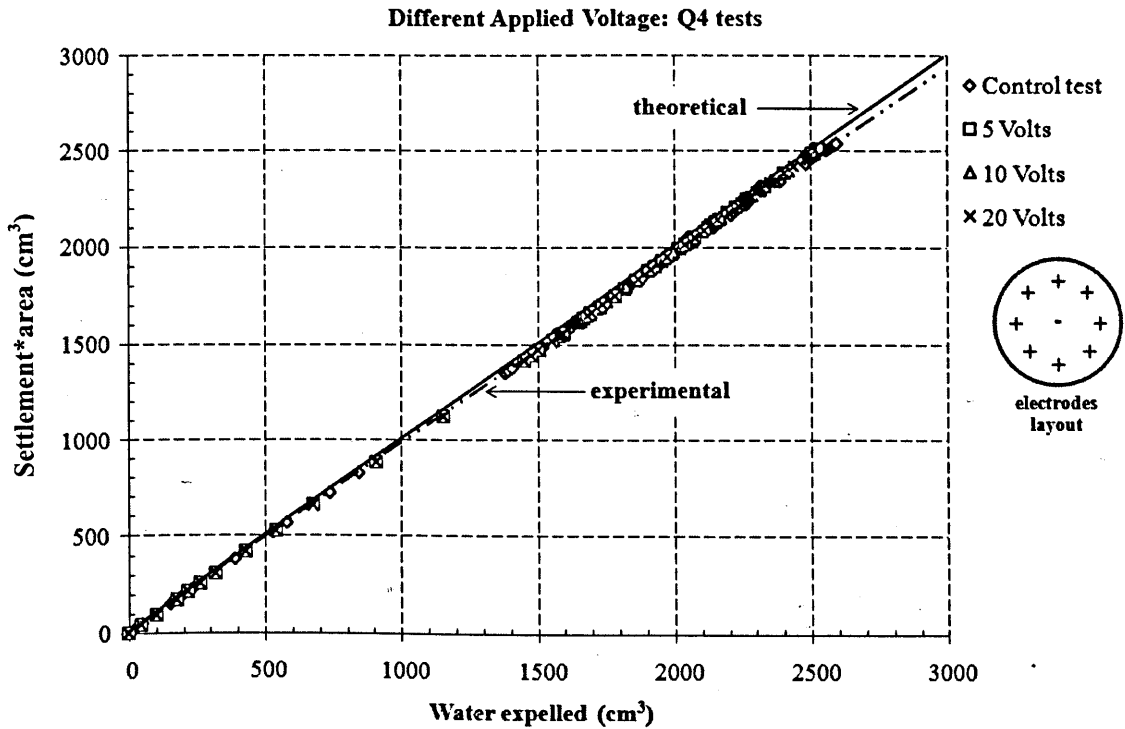


Figure D16 Result of different applied voltage on Q4 test series: settlement *area versus water expelled

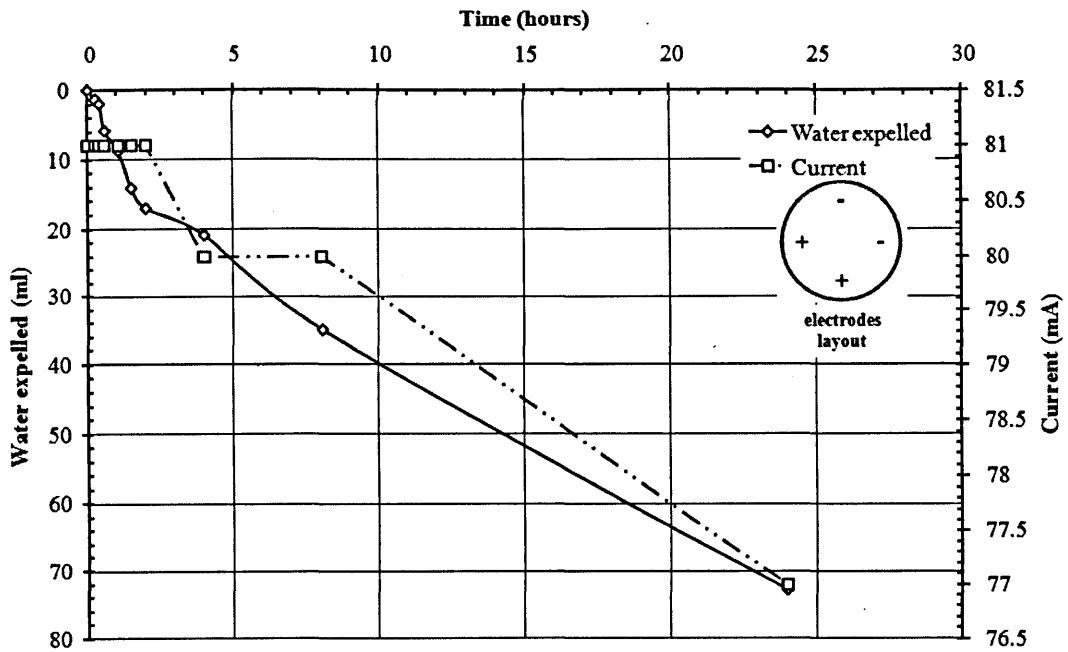


Figure D17 Results of A1V51d test: water expelled and current versus time

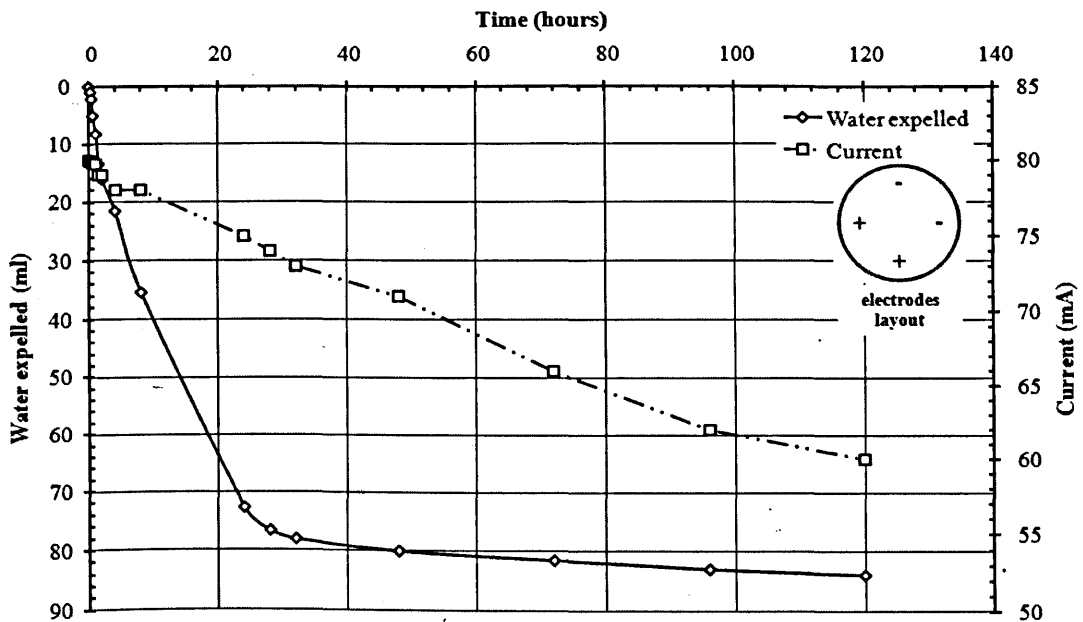


Figure D18 Results of A1V55d test: water expelled and current versus time

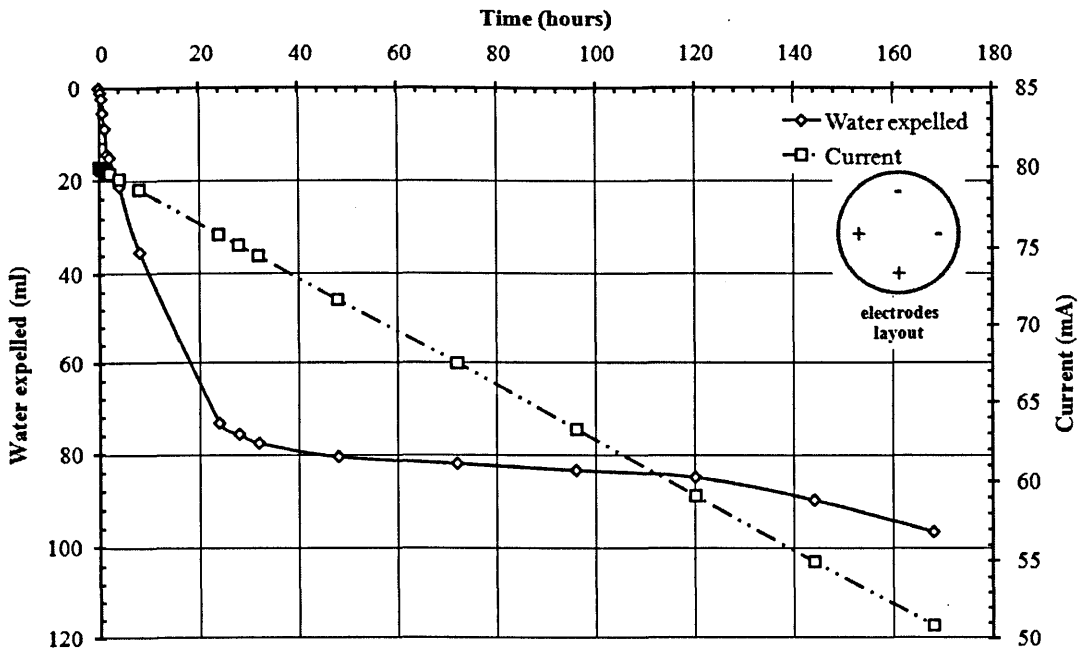


Figure D19 Results of A1V57d test: water expelled and current versus time

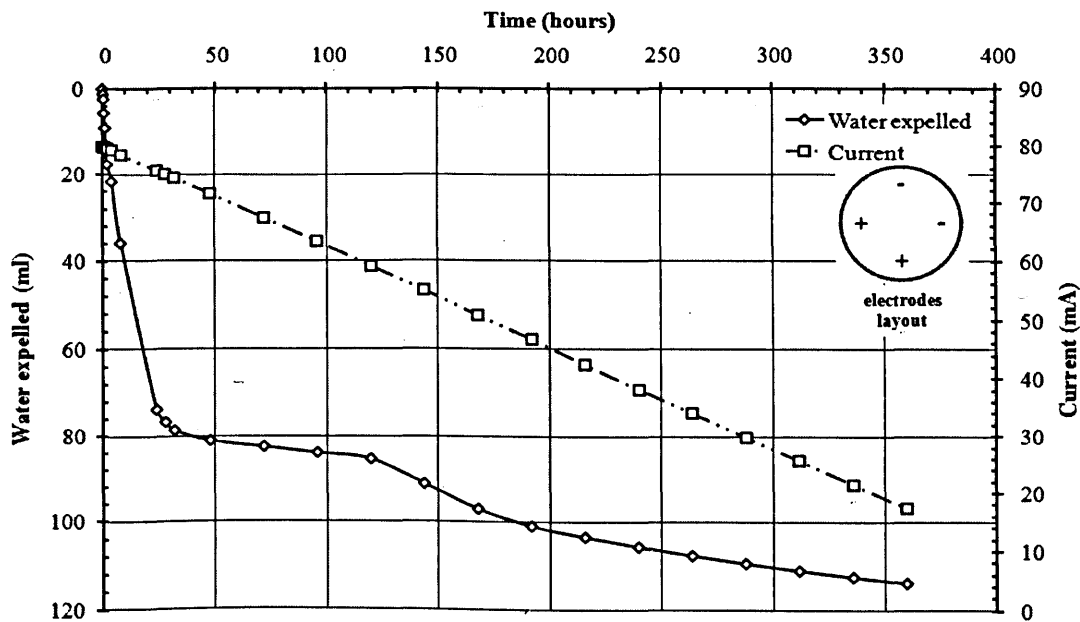


Figure D20 Results of A1V515d test: water expelled and current versus time

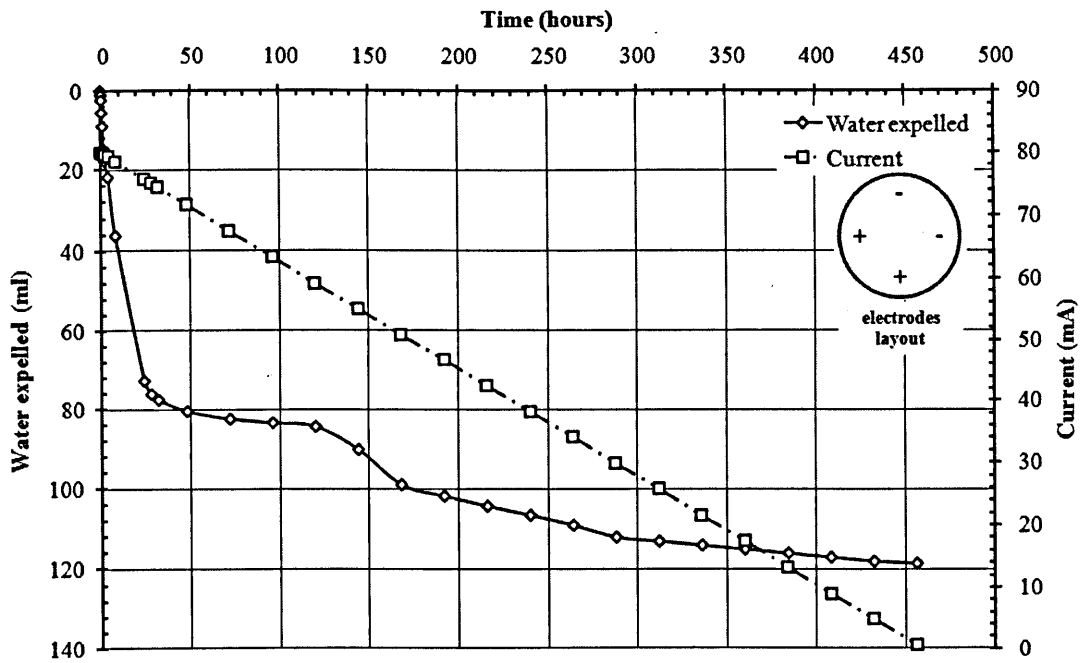


Figure D21 Results of A1V519d test: water expelled and current versus time

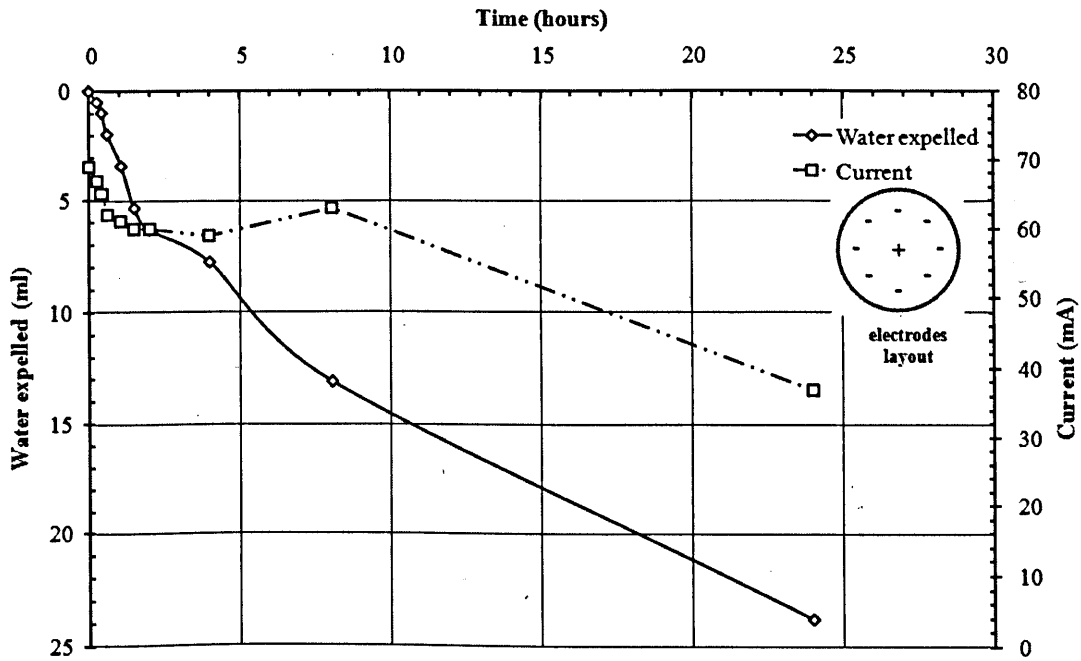


Figure D22 Results of Q3V51d test: water expelled and current versus time

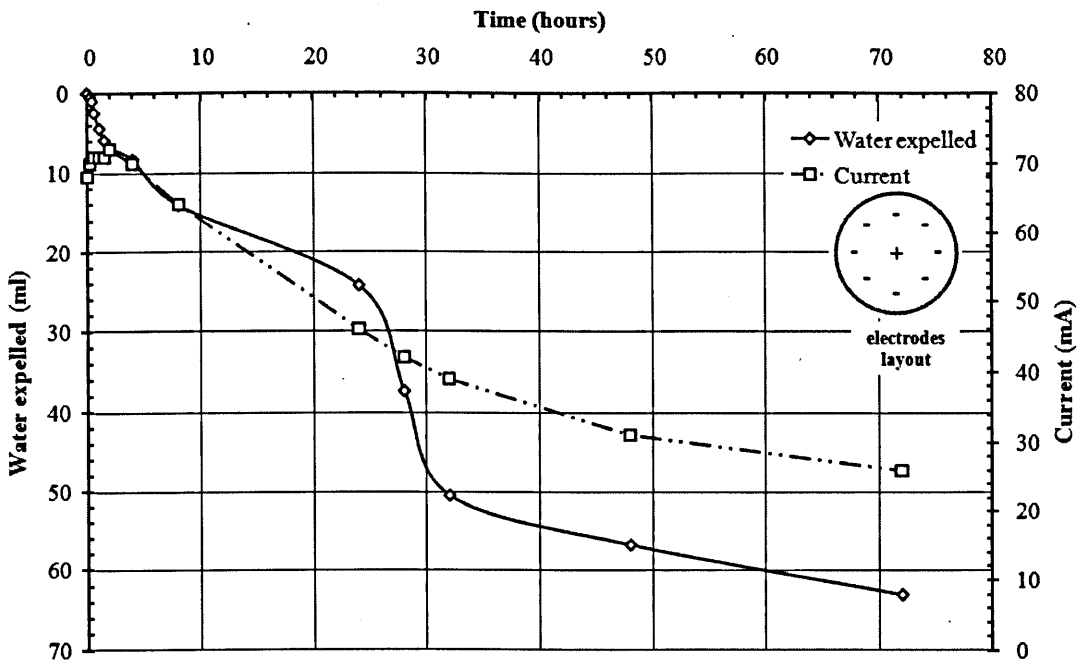


Figure D23 Results of Q3V53d test: water expelled and current versus time

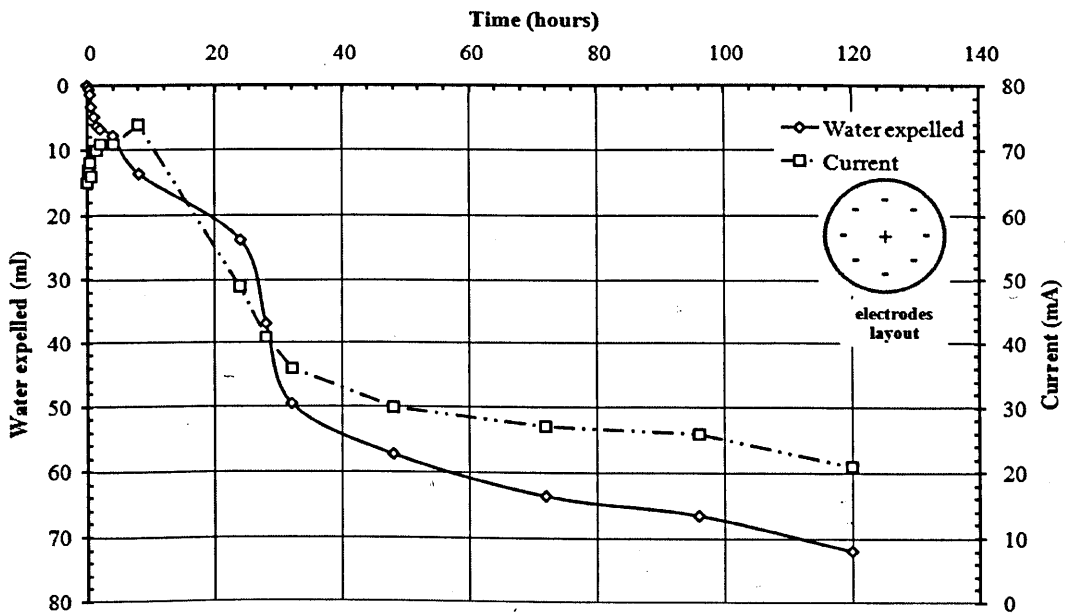


Figure D24 Results of Q3V55d test: water expelled and current versus time

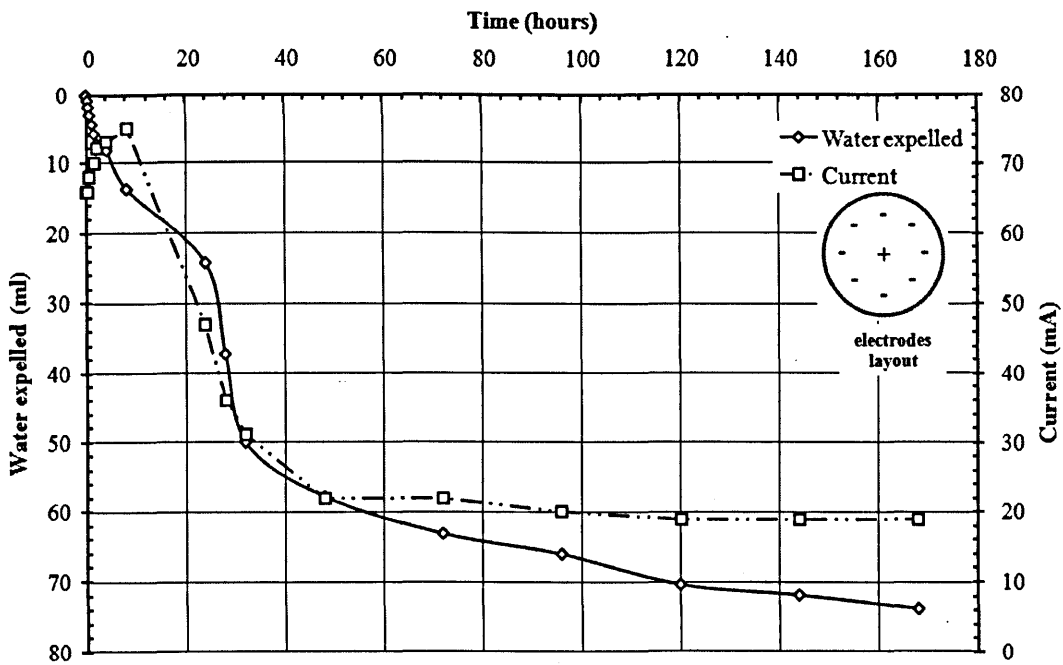


Figure D25 Results of Q3V57d test: water expelled and current versus time

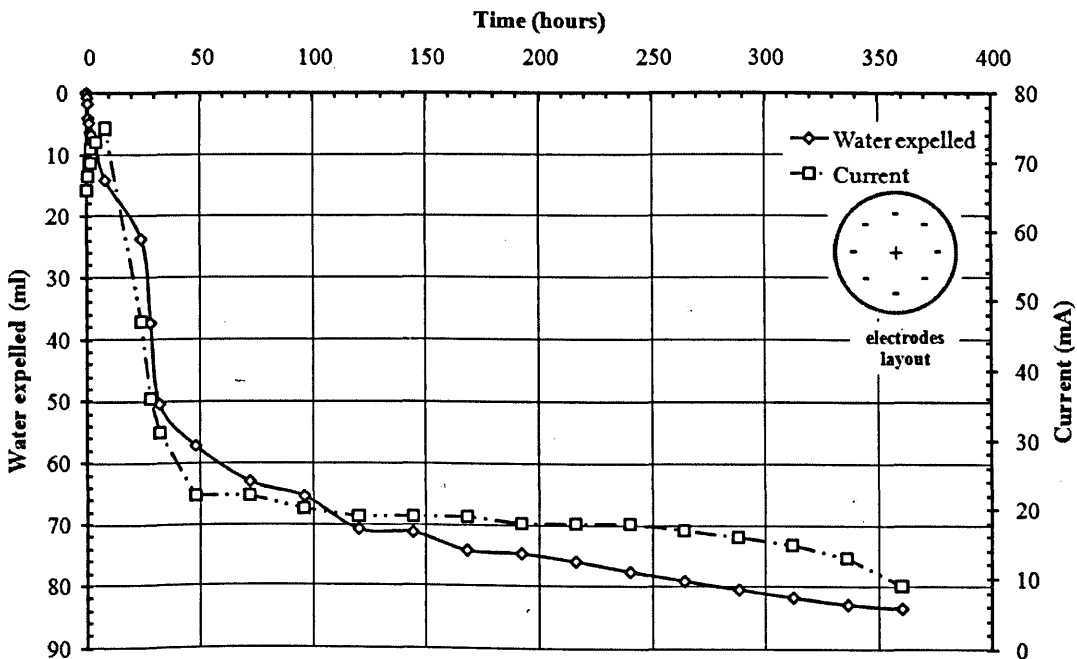


Figure D26 Results of Q3V515d test: water expelled and current versus time

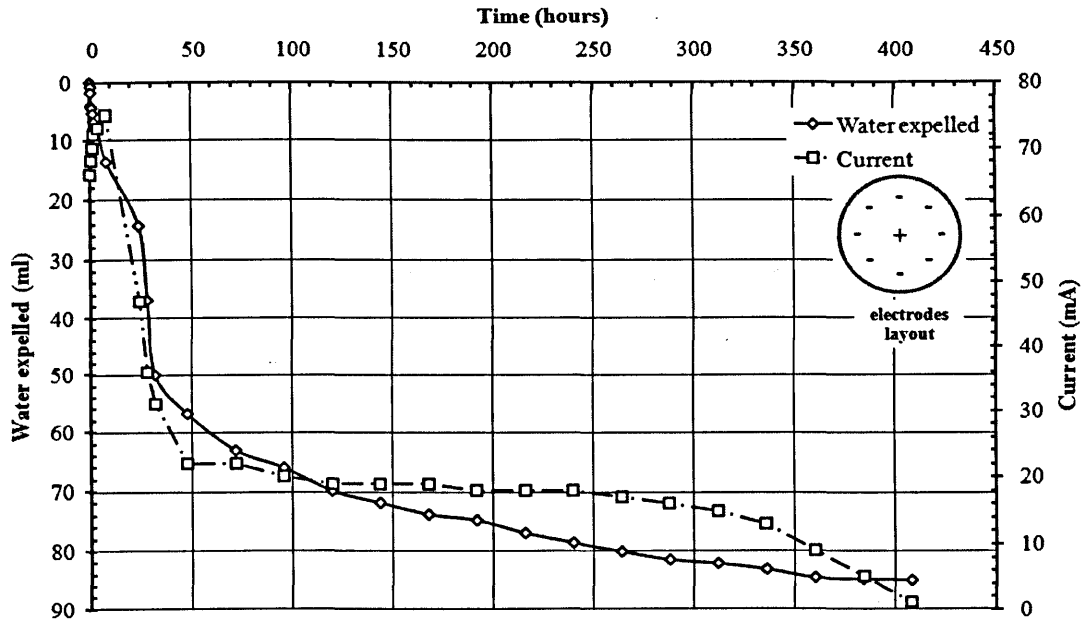


Figure D27 Results of Q3V517d test: water expelled and current versus time

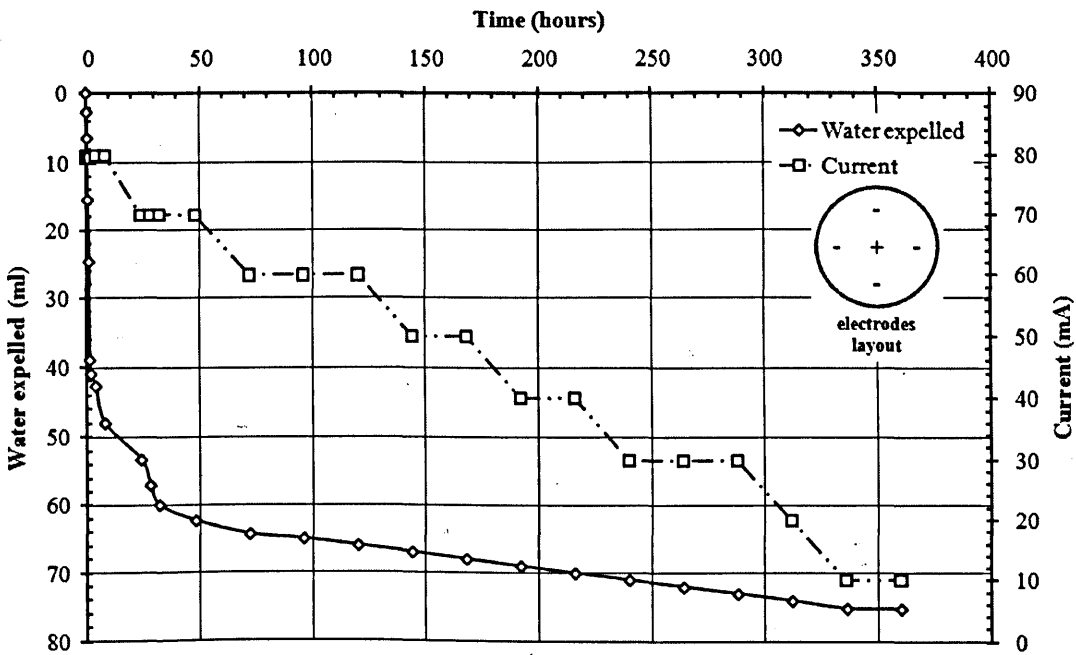


Figure D28 Results of Q1V515d test: water expelled and current versus time

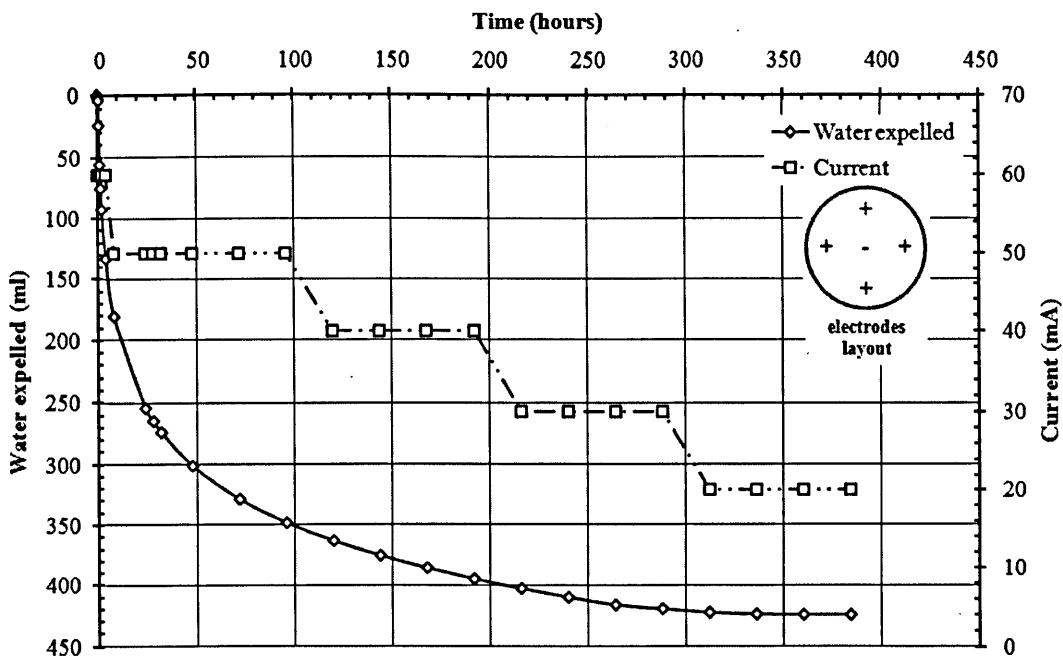


Figure D29 Results of Q2V516d test: water expelled and current versus time

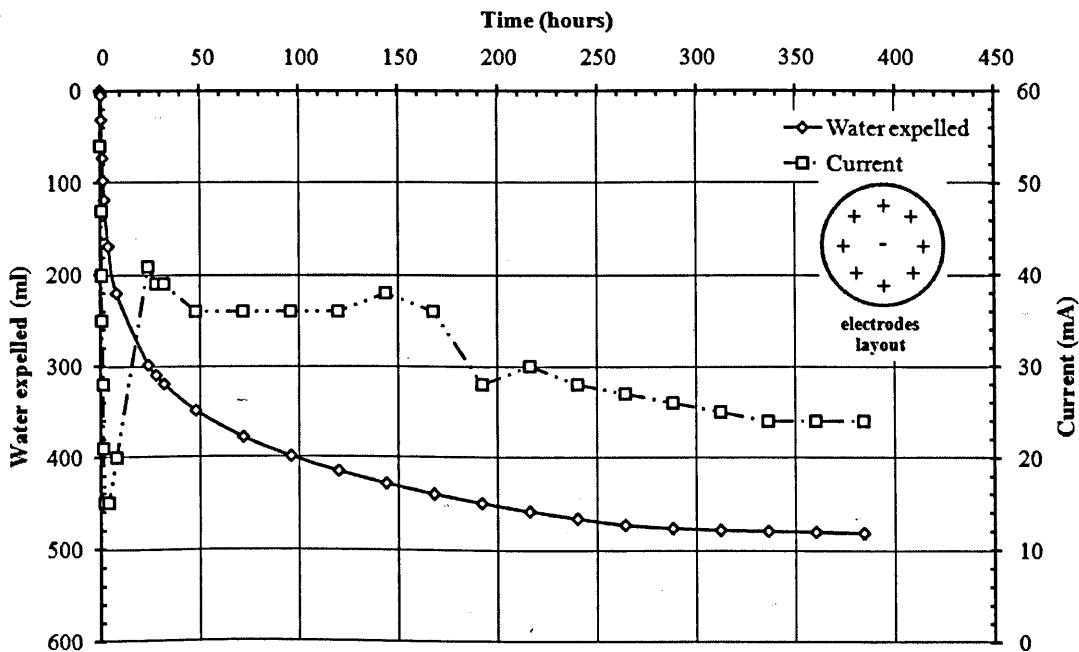


Figure D30 Results of Q4V516d test: water expelled and current versus time

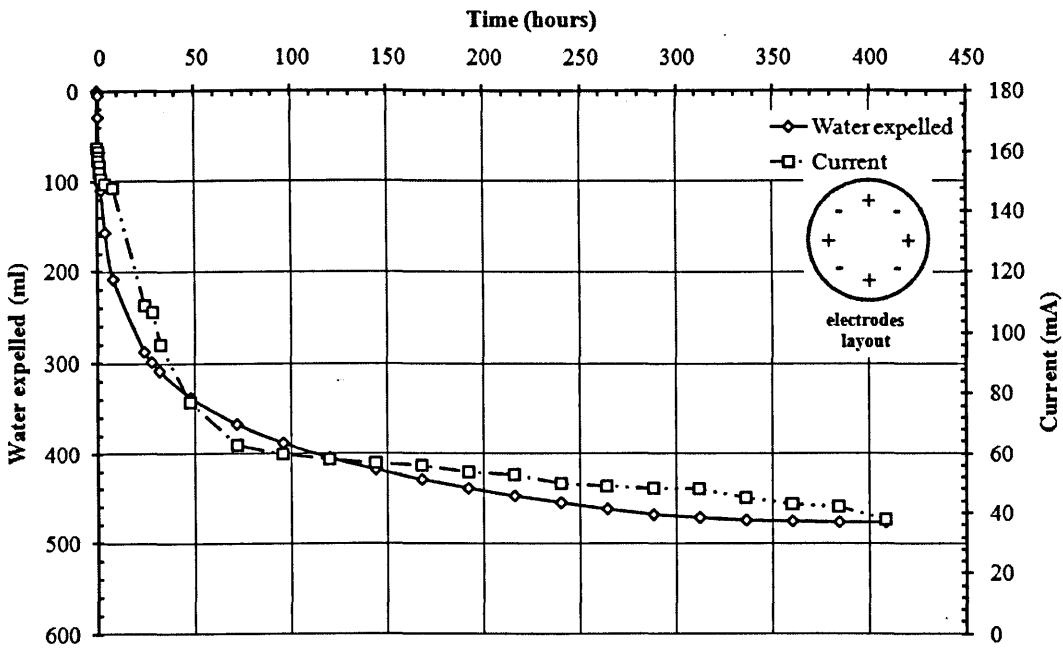


Figure D31 Results of A2V517d test: water expelled and current versus time

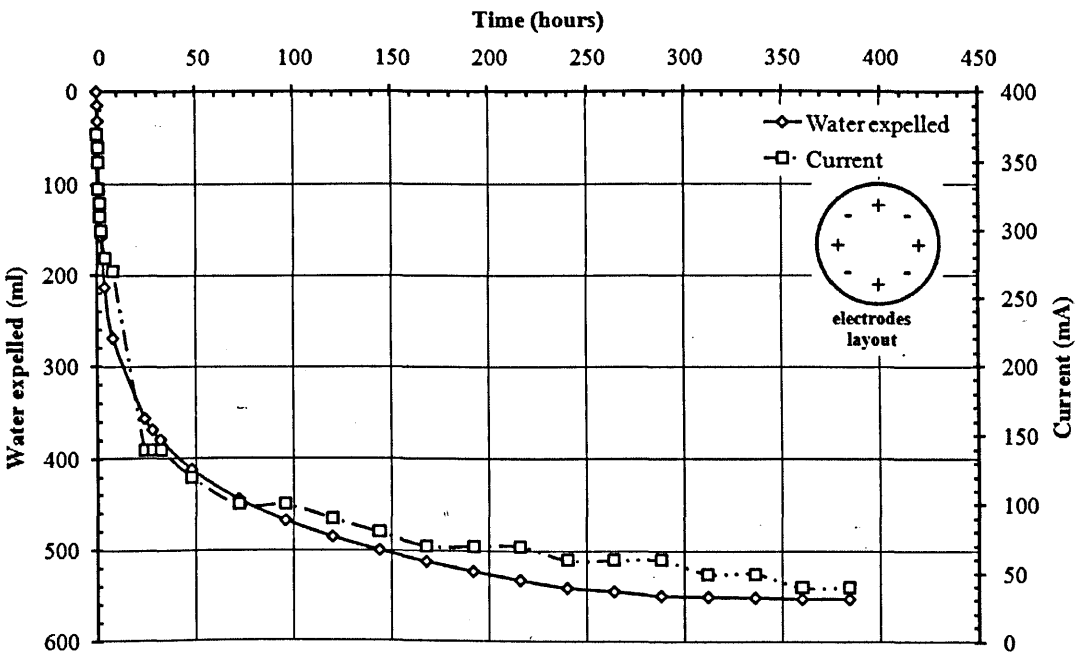


Figure D32 Results of A2V1016d test: water expelled and current versus time

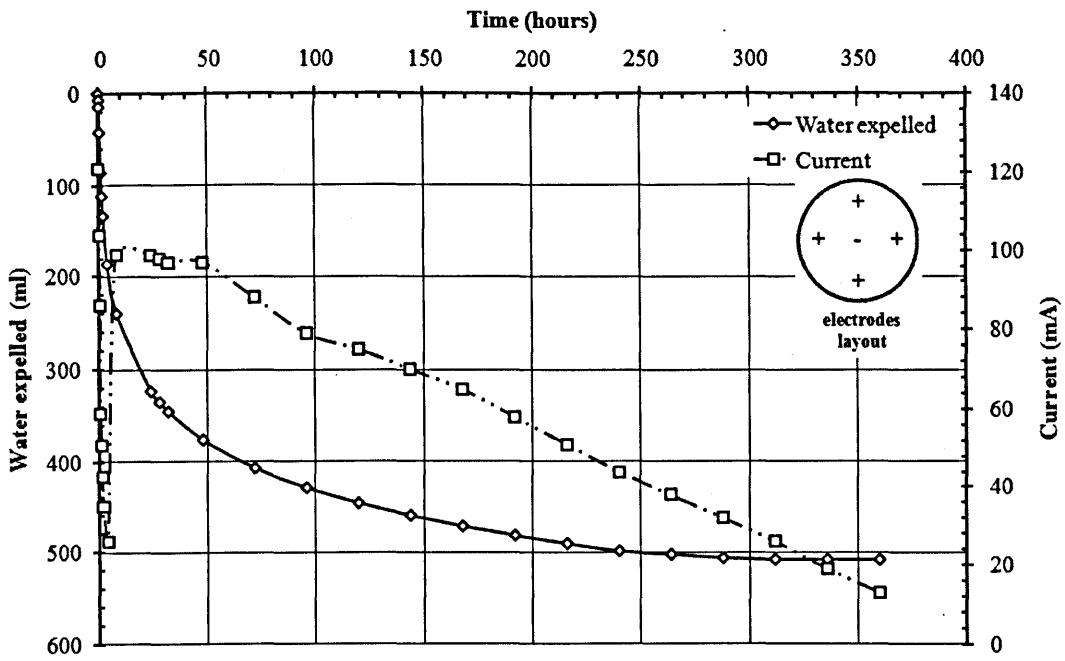


Figure D33 Results of Q2V1015d test: water expelled and current versus time

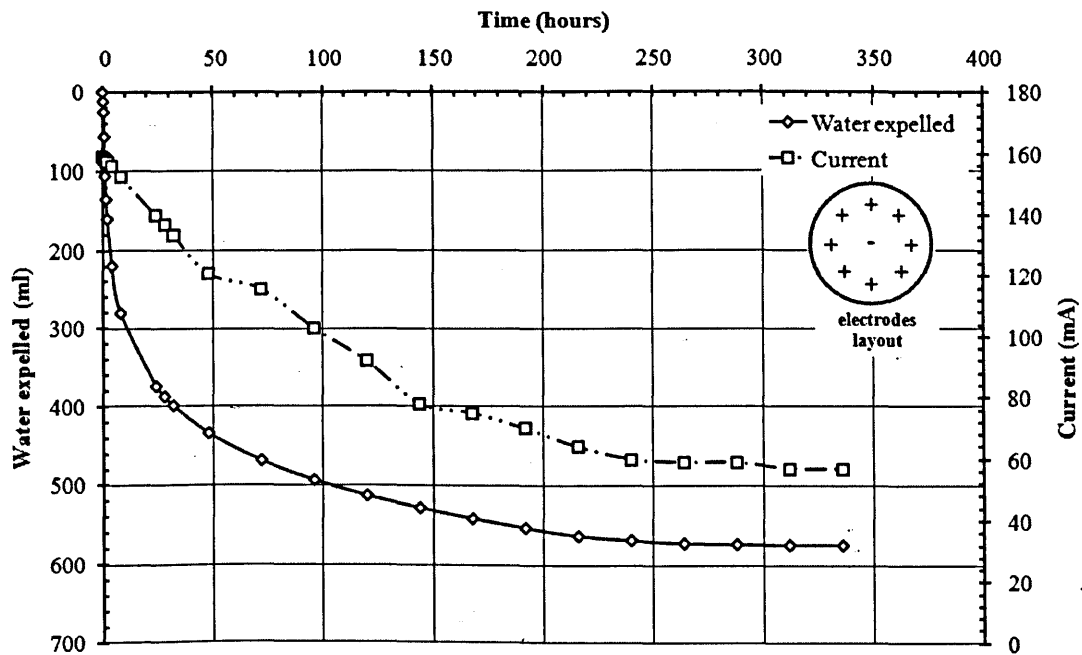


Figure D34 Results of Q4V1014d test: water expelled and current versus time

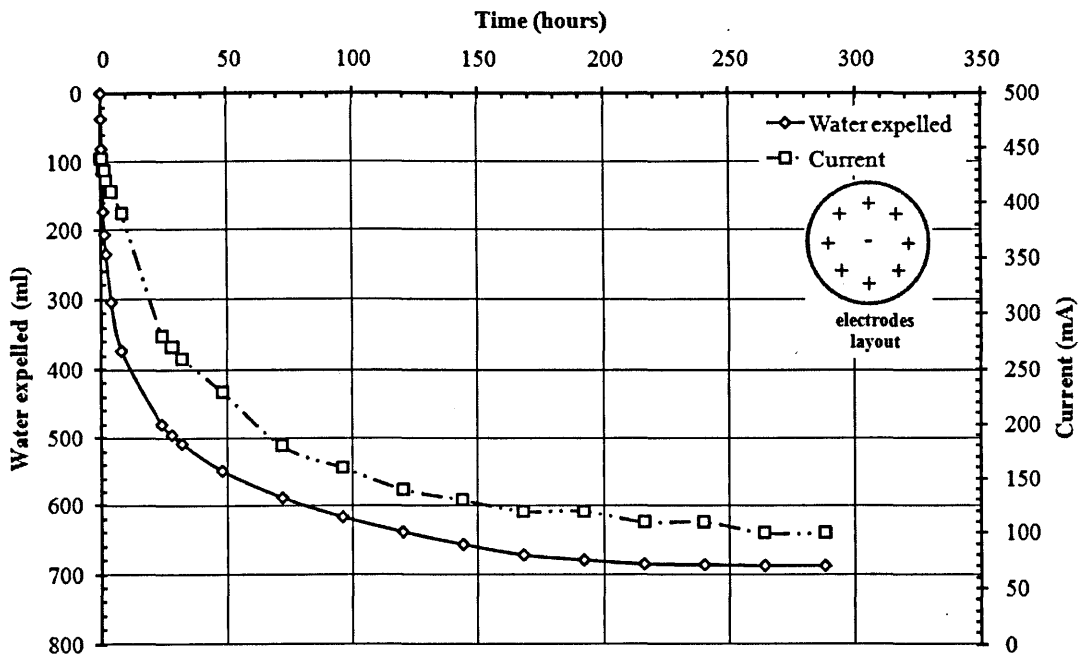


Figure D35 Results of Q4V2012d test: water expelled and current versus time

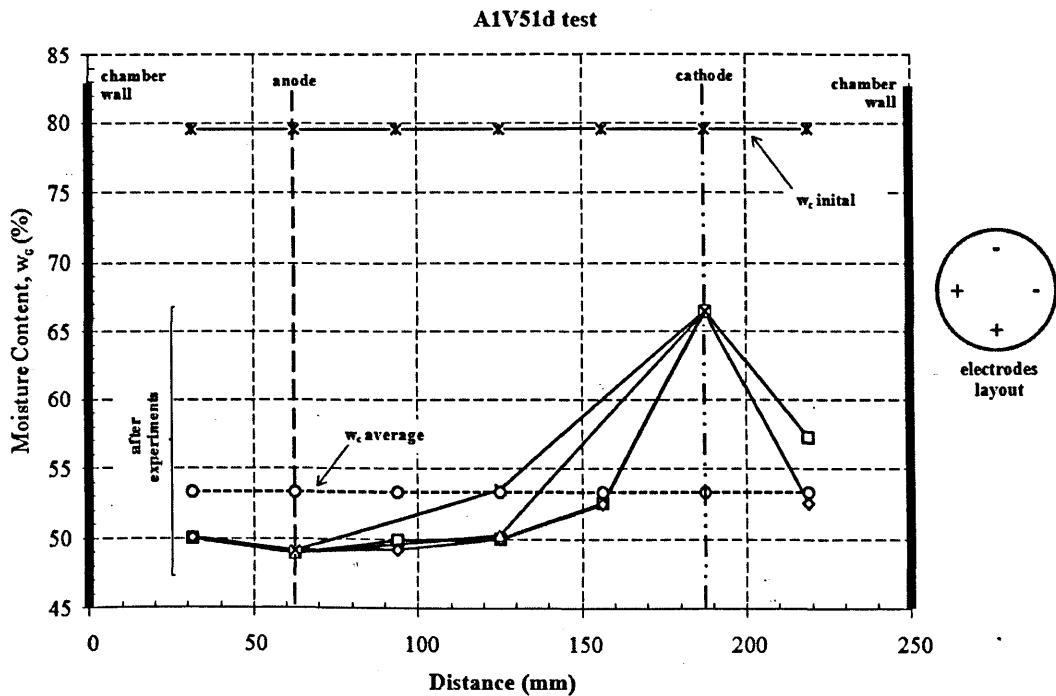


Figure D36 Results of A1V51d test: water content versus distance

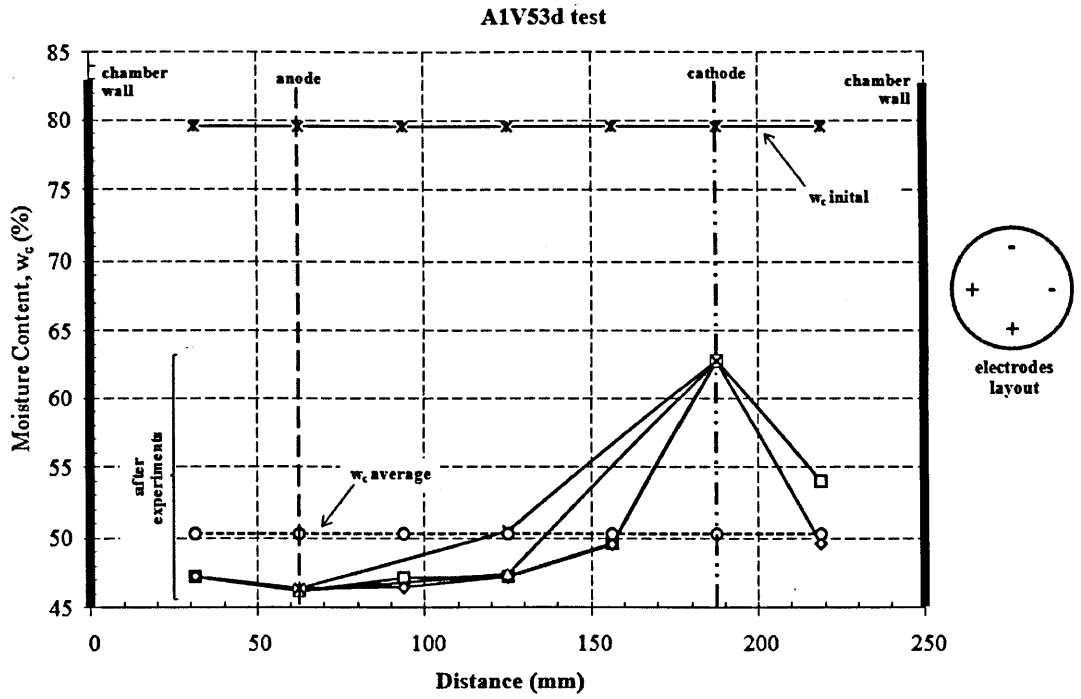


Figure D37 Results of A1V53d test: water content versus distance

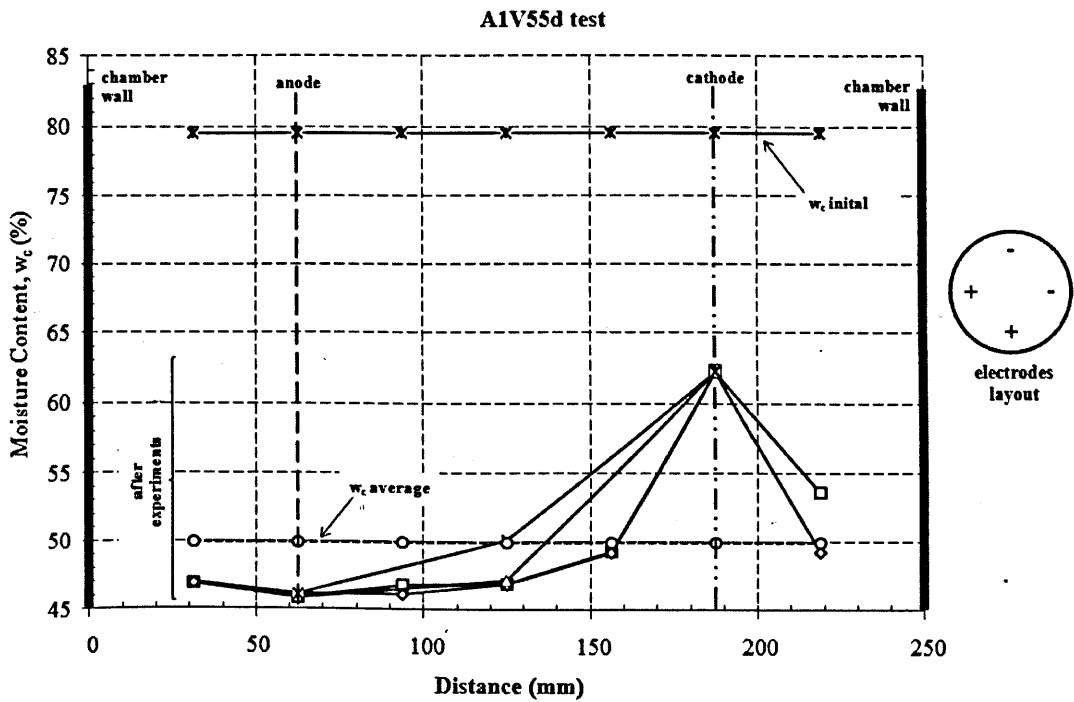


Figure D38 Results of A1V55d test: water content versus distance

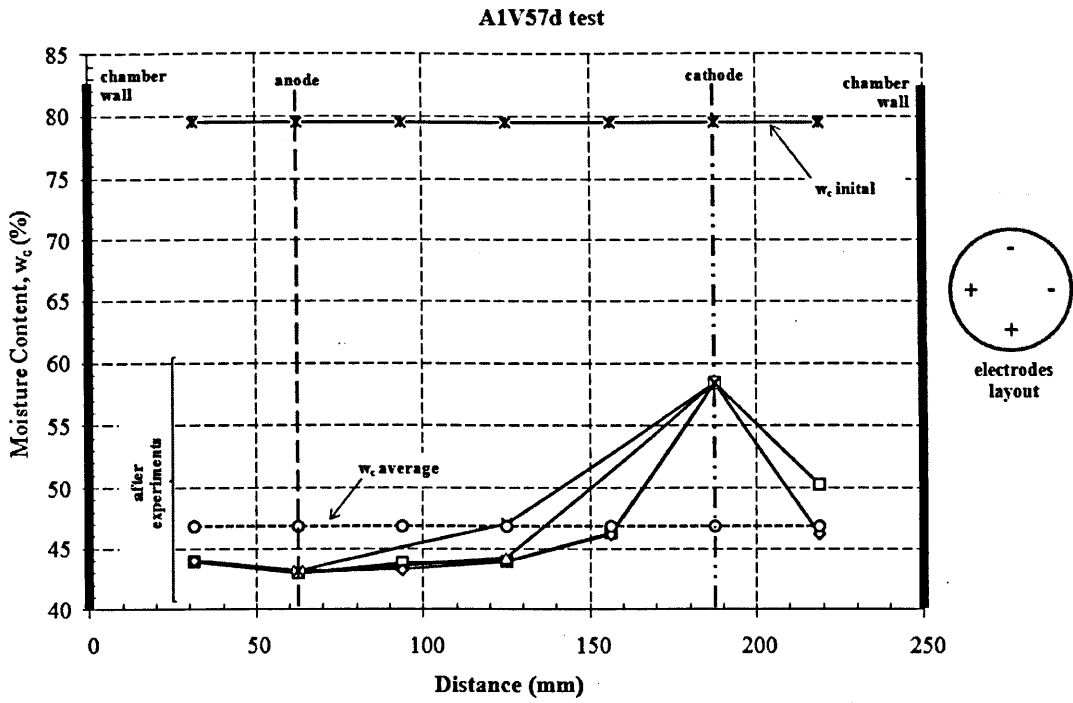


Figure D39 Results of A1V57d test: water content versus distance

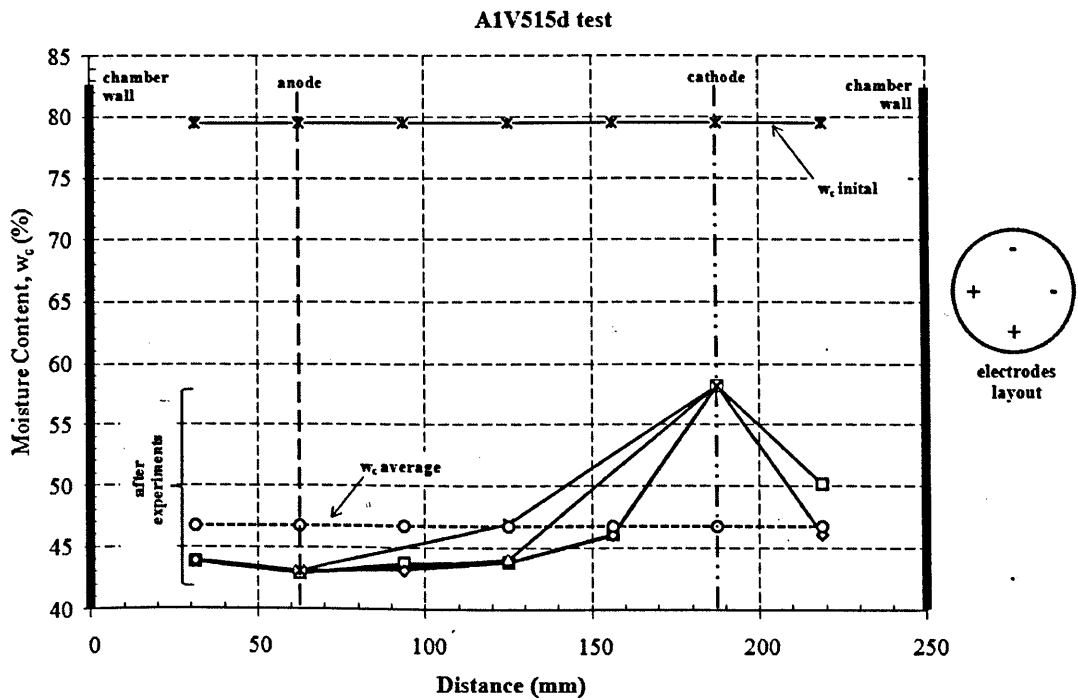


Figure D40 Results of A1V515d test: water content versus distance

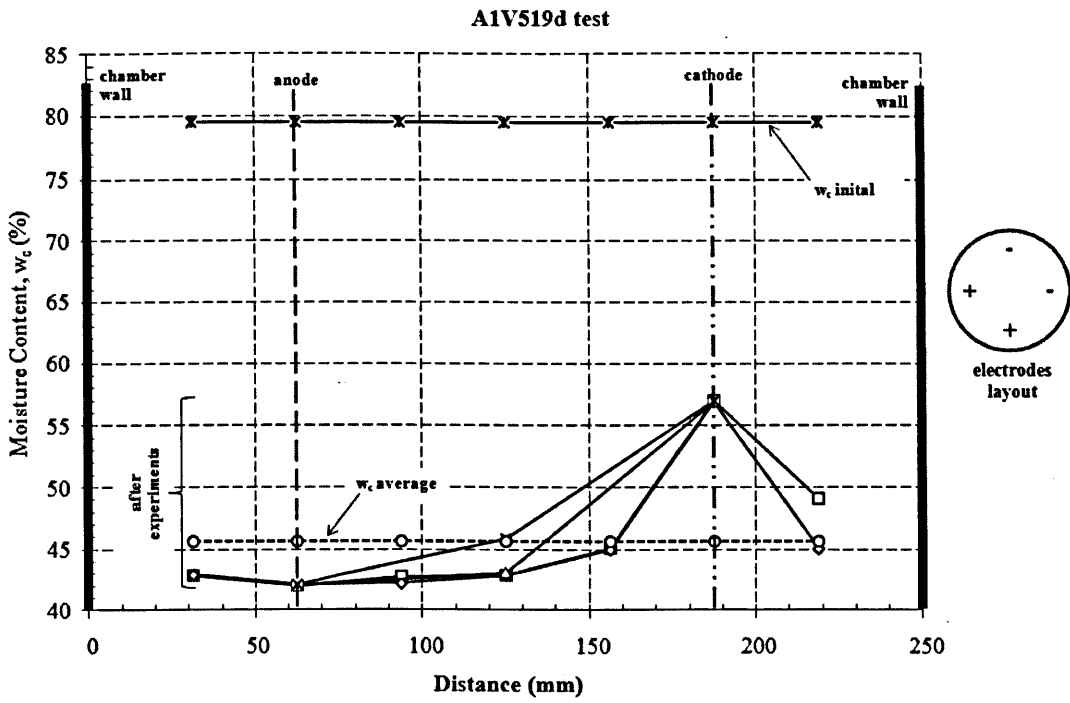


Figure D41 Results of A1V519d test: water content versus distance

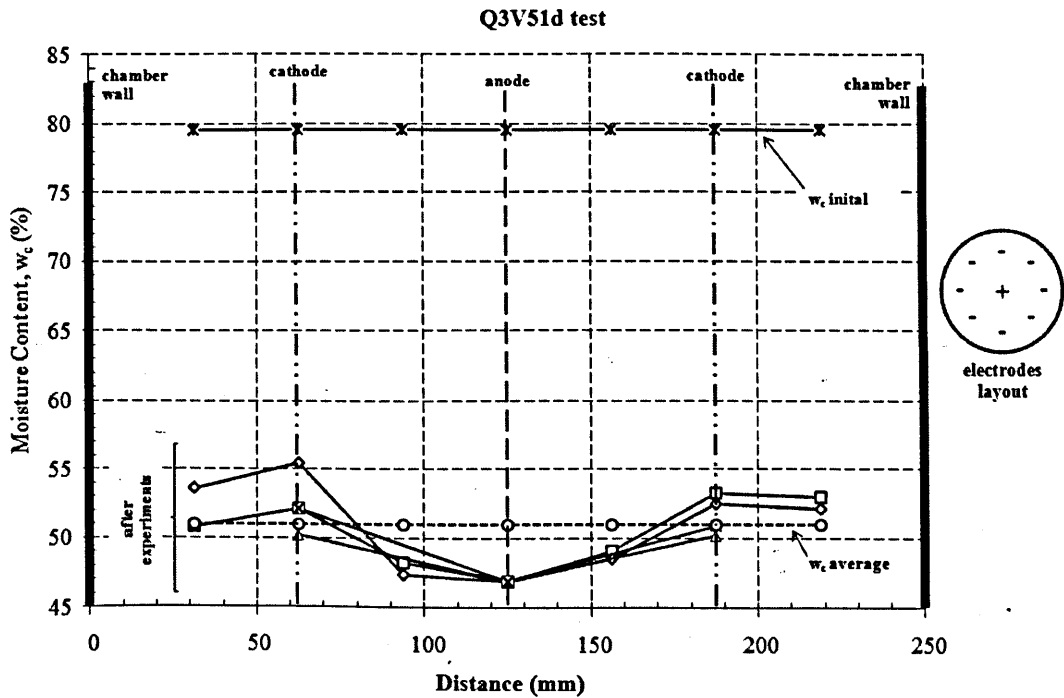


Figure D41 Results of Q3V51d test: water content versus distance

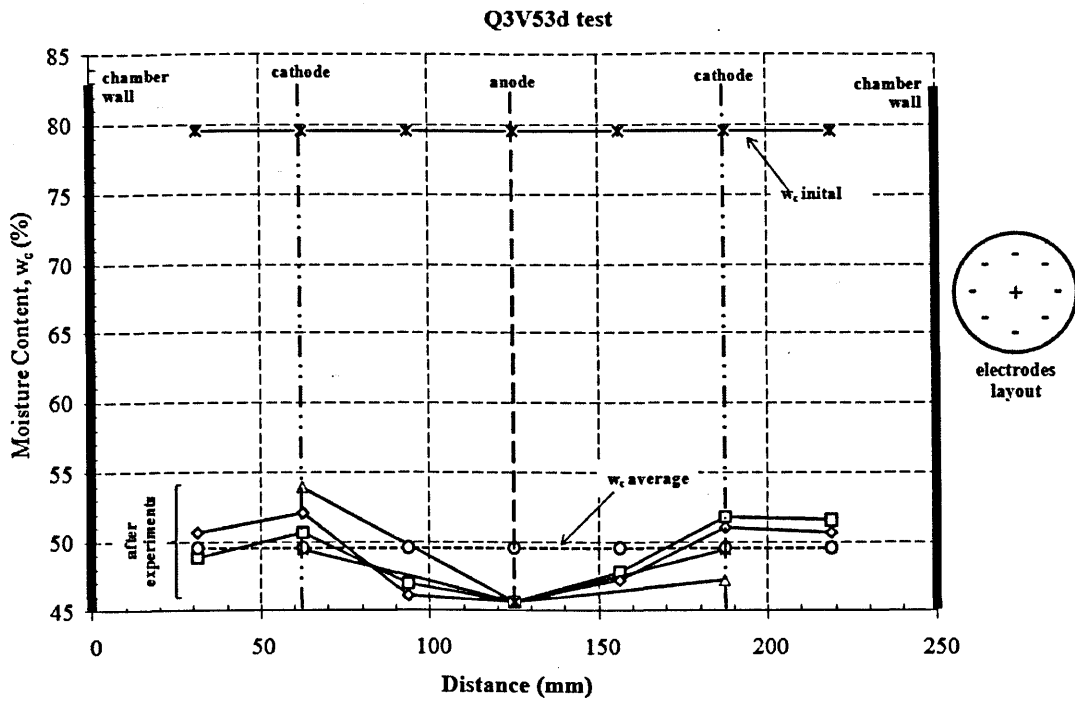


Figure D42 Results of Q3V53d test: water content versus distance

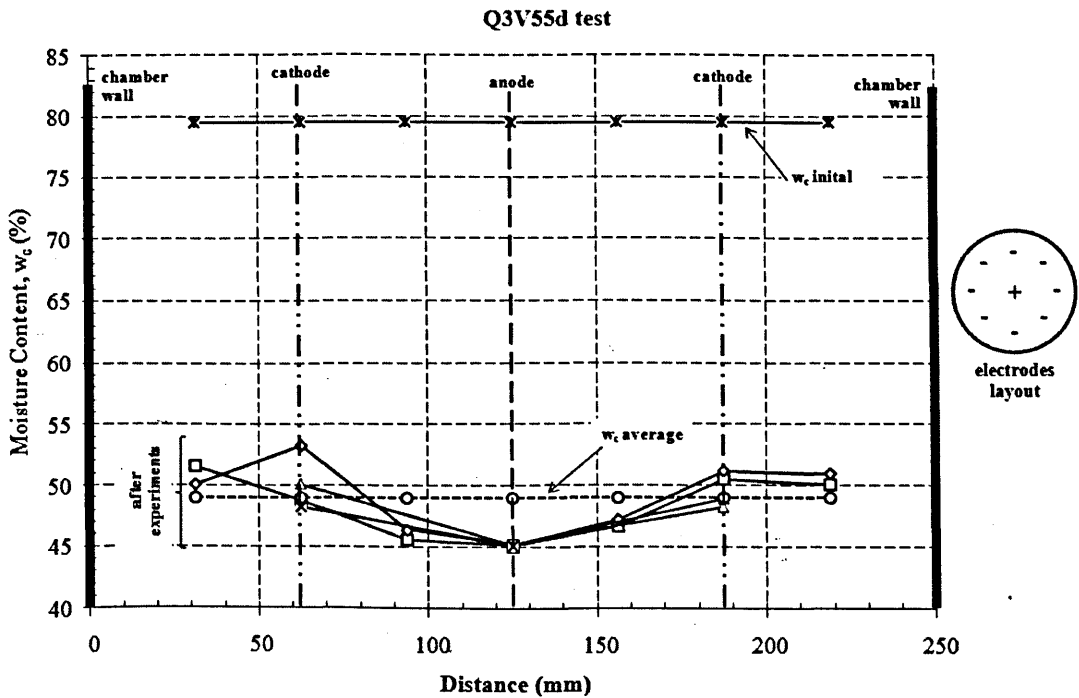


Figure D43 Results of Q3V55d test: water content versus distance

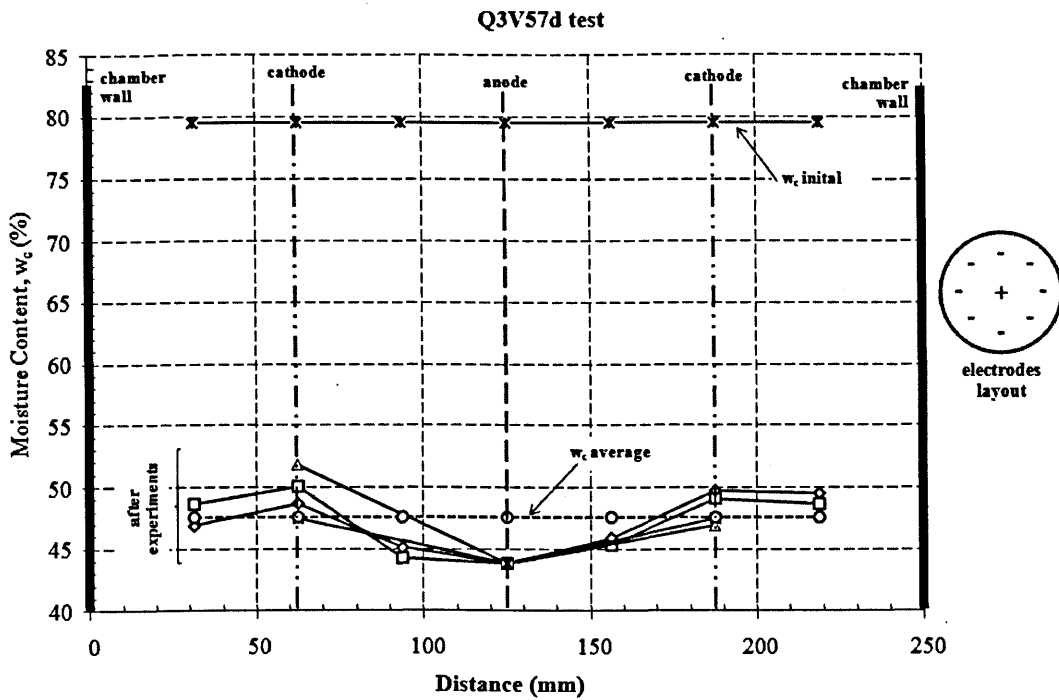


Figure D44 Results of Q3V57d test: water content versus distance

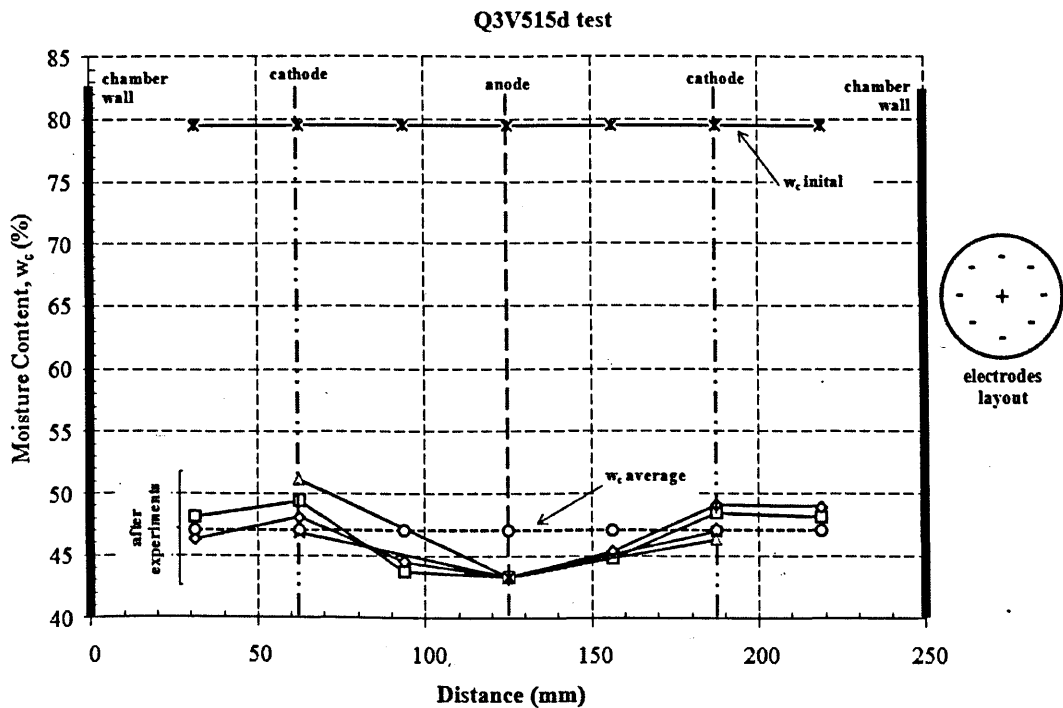


Figure D45 Results of Q3V515d test: water content versus distance

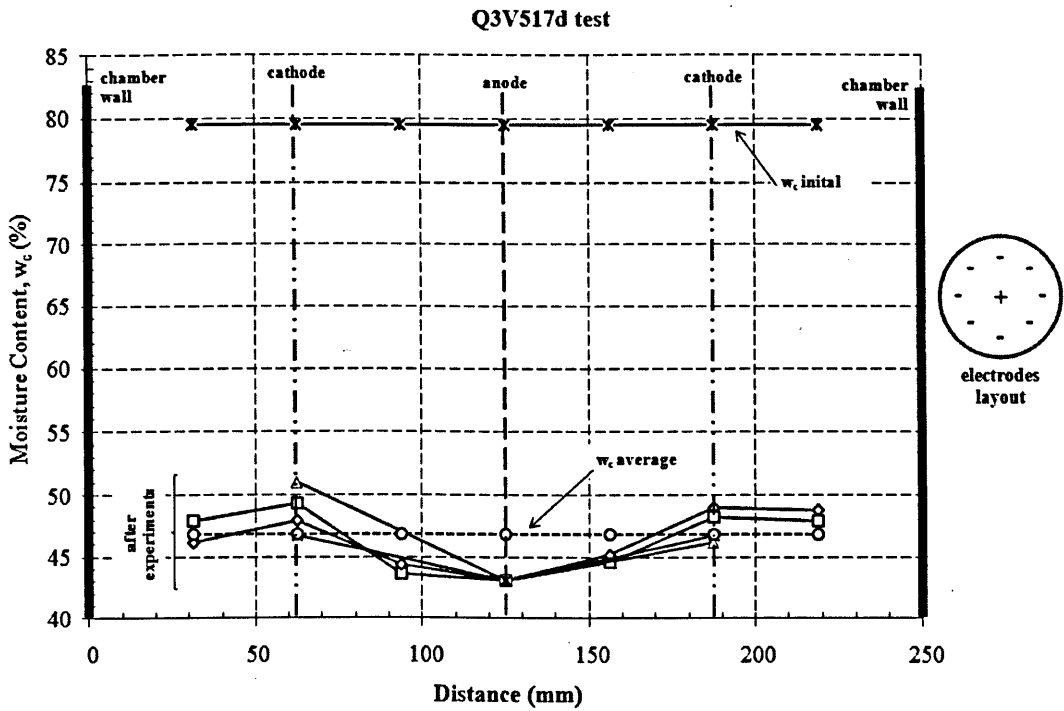


Figure D46 Results of Q3V517d test: water content versus distance

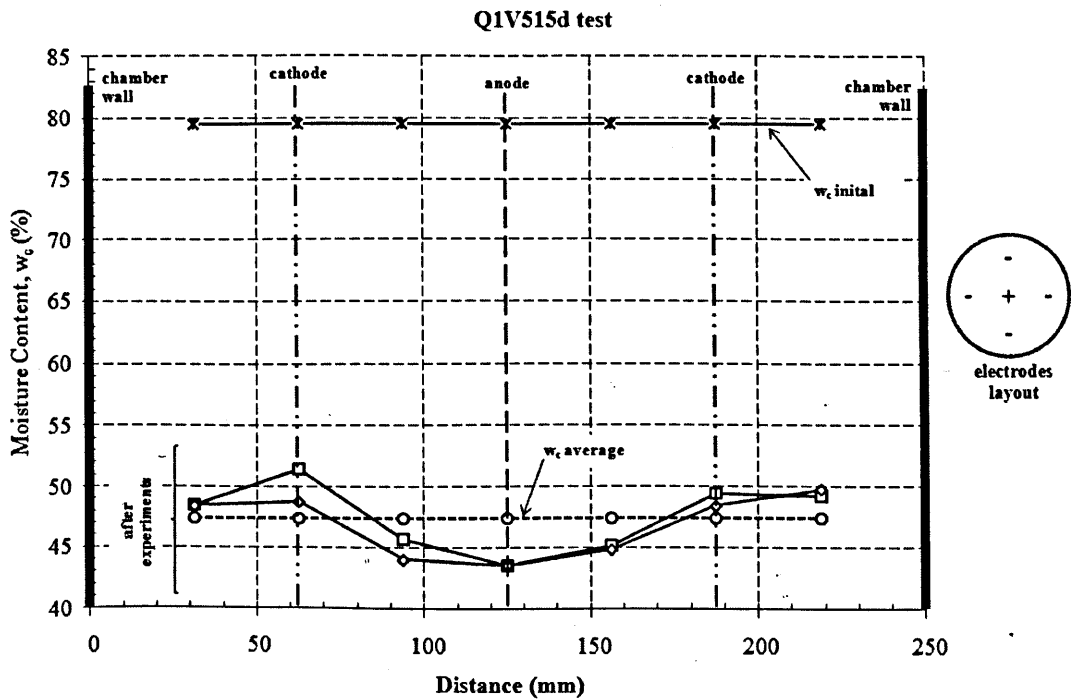


Figure D47 Results of Q1V515d test: water content versus distance

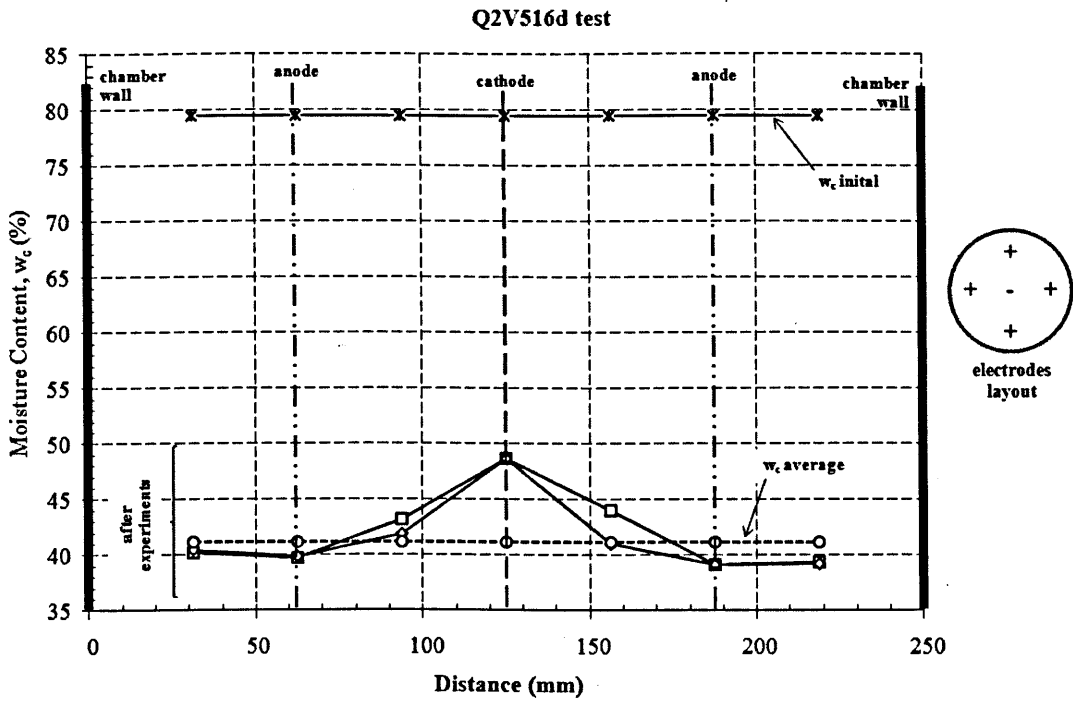


Figure D48 Results of Q2V516d test: water content versus distance

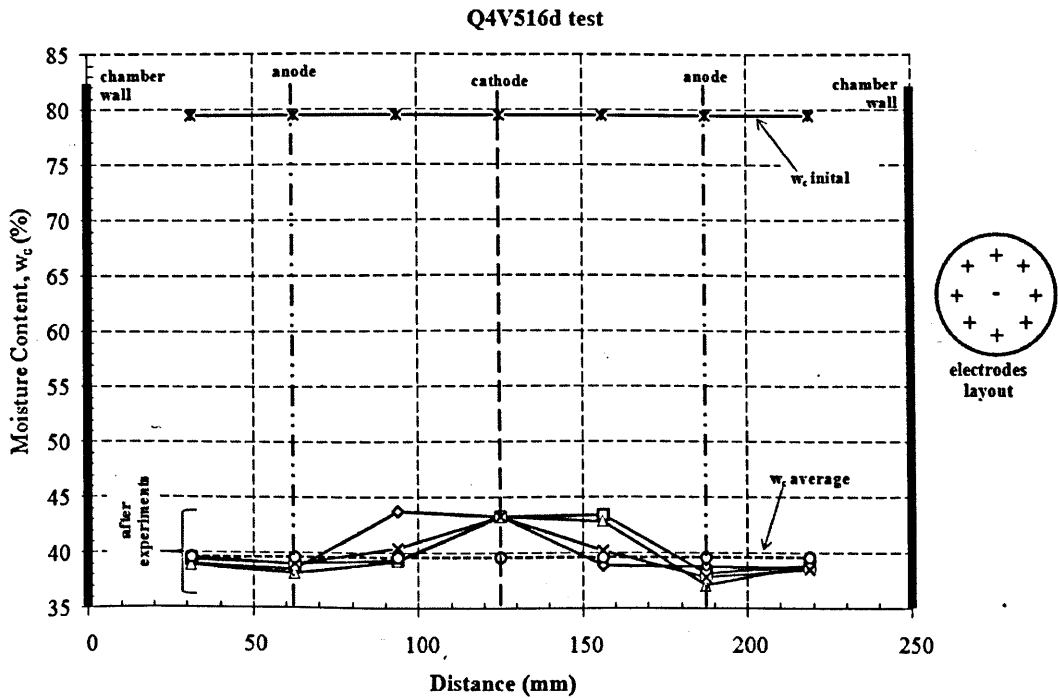


Figure D49 Results of Q4V516d test: water content versus distance

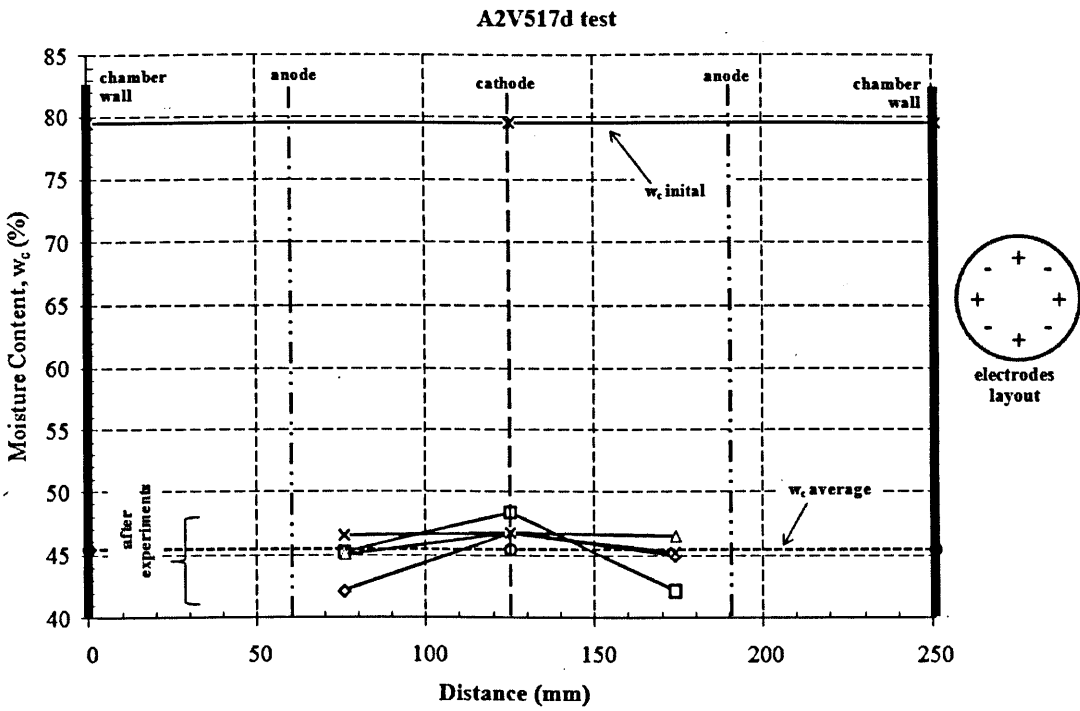


Figure D50 Results of A2V517d test: water content versus distance

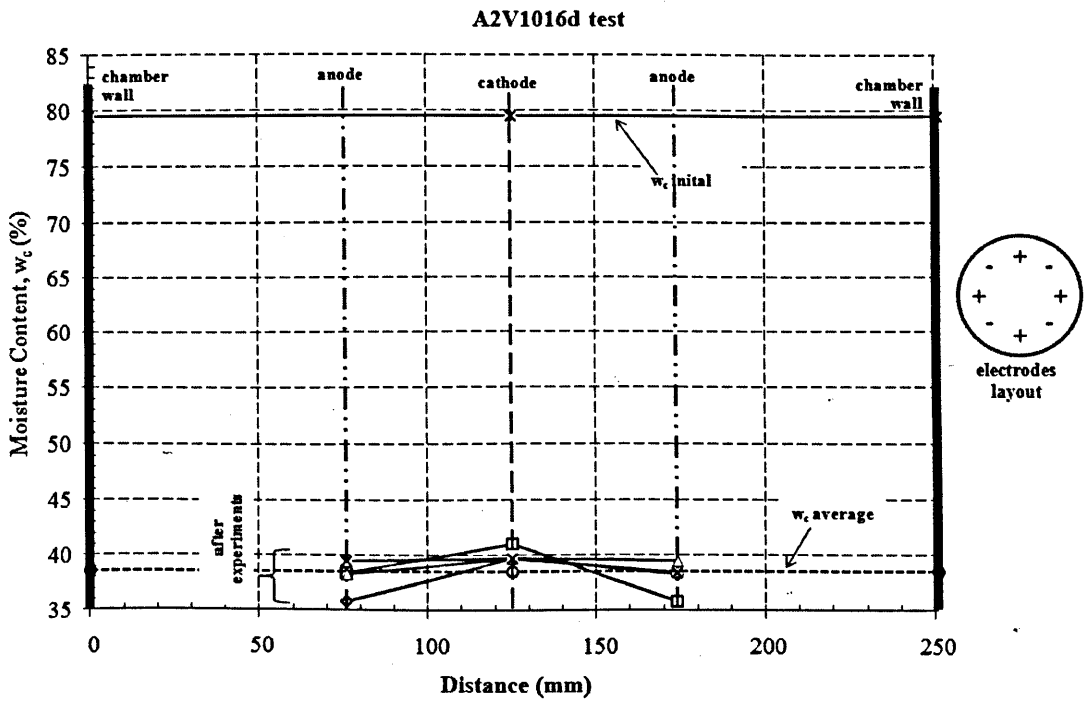


Figure D51 Results of A2V1016d test: water content versus distance

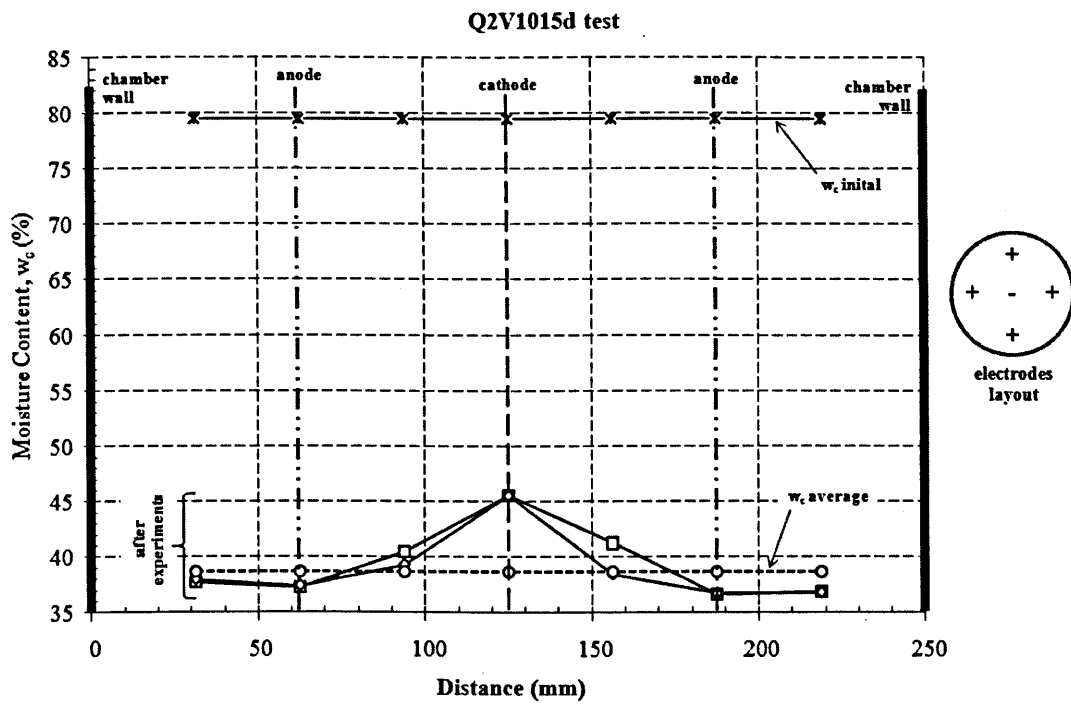


Figure D52 Results of Q2V1015d test: water content versus distance

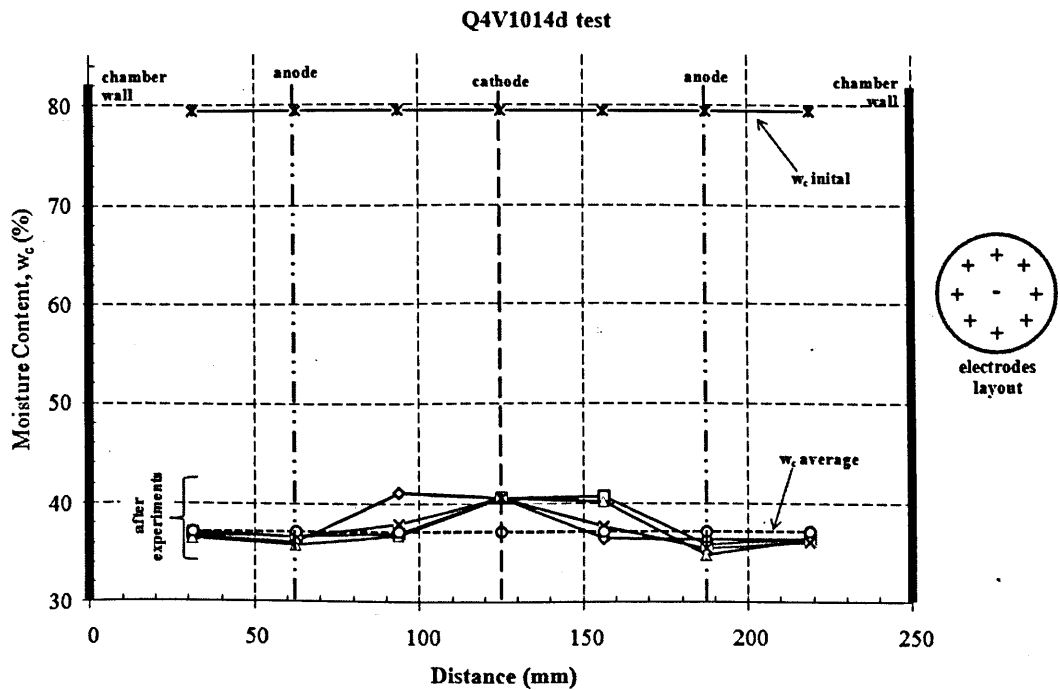


Figure D53 Results of Q4V1014d test: water content versus distance

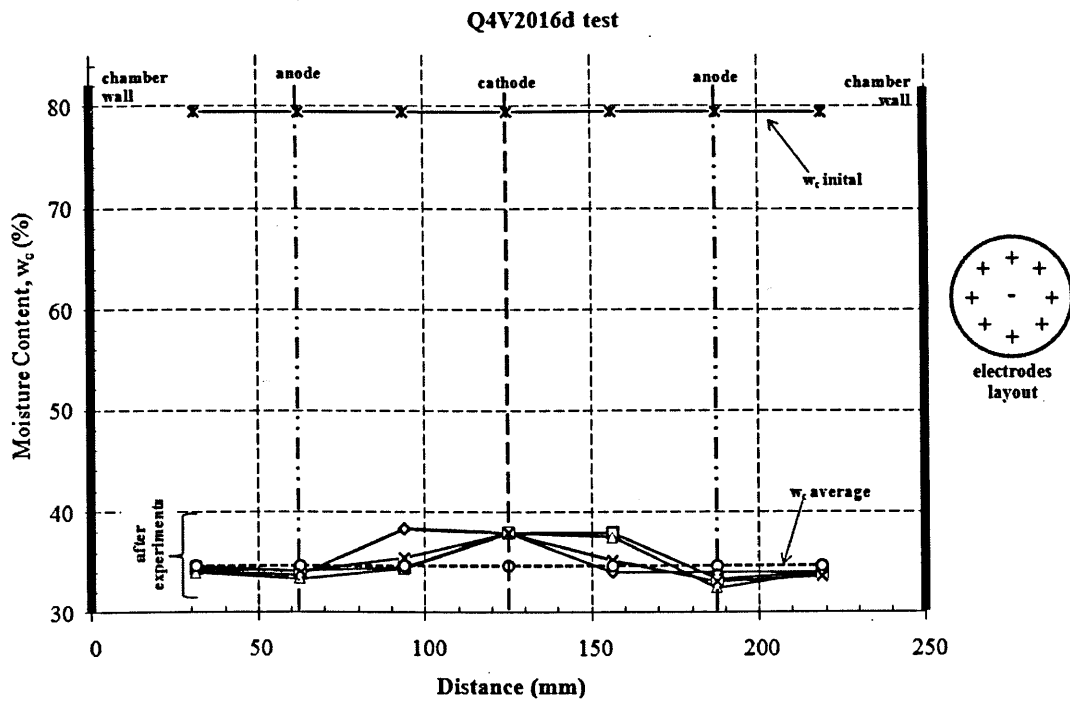


Figure D54 Results of Q4V2012d test: water content versus distance